AD NUMBER

AD011043

NEW LIMITATION CHANGE

TO

Approved for public release, distribution unlimited

FROM

Distribution authorized to DoD only; Test and Evaluation; 24 JAN 1953. Other requests shall be referred to Air Force Rocket Propulsion Laboratory, Edwards AFB, CA.

AUTHORITY

AFRPL ltr dtd 5 May 1972

| AD NUMBER |
| --- |
| AD011043 |
| CLASSIFICATION CHANGES |
| TO: unclassified |
| FROM: restricted |
| LIMITATION CHANGES |
| TO:<br>Distribution authorized to DoD only; Test and Evaluation; 24 JAN 1953. Other requests shall be referred to Air Force Rocket Propulsion Laboratory, Edwards AFB, CA. |
| FROM:<br>Controlling DoD Organization: Air Force Rocket Propulsion Laboratory, Edwards AFB, CA. |
| AUTHORITY |
| E.O. 10501 dtd 5 Nov 1953; Pre-dates formal DoD distribution statements. Treat as DoD only. |

AEROPHYSICS DEVELOPMENT CORPORATION

Pacific Palisades, Calif.

RESTRICTED

Date: 24 January 1953
Report Number: 2000-1-R1
Copy Number:

TECHNICAL REPORT

# PRELIMINARY PERFORMANCE STUDIES OF THE MULTI-JET

D. Bitondo
Project Engineer

and

E. L. Kumm

Approved by
W. Bollay

# DISCLAIMER NOTICE

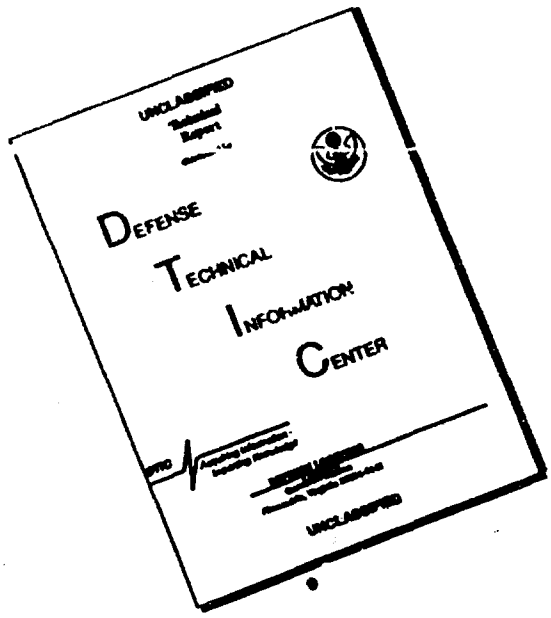


THIS DOCUMENT IS BEST QUALITY AVAILABLE. THE COPY FURNISHED TO DTIC CONTAINED A SIGNIFICANT NUMBER OF PAGES WHICH DO NOT REPRODUCE LEGIBLY.

| PREPARED BY | AEROPHYSICS DEVELOPMENT CORPORATION | REPORT NO 2000-1-R1 |
|---|---|---|
| CHECKED BY | PACIFIC PALISADES, CALIFORNIA | DATE Jan 24 1953 |

## ABSTRACT

The Multi_Jet engine consists of a large number of tiny pulse-jet tubes assembled into a matrix. It differs from the standard pulse-jet in that it achieves a shock compression prior to combustion and in addition completes the combustion at constant volume. The shock compression is achieved by the sudden closure of the exit valve. As a result a normal shock proceeds forward in the tube resulting in a pressure ratio of the order of 2. As the shock approaches the front end of the tube a front valve closes. Thus the compressed air is boxed into a closed volume. The combustion is achieved rapidly by surface combustion from hot ceramic tubes, the combustion proceeding radially inward in the tube. The constant volume combustion results, say, in a temperature ratio of about 5 and correspondingly another pressure ratio of 5. Thus the overall pressure ratio is of the order of 10. At this point the rear valve is opened to produce a jet thrust. After the flow is expanded, the front valve opens and the scavenging is completed.

A typical tube is about $\frac{1}{4}$ inch to $\frac{1}{2}$ inch in diameter and 6 inches long. A jet unit producing a thrust of 150 lbs at a maximum temperature of 3000°F has a diameter of about $8\frac{1}{4}$ inches, a weight of 43 lbs and a specific fuel consumption of 1.86 lbs/hr/lbs of thrust.

With current ceramic materials a peak gas temperature of 2500°F may be safely considered as the design cruising temperature. This contractor has tested a number of materials in single combustion tubes under pulsating conditions and satisfactorily demonstrated that they will withstand a gas temperature of 2500°F for extended periods. A number of promising ceramics have been developed with promise for withstanding a gas temperature of 3000°F; however, these have not yet been tested by this contractor.

The following table gives the performance characteristics of the engine at a flight speed (or helicopter tip speed) of 600 ft/sec:

| Temperature | | Thrust | Specific Fuel Consumption |
|---|---|---|---|
| | °F | Pounds | Pounds Per Hour / Pound of Thrust |
| | 2000°F | 94 lbs | 1.69 |
| Temperature of Cruise | 2200°F | 105 lbs | 1.73 |
| | 2500°F | 120 lbs | 1.80 |
| Temperature of Max. Power | 3000°F | 150 lbs | 1.86 |

Figure 5 gives the variation of the thrust and specific fuel consumption with flight velocity.

There are 160 tubes in this assembly and each tube fires 240 times per second. With the physical arrangement given in this report there are about 960 thrust pulses per second. The result is almost a steady net thrust since the expansion of each jet occupies about 25% of its firing cycle and the individual radial columns of tubes are fired in sequence. Thus the Multi-Jet engine should be much smoother and quieter than the conventional pulse-jet.

The Multi-Jet engine promises to be a very simple and inexpensive jet unit suitable particularly for helicopters and other subsonic aircraft and missile application. Preliminary design studies indicate that a helicopter powered by Multi-Jet engines has a greater range and endurance (for all payloads greater than 15% of the gross weight) than can be obtained with other types of powerplants. This comparison is shown in the table below:

Endurance in Hours for
Helicopters with Various Propulsion Systems

| Payload - % of Gross Weight | 30% | 20% | 15% |
|---|---|---|---|
| MULTI-JET | 3.40 | 4.40 | 5.00 |
| Piston-Engine | 1.60 | 3.70 | 5.00 |
| Pressure-Jet | 1.50 | 2.20 | 2.80 |
| Pulse-Jet | 1.45 | 1.80 | 2.00 |
| Ram-Jet | 0.70 | 0.90 | 1.00 |

PRELIMINARY PERFORMANCE STUDIES
OF THE MULTI-JET

24 January 1953

## FOREWARD

This report was prepared by the Aerophysics Development Corporation under U.S. Air Forde Contract Number AF 33(616)-37. This is the final Technical Report of the preliminary analysis carried out from 24 January 1952 to 24 January 1953 under the reaearch and development contract identified by Expenditure Order No. R-467-4 BR-1. This report is the last of a series issued in fulfillment of the above mentioned contract.

Included among those who cooperated in these preliminary studies are J. Beggs, who worked on the preliminary design and preliminary layouts of the engine; Dr. A. T. Zahorski, who assisted with the structural considerations; J. B. Kendrick, who assisted with the preliminary design of an overall helicopter configuration; D. Woestenburg who built and installed the experimental equipment and assisted in running the experimental tests.

The author is particularly indebted to Dr. W. Bollay, who originated the idea of the Multi-Jet and, under whose able guidance this work was undertaken. His stimulating, active interest throughout the various stages of the present investigation was deeply appreciated.

| PREPARED BY | AEROPHYSICS DEVELOPMENT CORPORATION | REPORT NO. 2000-1-R1 |
|---|---|---|
| CHECKED BY | PACIFIC PALISADES, CALIFORNIA | DATE. Jan 24 1953 |

## LIST OF SYMBOLS

$a$ - Velocity of sound - ft/sec

$C_T$ - Thrust coefficient - $\frac{F}{A\,g}$

$D$ - Tube diameter - feet

$F$ - Thrust - lbs.

$f$ - Specific fuel consumption- $\frac{\text{lbs.fuel 1 hour}}{\text{lb. thrust}}$

$I_D$ - Impulse of gases admitted at the intake - lb.secs.

$I_{NET}$ - Net impulse of gases per cycle - lb. secs.

$I_S$ - Impulse of gases discharged during scavenging.

$I_V$ - Impulse of gases discharged during thrust phase.

$L$ - Length of combustion tubes - feet

$M$ - Mach number

$M_d$ - Mach number of flow in combustion tube during intake = $M_1$

$P$ - Pressure - lbs./sq.ft.

$P_{3\,AVG}$ - Maximum average cycle pressure in tube - lbs/sq.ft.

$S_a$ - Air specific impulse - $\frac{\text{lbs. thrust}}{\text{lbs. of air/sec.}}$

$T$ - Temperature

$u$ - Fluid particle velocity - ft./sec.

$\bar{u}_e$ - Mean effective exit velocity - ft./sec.

$V$ - (or Vol.) - Total volume of a combustion tube - ft.

$w_a$ - Air flow - lbs./sec.

$w_f$ - Fuel flow - lbs./sec.

$W$ - Lbs. of air in the tube

| PREPARED BY | AEROPHYSICS DEVELOPMENT CORPORATION | REPORT NO 2000-1-R1 |
|---|---|---|
| CHECKED BY | PACIFIC PALISADES, CALIFORNIA | DATE Jan 24 1953 |

$\delta$ - $\frac{P_{psf}}{2116}$

$\theta$ - $\frac{T°R}{520}$

$\eta$ - Inlet diffuser efficiency - $\frac{P_{it}}{P_{ot}}$

$\tau_B$ - Duration of burning - secs.

$\tau_C$ - Duration of pulse compression - secs.

$\tau_o$ - Duration of time from the instant the valve starts opening to the instant that it is closed - secs.

$\tau_S$ - Duration of scavenging - secs.

$\tau_V$ - Time required for the valve to open or close - secs.

$\tau_{TOT}$ - Duration of one cycle - secs.

$\tau_E$ - Duration of exhaust

$\rho_{3AVG}$ - Average density of the air in the tube just before discharge - slugs/cu.ft.

$\rho_{2AVG} = \rho_{3AVG}$

$\dot{\xi}$ - Velocity of the shock wave with respect to the fluid particles in front of the wave.

$\mathcal{I}$ - Characteristic mass flow - $\frac{\text{lbs. of air/sec.}}{\text{sq.ft. of frontal area}}$

SUBSCRIPTS

o - Free stream or ambient conditions.

1 - Flow conditions in the tube after leaving the inlet diffuser.

2 - Flow conditions in the tube after passing through the shock wave.

3 - Flow conditions in the tube after burning.

N - Nozzle or exit flow conditions.

SL - Sea level conditions.

t - Supply conditions.

SUPERSCRIPTS

(′) - (prime) - Variable steady flow conditions while the tube is exhausting.

(″) - (double prime) - Conditions of the flow at the tube outlet.

PRELIMINARY PERFORMANCE STUDIES OF THE MULTI-JET

CONTENTS


| | | Page |
|---|---|---|
| ABSTRACT | ..... | ii |
| FOREWORD | ..... | iv |
| LIST OF SYMBOLS | ..... | v |
| INTRODUCTION | ..... | ix |
| PART I | Conclusions and Recommendations. | x |
| PART II | Performance, Analysis, and design of Multi-Jet..... | 20 |
| BIBLIOGRAPHY | ..... | 209 |

## INTRODUCTION

This report gives the preliminary performance analysis of the Multi-Jet. It describes:

(1) The cycle

(2) The ideal performance of a single Tube

(3) The actual performance of a single Tube

(4) The performance of a large supersonic unit

(5) The performance of a small subsonic unit

(6) The materials that can be used and the feasibility of practical applications

(7) The preliminary experimental test runs of a single tube model.

The report is divided into two parts. Part I gives the results and conclusions of the overall program. It also includes the recommendations for further study. Part II describes the technical details of the Multi-Jet and derives the basic equations of the cycle of operation.

PART I

CONCLUSIONS AND RECOMMENDATIONS

CONTENTS

| | | Page |
|---|---|---|
| SECTION I | Description and Results | 1 |
| SECTION II | Conclusions and Recommendations | 18 |

ILLUSTRATIONS

| FIGURE | | Page |
|---|---|---|
| 1. | Ideal Cycle..... | 2 |
| 2. | Comparison of Steady and Non-Steady Compression..... | 3 |
| 3. | Perspective View of the Multi-Jet.. | 5 |
| 4. | Construction Materials of the Multi-Jet..... | 7 |
| 5. | Performance of the Multi-Jet..... | 9 |
| 6. | Performance of a Ramjet..... | 10 |
| 7. | Comparison of Payloads..... | 11 |
| 8. | Helicopter Multi-Jet Fuel System.... | 14 |
| 9. | Perspective Drawing of 36" Engine.. | 15 |
| 10. | Performance of the 36" Diameter Engine..... | 17 |

PREPARED BY
CHECKED BY
AEROPHYSICS DEVELOPMENT CORPORATION
PACIFIC PALISADES, CALIFORNIA
REPORT NO 2000-1-R1
DATE Jan 24, 1953

# SECTION I

## DESCRIPTION AND RESULTS

### 1.1 Description of the Ideal Cycle

The principle of operation of the Multi-Jet engine can be understood most simply by first considering the limiting case of an ideal cycle. Consider a simple tube of constant cross-section through which air is flowing at a Mach Number = $M_1$. This tube is mounted on a vehicle (airplane or helicopter tip moving at a Mach Number $M_o$. This is shown in Figure 1 (a). The air flow is suddenly stopped by the closure of valve A as shown in Figure 1 (b). As a result the air at the end, near A, is suddenly brought to rest and a compression shock S travels upstream at a velocity slightly greater than the velocity of sound $a_1$ (measured with respect to the moving air particles). When this compression shock S reaches the upstream end, a valve B is suddenly closed. This is shown in Figure 1 (c). The air compressed by the shock wave S has a pressure ratio $P_2/P_1$ and a temperature ratio $T_2/T_1$. It will be noted that if, for example, $M_1 = 0.6$ then $P_2/P_1 = 2.17$ and $T_2/T_1 = 1.27$. If this air had been compressed by isentropic compression then it would have reached a pressure rise

$$\frac{\Delta P_{ISENT}}{P_1} = \frac{P_{1t} - P_1}{P_1} = 0.275$$

As a result of the non-steady compression, a pressure rise

$$\frac{\Delta P_{SHOCK}}{P_1} = \frac{P_2 - P_1}{P_1} = 1.17$$

was obtained. The ratio $\Delta P_{SHOCK}/\Delta P_{ISENT}$ is shown in Figure 2. The air is now heated by constant volume combustion to a temperature $T_3$ shown in Figure 1 (d). During the constant volume heating cycle $P_2 v_2 = R T_2$, $P_3 v_3 = R T_3$ and since $v_2 = v_3$ then $P_3/P_2 = T_3/T_2$.

If the temperature ratio $T_3/T_2 = 4.60$ for example, corresponding to a temperature $T_3 = 3030^\circ R$ ($2570^\circ F$), then $P_3/P_2 = 4.6$. If in addition $M_o = M_1 = 0.6$, then the resultant pressure ratio is $P_3/P_1 = 4.6 \times 2.17 = 10$. At this stage of the cycle the rear valve A is opened and the hot high pressure gases are permitted to expand rearward, as shown in Figure 1 (e). When the pressure inside the tube is reduced to the total pressure of the inlet flow $M_o$ the inlet valve B is opened. The inlet flow traveling at a Mach Number $M_o$ is brought to rest at the mouth of the tube. Meanwhile at the exit of the tube the ambient static pressure is lower than the pressure in the tube. Therefore,

| PREPARED BY | AEROPHYSICS DEVELOPMENT CORPORATION | REPORT NO 2000-1-R1 |
|---|---|---|
| CHECKED BY | PACIFIC PALISADES, CALIFORNIA | DATE Jan 24 1953 |

FIGURE 1

# IDEAL CYCLE

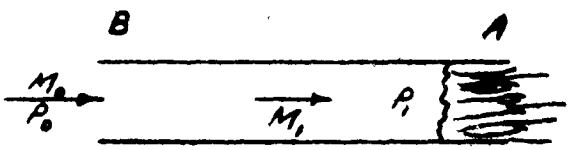


ⓐ SCAVENGING

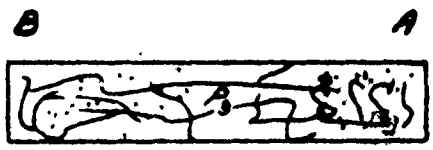


ⓓ BURNING

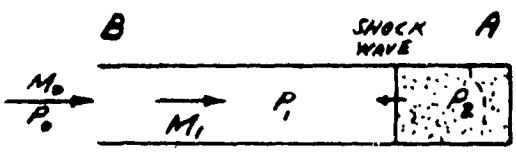


ⓑ SHOCK COMPRESSION

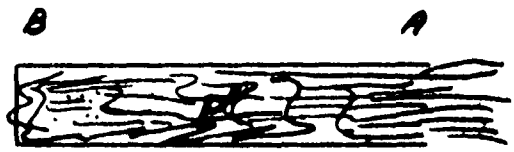


ⓔ DISCHARGE

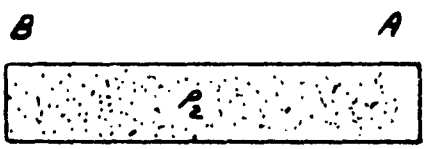


ⓒ SHOCK COMPRESSION

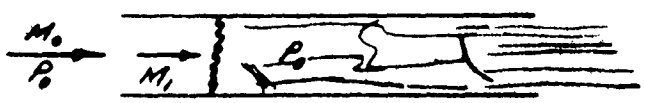


ⓕ SCAVENGING

| PREPARED BY | AEROPHYSICS DEVELOPMENT CORPORATION | REPORT NO 2000-1-R1 |
|---|---|---|
| CHECKED BY | PACIFIC PALISADES, CALIFORNIA | DATE Jan 24 1953 |

FIGURE 2

## COMPARISON OF STEADY AND NON-STEADY COMPRESSION

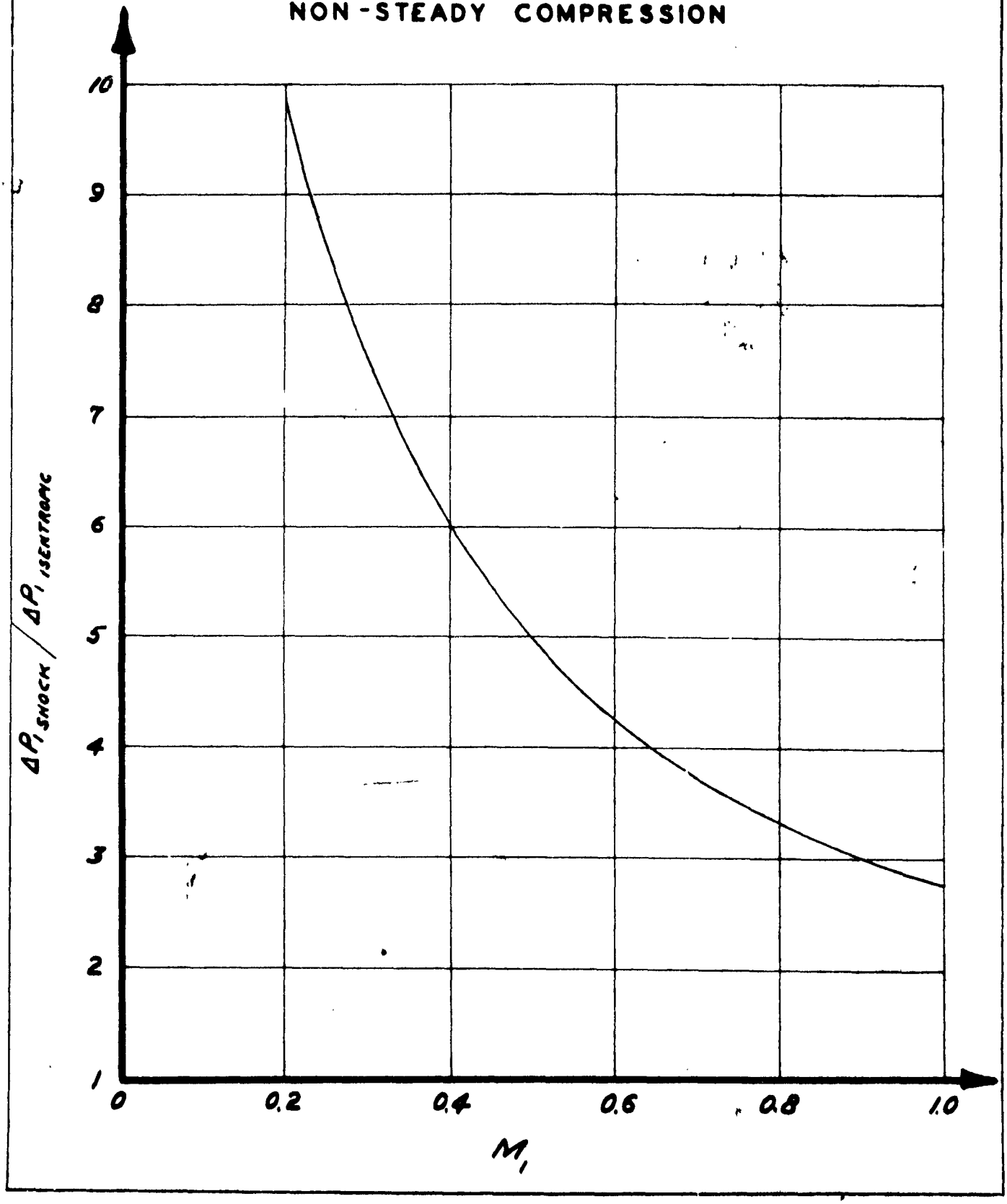

the reaminder of the burnt gases continue to flow out of the tube. The flow at the entrance of the tube has been brought to rest while the inlet valve was closed. As the valve is opened the inlet air begins to flow into the tube. This flow may be compared to the steady flow of air in a stream-tube towards a stagnation point and then again away from the stagnation point. A more exact analysis of this flow using the method of characteristics is carried out in a later section. Thus new fuel-air mixture flows into the tube replacing the remainder of the burnt gases from the previous cycle. This is shown in Figure 1 (f). When the tube is completely filled with a new charge the rear valve closes and a new cycle is started.

## 1.2 Description of the Multi-Jet Suitable for Helicopter Propulsion

The performance characteristics of a Multi-Jet with a maximum diameter of 8¼" were computed. The total length of this engine is 21⅛ inches. This includes the inlet duct, diffuser and a short outlet duct. A perspective drawing of the complete engine is given in Figure 3. The main body of the engine consists of an assembly of tubes arranged longitudinally in a cylindrical fashion. The packing arrangement is preferably such as to obtain as much combustion volume as possible in the 8¼ inch diameter cylinder. The tubes are arranged in a group of six circles with the tubes on the outer circle having the larger diameter, and the tubes in the inner circle having the smallest diameter. The inside diameter of each of the tubes from the outer to the inner circles is 0.51", 0.47", 0.40", 0.29", 0.28" and 0.25" respectively. There are 32 tubes in each circular row. The length of all the tubes is 6 inches. The total cross-sectional area of the combustion tubes is 25.0 square inches which is 49.5% of the total frontal area. The tubes are surrounded by a packing consisting of Fiberfrax which acts as a insulating material as well as providing a shock-proof method of holding the tubes. This material resembles cotton wool and can be packed with various densities around the tubes. It will withstand temperatures up to 2500°F without any adverse effects, and up to 3000°F with sintering.

Arranged to rotate on the face of the front wall at the inlet end of the tubes is the inlet valve, having four diametrically opposed pie-shaped portions. Arranged to rotate on the face of the back wall at the exhaust end of the tubes is the exhaust valve also having four diametrically opposed pie-shaped portions. The open portion of the inlet valve is so arranged that fuel and air is allowed to flow into the tube at the proper time and the solid portion is so arranged that burning and exhaust can occur in the tube at the correct time as the inlet valve revolves. The exhaust valve is similarly arranged to rotate on a common shaft with the inlet valve and to allow discharge and scavenging to occur when the open portion is opposite the tube opening and pulse compression and burning to occur when the closed portion is opposite the tube opening. The configuration can be seen on Figure 3.

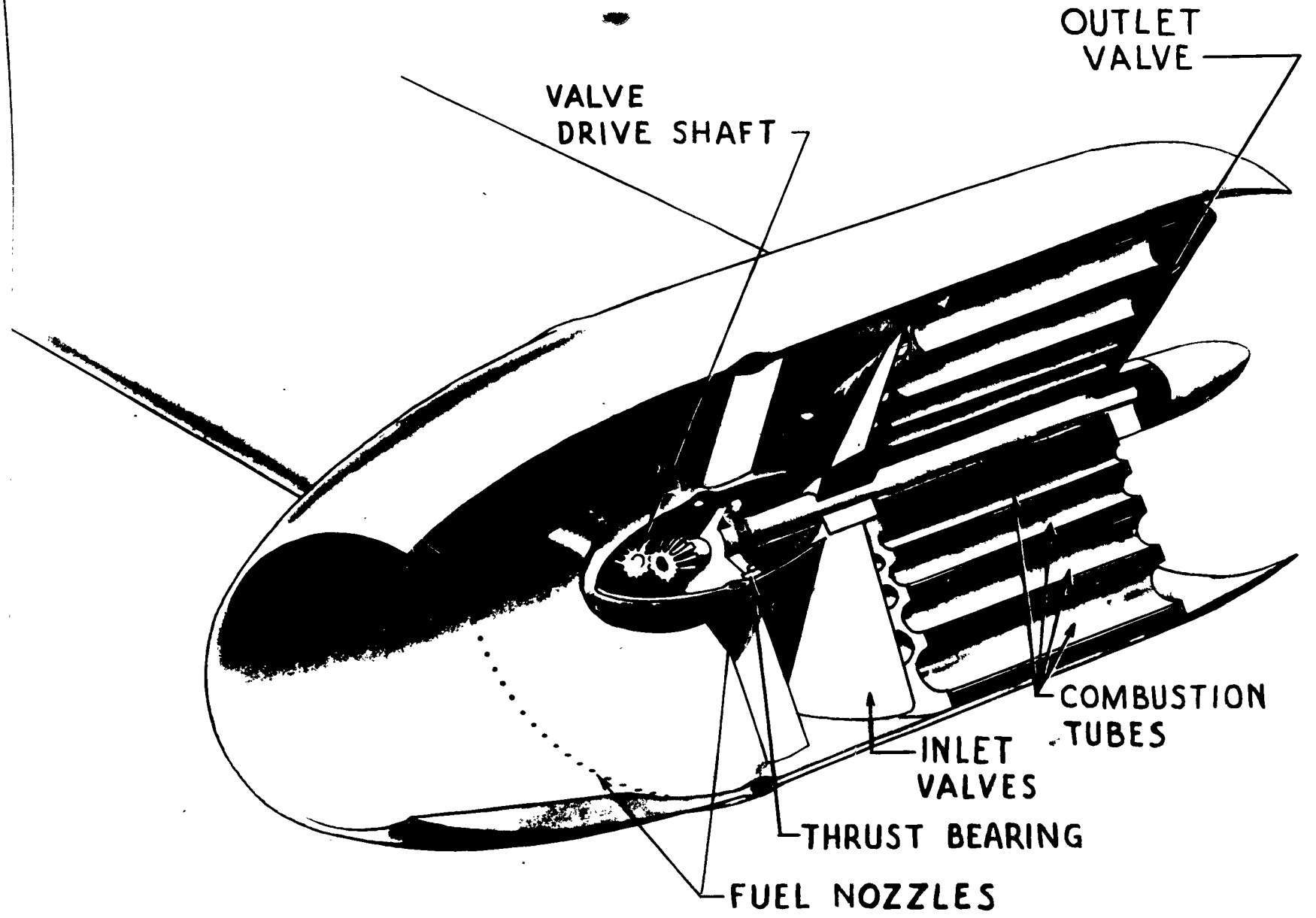


FIGURE 3

**PERSPECTIVE VIEW OF THE MULTI - JET**

| PREPARED BY | AEROPHYSICS DEVELOPMENT CORPORATION | REPORT NO 2000-1-R1 |
|---|---|---|
| CHECKED BY | PACIFIC PALISADES, CALIFORNIA | DATE Jan 24,1953 |

The total weight of the engine is 43 lbs including the outer cowling and inlet ducting and diffuser. This weight is computed under the assumption that Metamic tubes are used as combustion chambers. At this time the materials for an engine operating at a maximum cycle gas temperature of 2500°F can be readily obtained. As shown on Figure 4, the various parts can be made from the following materials:

Outer skin - aluminum

Inner diffuser skin (Aft of fuel nozzles) - enameled steel (Solaramic or similar process)

Inlet valve and central fairing - enameled steel

Outlet duct - enameled steel

Exhaust Valve - enameled steel

Surfaces of valves facing tubes - coated with refractory cement (Adachrome Super Plastic Cement)

Front and rear headers - castable Refractory (B & W Kromecast)

Combustion Tubes - Metamic Type LT-1

Spaces between tubes and central shaft packed with Fiberfrax.

The above materials have been tried and proven in a single tube mock-up model of the Multi-Jet and all have withstood the temperatures quite well. The model was operated for periods up to 15 minutes at maximum gas cycle temperatures of 2500°F. It was also operated for short periods at gas temperature of 3000°F. None of the above materials failed during these runs.

The enameled steel will take temperatures up to 1800°F. The refractory cement facing on the valves is good to 3000°F and has excellent adherent properties with steel. The castable refractory on each end of the tube matrix withstands temperatures up to 3000°F. The fiberfrax can take temperatures up to 2400°F without any effects. It will withstand temperatures up to 3000°F for a short time. The metamic tubes have been tested at 2400°F to give a strength of 3200 psi tensile. With a maximum cycle gas temperature of 2500°F the top steady state temperature of the tube walls is 2300°F. The rear valve and the central shaft are fuel cooled. The inlet valve is air cooled. These materials have actually been tested in the test rig mock-up of the Multi-Jet and have stood up through many test runs. Figure 4 is a sketch of the Multi-Jet showing the materials used for the important parts.

AEROPHYSICS DEVELOPMENT CORPORATION

PACIFIC PALISADES, CALIFORNIA

REPORT NO. 2000-1-R1

DATE Dec. 10, 1953

FIGURE 4

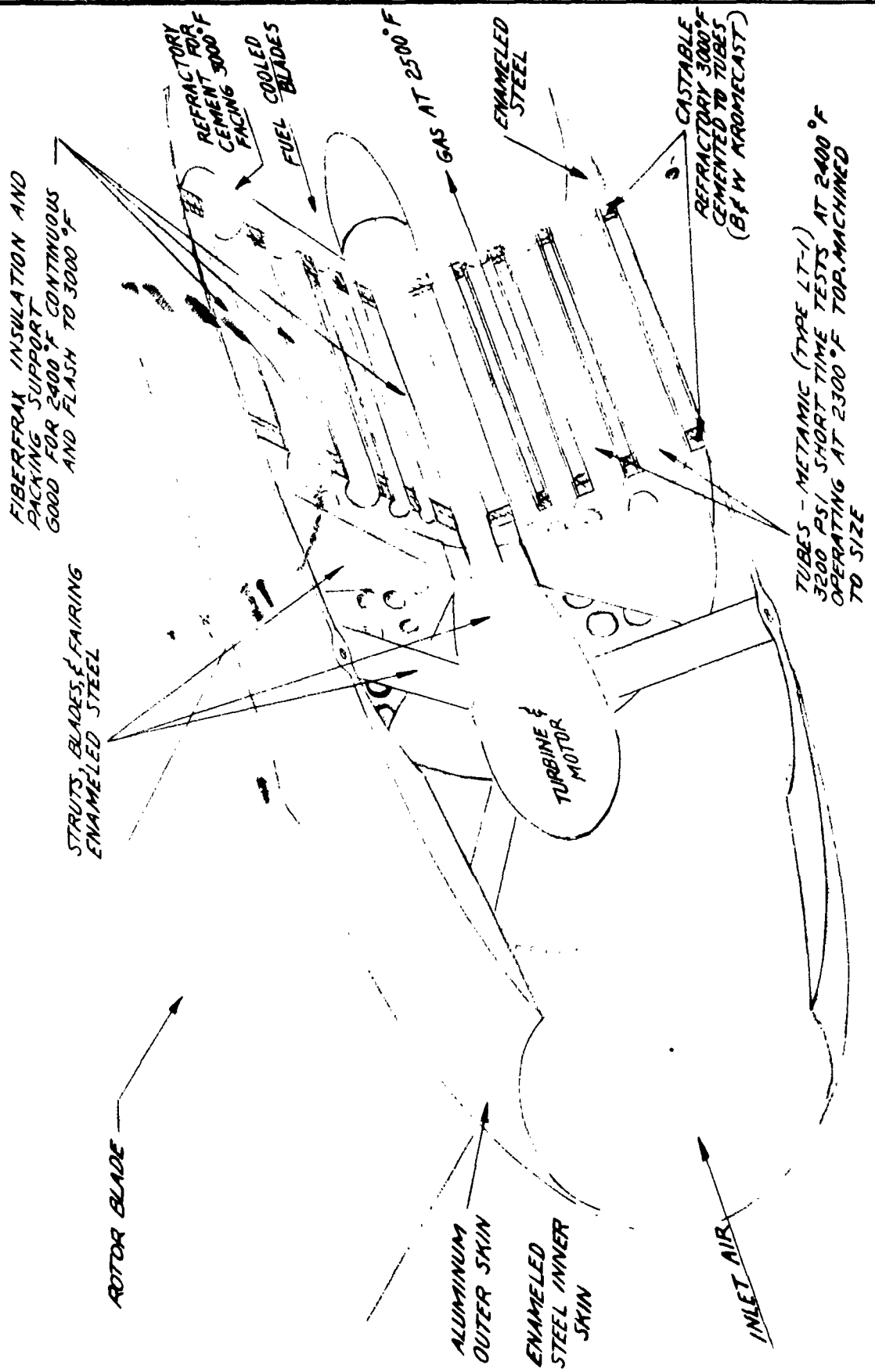


MATERIALS FOR THE MULTI-JET

The above engine can be safely run up to a maximum cycle gas temperature of 2500°F. There are materials that have been developed which will make it possible to run the maximum cycle temperature to 3000°F but these materials were not tested in the present model. It is expected that with future development a maximum cycle gas temperature of 3000°F can be reached. For example, molybdenum tubes with a disilicide coating can take temperatures up to 3000°F but at present are expensive.

1.3 Performance

Figure 5 is a composite graph of the important performance characteristics of an 8¼" maximum diameter Multi-Jet. The weight-thrust ratios for typical design or operating points are given. A check of these points shows the advantages of the Multi-Jet over the Pulsejet. The approximate characteristics of the 7½" diameter Pulsejet developed by the American Helicopter Co. are reported to be as follows:

1. Tip speed - 275 ft/sec
2. Thrust - 45 lbs.
3. Specific fuel consumption - 4.5 lbs/lb-hour
4. Weight - 30 lbs

The above figures are approximate. A comparison of the above values with Figure 5 shows that the thrust per frontal area for the Multi-Jet is about 2½ times greater. The weight-thrust ratio is about ½ for the Multi-Jet. The specific fuel consumption is about 1/3. Furthermore the Multi-Jet can be operated at any tip speed with little change in its performance characteristics.

Figure 6 gives the performance characteristic of an 8¼" diameter ramjet. This curve was obtained from Reference 13. The actual curve in Reference 13 gives the performance of a 6" diameter ramjet. The thrust curves plotted on Figure 6 represent an 8¼" diameter ramjet and it was assumed that the specific fuel consumption and the thrust per unit frontal area remained the same as for the 6" diameter jet described in Reference 13. Again by comparing with Figure 5 we see the better performance of the Multi-Jet. The ramjet excels only in its low weight. At low tip speeds the ramjet is too inefficient in both its fuel consumption and its thrust performance. The absence of static thrust makes the starting of a ramjet powered helicopter quite involved.

The biggest advantage of the Multi-Jet can be seen when a comparison is made of the payload carried by the various helicopters powered by different propulsion systems. This comparison can be seen on Figure 7. The comparison of the piston driven helicopter, with the

AEROPHYSICS DEVELOPMENT CORPORATION

PACIFIC PALISADES, CALIFORNIA

REPORT NO. 2000-1-R1

DATE Jan 24, 1953

FIGURE 5

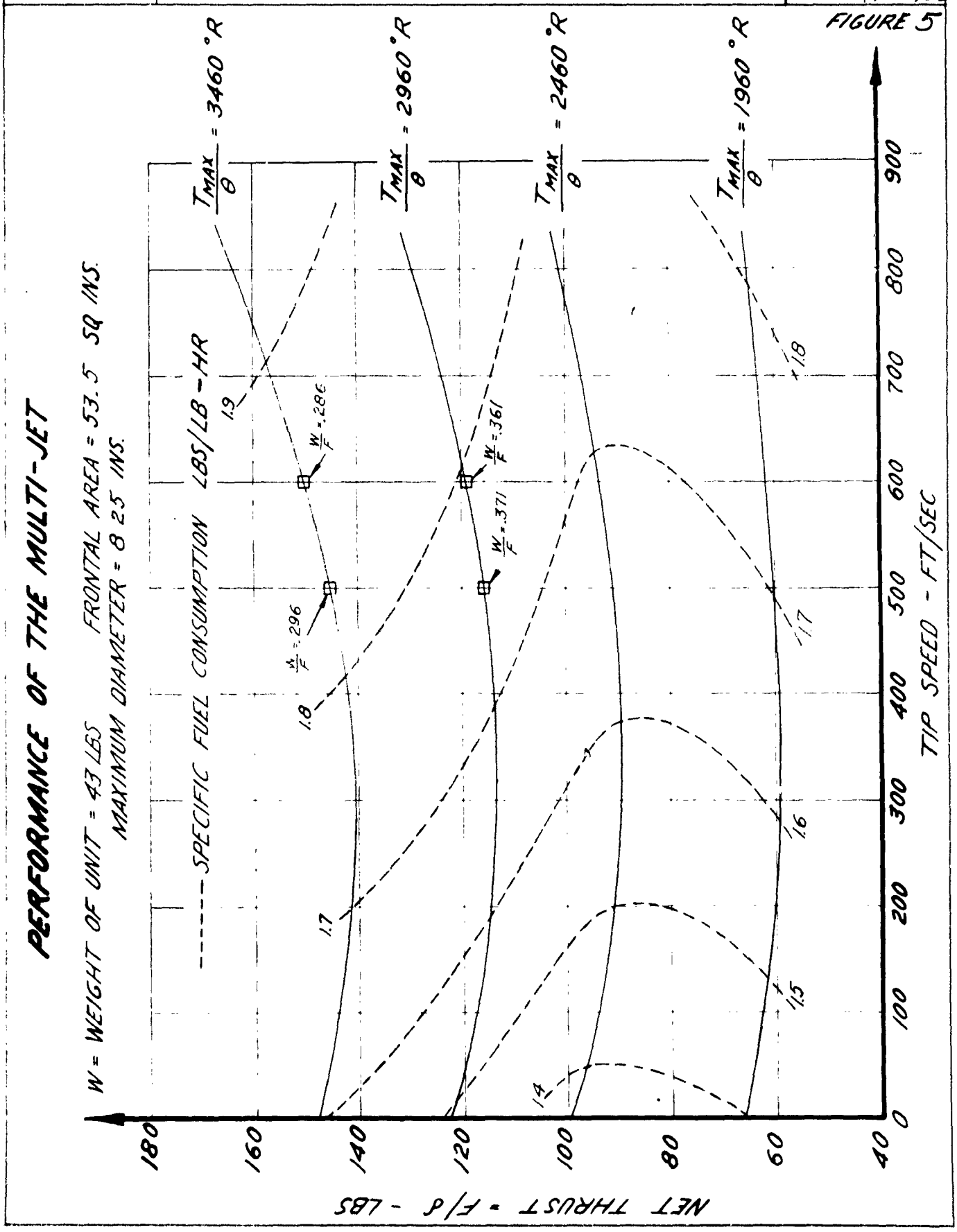

| PREPARED BY | AEROPHYSICS DEVELOPMENT CORPORATION | REPORT NO 2000-1-R1 |
|---|---|---|
| CHECKED BY | PACIFIC PALISADES, CALIFORNIA | DATE Jan 24, 1953 |

FIGURE 6

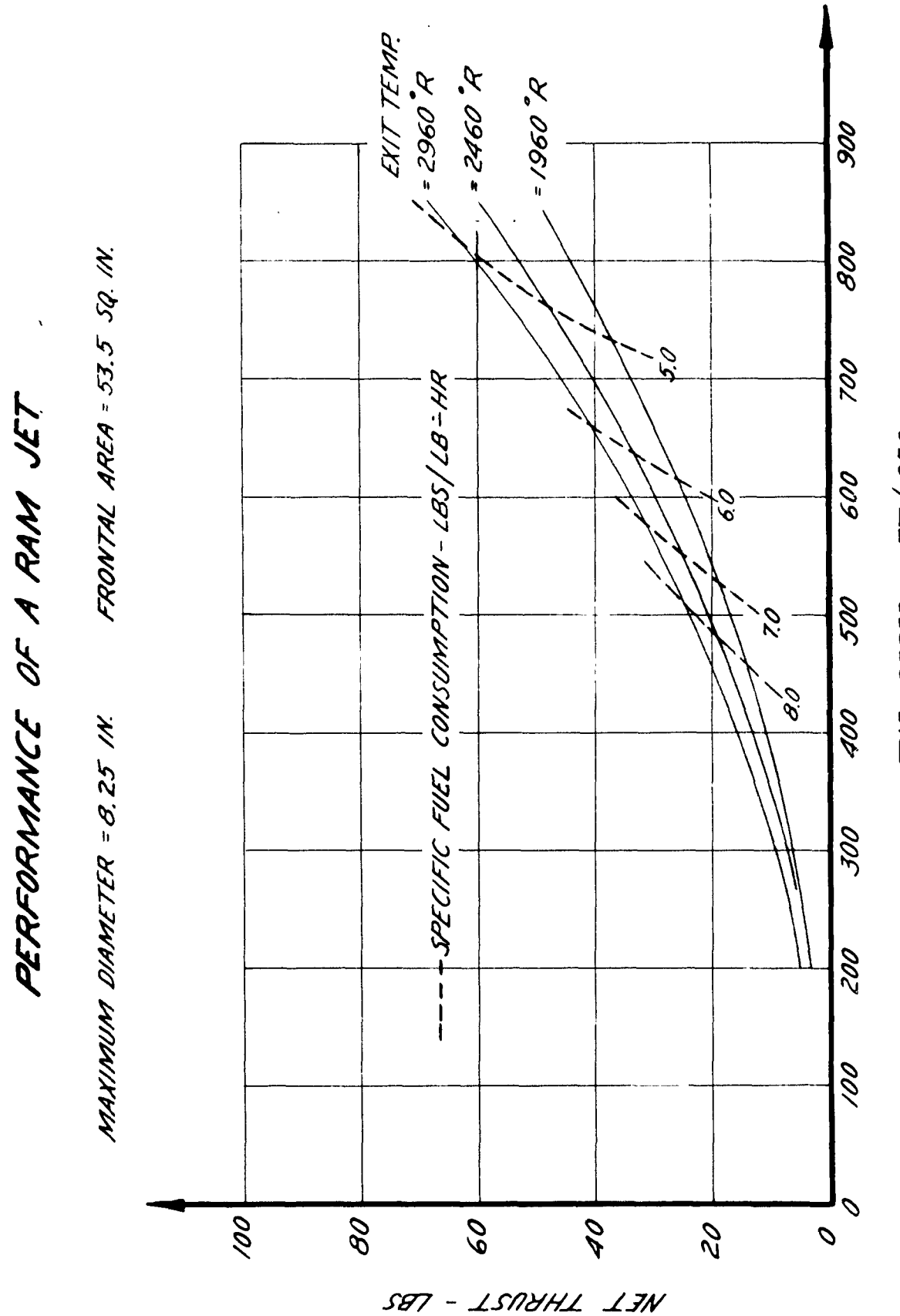

| | | |
|---|---|---|
| | AEROPHYSICS DEVELOPMENT CORPORATION | 2000-1-R1 |
| | P O BOX 657 PACIFIC PALISADES CALIFORNIA | Jan 24 1953 |

FIGURE 7

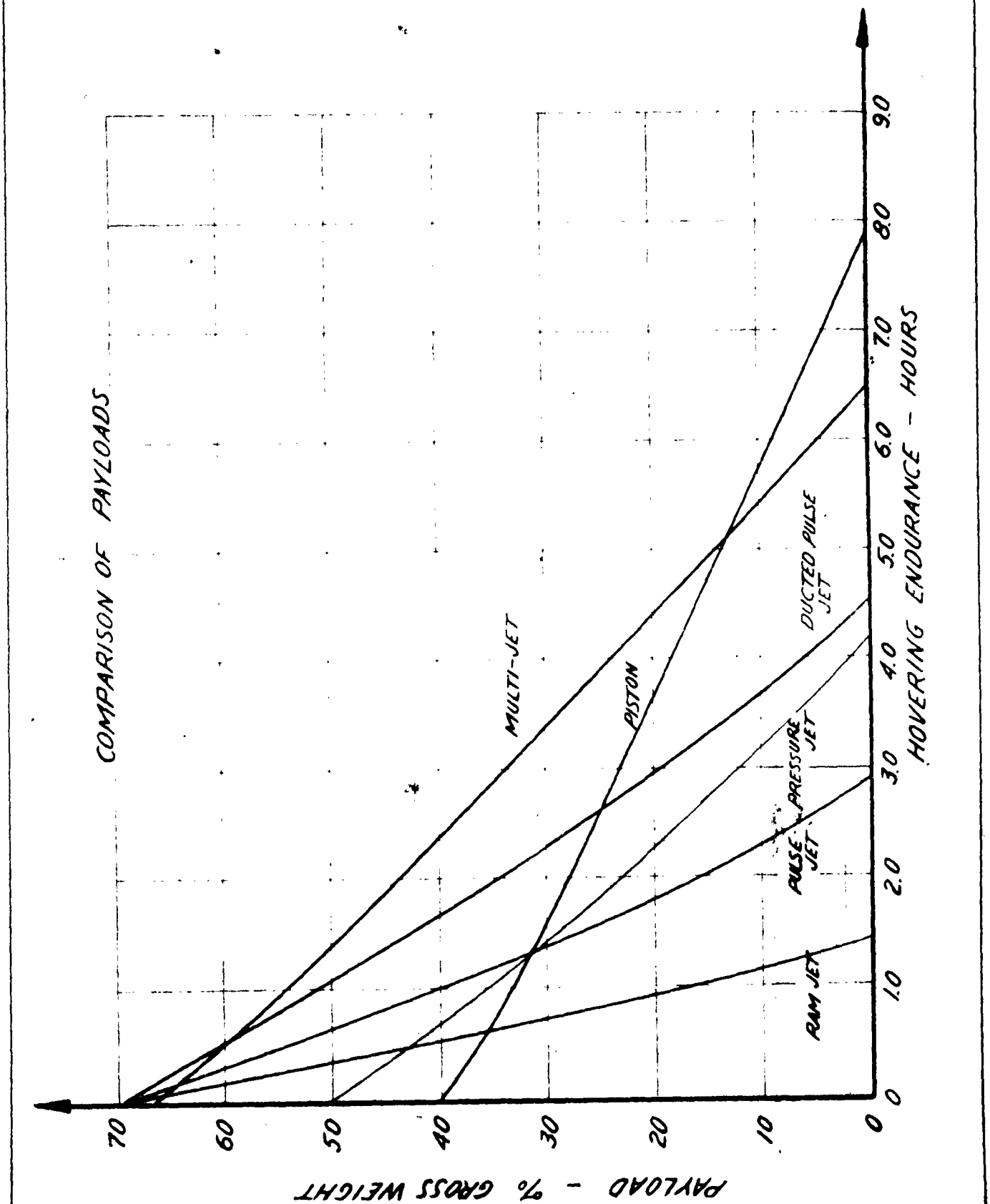

with the jet helicopters shows the superior carrying capacity of the piston helicopter for long range hauls. The jet type helicopters show their superior carrying capacity for the short haul operations. The reasons for the above characteristics are well known. The lower specific fuel consumption of the piston engine in spite of its higher engine weight makes it possible for it to travel the farthest with the greater load. Due to the lower weight of the jet units, the jet helicopters can carry more payload for the shorter distances.

On the other hand the Multi-Jet powered helicopter combines the advantages of the two above mentioned systems. The weight of the Multi-Jet units are only slightly higher than that of the other jet units while its fuel consumption is much lower. In spite of its fuel consumption being higher than the piston engine, the Multi-Jet powered helicopter can carry a greater payload than the piston driven helicopter over the same range due to its lower weight. Except for the extremely long ranges where the payload amounts to only 10% of the gross weight or less the Multi-Jet is superior to the piston driven helicopter. The above comparisons can be seen in Figure 7 which was obtained from Reference 12.

1.4 Operation of the Multi-Jet

A single tube mock-up of the Multi-Jet was constructed and test run. The main purpose of the model was to investigate the following problems:

1. Testing of tube materials under actual operating conditions.
2. Investigation of methods of mounting tubes.
3. Connected pipe test of the valved single tube model to determine if the cycle can be sustained and if the fuel-air mixture is re-ignited and burned in each succeeding cycle.

Due to the pulsating character of the flow no instantaneous measurements could be taken of the air or fuel flow. The experiments did indicate that a net thrust was obtained and that combustion was taking place due to the fact that the tube did not cool down during a run. A six inch tube of $\frac{1}{8}$ inch inside diameter was used.

The tube was preheated by means of a flame holder operating under a low air flow velocity. It is proposed to use a similar method to heat the tubes in the actual unit. It was found that the tubes had to be preheated to about 1800°F before the cycle could be started.

In the actual unit mounted on the blade tip of a helicopter rotor the valves can be rotated by means of a fuel-driven turbine. The fuel will be under a high pressure due to the centrifugal forces produced

by the rotating blades and this pressure can be utilized to turn the valves. A schematic diagram of the fuel system, the helicopter rotor speed control, and the Multi-Jet valve drive and speed control is shown in Figure 8.

Starting of the engine is presently considered to be accomplished as follows: A line from a pressurized gas container in the fuselage will dirve the rotary valve independently of the fuel motor by means of a small gas turbine at a rate higher than in steady state operation. Rotation of the valves and the ejector action of the air from the gas turbine will induce a small air flow through the engine. A small fuel flow also results by the fuel motor acting as a pump and this fuel is injected at the front of the engine. Ignition is obtained in this region by means of spark plugs and the fuel-air mixtures burning partially expand through the engine developing a small amount of thrust while the combustion tubes are being heated. When the combustion tubes are sufficiently heated to cause auto ignition of the incoming fuel-air mixture, thrust will increase rapidly allowing the blades to rotate. As the rotational speed increases the fuel pressure increases and the rotary valve may then be driven by the fuel motor instead of the compressed gas turbine. This "bootstrap" arrangement is believed to be a practical way of starting the engines but, of course, must be experimentally demonstrated.

External heated air supplies could, of course, be used for pre-heating the combustion tubes but such an arrangement involves rather bulky and heavy equipment which may not be easily available at various places the helicopter may desire to land.

## 1.5 Description of a 36" Diameter Engine

The cut-away perspective view of Figure 9 shows the general configuration of the Multi-Jet engine capable of supersonic flight.

The combustion chambers are arranged as a set of parallel cylindrical tubes in a drum-like cylinder whose outside diameter is 36 inches. This drum-like cylinder contains two end walls between which are mounted the combustion tubes. The tubes are arranged in a group of six concentric circles with the tubes on the outer circle having the larger diameter, and gradually decreasing in diameter to the inner circle of tubes of the smallest diameter. The inside diameter of the tubes from the outer to the inner circles are 2.62", 2.22", 1.87", 1.50", 1.23" and 1.02" respectively. There are 32 tubes in each row. The length of the tubes is 15 inches. The cross-sectional area of the combustion tubes is 506 square inches or 49.5% of the maximum cross-sectional area of the engine. The diameter of the engine is 36 inches and the total length is 45 inches. The total dry weight of the engine is approximately 1000 pounds.

AEROPHYSICS DEVELOPMENT CORPORATION
P O BOX 657 PACIFIC PALISADES CALIFORNIA

2000-1-R1
Jan 24 1953

Figure 8

## HELICOPTER MULTI-JET FUEL SYSTEM

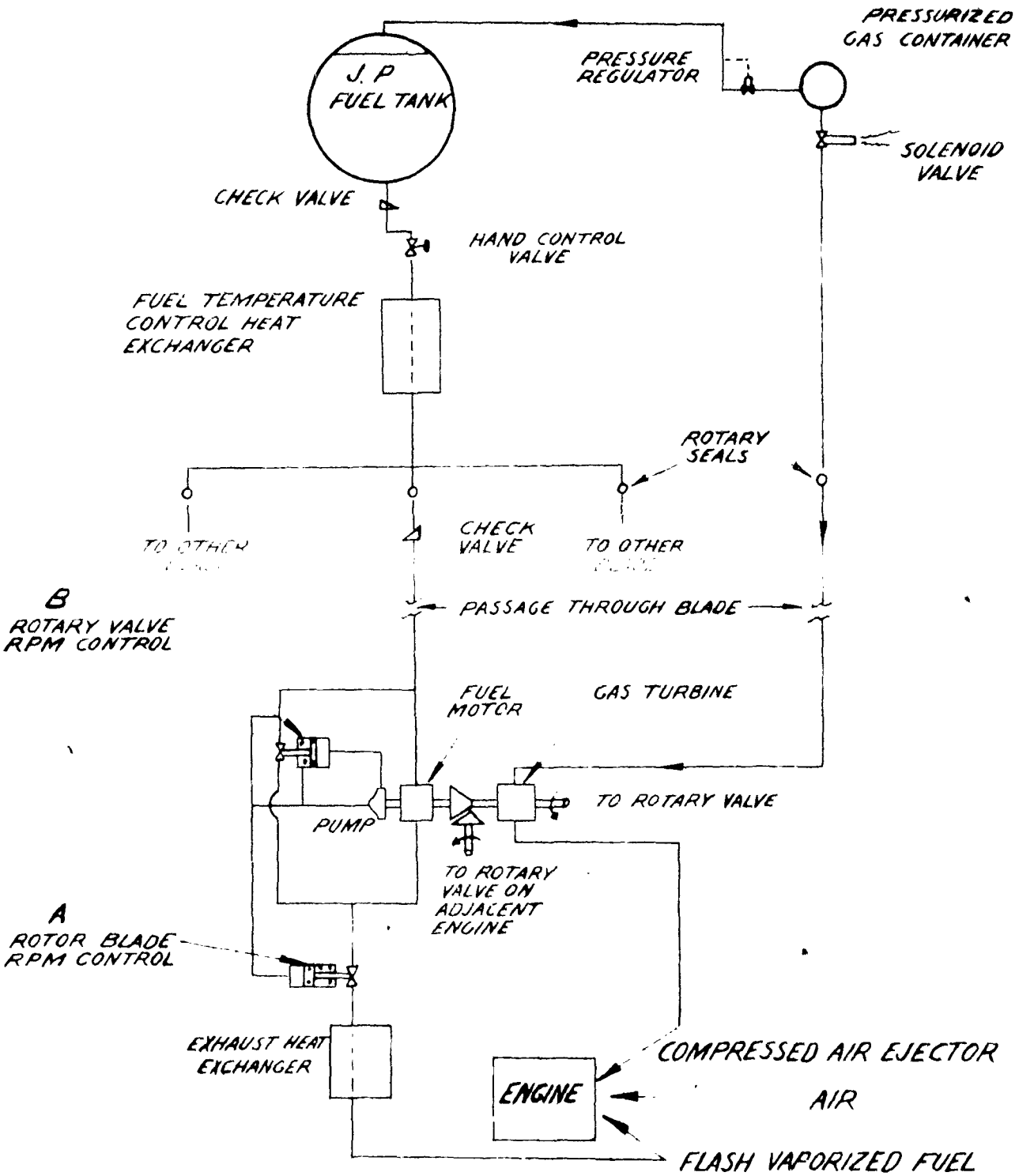

AEROPHYSICS DEVELOPMENT CORPORATION

PACIFIC PALISADES, CALIFORNIA

FIGURE 9

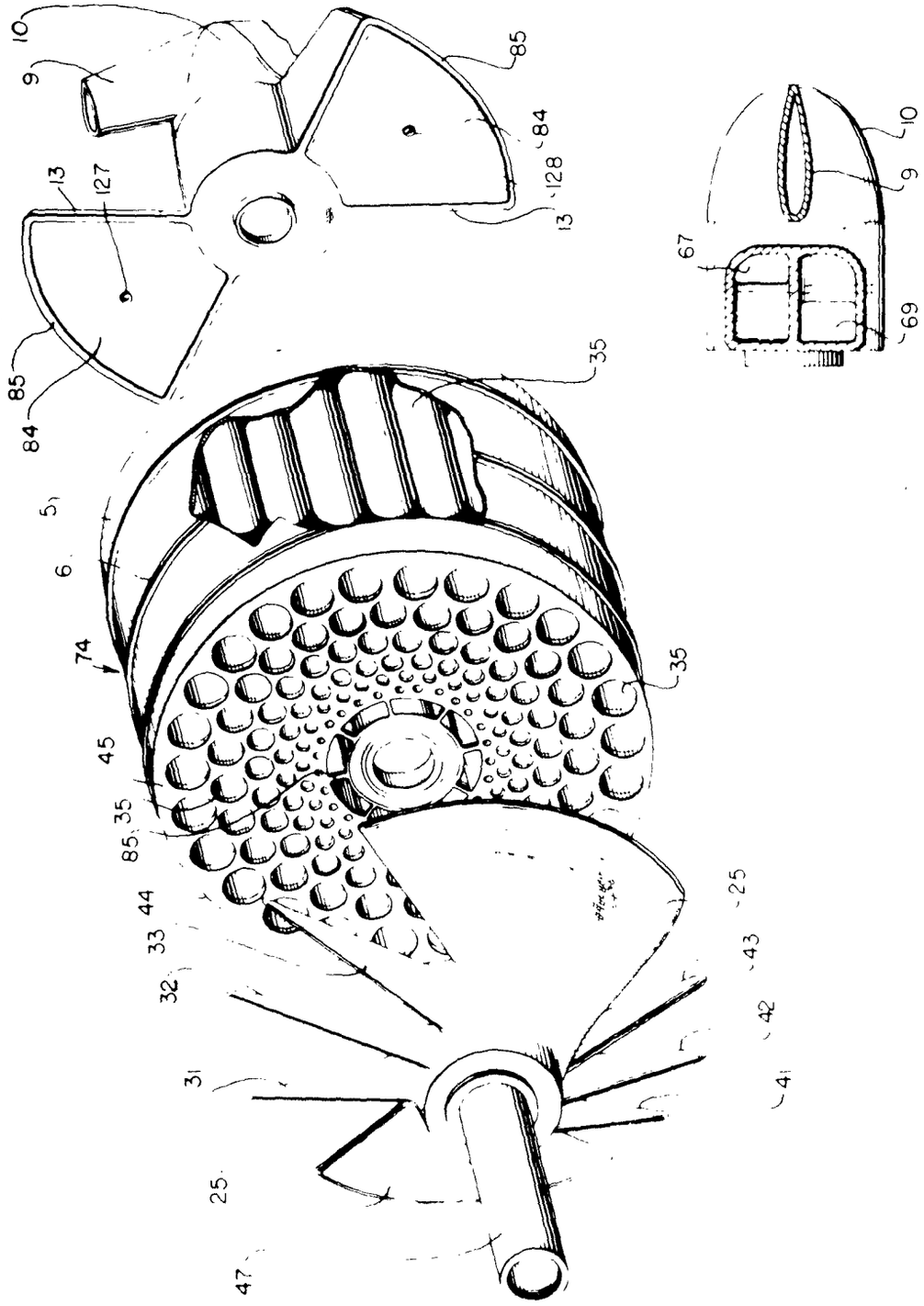


PERSPECTIVE VIEW OF BASIC COMPONENTS OF THE 36" MULTI-JET

Two rotating plates each having two pie-shaped cutouts, mounted at the ends of a shaft passing through the center of the cylinder serve as inlet and exhaust valves respectively. The cut-outs on the plates are so arranged that there is a force balance about the the center line of rotation. The open cut-out of the inlet valve will provide the proper time for the inlet of fuel and air to the tubes. The cut-outs of the exhaust valve provide the proper time for exhaust of gases out the outlet end of the tubes.

1.6 Performance of the 36" Diameter Engine

Figure 10 gives a composite plot of the thrust and specific fuel consumption of a 36" diameter Multi-Jet engine. The static weight/thrust ratio = 0.25 and is somewhat better than a turbo jet. The specific fuel consumption is higher, about 1.0 to 1.8 lbs of fuel/hour per lb of thrust. The whole unit is much lighter (about $\frac{1}{2}$ that of a turbo-jet and much shorter than a conventional turbo-jet. The Multi-Jet engine should be very much cheaper to build than an equivalent thrust turbo-jet. This type of engine can advantageously be used to replace turbor-jets in an expendable type of missile. Since the engine is simpler and cheaper to build than a turbo-jet and since the Multi-Jet's performance is comparable to a turbo-jet its use on an expendable missile (subsonic or supersonic) is desirable. There are two disadvantages of this unit relative to the turbo-jet. These are (1) its low characteristic mass flow (between 6 and 7), and, (2) its lower thrust/unit frontal area. (about 600 pounds per square foot.) However, by careful design of the missile, the inlet diffuser and the arrangement of the Multi-Jet units, it is possible to obtain an efficient missile configuration. This is especially true if the maximum diameter of the missile body is determined by factors other than the engine diameter. It is expected that with future development in the design and arrangement of combustion tubes the Multi-Jet would allow significantly higher characteristic mass flows and higher thrusts per unit frontal area.

The Multi-Jet can also compete with the ram-jet due chiefly to the former's lower specific fuel consumption. Since the Multi-Jet can supply static thrust the complexity of a large rocket boost system required for a ram-jet is unnecessary.

| PREPARED BY | AEROPHYSICS DEVELOPMENT CORPORATION | REPORT NO. 2000-1-R1 |
|---|---|---|
| CHECKED BY | PACIFIC PALISADES, CALIFORNIA | DATE Jan 24 1953 |

FIGURE 10

PERFORMANCE OF A 36" DIAMETER MULTI-JET

WEIGHT = 1000 LBS
FRONTAL AREA = 7.05 SQ FT

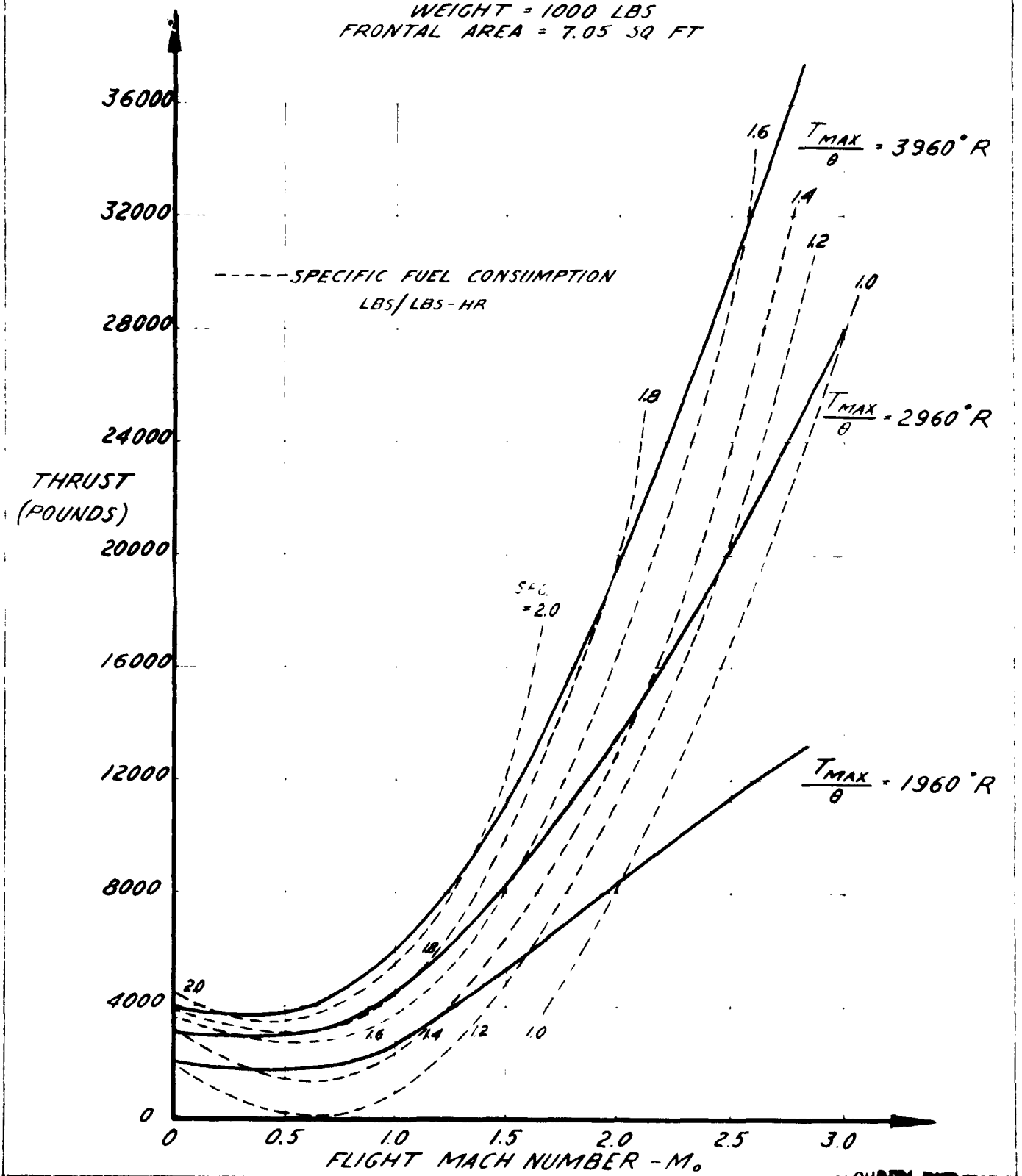

## SECTION II

## RECOMMENDATIONS

The Multi-Jet engine promises to be a simple and inexpensive jet unit suitable particularly for helicopters and other aircraft and missile application. Preliminary design studies indicated that although the specific fuel consumption of the Multi-Jet is more than that of the reciprocating engine, the much lower weight makes it possible for a Multi-Jet propelled helicopter to carry more payload for long as well as short range operations.

The Multi-Jet combines the simplicity of the pulsejet with an engine whose specific fuel consumption is less than half that of the pulsejet. The specific weight is somewhat less than a turbo-jet while its specific fuel consumption is only slightly higher. The Multi-Jet's durability and reliability should be far better than the conventional pulsejet; however, the cost in reasonable quantities is expected to be only slightly higher. Since each unit is made up of a large number of combustion chambers, the cycling arrangement makes it possible to superimpose the pulses to result in a nearly constant thrust, with only a small resulting ripple.

The main emphasis on the future work should be on an extensive experimental program to determine the actual performance and critical design points.

The work with a single tube model of the Multi-Jet should be continued. This experimental phase should include the testing of as many ceramic materials as are obtainable. In this way it is felt that the present maximum cycle temperature of 2500°F can be raised to 3000°F. The single tube test model should be built to exacting dimensions and must be cooled throughout so that accurate, quantitative results can be obtained. Valve clearances must be known and must be strictly maintained during a test run. Since the model will be constructed partially of steel, cooling of some parts will be necessary. This test program will be aimed at determining the optimum length for the combustion tubes, the optimum valve configuration operating wall temperatures, fuel-air ratios and starting wall temperatures. Due to the pulsating nature of the inlet and outlet flows special instrumentation will be required to measure fuel flow, air flow, thrust, and the variation of pressure and temperature during a cycle.

Since the inlet and outlet conditions of the actual engine cannot be simulated in a single tube model further testing sould include a single row of combustion tubes arranged in a circle having a diameter of 8". In this way the pulsating flow in the inlet pipe can be eliminated. The area ratios between the inlet duct and the tube inlets and, the exit duct and the tube outlets can be adjusted in

the single row test engine to simulate the ratios on the actual proposed engine.

From the very simple tests that have been conducted on the mock-up model of a single tube unit, there have been obtained many useful ideas that can be incorporated in the engine. The questions regarding the mounting of the tubes have been answered and the problem of obtaining high strength, high temperature materials has been definitely solved for cycle temperatures up to 2500°F. A preliminary design analysis of the important and critical components was carried out and there appear to be no known difficulties regarding the procurement of materials, the structural design and the manufacturing of an actual unit.

The tests themselves have exhibited the fact that the cycle is feasible and that the cycle is sustained as the tube is opened and closed by the valves. The model also exhibited net thrust. Due to the pulsating character of the flow and the lack of proper instrumentation it was not possible to make quantitative measurements on the test model. Since the contract was not primarily an experimental investigation, the funds available for instrumentation and equipment was limited. However a crude single tube model was constructed in order to prove the fact that the cycle could be sustained and that ignition of the fuel could be obtained in the hot ceramic tubes as well as providing a simulated test of the various materials.

The performance analysis does not indicate any critical points in the cycle. The curves given on Figure 5 include the performance of an engine operating on an actual cycle. Frictional flow losses, mass flow and pressure loss - due to the slow valve opening and closing times, and valve leakage losses are all included. The leakage losses were computed under the assumption that the leakage flow was conducted directly to the environmental static pressure. Actually the flow must travel through long narrow passages between the flat valve face and the flat surface of the header before it reaches the outside. The tubes in the outer circle will be the only ones that can possibly lose the amount computed. A loss of 8% of the total mass flow through the engine was computed for valve clearances of 0.002". Actually due to the above considerations it is estimated that about 3% of the mass flow will be lost when the valve clearances are 0.002". In making the performance computations, a loss of 8% was used so that the maximum allowable valve clearances could possibly be raised to 0.006". It is felt that a clearance of about 0.004" can be maintained between the combustion tube faces and the rotary valves.

PART II

PERFORMANCE, ANALYSIS AND DESIGN OF THE MULTI-JET

CONTENTS


| | | Page |
|---|---|---|
| SECTION I | Basic Cycle of Operation | 27 |
| SECTION II | Derivation of the Basic Equations | 30 |
| SECTION III | Ideal Cycle Performance of a Single Tube | 45 |
| SECTION IV | Actual Cycle Performance of a Single Tube | 69 |
| SECTION V | Performance and Design Analysis of a 36" Diameter Engine | 104 |
| SECTION VI | Performance and Design Analysis of an 8" Diameter Engine | 139 |
| SECTION VII | Effect on Helicopter Design and Performance of the Design of Combustion | 166 |
| SECTION VIII | Analysis of the Design of Combustion Tubes | 172 |
| SECTION IX | Experimental Results | 183 |
| BIBLIOGRAPHY | | 209 |
| APPENDIX I | Ideal Cycle Performance of a Single Tube | 212 |
| APPENDIX II | Actual Cycle Performance of a Single Tube | 214 |
| APPENDIX III | Performance Computations for the Supersonic Engine- | 215 |
| APPENDIX IV | Computations for the Ideal Cycle | 221 |
| APPENDIX V | Computations for the Actual Cycle | 223 |
| APPENDIX VI | Helicopter Multi-Jet Fuel System | 224 |
| TABLES | | 228 |

CONTENTS

ILLUSTRATIONS


| Figure | | Page |
|---|---|---|
| 1. | Basic Cycle | 28 |
| 2. | Mach Number of the Shock Wave | 31 |
| 3. | Pressure and Temperature Ratios after the Shock Wave | 32 |
| 4. | Duration of Discharge | 35 |
| 5. | Variation of Chamber Pressure with Time | 36 |
| 6. | Variation of Weight Flow with Time | 37 |
| 7. | Variation of Exit Velocity with Time | 38 |
| 8. | Variation of Thrust with Time during the Thrust Phase | 40 |
| 9. | Impulse of the Discharging Gases | 41 |
| 10. | Impulse Function | 43 |
| 11. | Fuel-Air ratio | [illegible] |
| 12. | Comparison of Steady and Non-Steady Compression | 46 |
| 13. | Ideal Cycle | 47 |
| 14. | Specific Fuel Consumption | 50 |
| 15. | Specific Fuel Consumption | 51 |
| 16. | Specific Fuel Consumption | 52 |
| 17. | Specific Fuel Consumption | 53 |
| 18. | Specific Fuel Consumption | 54 |
| 19. | Specific Fuel Consumption | 55 |
| 20. | Thrust per Unit Tube Area | 57 |
| 21. | Thrust per Unit Tube Area | 58 |
| 22. | Average Thrust per Cycle | 59 |
| 23. | Air Specific Impulse | 60 |

| PREPARED BY | AEROPHYSICS DEVELOPMENT CORPORATION | REPORT 2000-1-R1 |
|---|---|---|
| CHECKED BY | PACIFIC PALISADES, CALIFORNIA | DATE Jan 24 1953 |

CONTENTS


| Figure | | Page |
|---|---|---|
| 24. | Air Specific Impulse | 61 |
| 25. | Air Specific Impulse | 62 |
| 26. | Thrust per Unit Tube Area | 64 |
| 27. | Specific Fuel Consumption | 65 |
| 28. | Air Specific Impulse | 66 |
| 29. | Thrust Coefficient | 67 |
| 30. | Characteristic Mass Flow | 68 |
| 31. | Ideal Formation of the Pulse Compression Wave | 69 |
| 32. | Actual Formation of the Pulse Compression Wave | 70 |
| 33. | Ideal Closure of the Front Valve | 72 |
| 34. | Actual Closure of the Front Valve | 74 |
| 35. | Rotational Flow [illegible] Constant Area Duct | 75 |
| 36. | Pressure in a Constant Mach Number Duct with Friction and Pulse Compression | 78 |
| 37. | Static Pressure in a Constant Mach Number Duct with Friction and Pulse Compression $M_o$ = 0.25 | 79 |
| 38. | Static Pressure in a Constant Mach Number Duct with Friction and Pulse Compression $M_o$ = 0.50 | 80 |
| 39. | Static Pressure in a Constant Mach Number Duct with Friction and Pulse Compression $M_o$ = 0.75 | 81 |
| 40. | Mean Effective Exit Velocity | 83 |
| 41. | Duration of Pulse Compression and Scavenging | 85 |
| 42. | Fuel-Air Ratios | 87 |
| 43. | Thrust per Unit Frontal Area $M_o$ = 0.25 | 88 |
| 44. | Thrust per Unit Frontal Area $M_o$ = 0.50 | 89 |
| 45. | Thrust per Unit Frontal Area $M_o$ = 0.75 | 90 |

| PREPARED BY | AEROPHYSICS DEVELOPMENT CORPORATION | REPORT NO 2000-1-R1 |
|---|---|---|
| CHECKED BY | PACIFIC PALISADES, CALIFORNIA | DATE Jan 24 1953 |

CONTENTS


| Figure | | Page |
|---|---|---|
| 46. | Specific Fuel Consumption $M_o$ = 0.25 | 91 |
| 47. | Specific Fuel Consumption $M_o$ = 0.50 | 92 |
| 48. | Specific Fuel Consumption $M_o$ = 0.75 | 93 |
| 49. | Air Specific Impulse $M_o$ = 0.25 | 94 |
| 50. | Air Specific Impulse $M_o$ = 0.50 | 95 |
| 51. | Air Specific Impulse $M_o$ = 0.75 | 96 |
| 52. | Thrust Coefficient $M_o$ = 0.25 | 97 |
| 53. | Thrust Coefficient $M_o$ = 0.50 | 98 |
| 54. | Thrust Coefficient $M_o$ = 0.75 | 99 |
| 55. | Characteristic Mass Flow $M_o$ = 0.25 | 100 |
| 56. | Characteristic Mass Flow $M_o$ = 0.50 | 101 |
| 57. | Characteristic Mass Flow $M_o$ = 0.75 | 102 |
| 58. | Perspective Drawing of a 36" Multi-Jet | 105 |
| 59. | Sectional View of a 36" Multi-Jet | 106 |
| 60. | Wave Diagram for $M_o$ = 2.80 | 110 |
| 61. | Wave Diagram for Discharge Phase | 113 |
| 62. | Wave Configuration Produced when Inlet Valve Opens | 114 |
| 63. | Wave Diagram for $M_o$ = 2.00 | 116 |
| 64. | Wave Diagram for $M_o$ = 1.00 | 117 |
| 65. | Wave Diagram for $M_o$ = 0 | 118 |
| 66. | Valve Timing Diagram | 119 |
| 67. | Valve Diagram | 120 |
| 68. | Variation of K with $P_3/P_o$ | 121 |
| 69. | Thrust of 36" Multi-Jet | 124 |

| PREPARED BY | AEROPHYSICS DEVELOPMENT CORPORATION | REPORT NO 2000-1-R1 |
|---|---|---|
| CHECKED BY | PACIFIC PALISADES, CALIFORNIA | DATE Jan 24 1953 |

CONTENTS


| Figure | | Page |
|---|---|---|
| 70. | Specific Fuel Consumption | 125 |
| 71. | Air Specific Impulse | 126 |
| 72. | Thrust per Unit Frontal Area | 127 |
| 73. | Thrust Coefficient | 128 |
| 74. | Characteristic Mass Flow | 129 |
| 75. | Drag Coefficient of a Typical Missile | 130 |
| 76. | Drag and Thrust Coefficient at Sea Level | 132 |
| 77. | Drag and Thrust Coefficient at Altitude | 133 |
| 78. | Drag and Thrust at Sea Level | 134 |
| 79. | Perspective View of the 8" Multi-Jet | 140 |
| 80. | Ideal Thrust of 8" Multi-Jet | 141 |
| 81. | Ideal Specific Fuel Consumption | 142 |
| 82. | Ideal Air Specific Impulse | 143 |
| 83. | Ideal Thrust per Unit Frontal Area | 144 |
| 84. | Ideal Weight-Thrust Ratio | 145 |
| 85. | Ideal Thrust Coefficient | 146 |
| 86. | Ideal Characteristic Mass Flow | 147 |
| 87. | Burning Phase | 148 |
| 88. | Impulse for Various Flight Mach Numbers | 216 |
| 89. | Wave Diagram for $M_o = 0.75$ | 152 |
| 90. | Wave Diagram for $M_o = 0.$ | 153 |
| 91. | Valve Timing Diagrams | 154 |
| 92. | Actual Thrust of an 8" Multi-Jet | 155 |
| 93. | Actual Specific Fuel Consumption | 156 |

CONTENTS


| Figure | | Page |
|---|---|---|
| 94. | Actual Air Specific Impulse | 157 |
| 95. | Actual Thrust per Unit Frontal Area | 158 |
| 96. | Actual Weight-Thrust Ratio | 159 |
| 97. | Actual Thrust Coefficient | 160 |
| 98. | Actual Characteristic Mass Flow | 161 |
| 99. | Inlet Valve Configuration | 163 |
| 100. | Maximum Hovering Endurance | 169 |
| 101. | Comparison of Payloads | 170 |
| 102. | High Temperature Insulating Materials | 178 |
| 103. | Representative Temperature and Stress Profiles in the Tube Walls | 180 |
| 104. | Steady Flow Surface Combustion Flow Diagram | 184 |
| 105. | Rotary Valve Surface Combustion Flow Diagram | 186 |
| 106. | Experimental Test Layout - Rotary Valve Tests | 187 |
| 107. | Rotary Valve Construction | 187 |
| 108. | Rotary Valve with Thrust Plate | 189 |
| 109. | Installation of the Combustion Tube | 189 |
| 110. | Mounted Insulated Quartz Tube Ready for Testing | 190 |
| 111. | Alumina Tube Showing Thermal Shock | 190 |
| 112. | Quartz Tube with Expanded Section after Tested | 192 |
| 113. | Stupalith - A 2417 Melted Wall after Running | 192 |
| 114. | Graphite Tube after Five Minutes of Surface Combustion | 194 |
| 115. | Metamic Tube | 194 |
| 116. | Model of Intermittent and Steady State Surface Combustion | 196 |
| 117. | Rotary Valve Combustion Testing | 198 |

CONTENTS

| Figure | | Page |
|---|---|---|
| 118. | Colour Picture of Clear Quartz in Valve Mechanism - - - | 198 |
| 119. | Layout of Single Tube Rotary Valve - - - - - - - - - - | 200 |
| 120. | Fuel Valves and Preheater Assembly - - - - - - - - - - | 201 |
| 121. | Preheater Flame Holder and Needle Jet - - - - - - - - | 201 |
| 122. | Carbon Tubes - - - - - - - - - - - - - - - - - - - - - | 202 |
| 123. | Preheater Flame - - - - - - - - - - - - - - - - - - - | 202 |
| 124. | Surface Combustion Flame - - - - - - - - - - - - - - | 203 |
| 125. | Diagram of the Shock Tube - - - - - - - - - - - - - - | 205 |
| 126. | Photograph of the Shock Tube - - - - - - - - - - - - | 206 |
| 127. | Diaphragm Joint - - - - - - - - - - - - - - - - - - - | 206 |
| 128. | Temperature Rise due to Constant Volume Combustion - - | 219 |
| 129. | Temperature Rise due to Constant Pressure Combustion - | 220 |
| 130. | Helicopter Fuel System - - - - - - - - - - - - - - - | 225 |

| PREPARED BY | AEROPHYSICS DEVELOPMENT CORPORATION | REPORT NO 2000-1-R1 |
|---|---|---|
| CHECKED BY | PACIFIC PALISADES, CALIFORNIA | DATE Jan 24, 1953 |

## SECTION I

## BASIC CYCLE OF OPERATION

### 1.1 Description of the Cycle of Operation

In order to establish a nomenclature the operation of a basic cycle will be set forth. (See Figure 1)

(1) A vehicle assumed to be traveling at a Mach Number, $M_o$, takes in air and diffuses it to a Mach Number $M_1$, with a diffuser total pressure of $\eta = P_{t_1}/P_{t_o}$.

(2) The air passes through the intake valves, and it enters the duct at a Mach Number $M_1$.

(3) This air flows down the tube resulting in flow conditions at the tube exit of $M_1$, $P_{t_1}''$ and $P_1''$. The duration of scavenging = $\tau_s$.

(4) The exhaust valve is closed in a time $\tau_v$. This closing process is started just before the last bit of burned gases has been discharged and it is completed just as the last bit of scavenged air is discharged. This closing process sends forth a series of weak compression waves which combine, at a distance, into a normal shock wave.

(5) This normal shock wave travels up the tube raising the pressure and temperature to $P_2''$, $T_2''$ in the rear and $P_2$, $T_2$ in the front end.

(6) Just before the normal shock wave arrives at the front of the tube, the intake valve is closed in a time $\tau_v$, sending small expansion waves, which in the time $\tau_v$ travel a distance of $L_1$ feet.

(7) The time taken for the normal shock wave to travel up the tube = duration of pulse compression = $\tau_c$. The Mach Number of the wave $M_w$ will be a function of $M_1$.

(8) After the front and rear valves are closed the burning phase takes place. There are two methods used for ignition. In one case the normal shock wave is directed into a conical shaped dome at the front end of the tube where it is focused and strengthened to the point where detonation is initiated. The detonation wave then sweeps through the gases in a time $\tau_B$ raising the pressure and temperature to $P_3''$, $T_3''$ and $P_3$, $T_3$ in the back and front ends respectively. In the other case the ignition is obtained by means of surface combustion.

| PREPARED BY | AEROPHYSICS DEVELOPMENT CORPORATION | REPORT NO 2000-1-R1 |
|---|---|---|
| CHECKED BY | PACIFIC PALISADES, CALIFORNIA | DATE Jan 24,1953 |

FIGURE 1

## BASIC CYCLE

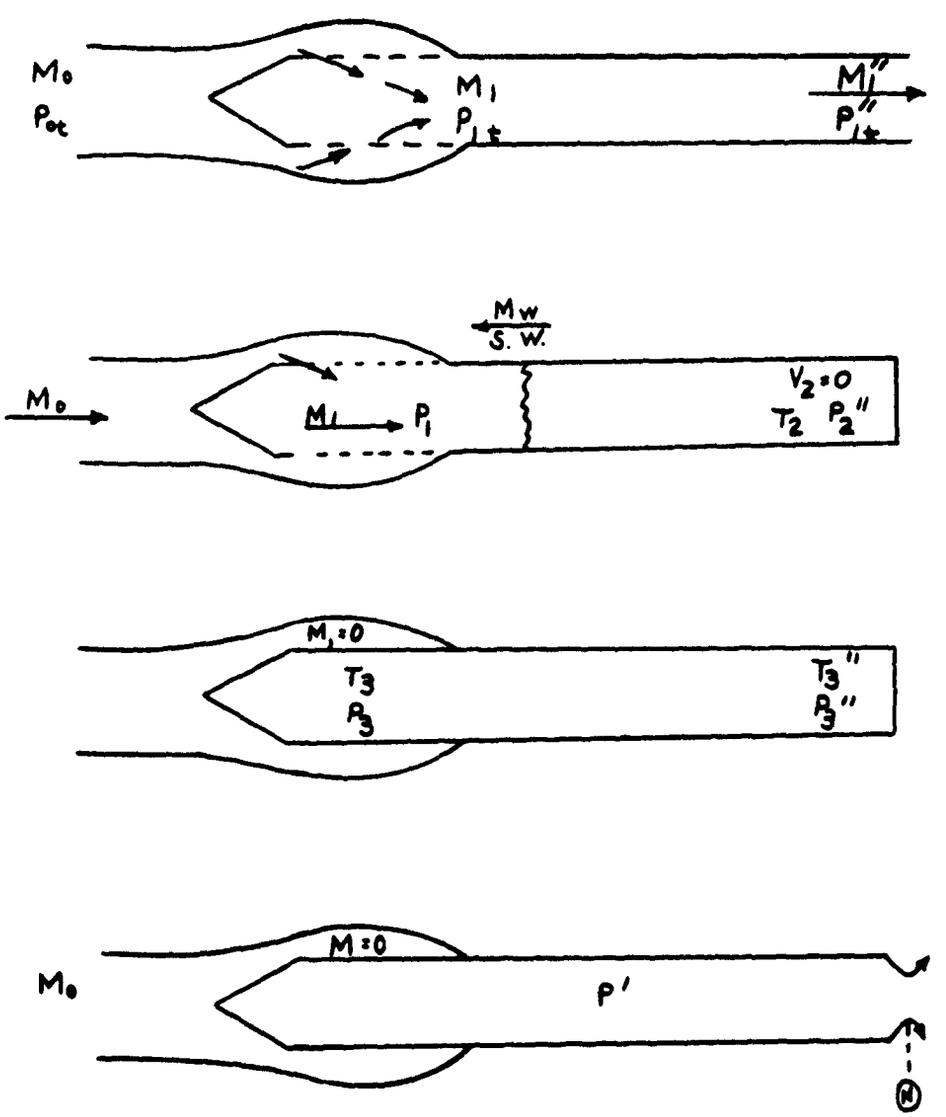

(9) The exhaust valve will open as soon as burning is completed. It can be designed to move at a predetermined variable rate so that a constant average thrust is obtained instead of a pulsating force during the exhaust part of the cycle or it can be made to open instantaneously. The time required for this process is $\tau_E$. The variable total pressure at the nozzle as the tube is exhausting will be denoted by $P'$. The condition at the nozzle will be denoted by a subscript N.

(10) When the pressure at the exhaust nozzle has dropped to atmospheric, the inlet valve is opened completely and scavenging is initiated. As shown by the experiments of Kadenacy (Reference 1) and others it is possible to permit the pressure in the duct to drop to sub-atmospheric values and to use this pressure difference to initiate the savenging part of the cycle. It is also hoped that the jet exhaust of each exhausting tube can be directed so that it will act as a jet pump and scavenge the other tubes.

(11) At the end of the exhaust phase the inlet valves open and scavenging is begun.

## SECTION II

## DERIVATION OF THE BASIC EQUATIONS

### 2.1 Equations Describing Pulse Compression

The velocity of the shock wave with respect to the fluid particles in front of the shock wave = $\dot{\xi}$. The velocity of the fluid particles in front of the shock wave = $u_1$. The absolute velocity of the shock wave = $\dot{\xi} - u_1$. From the tables of normal shock wave characteristics (References 2 and 3) the following relation can be found

$$\frac{\dot{\xi}}{a_1} = \sqrt{\frac{(\gamma-1) + (\gamma+1) P_2/P_1}{2\gamma}} \qquad \ldots(1)$$

We can write

$$\frac{\dot{\xi}}{a_1} - \frac{u_1}{a_1} = \sqrt{\frac{(\gamma-1) + (\gamma+1) P_2/P_1}{2\gamma}} - M_1$$

and therefore

$$M_w = \frac{\dot{\xi} - u_1}{a_1} = \sqrt{\frac{(\gamma-1) + (\gamma+1) P_2/P_1}{2\gamma}} - M_1 \qquad \ldots(2)$$

The above equation is plotted on Figure 2.

The relation between particle velocities and pressures before and after a normal shock wave is given by Courant and Friedrichs in Reference 4. In our notation, we have

$$u_2 = u_1 - (P_2 - P_1)\sqrt{\frac{2 a_1^2}{\gamma[(\gamma+1) P_2 + (\gamma-1) P_1] P_2}} \qquad \ldots(3)$$

Our boundary conditions give $u_2 = 0$. Remembering that $\frac{u_1}{a_1} = M_1$ and $P_1 = P_0$, (3) becomes

$$M_1 = \left(\frac{P_2}{P_1} - 1\right)\frac{1}{\gamma}\sqrt{\frac{2\gamma}{(\gamma+1) P_2/P_1 + (\gamma-1)}} \qquad \ldots(4)$$

This relation is plotted on Figure 3. The temperature ratio

$$\frac{T_2}{T_1} = \frac{P_2}{P_1}\left[\frac{(\gamma-1)(M_w + M_1)^2 + 2}{(\gamma+1)(M_w + M_1)^2}\right] \qquad \ldots(5)$$

| PREPARED BY | AEROPHYSICS DEVELOPMENT CORPORATION | REPORT NO. 2000-1-R1 |
|---|---|---|
| CHECKED BY | PACIFIC PALISADES, CALIFORNIA | DATE Jan 24, 1953 |

FIGURE 2

# MACH NUMBER OF SHOCK WAVE

$$M_w = \frac{\text{ABSOLUTE VELOCITY OF THE SHOCK WAVE}}{a_1}$$

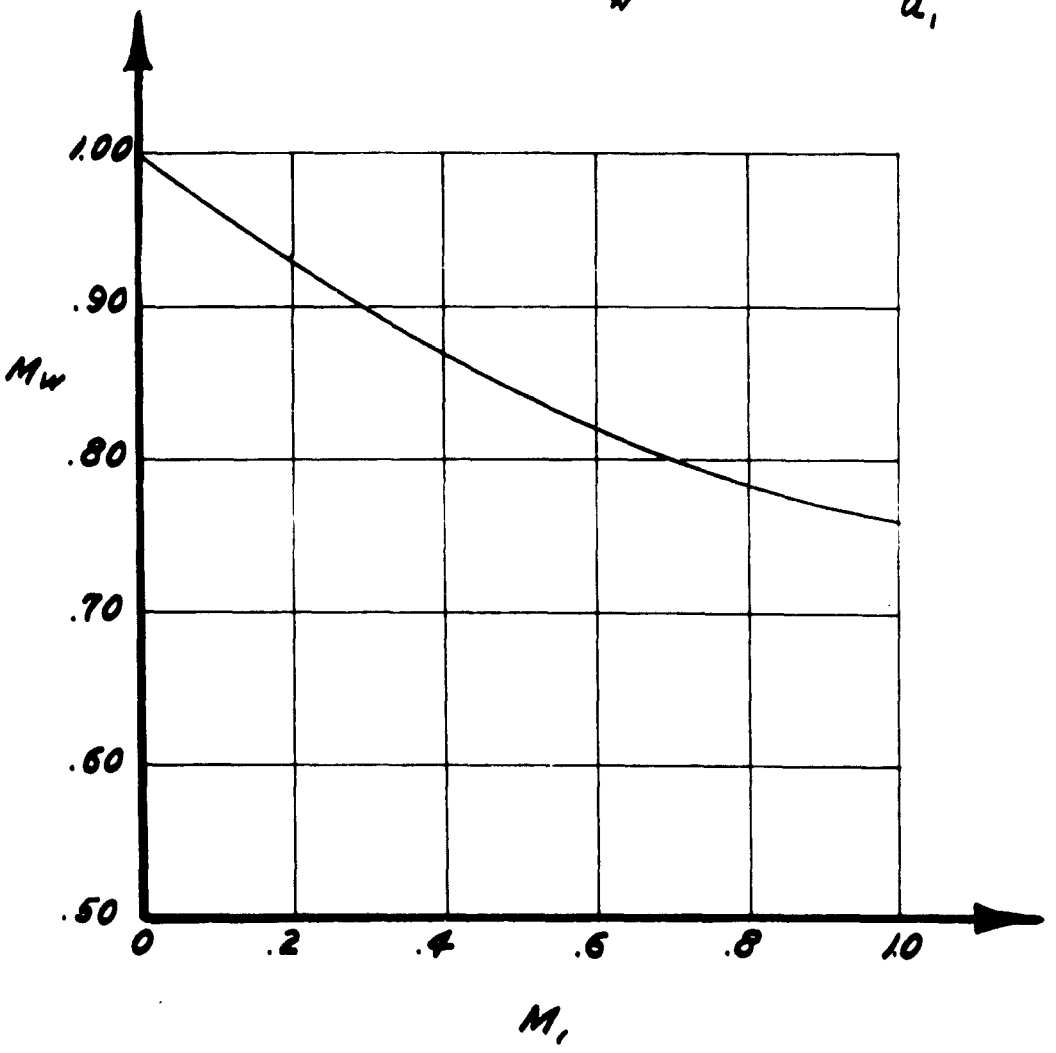

| PREPARED BY | AEROPHYSICS DEVELOPMENT CORPORATION | REPORT NO. 2000-1-R1 |
|---|---|---|
| CHECKED BY | PACIFIC PALISADES, CALIFORNIA | DATE Jan 24, 1953 |

FIGURE 3

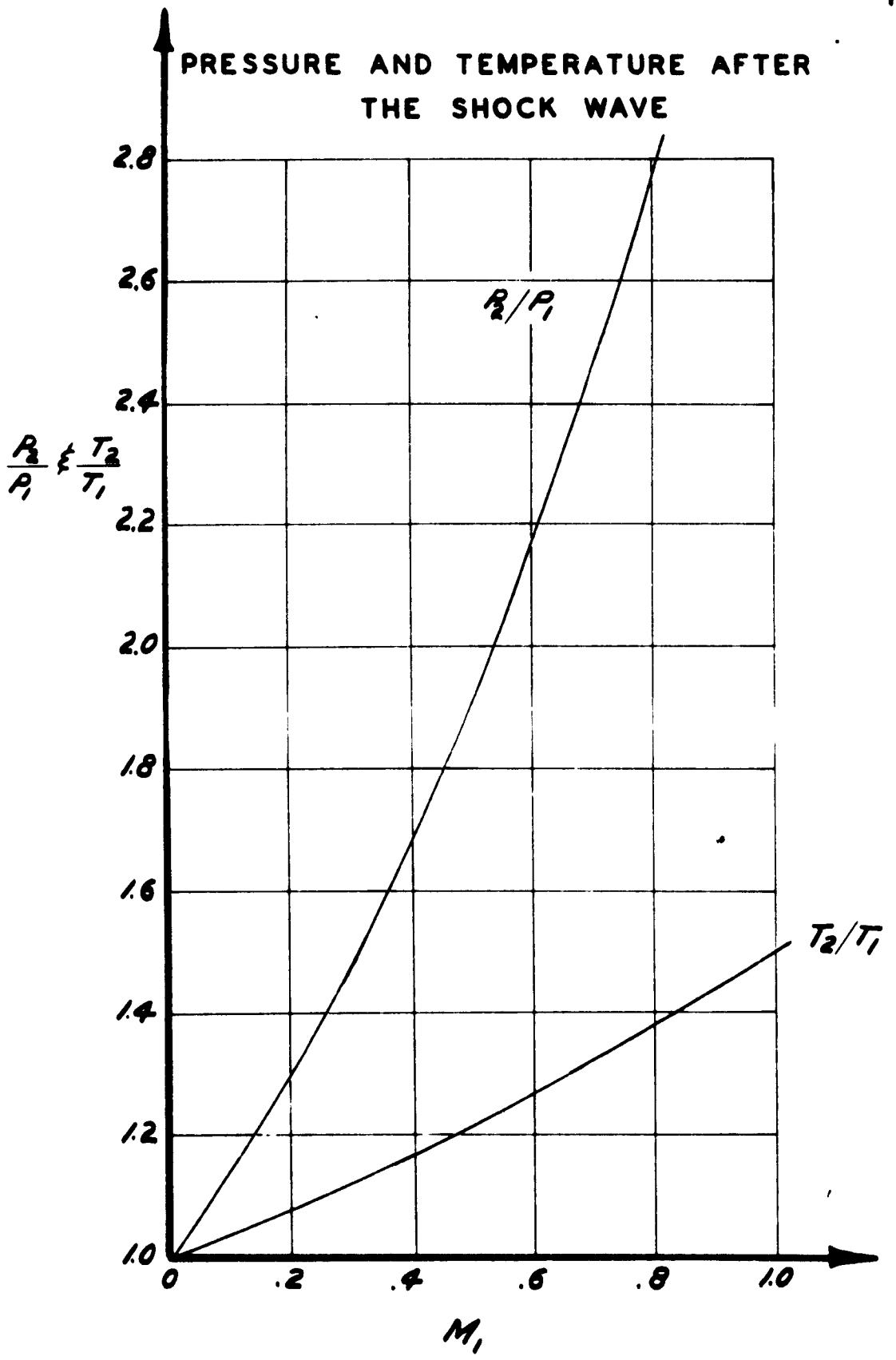

and is also plotted on Figure 3.

The density ratio $\frac{\rho_2}{\rho_1} = \frac{P_2}{P_1} \cdot \frac{T_1}{T_2}$ .

2.2 Equations for Exhaust Flow

The time, $\tau_E$, required for the gases to expand from the high pressure $P_3$ (Figure 1) to ambient pressure $P_0$, will be made of two parts:

1. The first part $\tau_{E_1}$, is the time taken for sonic flow at the exit nozzle.
2. The second part $\tau_{E_2}$, is the time taken for subsonic flow at the exit nozzle.

Weight Flow

$$w = \frac{dW'}{d\tau} \qquad \ldots(6)$$

W' is the instantaneous weight of gas in the chamber. Primed symbols denote the instantaneous values while the chamber is exhausting.

$$W = g \rho_3 A_N L \qquad \ldots(7)$$

$$w = g \frac{P_N A_N}{\rho' a'} \cdot \frac{\rho' a'}{\rho_3 a_3} \rho_3 a_3 A_N \qquad \ldots(8)$$

Where $A_N$ is the cross-sectional area in square feet of the combustion tubes and L is their length in feet. (i.e. $A_N = A_D$)

2.2.1 Choked Nozzle. Since the gas in the chamber is expanding isentropically

$$\frac{\rho'}{\rho_3} = \left(\frac{P'}{P_3}\right)^{\frac{1}{\gamma}} \quad \text{and} \quad \frac{a'}{a_3} = \left(\frac{P'}{P_3}\right)^{\frac{\gamma-1}{2\gamma}} \qquad \ldots(9)$$

Using (9) and substituting (7), equation (8) becomes

$$w = \varphi \left(\frac{\rho'}{\rho_3}\right)^{\frac{\gamma+1}{2}} W a_3 \frac{A_N}{A_D L} \qquad \ldots(10)$$

where

$$\varphi = \frac{\rho_N V_N}{\rho' a'}$$

Take (6) and substitute

$$W' = W \frac{\rho'}{\rho_3} \qquad \ldots(11)$$

(10) becomes $$w = -W \frac{d\, P'/P_3}{d\tau} \qquad \ldots(12)$$

Indicate $P'/P_3 = \sigma$ . Then equating (12) to (10) we get

$$\varphi \frac{A_N a_3}{A_0 \cdot L} d\tau = \frac{d\sigma'}{\sigma'^{\frac{\gamma+1}{2}}} \qquad \ldots(13)$$

For sonic nozzle flow

$$1 \geq \sigma \geq \frac{P_0}{P_3} \left(\frac{\gamma+1}{2}\right)^{\frac{1}{\gamma-1}}$$

Integrating and using the pressure ratio

$$\frac{\tau_{E_1}}{\frac{V}{A_N a_3}} = \frac{2}{\varphi(\gamma+1)} \left\{ \left[ \left(\frac{\gamma+1}{2}\right)^{\frac{\gamma}{\gamma-1}} \frac{P_0}{P_3} \right]^{\frac{1-\gamma}{2\gamma}} - 1 \right\} \qquad \ldots(14)$$

2.2.2 Subsonic Nozzle. Take equation (13)

$$\frac{\Delta\sigma}{\varphi \sigma^{\frac{\gamma+1}{2}}} = \frac{\Delta \tau_{E_2}}{\frac{V}{A_N a_3}} \qquad \ldots(15)$$

then $$\tau_E = \tau_{E_1} + \tau_{E_2}$$

A plot of these relations is given in Figure 4. Equations (13) and (15) can be used to give the variation of $P'/P_0$ with time. See Figure 5.

2.2.3 Weight Flow. Take equation (8)

$$w = \varphi \left(\frac{P'}{P_3}\right)^{\frac{\gamma+1}{2\gamma}} g \rho_3 a_3 A_N \qquad \ldots(16)$$

$$\frac{w}{g \rho_3 a_3 A_N} = \varphi \left(\frac{P'}{P_3}\right)^{\frac{\gamma+1}{2\gamma}} \qquad \ldots(17)$$

Using the relation between $P'/P_3$ and $\tau_E$ , the weight flow can be plotted against time. See Figure 6.

2.2.4 Discharge Velocity.

$$\frac{V_N}{a_3} = \sqrt{\frac{2}{\gamma-1} \left(\frac{P'}{P_3}\right)^{\frac{\gamma-1}{\gamma}} \left[1 - \left(\frac{P_N}{P'}\right)^{\frac{\gamma-1}{\gamma}}\right]} \qquad \ldots(18)$$

This relation is plotted on Figure 7.

AEROPHYSICS DEVELOPMENT CORPORATION

PACIFIC PALISADES, CALIFORNIA

FIGURE 4

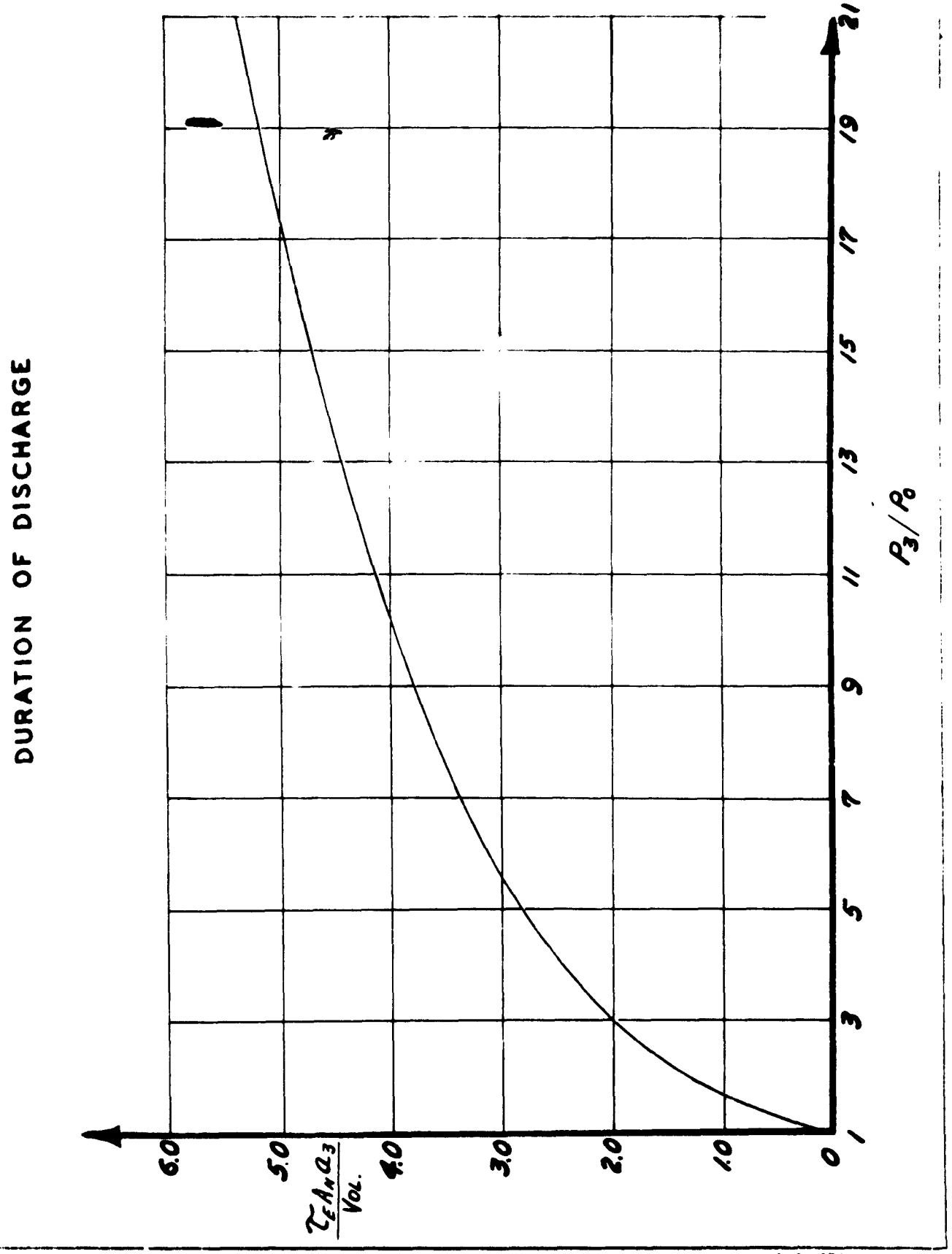

| PREPARED BY | AEROPHYSICS DEVELOPMENT CORPORATION | REPORT NO 2000-1-R1 |
|---|---|---|
| CHECKED BY | PACIFIC PALISADES, CALIFORNIA | DATE Jan 24, 1953 |

VARIATION OF CHAMBER PRESSURE WITH TIME — FIGURE 5

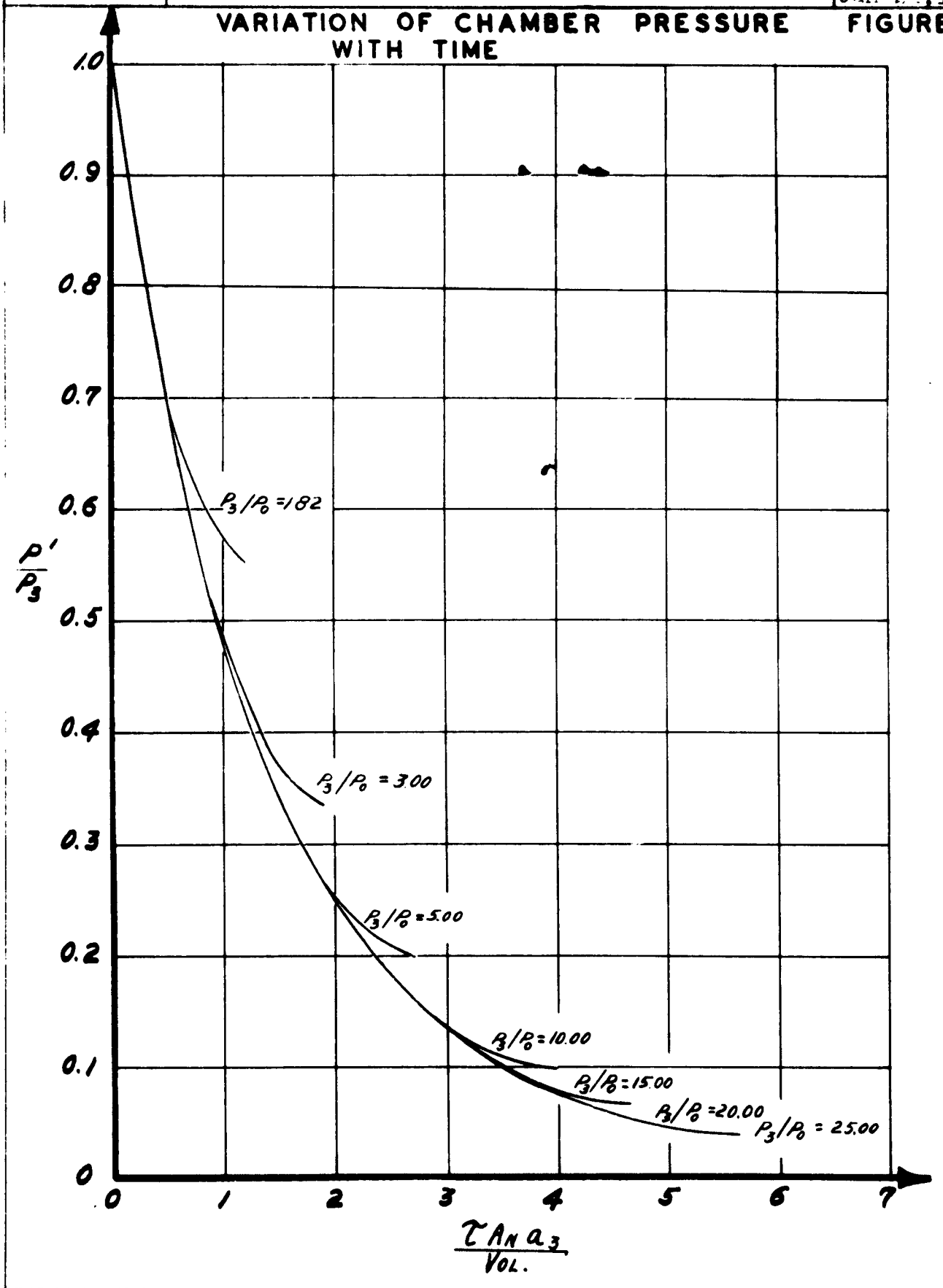

| PREPARED BY | AEROPHYSICS DEVELOPMENT CORPORATION | REPORT NO. 2000-1-R1 |
|---|---|---|
| CHECKED BY | PACIFIC PALISADES, CALIFORNIA | DATE Jan 4, 1953 |

FIGURE 6

## VARIATION OF WEIGHT FLOW WITH TIME

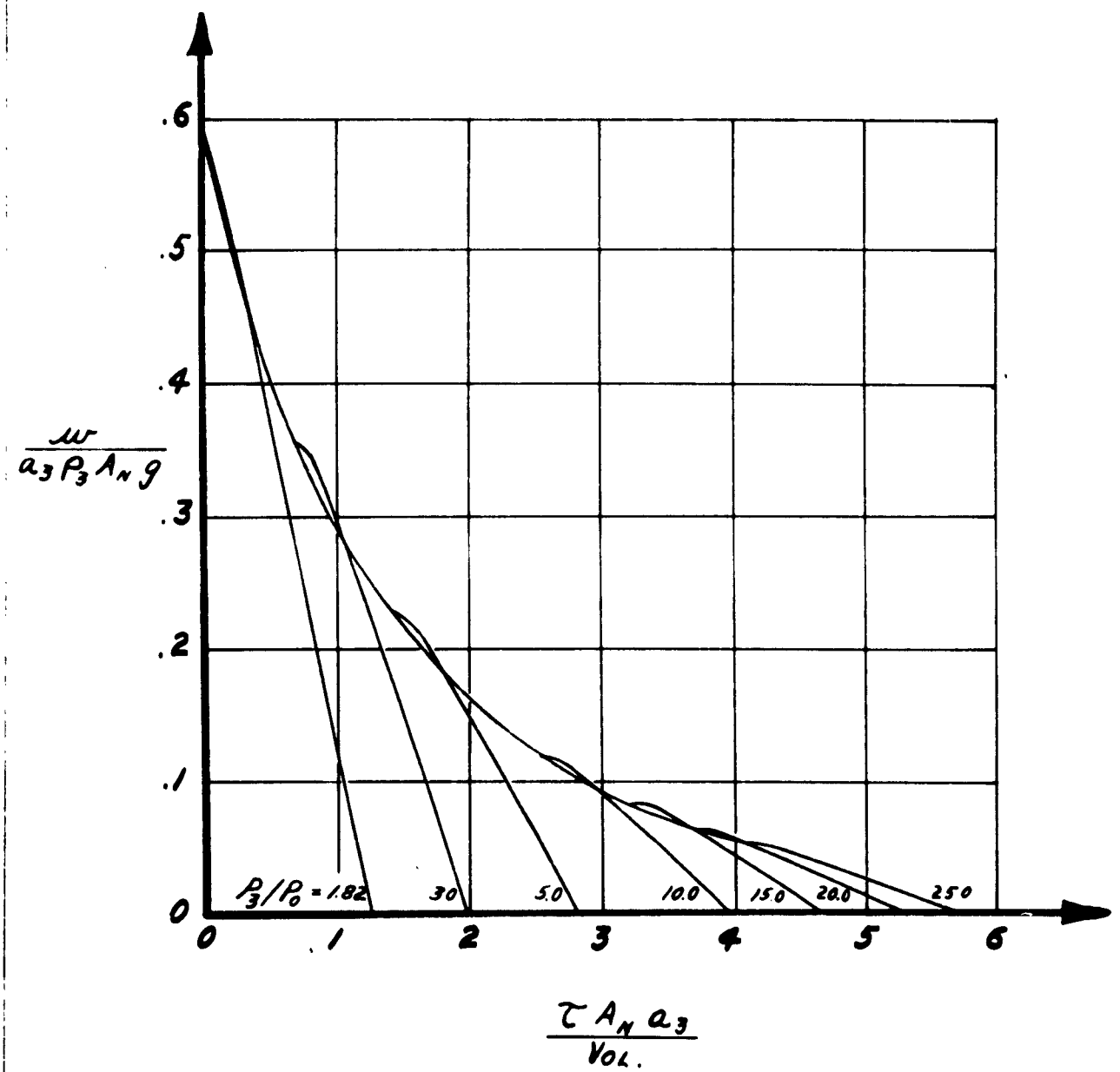

| PREPARED BY | AEROPHYSICS DEVELOPMENT CORPORATION | REPORT NO 2000-1-R1 |
|---|---|---|
| CHECKED BY | PACIFIC PALISADES, CALIFORNIA | DATE Jan 24, 1953 |

FIGURE 7

## VARIATION OF EXIT VELOCITY WITH TIME

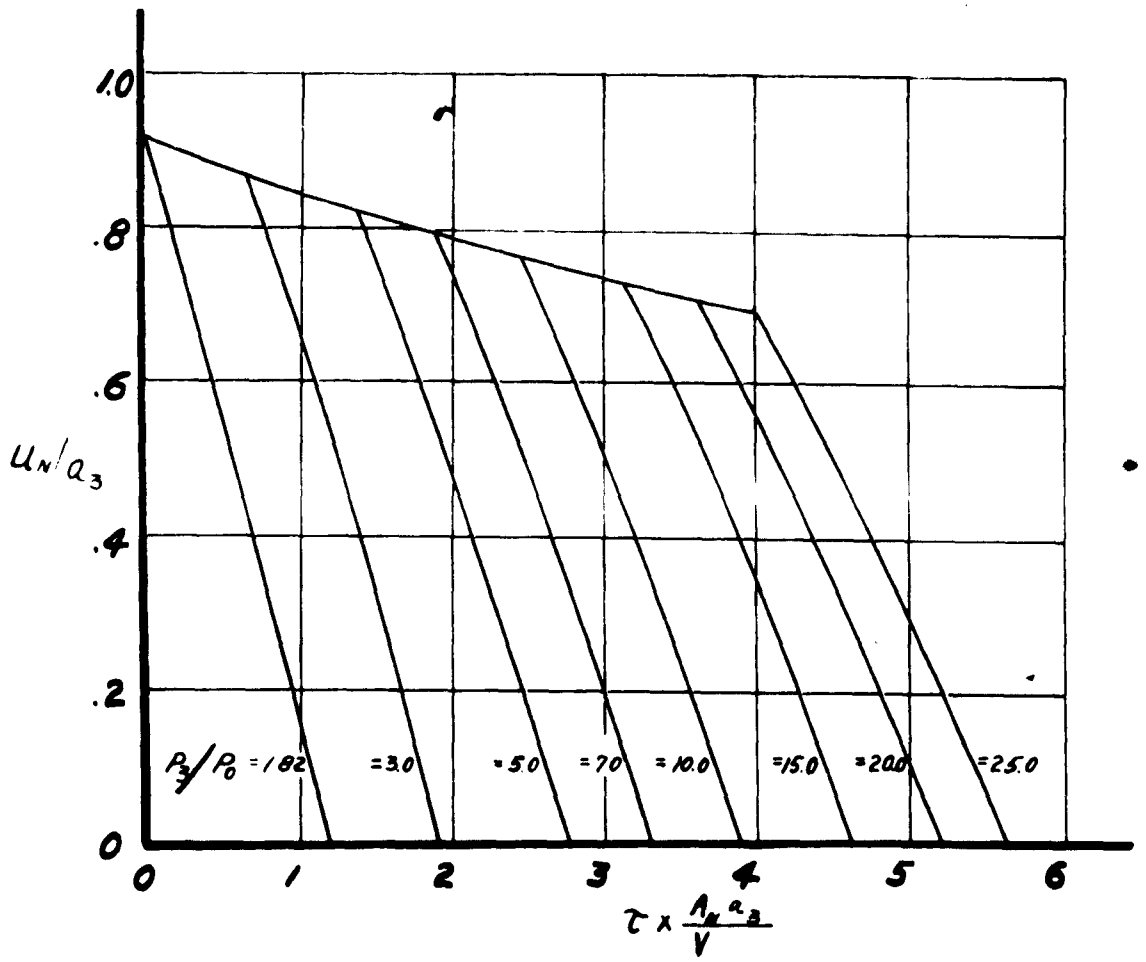

2.2.5 Thrust

$$F = \dot{m} V_N + A_N (P_N - P_o) \qquad \ldots(19)$$

For sonic throat

$$P_N = \left(\frac{2}{\gamma+1}\right)^{\frac{\gamma}{\gamma-1}} P'$$

For subsonic throat

$$P_N = P_o$$

Dimensionless Thrust:

$$\frac{F}{g \rho_3 a_3^2 A_N} = \frac{V_N}{a_3} \cdot \frac{w/g}{g \rho_3 a_3 A_N} + \frac{P_3 A_N}{a_3^2 g \rho_3 A_N} \left(\frac{P_N}{P_3} - \frac{P_o}{P_3}\right) \qquad \ldots(20)$$

The variation of thrust with time can be found by using equations (13), (17), (15), and (13) with (20) and are plotted on Figure 8.

2.2.6 Impulse

$$I = F \cdot \tau_E$$

In calculating the area under the thrust versus time curves, the assumption was made that the chamber pressure $P'$, would fall only to where $P' = P_{ot}$ or the total pressure of the ambient flow.

$$\frac{I_V}{a_3 g \rho_3 V} = \frac{F}{a_3^2 g \rho_3 A_N} \cdot \frac{\tau_E}{V/A_N a_3} \qquad \ldots(21)$$

The impulse is plotted on Figure 9 against the pressure ratio $P_3/P_o$. We can write

$$\frac{I_G}{a_o \rho_o g V} = \frac{I_G}{a_3 \rho_3 g V} \cdot \frac{\rho_3}{\rho_o} \cdot \frac{a_3}{a_o} \qquad \ldots(22)$$

Where $\rho_3/\rho_o$ and $a_3/a_o$ are functions of $M_o$ and $P_3/P_o$. Remember that in this ideal case $M_1 = M_o$.

The impulse due to air intake drag, $I_D$ = total mass flow X inlet velocity.

$$\frac{I_D}{a_o \rho_o g V} = \frac{V \rho_3}{V \rho_o} \cdot \frac{M_o a_o}{g a_o} = \frac{M_o}{g} \cdot \frac{\rho_3}{\rho_o} \qquad \ldots(23)$$

$I_{(net)} = I_G - I_D$

AEROPHYSICS DEVELOPMENT CORPORATION
PACIFIC PALISADES, CALIFORNIA

REPORT NO 2000-1-R1
DATE Jan 24 1953

FIGURE 8

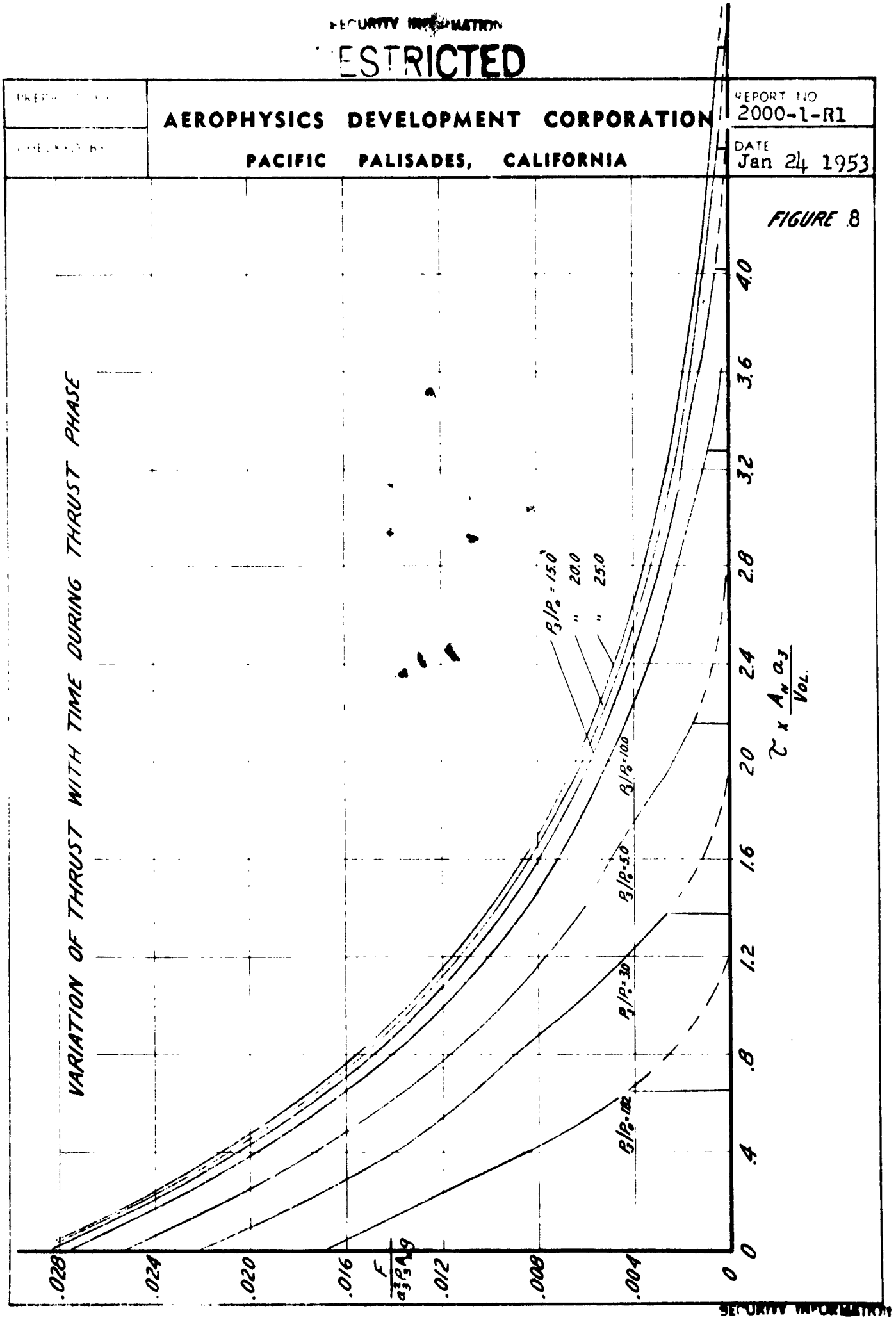

| PREPARED BY | AEROPHYSICS DEVELOPMENT CORPORATION | REPORT NO. 2000-1-R1 |
|---|---|---|
| CHECKED BY | PACIFIC PALISADES, CALIFORNIA | DATE Jan 24, 1953 |

FIGURE 9

## IMPULSE OF THE DISCHARGING GASES

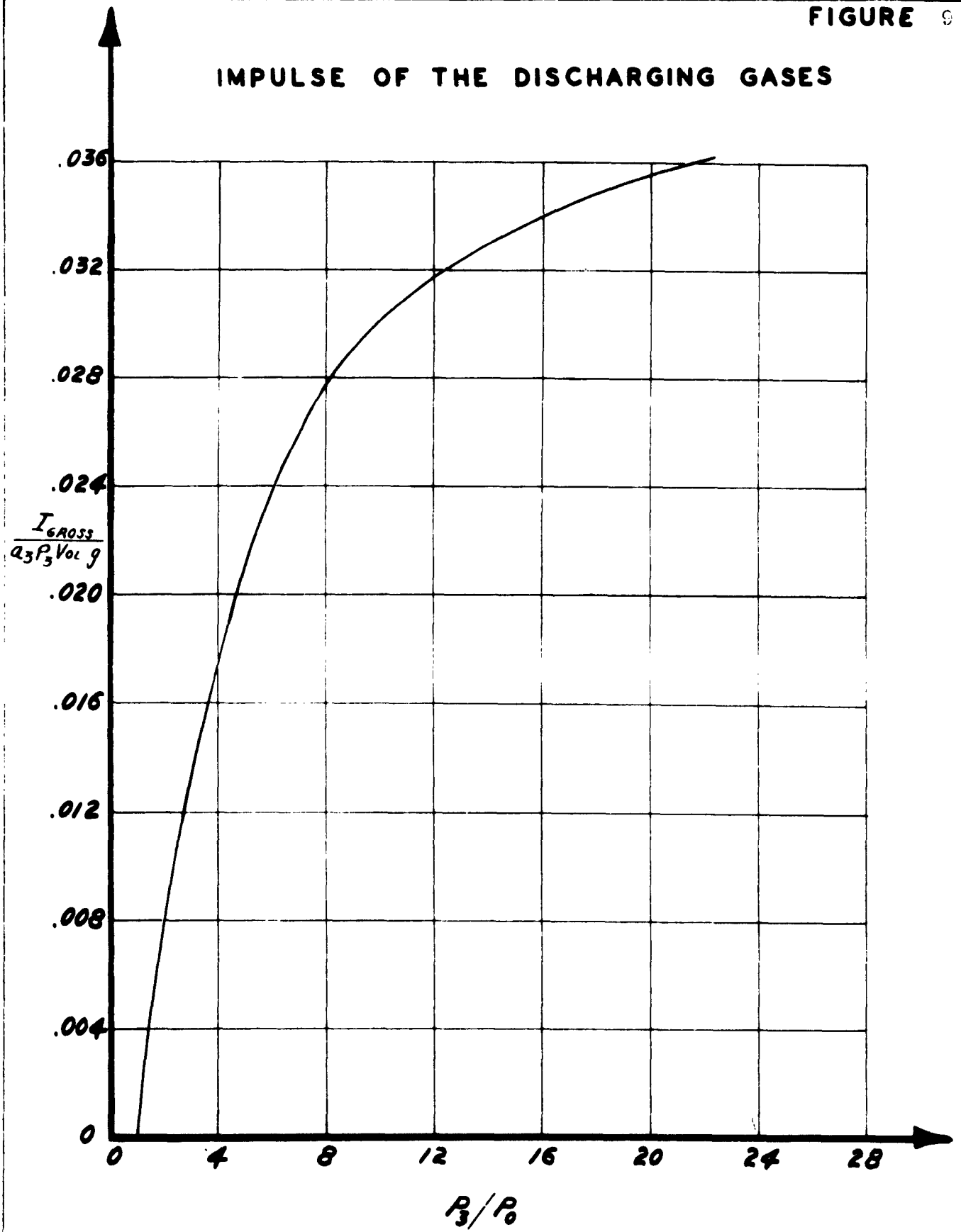

This function is plotted on Figure 10. The above non-dimensional functions are also tabulated in Table I. These non-dimensional functions are used as the basis for the analysis of the Multi-Jet.

2.3 Equations for the Fuel-air Ratio

The fuel-air ratio was computed from the increase in internal energy of the mixture after burning. The tables in Keenan and Kay, Reference 5, and charts by Satterfield, Williams and Hottel, Reference 6, give the value of the internal energy before and after burning for various fuel-air mixtures. For these first calculations the values from the table for 200% theoretical air in Reference 5 were used and if $T_3$ went above 3900°R then the chart for 0.8F in Reference 6 was used. Actually, the internal energy at $T_3$ would be a function of the fuel-air ratio and in order to compute the F/A ratio the method of successive approximations must be used. On the other hand since the variation of the internal energy at $T_3$ varies so little with fuel-air ratio this method was discarded for these first calculations. The fuel-air ratios are plotted on Figure 11.

| PREPARED BY | AEROPHYSICS DEVELOPMENT CORPORATION | REPORT NO 2000-1-R1 |
|---|---|---|
| APPROVED BY | PACIFIC PALISADES, CALIFORNIA | DATE Jan 24, 1958 |

FIGURE 10

## IMPULSE FUNCTION

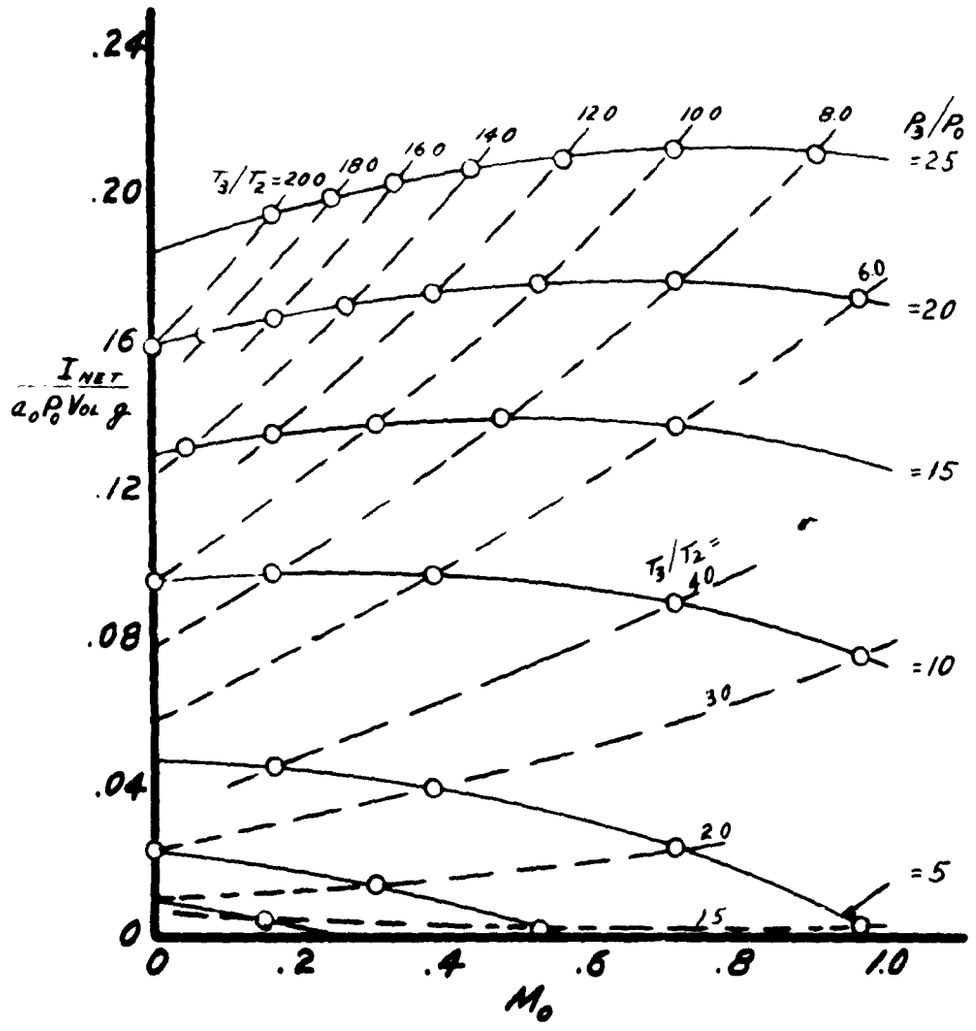

| PREPARED BY | AEROPHYSICS DEVELOPMENT CORPORATION | REPORT NO. 2000-1-R1 |
|---|---|---|
| CHECKED BY | PACIFIC PALISADES, CALIFORNIA | DATE Jan 14, 1953 |

FIGURE 11

## FUEL - AIR RATIOS

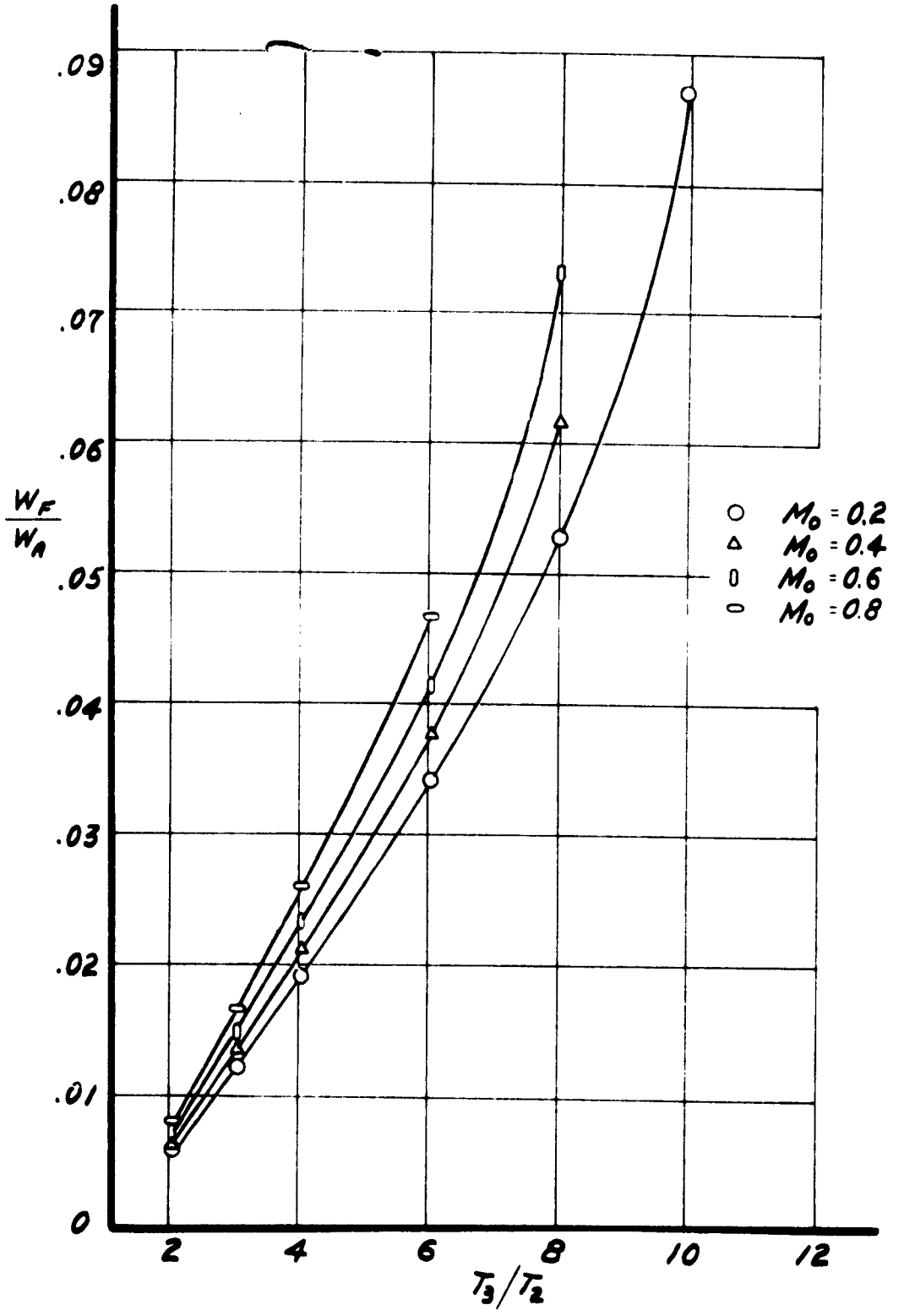

SECTION III

IDEAL CYCLE PERFORMANCE OF A SINGLE TUBE

## 3.1 Assumptions

The first computations were carried out for a simplified ideal cycle. The assumptions made for this first part of the investigation are:

(1) The flow Mach Number during scavenging, $M_1$, is equal to the flight Mach Number $M_o$.

(2) Frictional flow losses are neglected. ($P_1 = P_1' = P_o$ ; $P_{t_o} = P_{t_1}$)

(3) The duct consists of a straight through flow system.

(4) Inlet and exhaust valves open and close in zero time.

(5) There will be no contraction or expansion of the jet exhaust at the exit.

(6) Combustion efficiency will be 100 ; the heating value of the fuel will be taken at 18,500 BTU/lb of fuel, with no dissociation of products of combustion and; the final conditions are given by constant volume burning.

(7) The time required for combustion will be calculated under the assumption that burning took place through a detonation wave and was assumed to be $\tau_B$ = 0.010 secs.

## 3.2 Description of the Ideal Cycle

The principle of operation of the Multi Jet engine can be understood most simply by first considering the limiting case of an ideal cycle. Consider a simple tube of constant cross-section through which air is flowing at a Mach Number = $M_1$. This tube is mounted on a vehicle (airplane or helicopter) moving at a Mach Number $M_o$. This is shown in Figure 13 (a). The air flow is suddenly stopped by the closure of valve A as shown in Figure 13 (b). As a result, the air at the end, near A, is suddenly brought to rest and a compression shock S travels upstream at a velocity somewhat greater than the velocity of sound $a_1$, (measured with respect to the moving air particles). When this compression shock S reaches the upstream end, a valve B is suddenly closed. This is shown in Figure 13 (c). The air compressed by the shock S has a pressure

This function is plotted on Figure 10. The above non-dimensional functions are also tabulated in Table I. These non-dimensional functions are used as the basis for the analysis of the Multi-Jet.

2.3 Equations for the Fuel-air Ratio

The fuel-air ratio was computed from the increase in internal energy of the mixture after burning. The tables in Keenan and Kay, Reference 5, and charts by Satterfield, Williams and Hottel, Reference 6, give the value of the internal energy before and after burning for various fuel-air mixtures. For these first calculations the values from the table for 200% theoretical air in Reference 5 were used and if $T_3$ went above 3900°R then the chart for 0.8F in Reference 6 was used. Actually, the internal energy at $T_3$ would be a function of the fuel-air ratio and in order to compute the F/A ratio the method of successive approximations must be used. On the other hand since the variation of the internal energy at $T_3$ varies so little with fuel-air ratio this method was discarded for these first calculations. The fuel-air ratios are plotted on Figure 11.

| PREPARED BY | AEROPHYSICS DEVELOPMENT CORPORATION | REPORT NO 2000-1-R1 |
|---|---|---|
| CHECKED BY | PACIFIC PALISADES, CALIFORNIA | DATE Jan 24, 1953 |

FIGURE 10

# IMPULSE FUNCTION

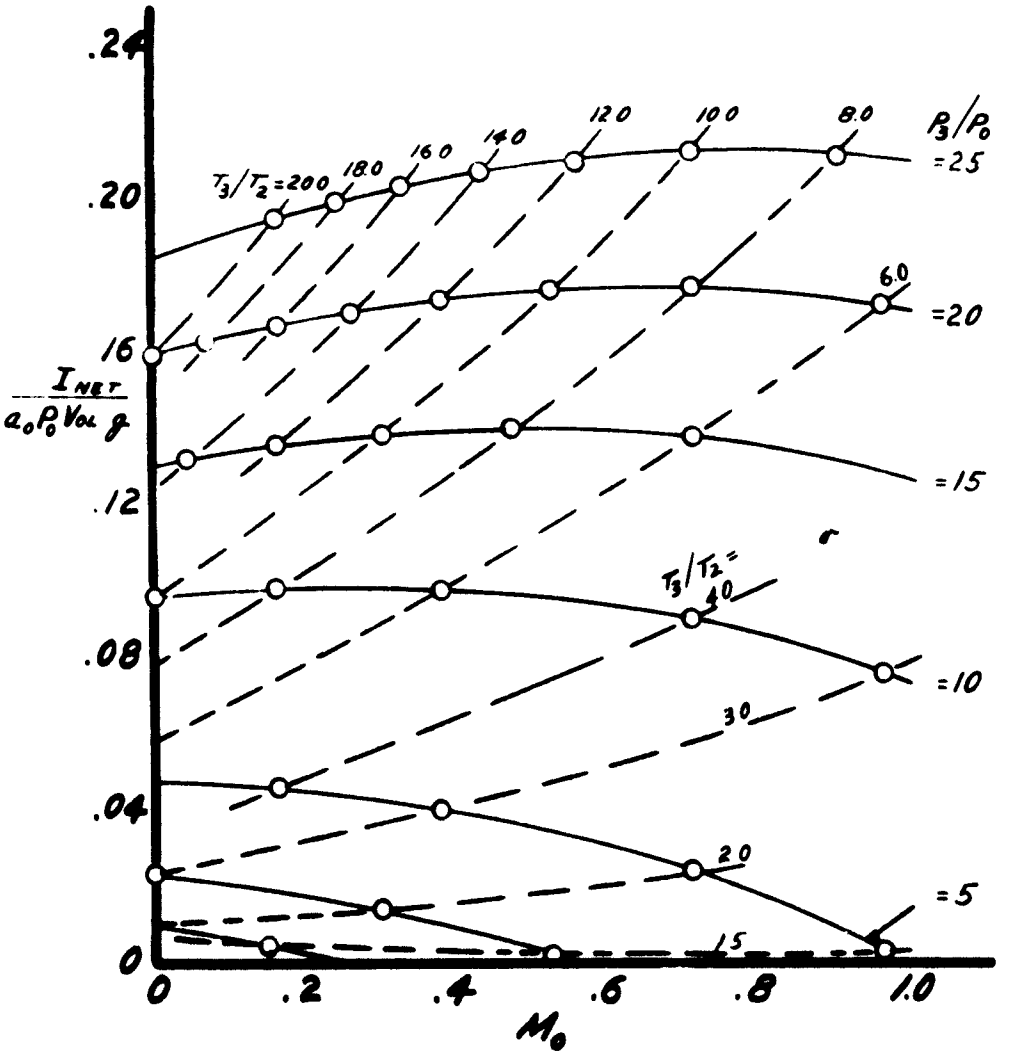

| PREPARED BY | AEROPHYSICS DEVELOPMENT CORPORATION | REPORT NO 2000-1-R1 |
|---|---|---|
| CHECKED BY | PACIFIC PALISADES, CALIFORNIA | DATE Jan 24, 1953 |

FIGURE 11

## FUEL - AIR RATIOS

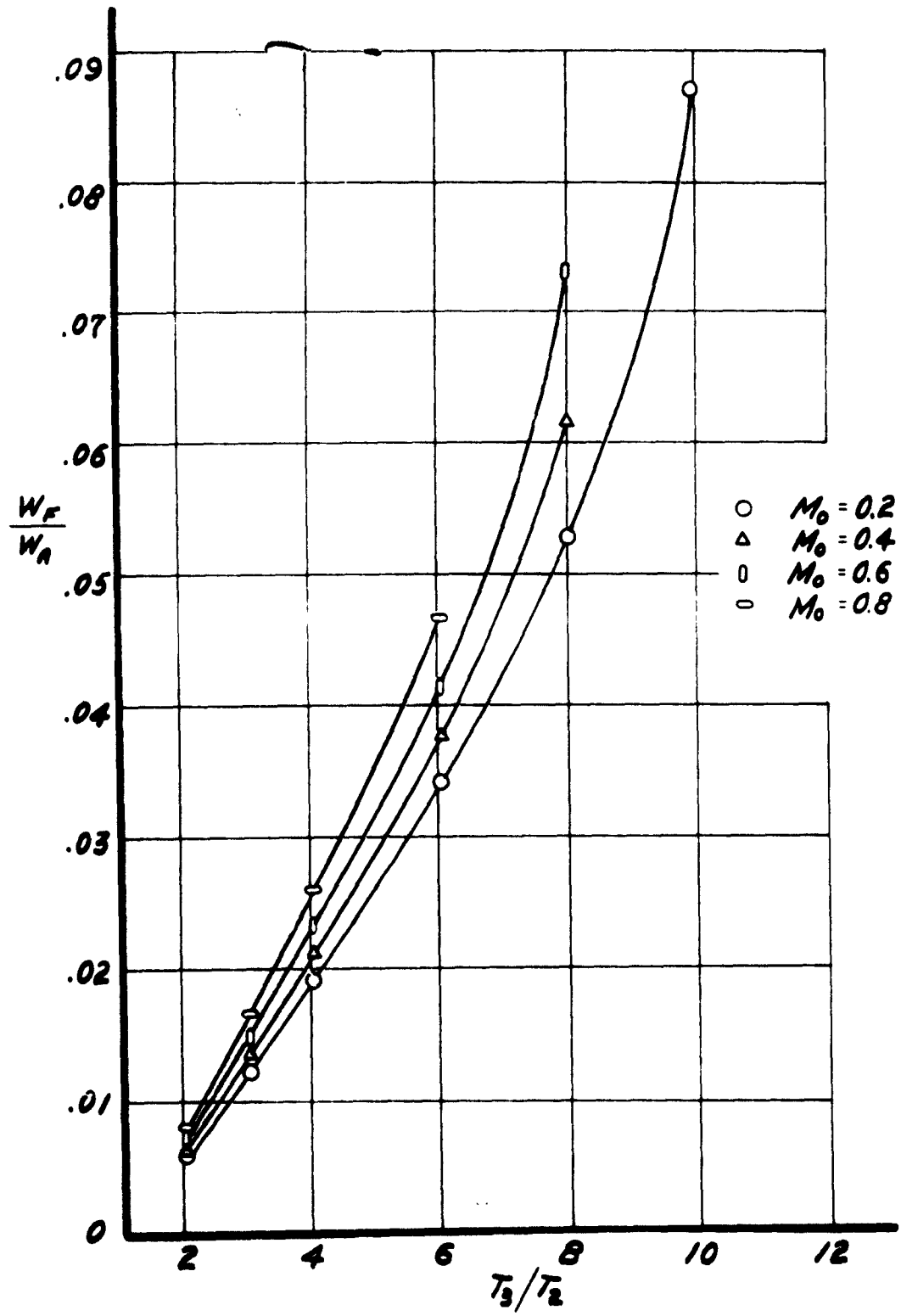

SECTION III

IDEAL CYCLE PERFORMANCE OF A SIMPLE TUBE

## 3.1 Assumptions

The first computations were carried out for a simplified ideal cycle. The assumptions made for this first part of the investigation are:

(1) The flow Mach Number during scavenging, $M_1$, is equal to the flight Mach Number $M_0$.

(2) Frictional flow losses are neglected. ($P_1 = P_1'' = P_0$ ; $P_{t_0} = P_{t_1}$)

(3) The duct consists of a straight through flow system.

(4) Inlet and exhaust valves open and close in zero time.

(5) There will be no contraction or expansion of the jet exhaust at the exit.

(6) Combustion efficiency will be 100%; the heating value of the fuel was taken as 18,700 BTU/lb of fuel, with no dissociation of products of combustion and; the final conditions are given by constant volume burning.

(7) The time required for combustion will be calculated under the assumption that burning took place through a detonation wave and was assumed to be $\tau_B$ = 0.010 secs.

## 3.2 Description of the Ideal Cycle

The principle of operation of the Multi Jet engine can be understood most simply by first considering the limiting case of an ideal cycle. Consider a simple tube of constant cross-section through which air is flowing at a Mach Number = $M_1$. This tube is mounted on a vehicle (airplane or helicopter) moving at a Mach Number $M_0$. This is shown in Figure 13 (a). The air flow is suddenly stopped by the closure of valve A as shown in Figure 13 (b). As a result, the air at the end, near A, is suddenly brought to rest and a compression shock S travels upstream at a velocity somewhat greater than the velocity of sound $a_1$, (measured with respect to the moving air particles). When this compression shock S reaches the upstream end, a valve B is suddenly closed. This is shown in Figure 13 (c). The air compressed by the shock S has a pressure

| PREPARED BY | AEROPHYSICS DEVELOPMENT CORPORATION | REPORT NO 2000-1-R1 |
|---|---|---|
| CHECKED BY | PACIFIC PALISADES, CALIFORNIA | DATE Jan 24 1953 |

FIGURE 12

## COMPARISON OF STEADY AND NON-STEADY COMPRESSION

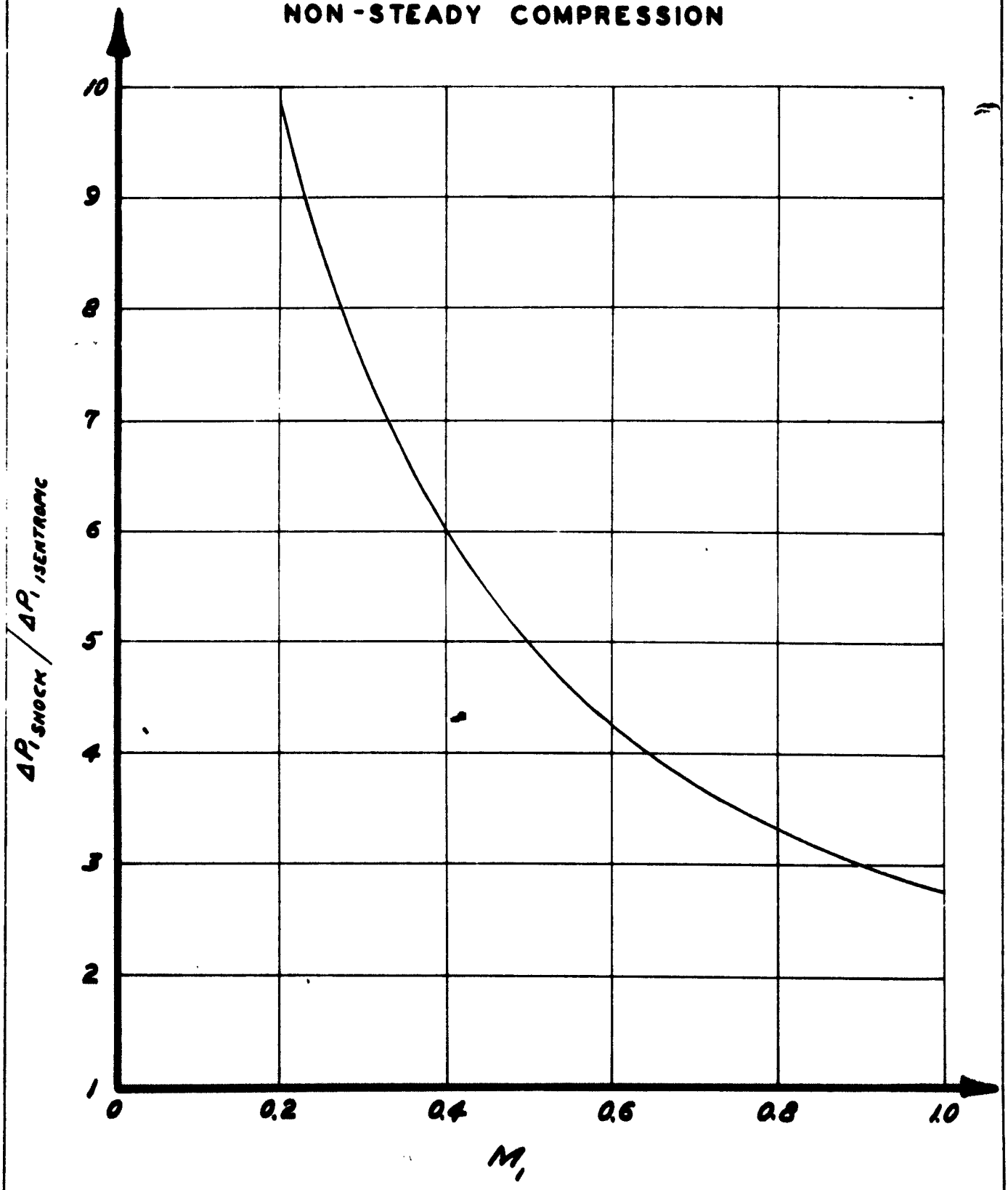

| PREPARED BY | AEROPHYSICS DEVELOPMENT CORPORATION | REPORT NO 2000-1-R1 |
|---|---|---|
| CHECKED BY | PACIFIC PALISADES, CALIFORNIA | DATE Jan 24 1953 |

FIGURE 13

# IDEAL CYCLE

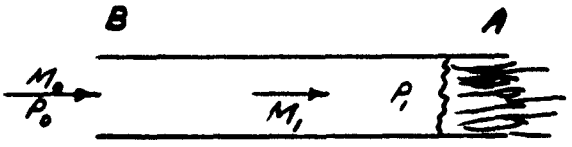


(a) SCAVENGING

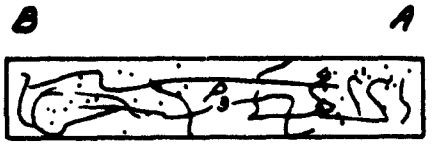


(d) BURNING

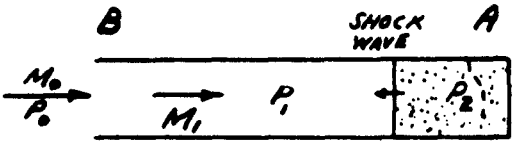


(b) SHOCK COMPRESSION


(e) DISCHARGE

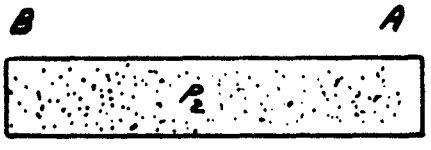


(c) SHOCK COMPRESSION

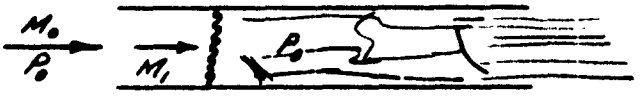


(f) SCAVENGING

ratio $P_2/P_1$, and a temperature ratio $T_2/T_1$. It will be noted that if, for example, $M_1 = 0.8$ then $P_2/P_1 = 0.8$ then $P_2/P_1 = 2.17$ and $T_2/T_1 = 1.27$. If this air has been compressed by steady, isentropic compression, then it would have reached a pressure rise.

$$\frac{\Delta P_{ISENT}}{P_0} = \frac{P_{0_2} - P_0}{P_0}$$

As a result of the non-steady compression, a pressure rise

$$\frac{\Delta P_1}{P_0} = \frac{P_2 - P_0}{P_0} = 1.17$$

was obtained. The ratio

$$\frac{\Delta P_{1\ SHOCK}}{\Delta P_{\ ISENT}}$$

is shown in Figure 12.

The air is now heated by constant volume combustion to a temperature $T_3$, shown in Figure 13 (d). During the constant volume heating cycle $P_2 = \rho_2 R T_2$, $P_3 = \rho_3 R T_3$ and since $\rho_2 = \rho_3$, then $P_3/P_2 = T_3/T_2$. If the temperature ratio $T_3/T_2 = 4.30$ for example, corresponding to a temperature $T_3 = 3030^{\circ}R$ ($1570^{\circ}F$) then $P_3/P_2 = 4.30$. If, in addition, $M_0 = M_1 = 0.80$, then the resulting pressure ratio is $P_3/P_0 = 4.8 \times 2.17 = 10$. At this stage of the cycle, the rear valve A is opened and the hot high pressure gases are permitted to expand rear-ward, as shown in Figure 13 (e). When the pressure inside the tube is reduced to the total pressure of the inlet flow $P_{0_2}$, the inlet valve B is opened. The inlet flow traveling at a Mach Number $M_0$ is brought to rest at the mouth of the tube. Meanwhile, at the exit of the tube, the ambient static pressure is lower than the pressure in the tube; therefore, the remainder of the burnt gases continue to flow out of the tube. The flow at the entrance of the tube has been brought to rest while the inlet valve was closed. As the valve is opened, the inlet air begins to flow into the tube. This flow may be compared to the steady flow of air in a stream-tube towards a stagnation point and then again away from the stagnation point. Thus new fuel-air mixture flows into the tube replacing the remainder of the burnt gases from the previous cycle. This is shown in Figure 13 (f). When the tube is completely filled with a new charge, the rear valve closes and a new cycle is started.

This ideal cycle is composed of four phases:

(1) Scavenging and Intake
(2) Shock Compression
(3) Combustion at Constant Volume
(4) Expansion

## 3.3 Derivation of the Performance Characteristics

The pulse or shock compression is obtained by means of the shock wave formed by the closure of the exhaust valve. This shock wave is formed at the exhaust valve and travels upstream, stopping the incoming fluid particles and compressing them to a higher

pressure. The relations between the Mach Number of the duct flow, $M_1$, the pressure ratio, $P_2/P_1$ and the temperature ratio $T_2/T_1$, are derived in Section II, and are given on Figure 3. The absolute velocity of the shock wave is $\xi - u$, and the velocity of sound ahead of the wave is $a_1$. The Mach Number of the wave $M_w = \frac{\xi - u}{a_1}$ is given in Figure 2.

From these two figures, the pressure ratio and the time required for shock compression may be found. The duration of shock compression $\tau_c$ is the time required for the wave to travel from the exhaust to the inlet valve.

When the shock arrives at the inlet or front end of the tube, the inlet valve closes, thus trapping the compressed fuel-air mixture in the tube. The fuel-air mixture is allowed to burn and the final temperatures and pressures will be determined by the efficiency of burning and the fuel-air ratio. From the assumptions we have:

(1) Burning efficiency = 100%.

(2) $\frac{T_3}{T_2} = \frac{P_3}{P_2}$ (constant volume burning).

(3) $T_3 = T_3''$ and $P_3 = P_3''$ (frictionless fluid flow).

The time required for burning will be taken as a constant value of 0.010 secs. Actually the combustion of the fuel-air will be carried out in two stages:

(1) The burning by a flame front traveling at very low velocities, 1 to 2 ft/sec.

(2) The burning by a detonation wave traveling at large velocities, 4000 to 5000 ft/sec. The variation of with various parameters (i.e. length, F/A ratio, etc.) is small enough to be neglected in these calculations, therefore a constant value of $\tau_B = 0.010$ secs. is used.

In this simplified ideal case the computations will be carried out with $M_0$ and $P_3/P_0$ as the variable parameters. It should be noted that, for this case, given values of $M_0$ and $P_3/P_0$ uniquely determine the value of $T_3/T_0$.

The Specific Fuel Consumption is given by the following equation

$$\frac{f}{\sqrt{\theta}} = \frac{\mu v_f}{\mu v_a} \cdot 3600 \quad \frac{V_g P_0 a_0}{I} \cdot \frac{P_3}{P_0} \cdot \frac{1}{a_{SL}} \qquad \ldots (24)$$

This is plotted on figure 14, 15, 16, 17, 18, and 19.

Let $\tau = 0$ when the inlet valve opens. Assume that the duration of the scavenging phase is given by the time taken for the gas interface at the inlet valve to travel down the tube at Mach

AEROPHYSICS DEVELOPMENT CORPORATION
PACIFIC PALISADES, CALIFORNIA

DATE Jan 2, 1953

FIGURE 3

## SPECIFIC FUEL CONSUMPTION

f - LBS. FUEL PER HOUR PER LB THRUST

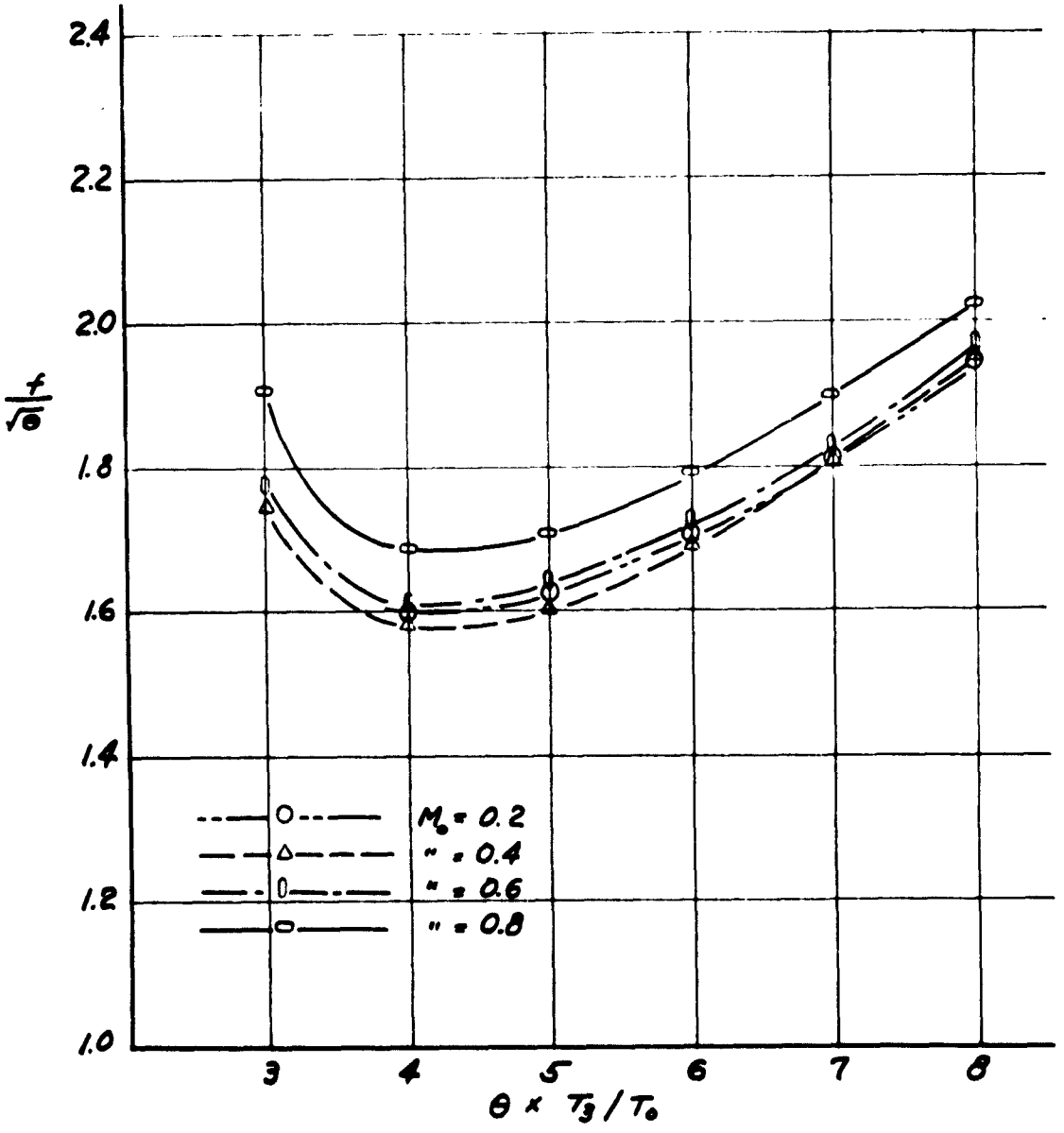

| PREPARED BY | AEROPHYSICS DEVELOPMENT CORPORATION | REPORT 2000-1-A1 |
|---|---|---|
| CHECKED BY | PACIFIC PALISADES, CALIFORNIA | DATE Jan 24, 1953 |

FIGURE 14

## SPECIFIC FUEL CONSUMPTION

f- LBS. FUEL PER HOUR PER LB THRUST

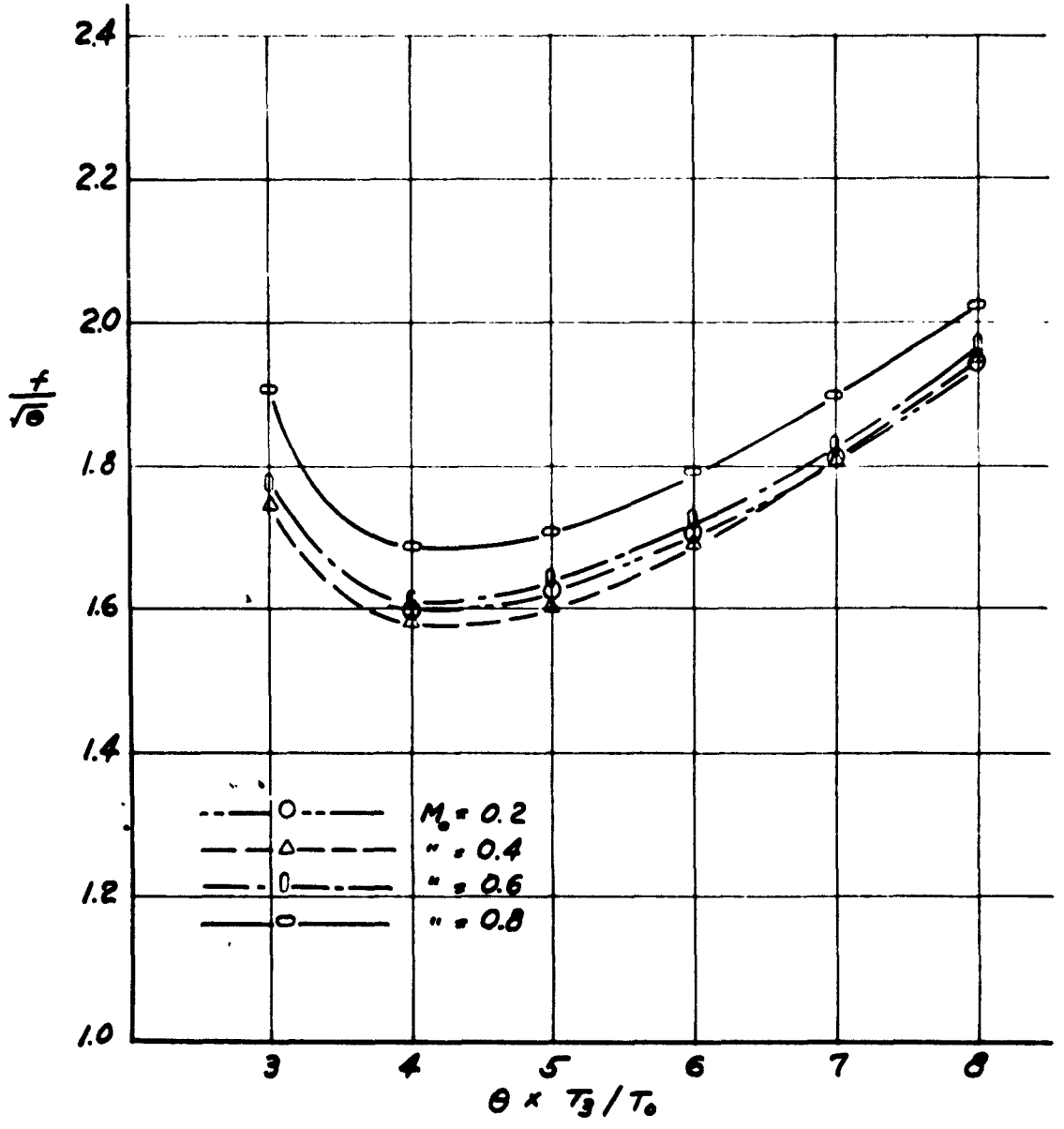

| PREPARED BY | AEROPHYSICS DEVELOPMENT CORPORATION | 1000-1-R1 |
|---|---|---|
| CHECKED BY | PACIFIC PALISADES, CALIFORNIA | DATE Jan 28, 1953 |

FIGURE 15

## SPECIFIC FUEL CONSUMPTION

f - LBS. FUEL PER HOUR PER LB. THRUST

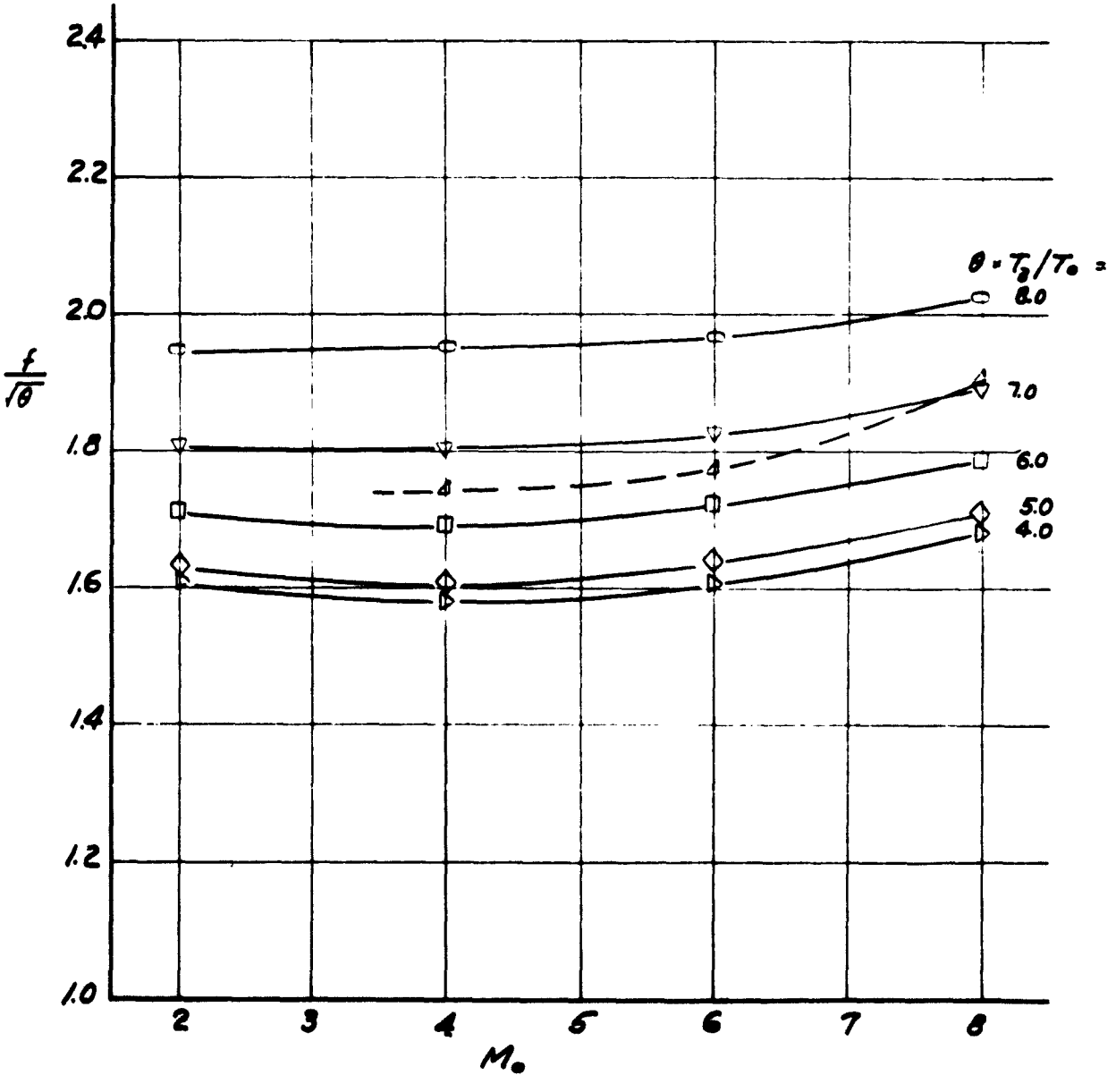

| PREPARED BY | AEROPHYSICS DEVELOPMENT CORPORATION | REPORT NO. 2000-1-R1 |
|---|---|---|
| CHECKED BY | PACIFIC PALISADES, CALIFORNIA | DATE Jan 24, 1953 |

FIGURE 16

SPECIFIC FUEL CONSUMPTION

f - LBS. FUEL PER HOUR PER LB. THRUST

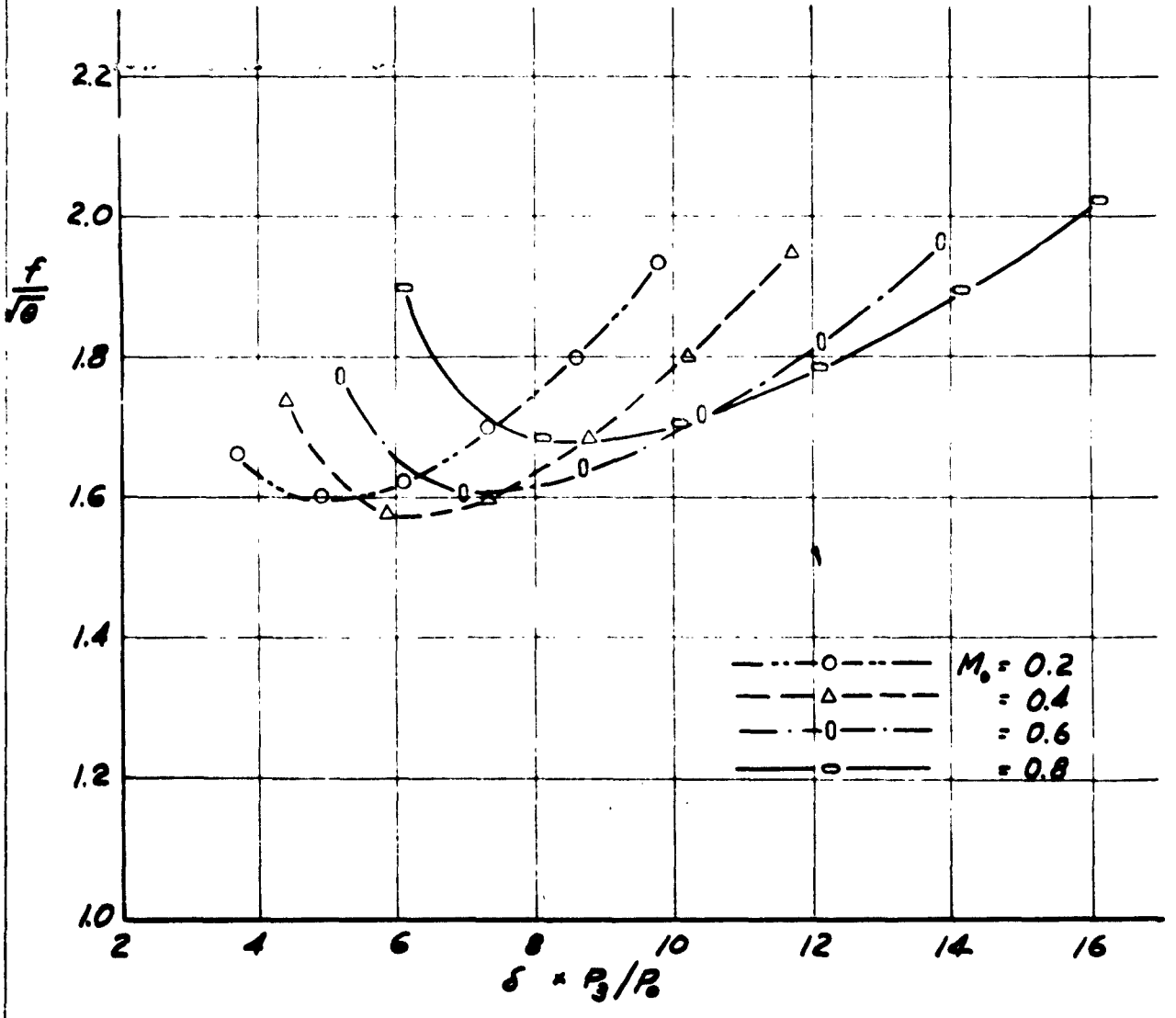

| PREPARED BY | AEROPHYSICS DEVELOPMENT CORPORATION | REPORT NO. 2000-1-R1 |
|---|---|---|
| CHECKED BY | PACIFIC PALISADES, CALIFORNIA | DATE Jan 24, 1953 |

FIGURE 17

SPECIFIC FUEL CONSUMPTION

f - LBS. FUEL PER HOUR PER LB. THRUST

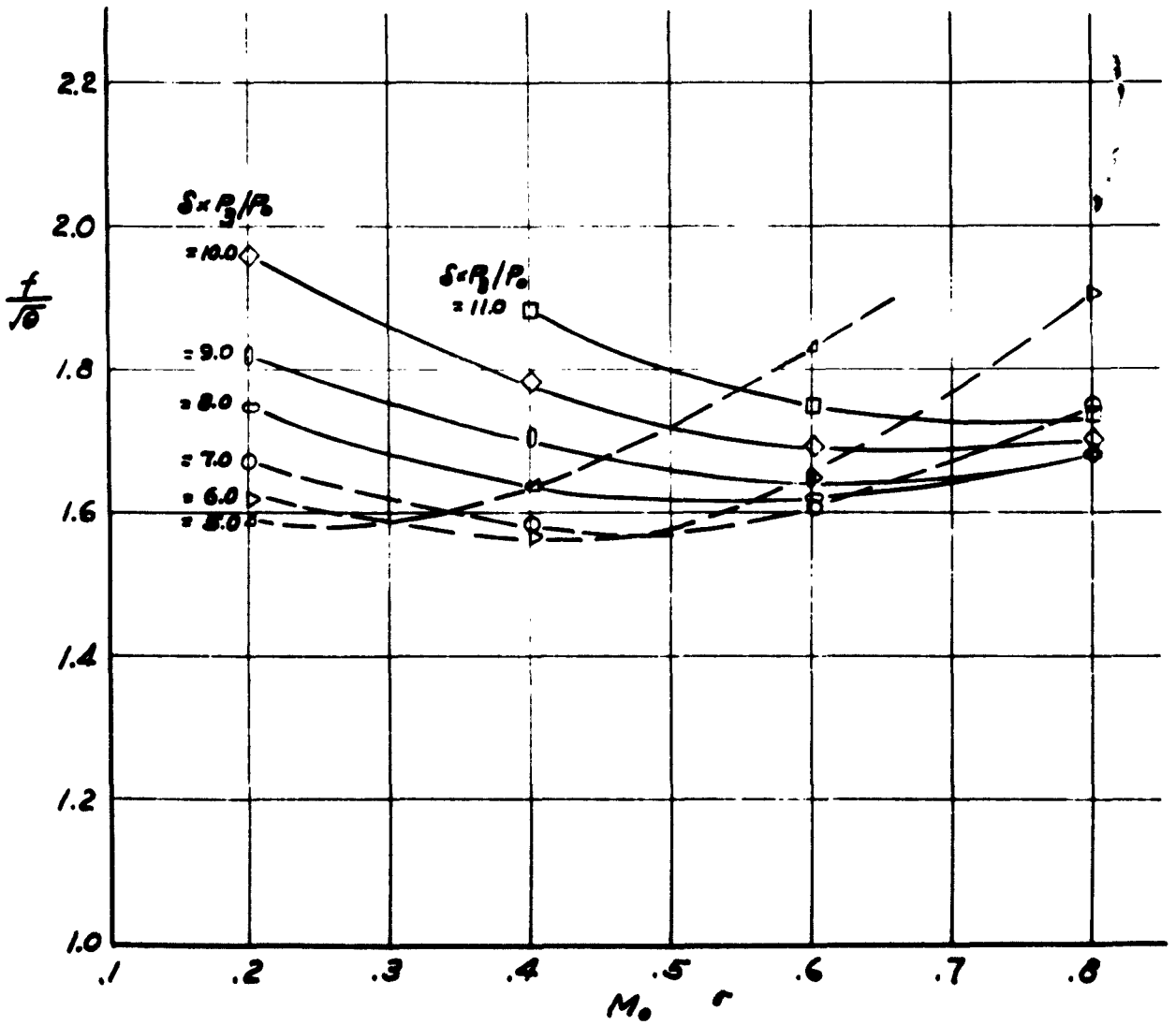

| PREPARED BY | AEROPHYSICS DEVELOPMENT CORPORATION | REPORT 2000-1-31 |
|---|---|---|
| CHECKED BY | PACIFIC PALISADES, CALIFORNIA | DATE Jan 24, 1953 |

FIGURE 18

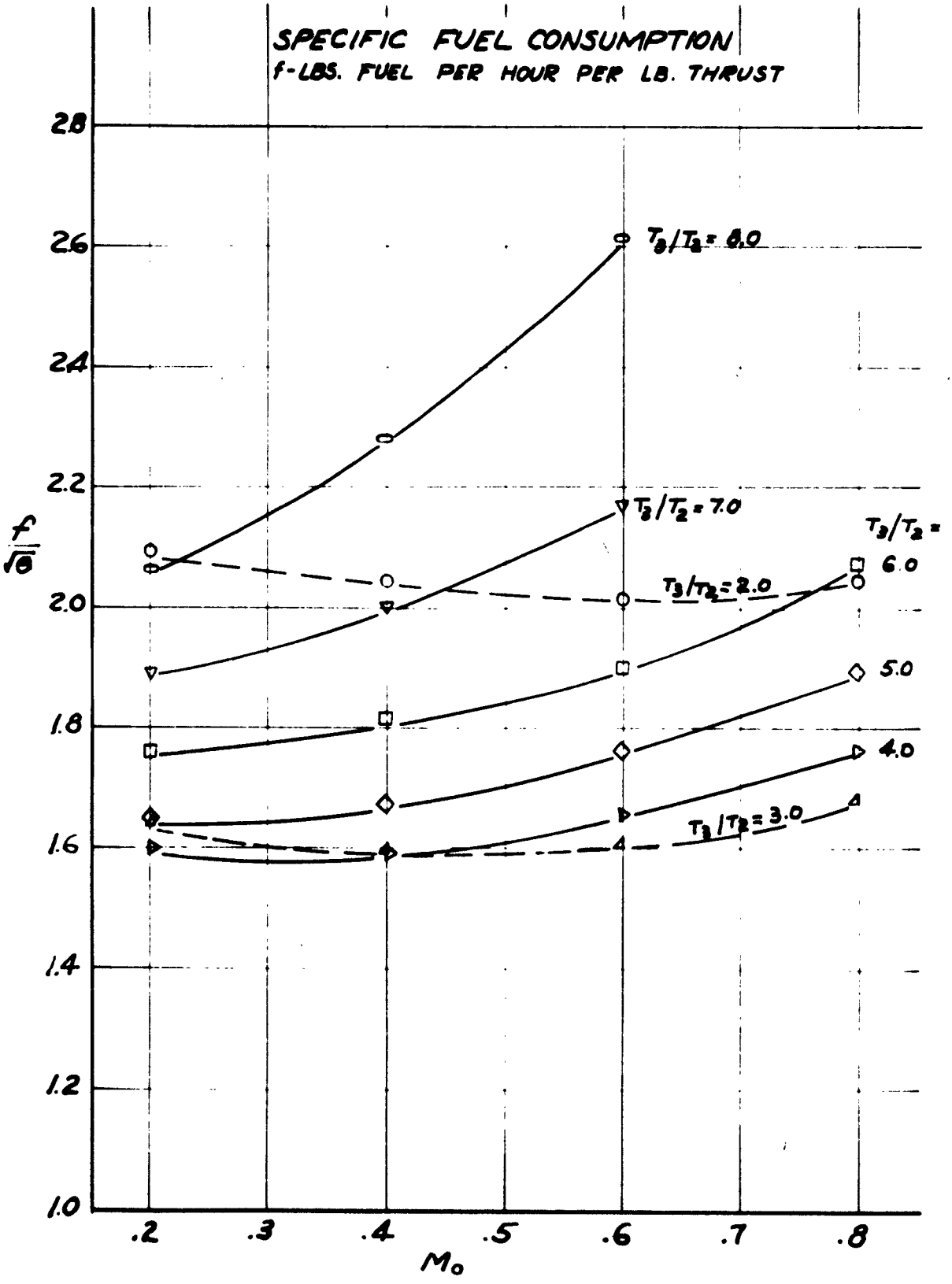

| PREPARED BY | AEROPHYSICS DEVELOPMENT CORPORATION | REPORT NO. 2000-1-R1 |
|---|---|---|
| CHECKED BY | PACIFIC PALISADES, CALIFORNIA | DATE Jan 24, 1953 |

FIGURE 19

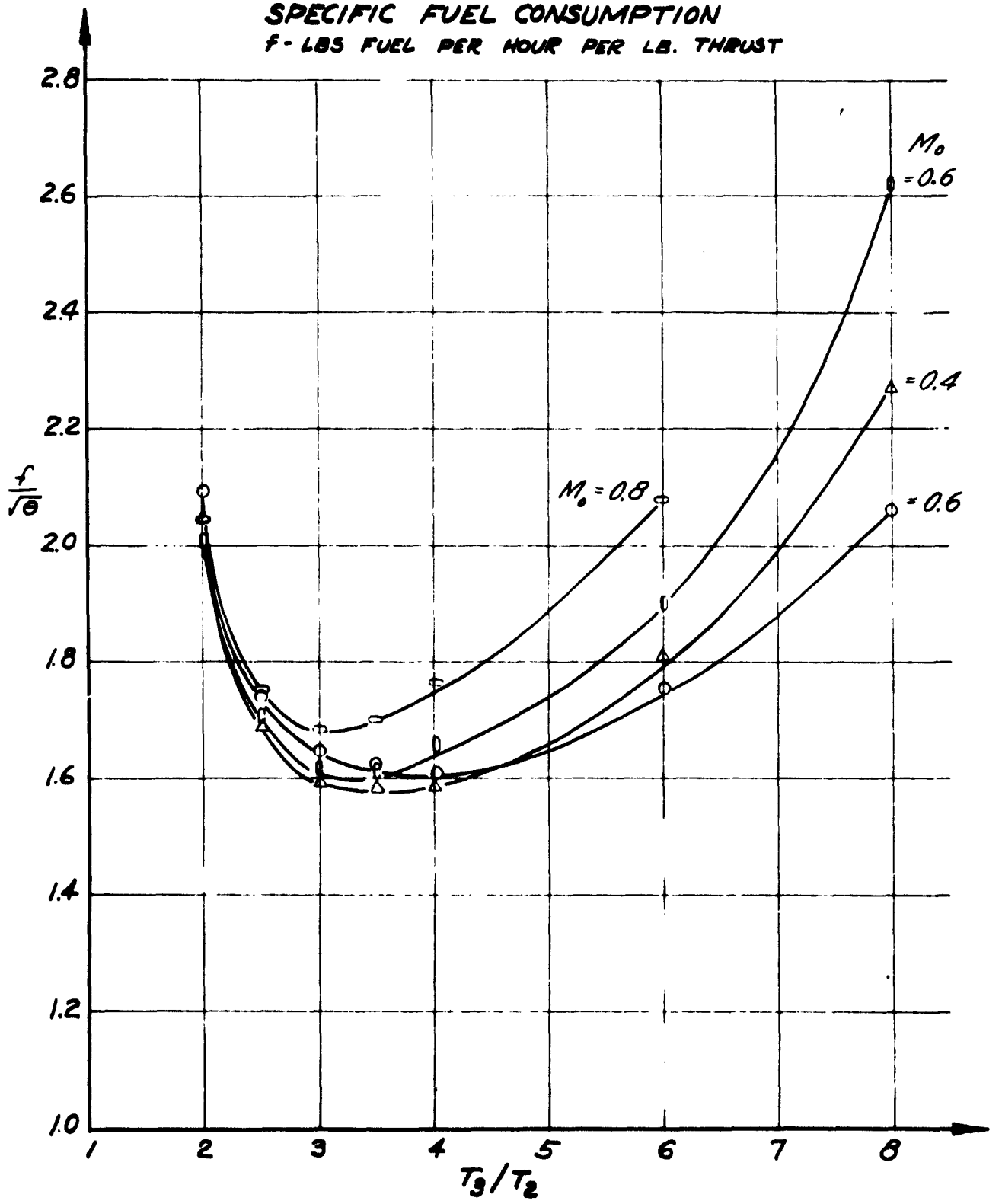

| PREPARED BY | AEROPHYSICS DEVELOPMENT CORPORATION | REPORT NO 2000-1-R1 |
|---|---|---|
| CHECKED BY | PACIFIC PALISADES, CALIFORNIA | DATE Jan 24,1953 |

Number $M_o$. Then

$$\frac{\tau_s}{L}\sqrt{\theta} = \frac{1}{M_o a_{SL}}\sqrt{\frac{T_o}{T_1}} \quad \ldots(25)$$

The duration of the pulse compression is assumed to be given by the time taken for the normal shock wave to travel from the exhaust valve to the inlet valve.

$$\frac{\tau_c}{L}\sqrt{\theta} = \frac{1}{M_w a_{SL}}\sqrt{\frac{T_2}{T_1}} \quad \ldots(26)$$

The duration of detonation and burning is assumed to be made up of two parts: (1) the time required for detonation to form, (2) the time required for the detonation to sweep over the rest of the gases.

$$\frac{\tau_B}{L}\sqrt{\theta} = K_c + \frac{1}{M_{DET} a_{SL}} \quad \ldots(27)$$

The duration of the exhaust phase is given by Figure 4.

$$\frac{\tau_E}{L}\sqrt{\theta} = \left[\frac{\tau_E}{V/A_N a_3}\right]\frac{a_1}{a_3}\frac{1}{a_{SL}} \quad \ldots(28$$

where $\tau_E/\frac{V}{A_N a_3}$ is a function of (Figure 4). Since is large, can be neglected. The total duration of one cycle can be assumed to vary directly with the length of the tube.

The average thrust per sq. ft. of nozzle area is

$$\frac{F}{A_N \delta} = \frac{I_{NET}}{a_o g \rho_o V_{OL}} \cdot \frac{L}{\tau\sqrt{\theta}} \cdot \frac{\gamma P_{SL}}{a_{SL}} \quad \ldots(29)$$

See Figures 20, 21, and 22 for a plot of this function.

Air Specific Impulse: (pounds of thrust per lb of air per sec.)

$$\frac{S_a}{\sqrt{\theta}} = \frac{F}{A_N \delta} \cdot \frac{V\delta}{W\sqrt{\theta}} \cdot \frac{\tau\sqrt{\theta}}{L} \quad \ldots(30)$$

Where the weight of air per cycle is given by

$$\frac{W\sqrt{\theta}}{V_{OL}\delta} = \frac{\rho_3}{\rho_o} P_{SL} \quad \ldots(31)$$

The plot of equation (30) can be found in Figures 23, 24, and 25.

The performance characteristics of a single tube engine operating under the conditions assumed at the beginning of this

| PREPARED BY | AEROPHYSICS DEVELOPMENT CORPORATION | REPORT NO 2000-1-R1 |
|---|---|---|
| CHECKED BY | PACIFIC PALISADES, CALIFORNIA | DATE Jan 24, 1953 |

FIGURE 20

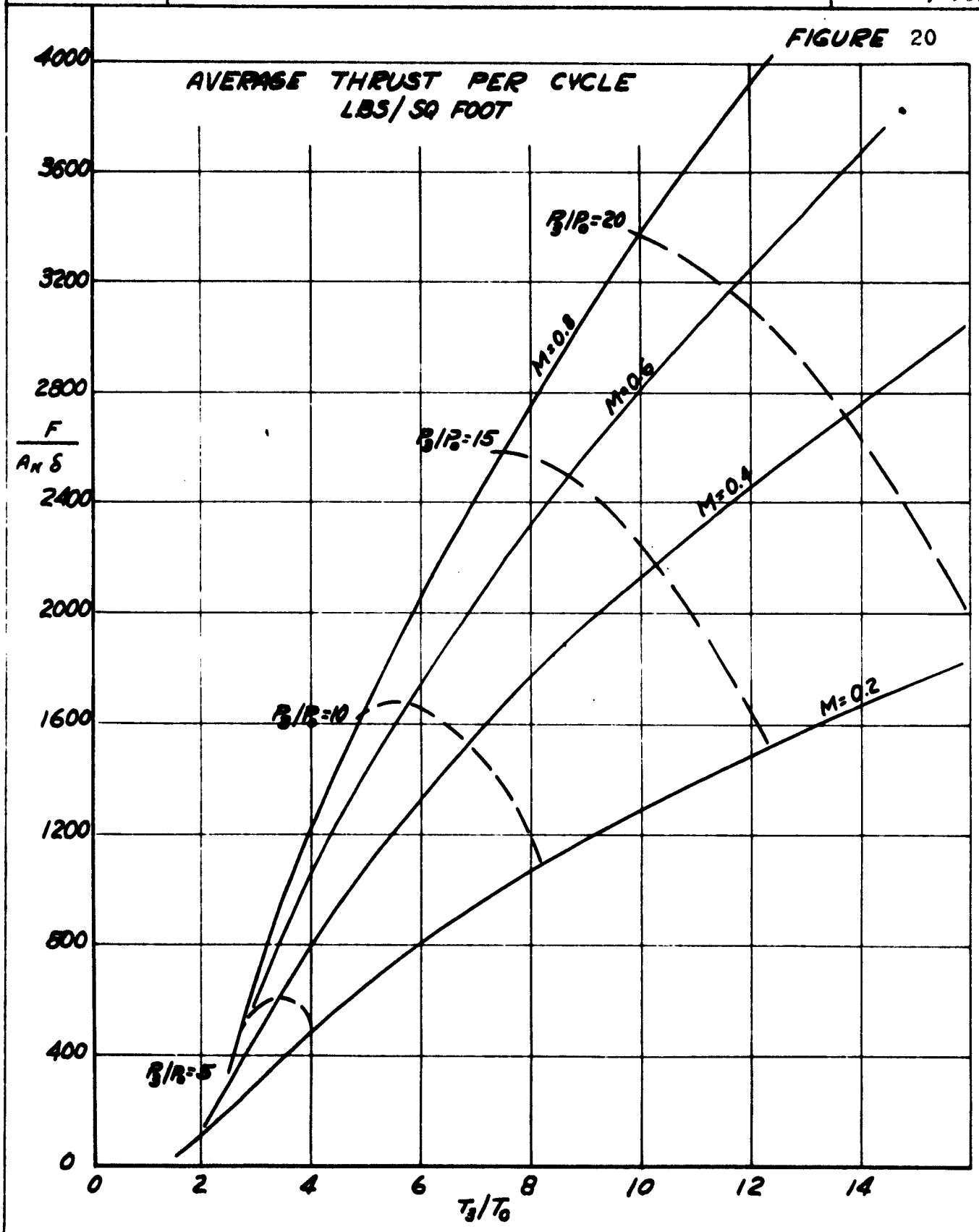

| PREPARED BY | AEROPHYSICS DEVELOPMENT CORPORATION | REPORT NO 2000-1-R1 |
|---|---|---|
| CHECKED BY | PACIFIC PALISADES, CALIFORNIA | DATE Jan. 24, 1953 |

FIGURE 21

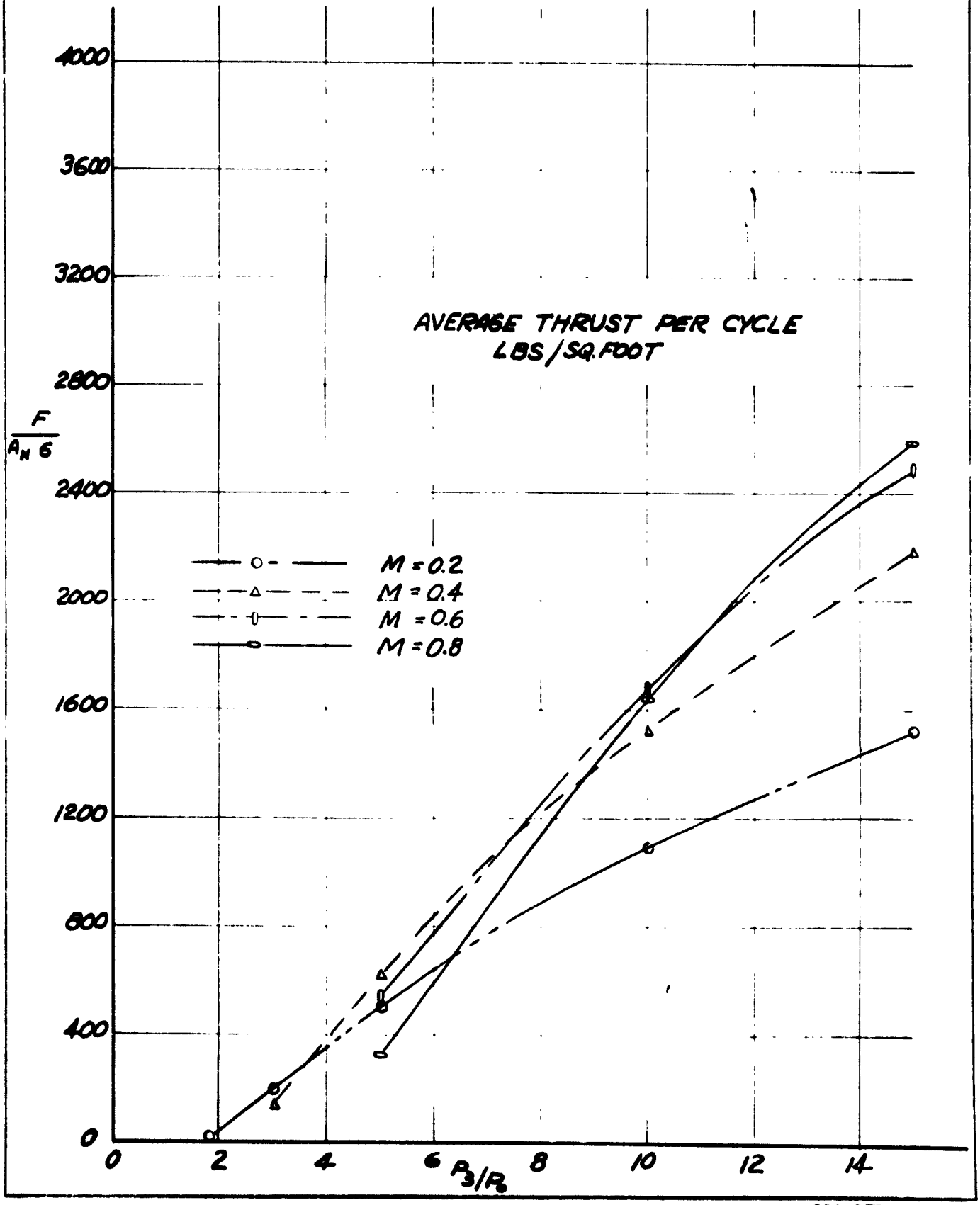

FIGURE 22

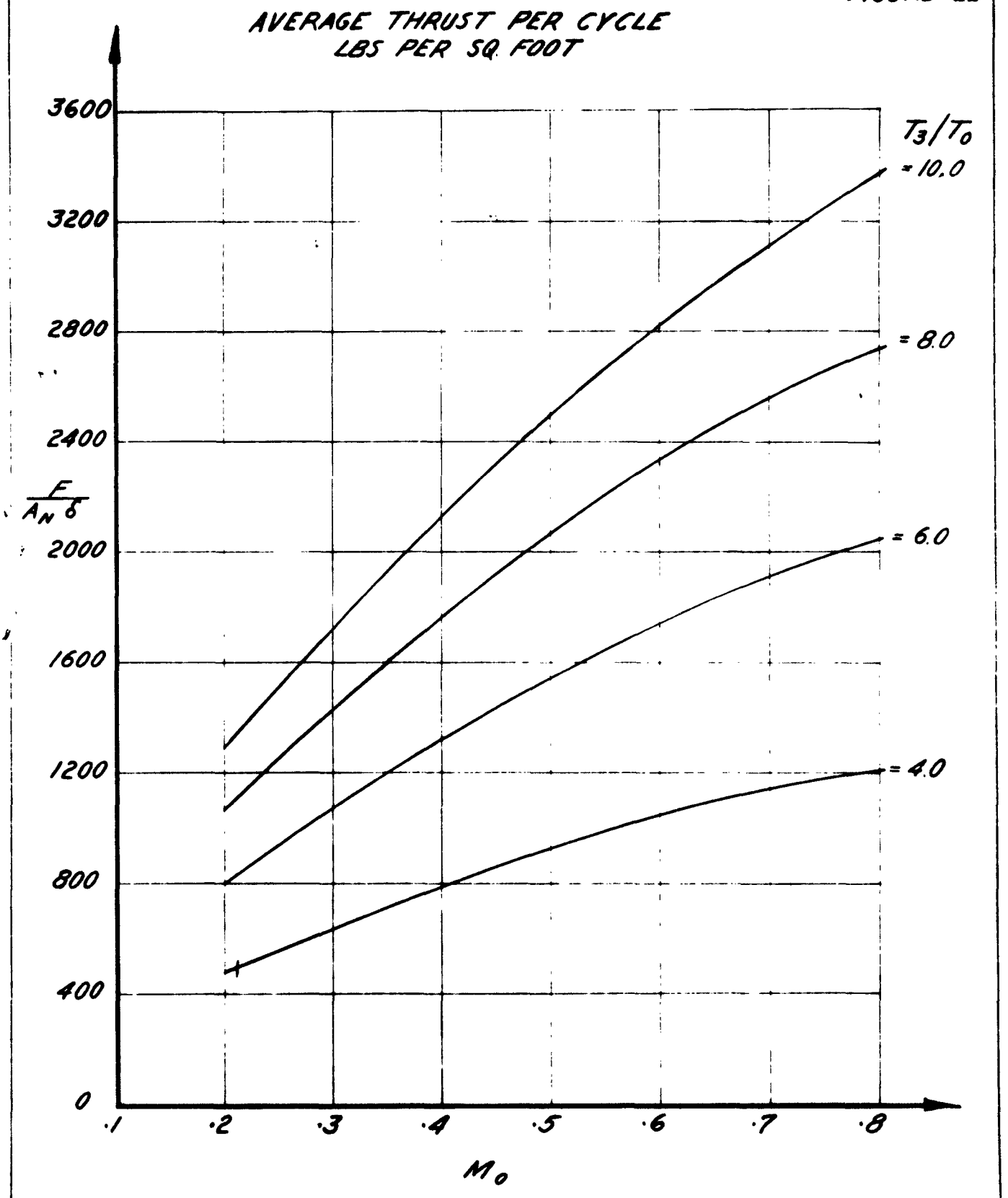
AVERAGE THRUST PER CYCLE
LBS PER SQ FOOT
3600
3200
2800
2400
$\frac{F}{A_N \delta}$
2000
1600
1200
800
400
0
.1
.2
.3
.4
.5
.6
.7
.8
$M_0$
$T_3/T_0$
= 10.0
= 8.0
= 6.0
= 4.0

| PREPARED BY | AEROPHYSICS DEVELOPMENT CORPORATION | REPORT NO. 2000-1-R1 |
|---|---|---|
| CHECKED BY | PACIFIC PALISADES, CALIFORNIA | DATE Jan 24, 1953 |

FIGURE 23

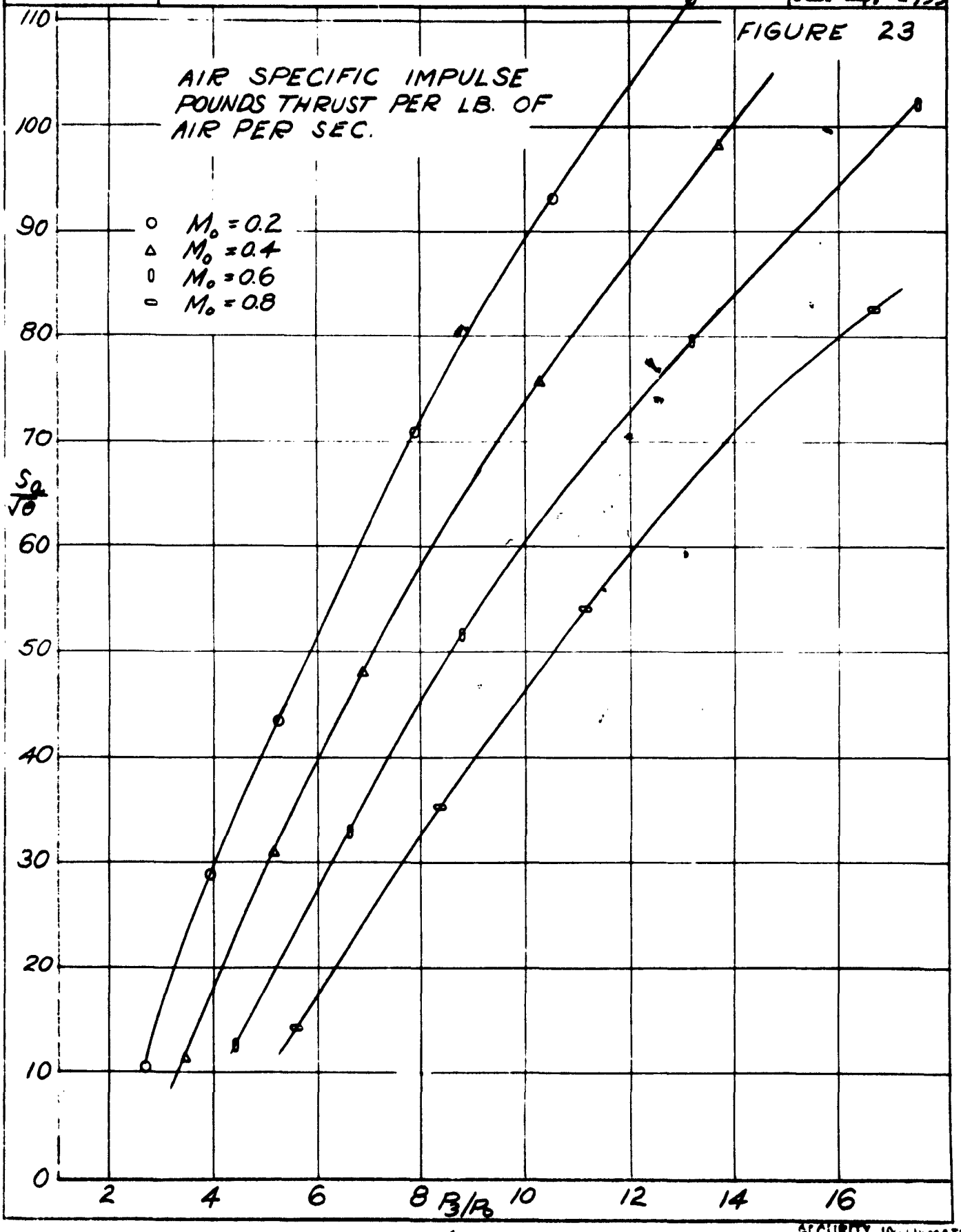

PREPARED BY

CHECKED BY

AEROPHYSICS DEVELOPMENT CORPORATION
PACIFIC PALISADES, CALIFORNIA

REPORT NO. 2000-1-R1

DATE Jan 24, 1953

FIGURE 24

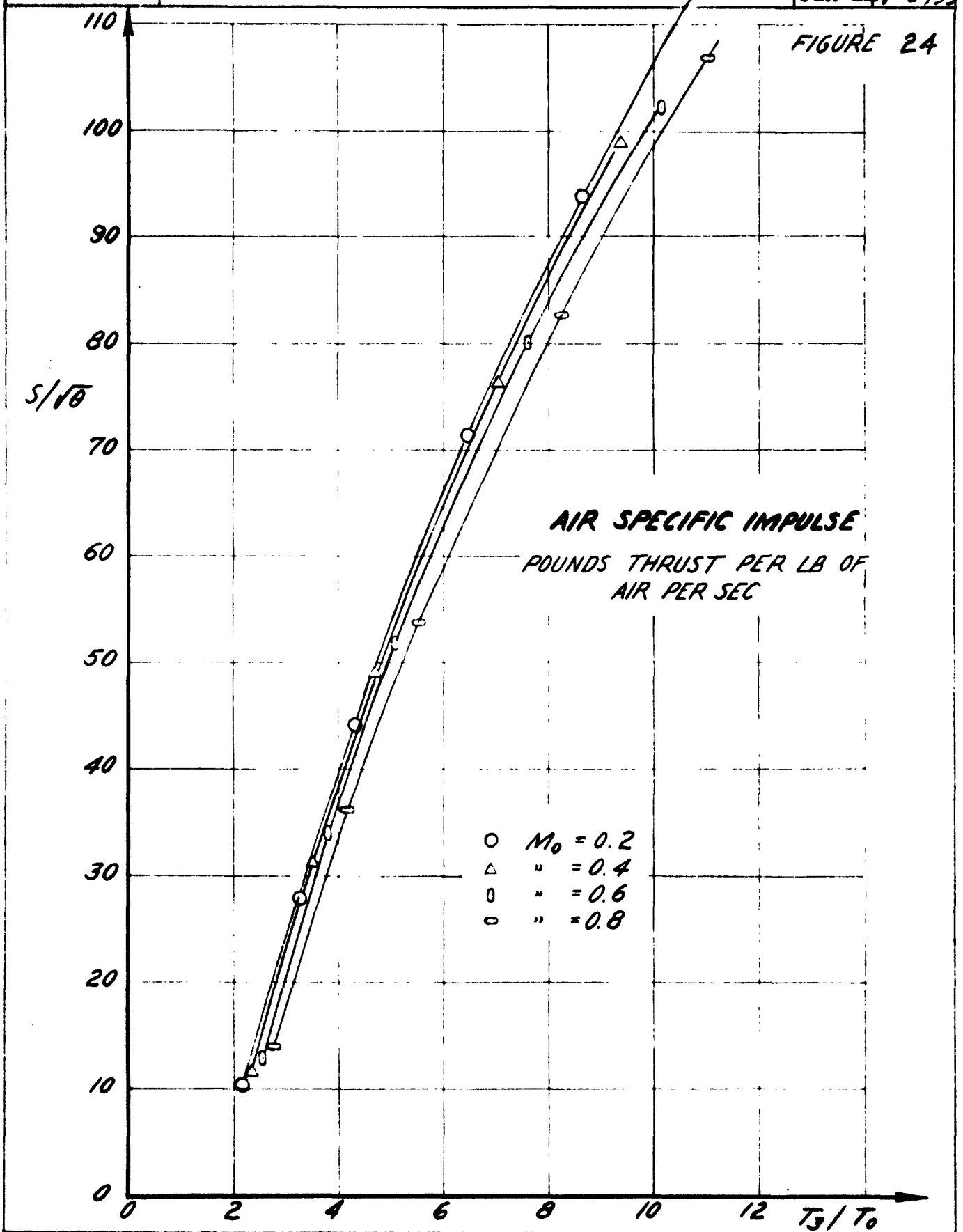

| PREPARED BY | AEROPHYSICS DEVELOPMENT CORPORATION | REPORT NO. 2000-1-R1 |
|---|---|---|
| CHECKED BY | PACIFIC PALISADES, CALIFORNIA | DATE Jan 2, 1953 |

FIGURE 25

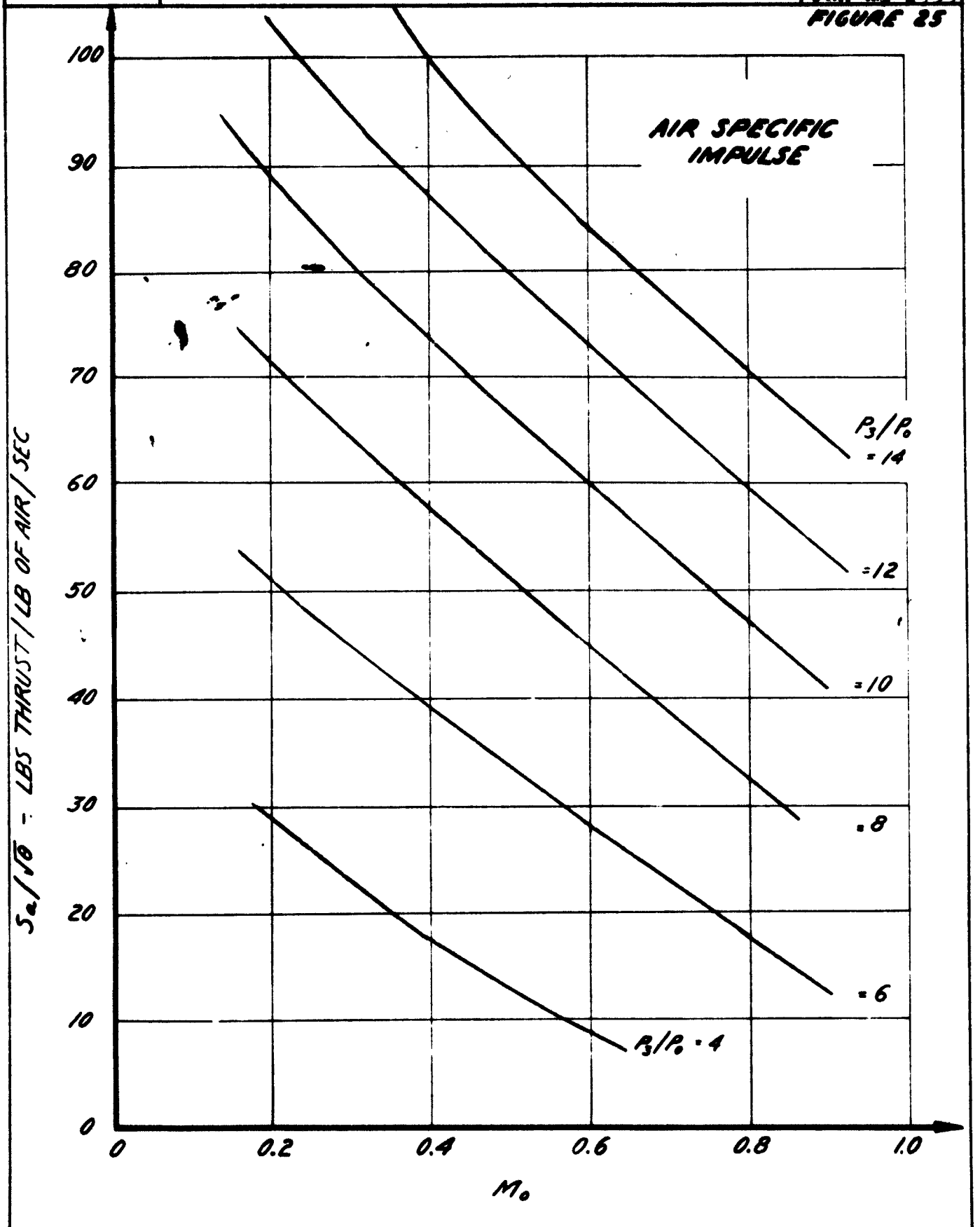

| PREPARED BY | AEROPHYSICS DEVELOPMENT CORPORATION | REPORT NO. 2000-1-R1 |
|---|---|---|
| CHECKED BY | PACIFIC PALISADES, CALIFORNIA | DATE Jan 24 1953 |

section are given in Figures 26 to 30. The thrust per sq. foot of frontal area, the specific fuel consumption, the air specific impulse, and the thrust coefficient are plotted against flight Mach Number for various top temperatures in Figures 26, 27, 28, and 29 respectively. Figure 30 gives the characteristic mass flow of a single tube engine. Tables 2 and 3 list the performance characteristics for the ideal case and are described in detail in Appendix I.

| PREPARED BY | AEROPHYSICS DEVELOPMENT CORPORATION | REPORT NO. 2000-1-R1 |
|---|---|---|
| CHECKED BY | PACIFIC PALISADES, CALIFORNIA | DATE Jan. 24 1953 |

FIGURE 26

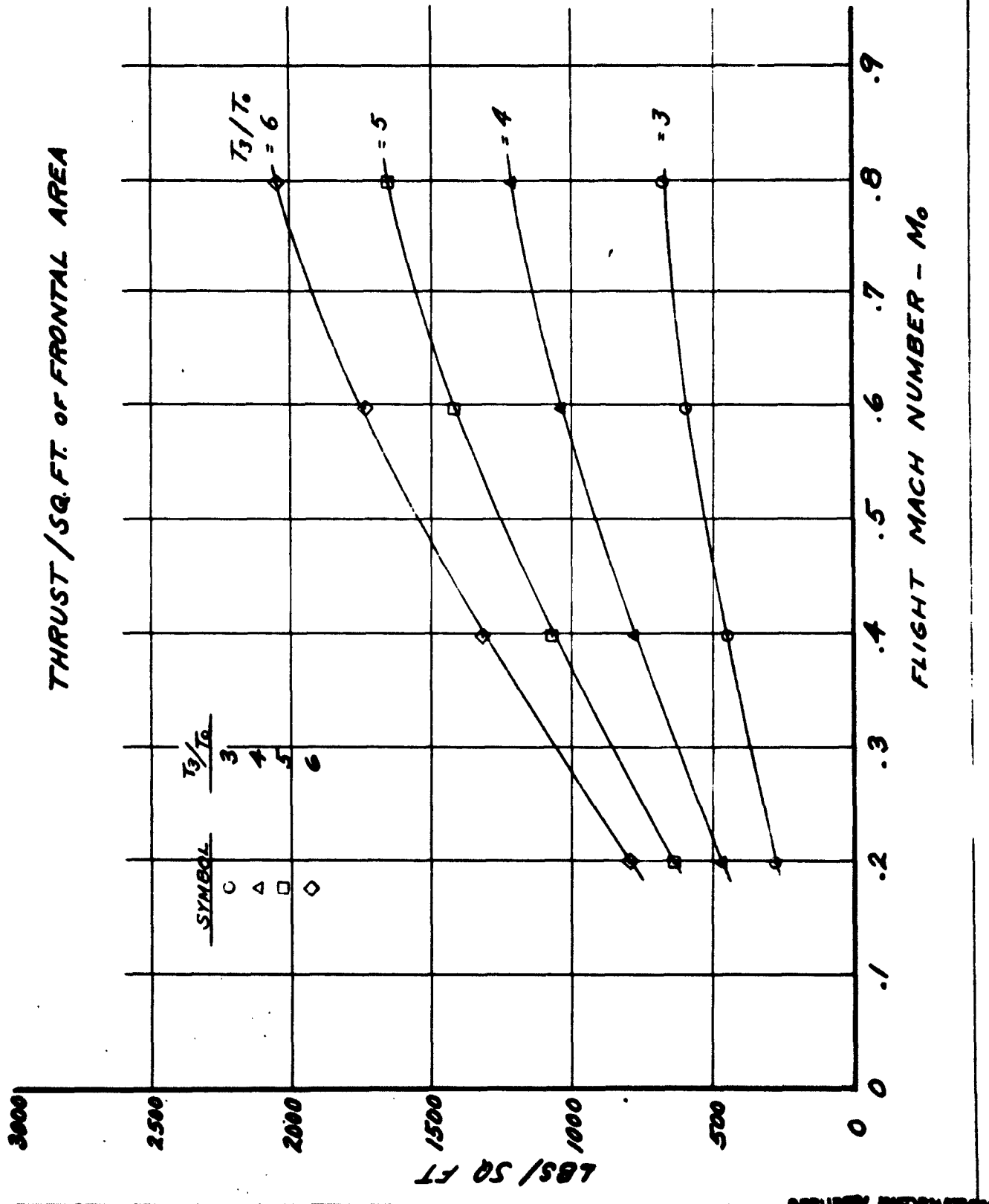

| PREPARED BY | AEROPHYSICS DEVELOPMENT CORPORATION | REPORT NO 2000-1-R1 |
|---|---|---|
| CHECKED BY | PACIFIC PALISADES, CALIFORNIA | DATE Jan 24 1953 |

FIGURE 27

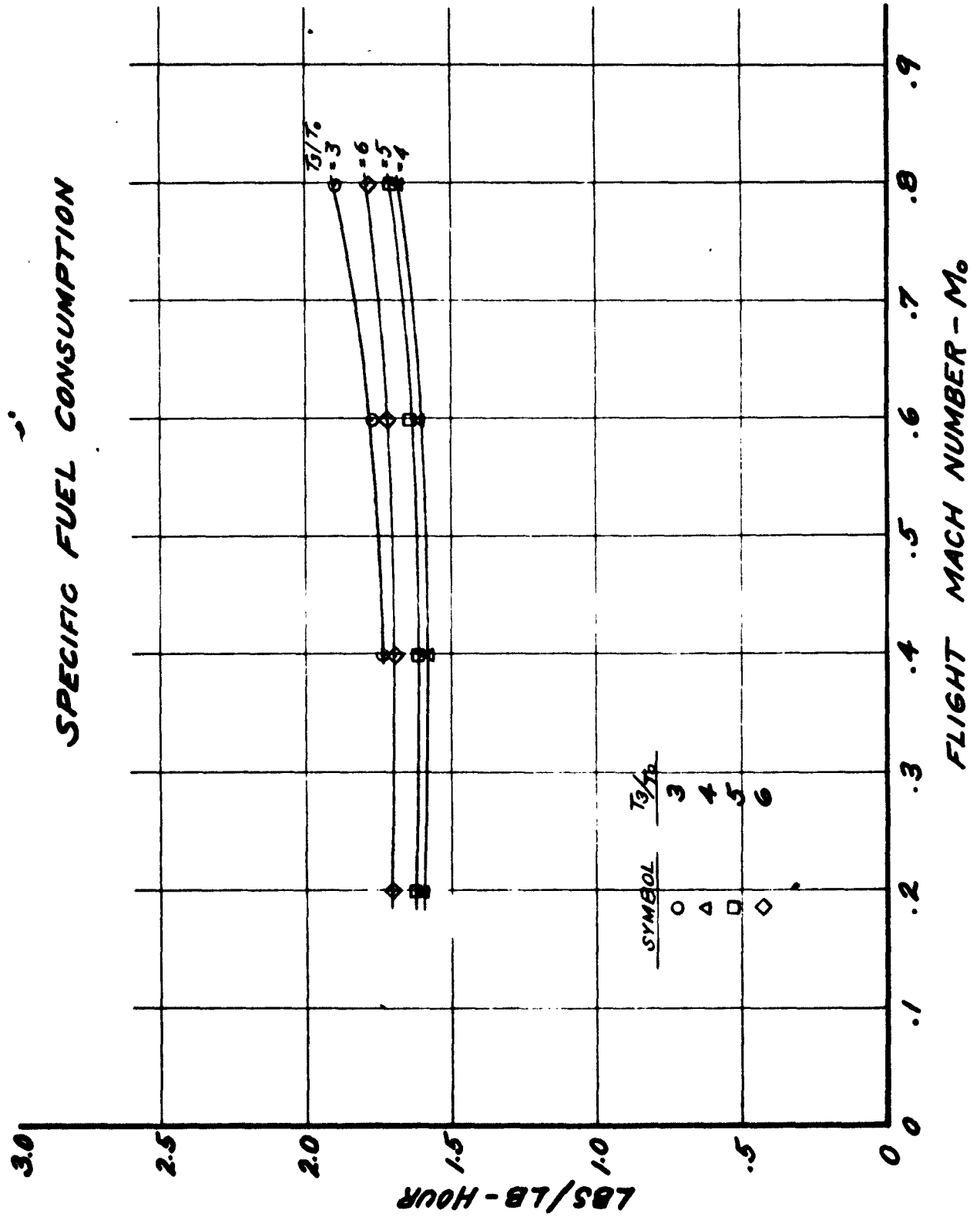

| PREPARED BY | AEROPHYSICS DEVELOPMENT CORPORATION | REPORT NO 2000-1-R1 |
|---|---|---|
| CHECKED BY | PACIFIC PALISADES, CALIFORNIA | DATE Jan 24 1953 |

FIGURE 28

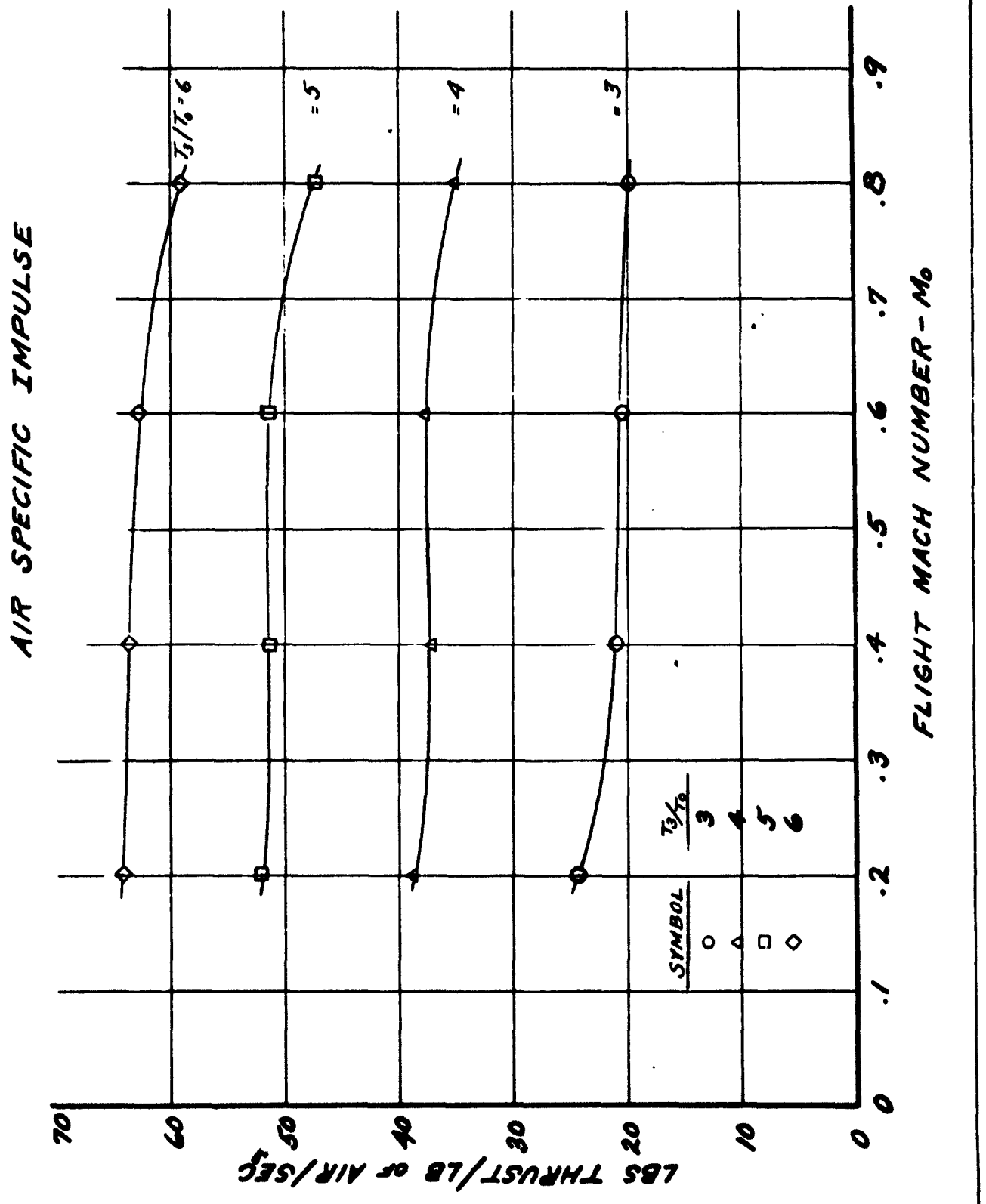

| PREPARED BY | AEROPHYSICS DEVELOPMENT CORPORATION | REPORT NO 2000-1-R1 |
|---|---|---|
| CHECKED BY | PACIFIC PALISADES, CALIFORNIA | DATE Jan 24 1953 |

FIGURE 29

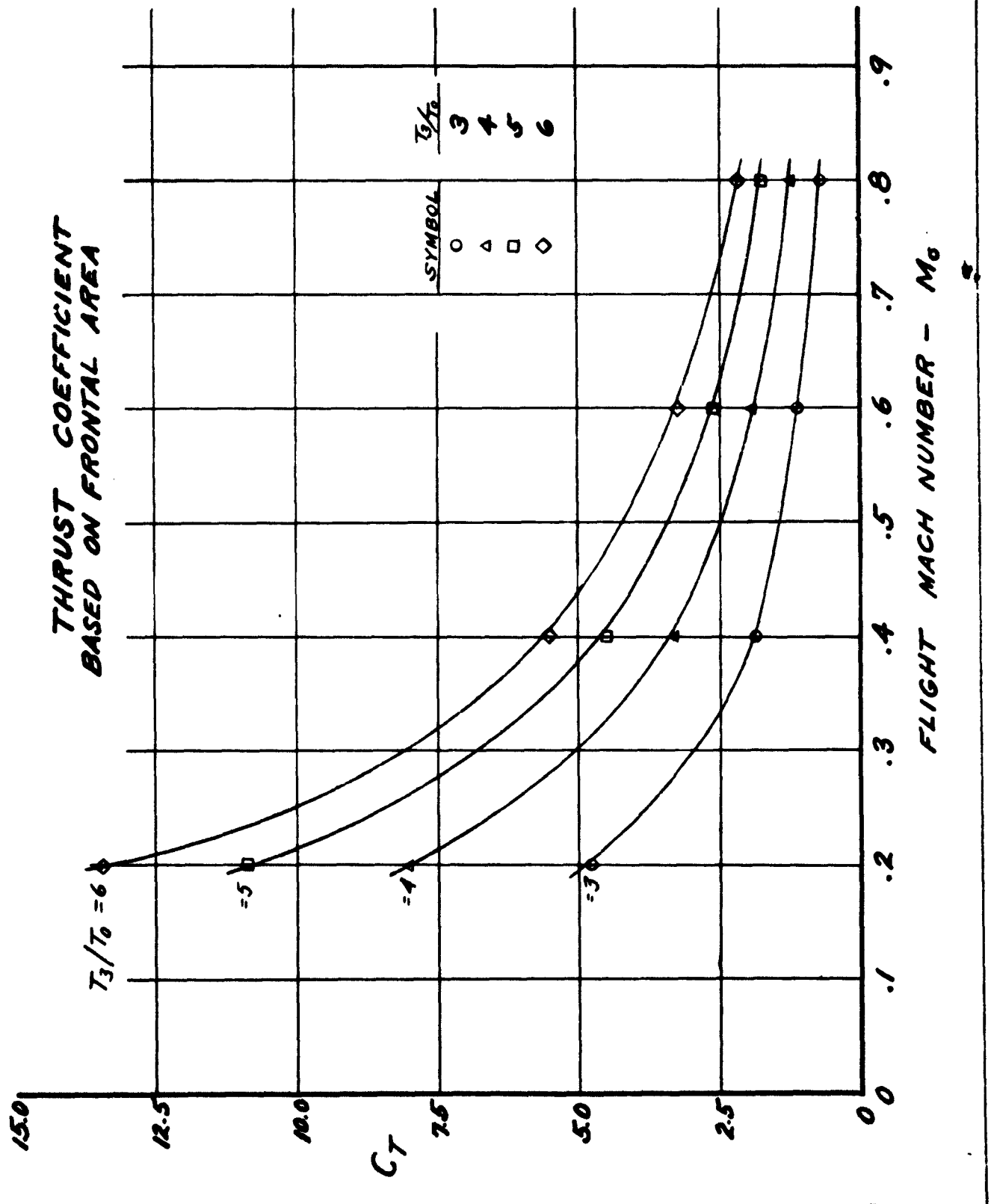

| PREPARED BY | AEROPHYSICS DEVELOPMENT CORPORATION | REPORT NO 2000-1-R1 |
|---|---|---|
| CHECKED BY | PACIFIC PALISADES, CALIFORNIA | DATE Jan 24 1953 |

FIGURE 30

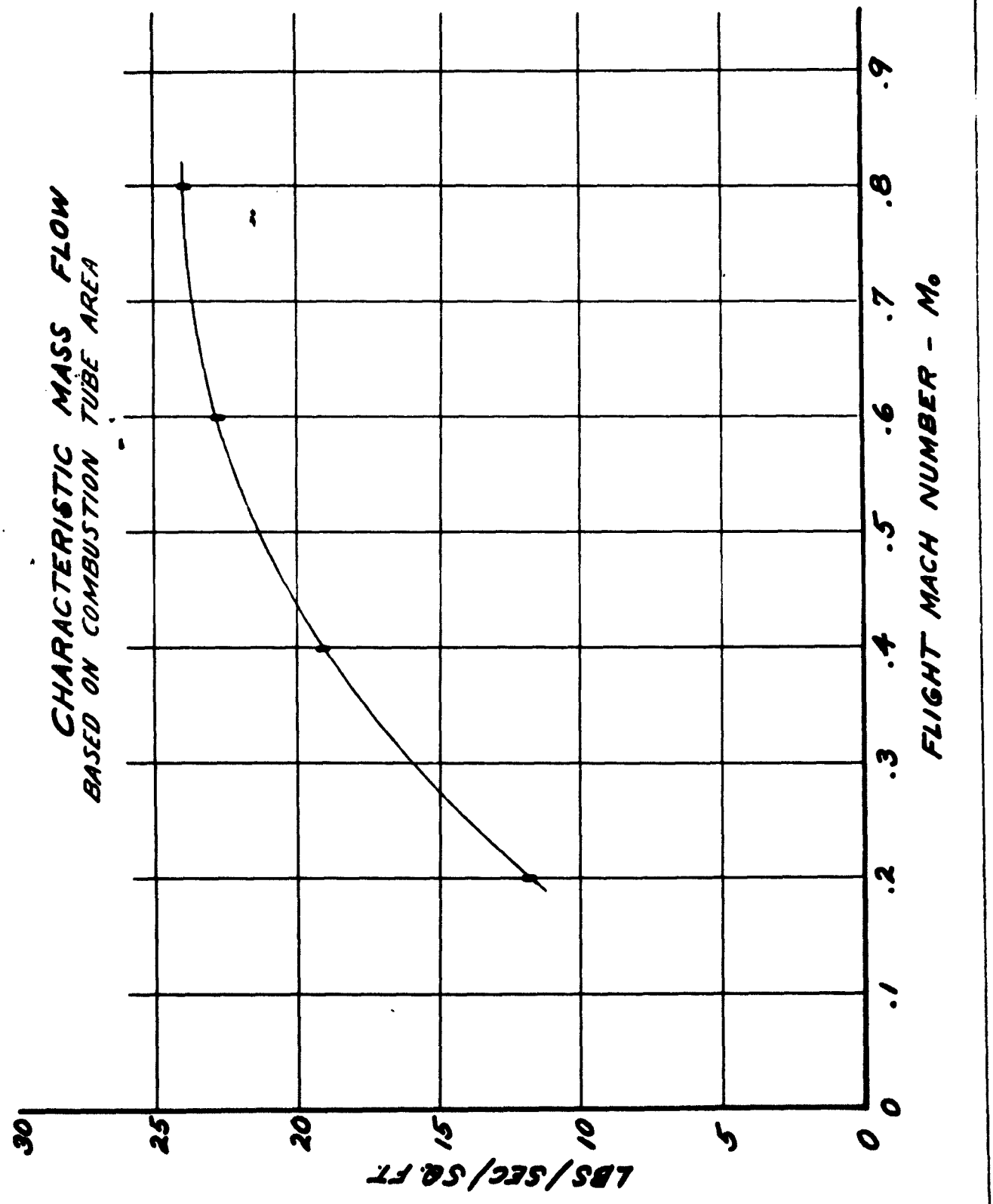

PREPARED BY | AEROPHYSICS DEVELOPMENT CORPORATION | REPORT NO 2000-1-R1
CHECKED BY | PACIFIC PALISADES, CALIFORNIA | DATE Jan. 24 1953

## SECTION IV

## ACTUAL CYCLE PERFORMANCE OF A SINGLE TUBE

### 4.1 Description and Assumptions

In the previous section the performance analysis of a single tube engine, with frictionless flow and ideal valve operation was computed. These first calculations gave an indication of the potentialities of this type of engine, but on the other hand, a fairer evaluation of the cycle could be made only with more realistic assumptions. These assumptions are:

1. The valves open or close within a finite time - $\tau_v$
2. The friction coefficient for flow in the tube is 0.02
3. Leakage losses will be neglected.
4. The duration of burning is assumed to be 0.010 seconds.

In these computations of the performance of a single tube, a definite physical configuration is not postulated. It is assumed that the engine consists only of a single tube or duct, with valves front and rear, that operate as assumed above.

### 4.2 Influence of the Opening and Closing Actions of the Valves on the Duct Flow

The closing action of the exhaust valve will produce the shock or pulse compression wave. If this valve could be closed in zero time, then the wave would be formed immediately. For this case see Figure 31 for the time-distance diagram of the conditions in the tube before and after the formation of the wave. The valve closes at $\tau = 0$ sending out a wave that stops the particles of air coming towards it. This is the ideal case and was treated in a previous section. In the actual case the valve will close in a finite time - $\tau_v$ . As it is closing it will send out a series of small compression waves which will finally converge at a point upstream from the valve and form a shock wave.

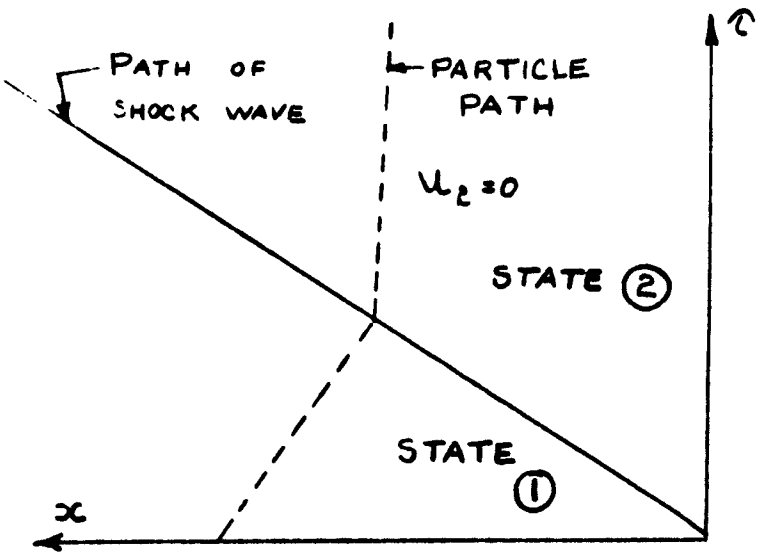


FIGURE 31

The distance required for the formation of the wave will be a function of $\tau_v$ and the duct Mach number $M_d$ or $M_1$. There remains therefore, the problem of finding the maximum allowable value of $\tau_v$ to produce a wave within a certain specified distance. It was decided that the wave be established within a foot of the valve position. The exact solution of this non-stationary wave problem requires a lengthy and tedious method of trial and error for each given value of $M_d$ and $\tau_v$. The method is given by Guderley (Reference 7) and others (Reference 8 and 9), but it was decided that for these first calculations certain simplifying assumptions would be made to reduce the work.

These assumptions are:

(1) The valve will send out signals (or compression waves), as it is closing, at the local speed of sound.

(2) The final state 2 behind the wave will be assumed to be the same as that produced by the ideal shock wave mentioned above.

(3) The first signal is sent out at a velocity of $a_1$, at the time $\tau = 0$. The last signal is sent out at a velocity of $a_2$ at time $\tau = \tau_v$. Their path in the (x,t) diagram will be assumed to be straight lines.

(4) The normal shock wave will form at the juncture of the last the first signals.

(5) No reflected waves due to the interaction of the signals will be assumed to travel back towards the valve.

In the actual case the final wave formed will be slightly weaker than that predicted by the ideal case, due to the interaction of the signals in the formation of the wave. This is small enough to be neglected, at this time. The time-distance diagram of the formation of the pulse compression wave is given in Figure 32.

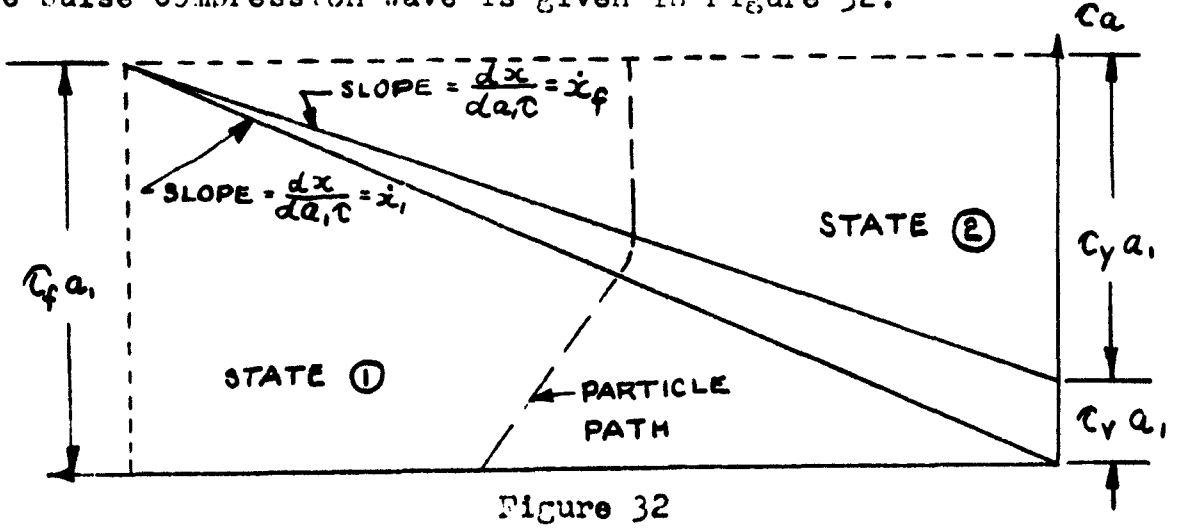


Figure 32

The slope of the first characteristic

$$\dot{x}_1 = \frac{dx_1}{d\tau_1 u_1} = \frac{a_1 - u_1}{a_1} = 1 - M_1 \qquad \ldots(32)$$

The slope of the last characteristic

$$\dot{x}_f = \frac{dx_2}{d\tau_2 a_2} = \frac{a_2}{a_1} \qquad \ldots(33)$$

These are given from the initial and final conditions for the ideal case. From the diagram, we have

$$\frac{x_w}{a_1 \tau_f} = \dot{x}_1 \quad \text{Now} \quad a_1 \tau_1 = a_1 \tau_v + a_1 \tau_y$$

$$a_1 \tau_y = \frac{x_w}{\dot{x}_f} \;, \quad \therefore a_1 \tau_1 = a_1 \tau_v + \frac{x_w}{\dot{x}_f}$$

$$\therefore \; x_w = x_1 \left( a_1 \tau_v + \frac{x_w}{\dot{x}_f} \right)$$

$$x_w = \frac{a_1 \tau_v}{\frac{1}{\dot{x}_1} - \frac{1}{\dot{x}_f}} \qquad \ldots(34)$$

$$x_w = \frac{a_1 \tau_v}{\frac{1}{1 - M_d} - \frac{a_1}{a_2}} \qquad \ldots(35)$$

Table 4 gives the maximum closing time required at each value of $M_d$ for the wave to form in the distance $x_w = 1$ foot. The results of the computation show that for a duct Mach number of 0.6, the maximum allowable time for closing is 1.45 millisecs.

The front valve will have to be closed before the normal shock wave arrives at the front end of the tube. Since the air particles are streaming past the valve when it closes, an expansion wave will be sent down the tube. Assume that the valve closes in zero time. Figure 33 gives the conditions on the (x,t) plane after the inlet valve has closed. For an expansion wave (Reference 4, page 95)

$$u_L = u_1 + \frac{2 a_1}{\gamma - 1} \left[ \left( \frac{P_L}{P_1} \right)^{\frac{\gamma - 1}{2\gamma}} - 1 \right] \qquad \ldots(36)$$

$$\frac{u_1}{a_1} = M_1 \;, \quad u_L = 0 \qquad \gamma = 1.40$$

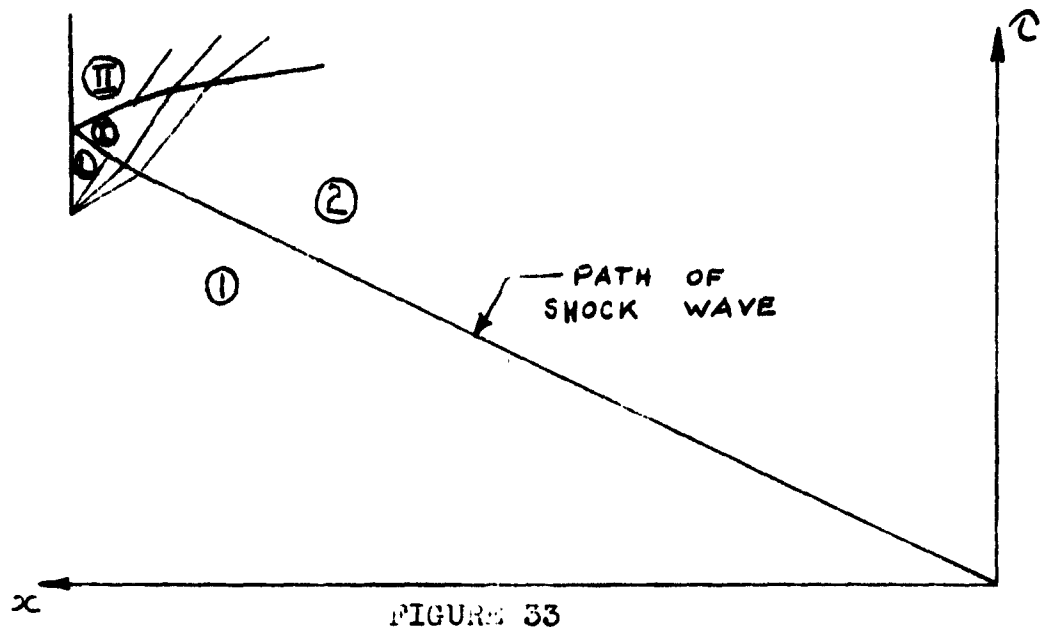


FIGURE 33

$$\therefore \frac{P_L}{P_1} = \left[1 - 0.2\, M_1\right]^7 \qquad \ldots(37)$$

For the case $M_1 = M_0 = 0.6$ , $P_L/P_1 = 0.41$

From the Pulse Compression $P_2/P_1 = 2.19$

The change from state (L) to (I) using equation (3)

$$u_I = u_L - (P_I - P_L)\sqrt{\frac{2\,a_L^2}{\gamma\left[(\gamma+1)P_I + (\gamma-1)P_L\right]P_L}} \qquad \ldots(38)$$

The change from state (2) to (I)

$$u_I = u_2 + \frac{2\,a_2}{\gamma-1}\left[\left(\frac{P_I}{P_4}\right)^{\frac{\gamma-1}{2\gamma}} - 1\right] \qquad \ldots(39)$$

$u_L = u_2 = 0$ and equating (38) and (39) and simplifying

$$\frac{2\gamma}{\gamma-1}\left(\frac{a_2}{a_1}\right)^2\left[\left(\frac{P_I}{P_1}\right)^{\frac{\gamma-1}{2\gamma}} - \left(\frac{P_2}{P_1}\right)^{\frac{\gamma-1}{2\gamma}}\right]^2\left(\frac{P_1}{P_2}\right)^{\frac{\gamma-1}{\gamma}} = \frac{\left(\frac{P_I}{P_1} - \frac{P_L}{P_1}\right)^2\left(\frac{a_L}{a_1}\right)^2}{\frac{P_L}{P_1}\left(\frac{\gamma+1}{\gamma-1} + \frac{P_L}{P_1}\right)} \qquad (40)$$

For $M_1 = 0.6$ , $\frac{P_2}{P_1} = 2.19$ , $\left(\frac{a_2}{a_1}\right)^2 = 1.27$

Solving by trial: since $\frac{P_L}{P_1} = 0.41$ $\therefore \left(\frac{a_L}{a_1}\right)^2 = 0.775$ (isentropic reations)

$$\therefore P_I/P_1 = 0.995$$

Using (39) and solving for $u_1/a_1 = 0.535$

$$M_I = \frac{u_I}{a_I} = \frac{u_I}{a_2} \cdot \frac{a_2}{a_I} = \frac{u_I}{a_2}\left(\frac{P_2}{P_1} \cdot \frac{P_1}{P_I}\right)^{\frac{1}{7}}$$

$$= 0.535\left(\frac{2.19}{0.995}\right)^{\frac{1}{7}} = 0.60 \qquad \ldots(41)$$

Since $M_I = 0.60$ and $M_{II} = 0$

Then $P_{II}/P_I = 2.19$ . We see that the strength of the reflected wave = the strength of the incident shock wave. This could have been deduced from our assumptions since second order effects are neglected in order to linearize the equations of shock reflection. Since our shock wave is relatively weak, this can be done with little error.

Summarizing we have

$$P_L/P_2 = 0.41 \qquad \ldots(42)$$

$$P_I/P_2 = 0.993 \qquad \ldots(43)$$

$$P_{II}/P_I = 2.19 \qquad \ldots(44)$$

We see that the pressure in state (L) has dropped to a low level, but that after the passage of the shock wave the pressure in (I) is nearly equal to the original pressure in state (1) . Due to the fact that the particles in state (I) are travelling towards the inlet valve, a reflected wave further increases the pressure up to $P_{II}$ which nearly equals the pressure $P_2$ . The overall effect of the closing of the front valve produces an expansion wave which reduces the pressure and temperature level in the region of the front valve. It is in this region that we wish to initiate the detonation. Since the temperature is lowered, the possibility of forming a detonation wave is reduced.

In the actual case, the inlet valve will not close in zero time, but will require a time $\tau_v$ . Assume that the wave arrives at the inlet just as the valve has closed. The conditions are shown on the (x,t) plane in Figure 34. At the time $\tau_c$ , the inlet valve is closed and the tube contains the full charge per cycle. The density will not

be uniform throughout the tube since from point F to R the pressure will be decreased through the expansion wave. A correction will have to be applied to give the mass of air per cycle. The pressure at R (behind the incident wave, but in front of the reflected wave) will correspond to that in (I) for the previous case, or

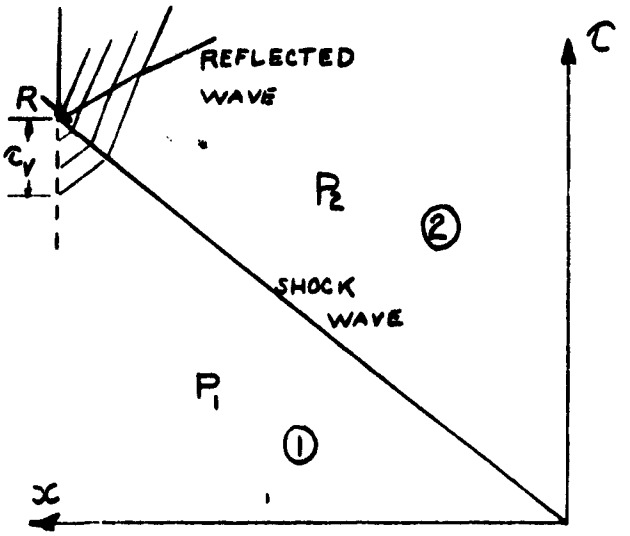


Figure 34

$$P_R = P_2 \qquad \ldots(45)$$

The distance $L_1$, from R to F is given by the distance the first signal travels in the time $\tau_v$. This is given approximately by

$$L_1 = \tau_v\, a_1 (1 + M_1) \qquad \ldots(46)$$

Assuming $\rho_R = \rho_1$ we can then find the mass of air in the tube.

## 4.3 Frictional Flow Losses

Two cases are investigated (1) the constant area duct; (2) the constant Mach number duct.

4.3.1 Pipe of Constant Area of Cross-section. In hydraulics the loss in head due to pipe friction is written

$$h_L = f \frac{L}{D} \frac{V^2}{2g} \qquad \ldots(47)$$

or $$\Delta P_L = f \frac{L}{D} \frac{1}{2} \rho V^2 \qquad \ldots(48)$$

where L = length of pipe
D = diameter of pipe

| PREPARED BY | AEROPHYSICS DEVELOPMENT CORPORATION | REPORT NO 2000-1-RJ |
|---|---|---|
| CHECKED BY | PACIFIC PALISADES, CALIFORNIA | DATE Jan 21 1953 |

FIGURE 35

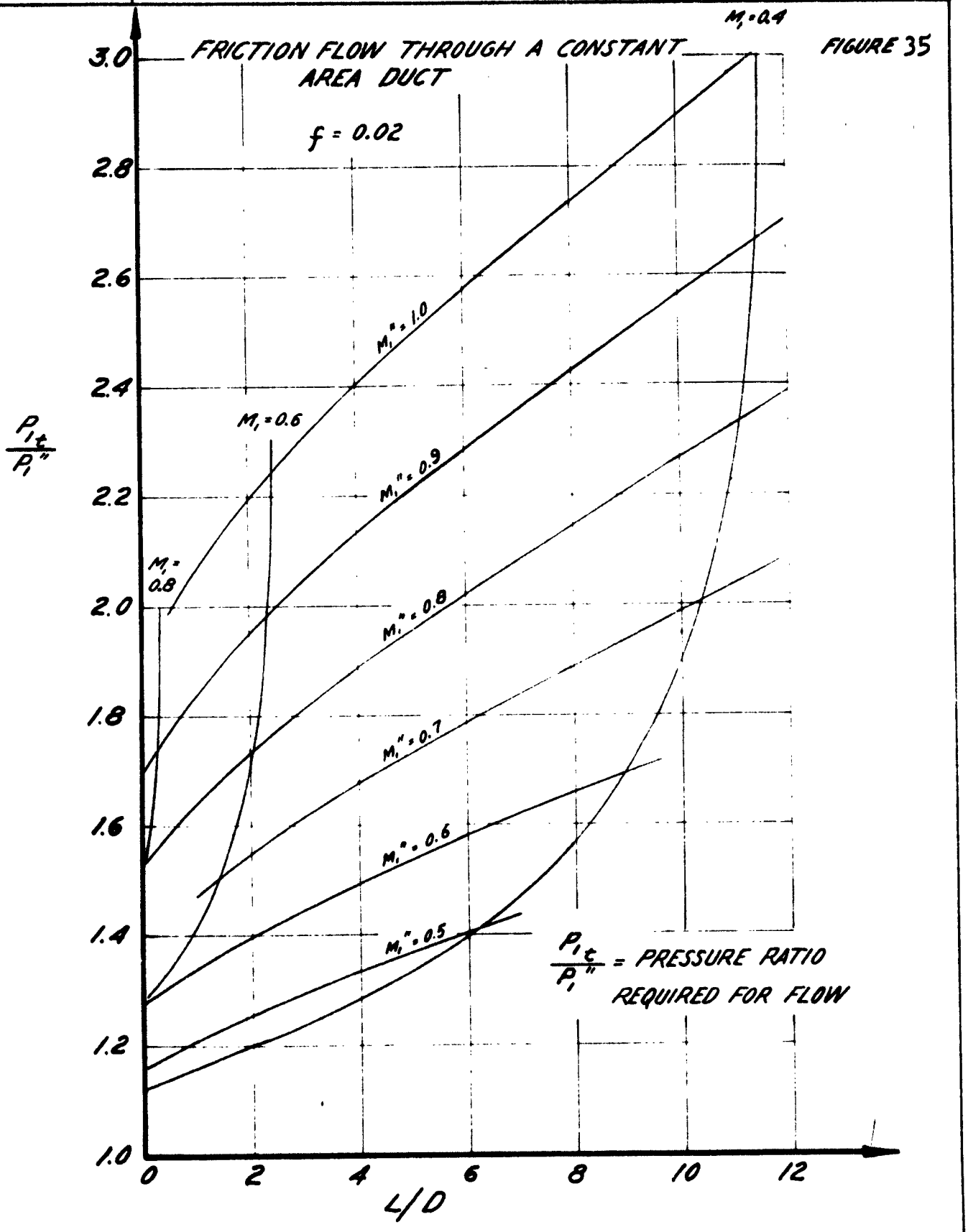

| PREPARED BY | AEROPHYSICS DEVELOPMENT CORPORATION | REPORT NO. 2000-1-R1 |
|---|---|---|
| CHECKED BY | PACIFIC PALISADES, CALIFORNIA | DATE Jan 24, 1953 |

For gas flows we write similarly, where $\Delta P_L$ = loss in total pressure.

$$\Delta P_L = f \frac{dL}{D} \frac{\gamma}{2} P M^2 \qquad \ldots(49)$$

$$\frac{2}{\gamma} \frac{1}{M_2} \frac{dP}{P} = \frac{f\, dL}{D} \qquad \ldots(50)$$

$$\frac{fL}{D} = \frac{2}{\gamma}\int_{M_1}^{M_1''} \frac{dP}{M^2 P} = \frac{2}{\gamma}\int_{M_1}^{'} \frac{dP}{M^2 P} - \frac{2}{\gamma}\int_{M_1''}^{'} \frac{dP}{M^2 P} = \Phi_1 - \Phi_1'' \qquad \ldots(51)$$

A flow with friction may be represented by a Fanno line ( $PV$ = constant) in the enthalpy-entropy diagram. These lines are tabulated by Keenan and Kaye (see Reference 5). (Note: Keenan and Kaye defines f such that $4f_{Keenan}$ = f hydr.) For $f_{hydr.} = 0.02$ and various inlet Mach Numbers the outlet Mach Numbers and the ratio of inlet total to exit static is plotted on Figure 35.

The curve shows that for the high values of $M_1 = 0.6$ the pressure ratio required to scavenge the tube must be $P_{t_1}/P_1'' > 1.38$ for $L/D = 25$ This value goes up to 2.25 for the $(L/D)_{MAX}$ for $M_1 = 0.6$. It is next to impossible to maintain such pressure ratios for a tube in flight and therefore it was decided to try a duct with variable cross-section or constant Mach Number.

4.3.2 Pipe with Constant Mach Number of the Flow.

Continuity $\rho U A$ = constant . . .(52)

Momentum $\frac{u^2}{2g} + \int \frac{dP}{\rho g} + h_L$ = constant . . .(53)

Energy $i + \frac{u^2}{2gJ}$ = constant . . .(54)

If $u$ = constant then from the energy equation

$i$ = constant = $c_p T$ . . .(55)

$T$ = constant

Since T = constant $\therefore$ M = constant

From the continuity equation

$$\frac{D_1''}{D_1} = \sqrt{\frac{\rho_1}{\rho_1''}} = \sqrt{\frac{P_1''}{P_1}} \quad \text{since } P = g\rho RT \qquad \ldots(56)$$

The total pressure variation is

$$\frac{P_t}{P} = \left[1 + \frac{\gamma - 1}{2} M^2\right]^{\frac{\gamma}{\gamma - 1}} = \text{constant} \qquad \ldots(57)$$

PREPARED BY | AEROPHYSICS DEVELOPMENT CORPORATION | REPORT NO 2000-1-R1
CHECKED BY | PACIFIC PALISADES, CALIFORNIA | DATE Jan 24, 1953

or $$\frac{P_{t_1}''}{P_{t_1}} = \frac{P_1''}{P_1} = \left(\frac{D_1}{D_1''}\right)^2 \qquad \ldots(58)$$

$d h_L = f \frac{dx}{D} \frac{u^2}{2g}$ and taking the momentum equation and differentiating

$$d h_L = f \frac{dx}{D} \frac{u^2}{2g} = -\frac{dP}{\rho g} \qquad \ldots(59)$$

$$\frac{dP}{\rho g} = RT \frac{dP}{P} = -RT\, 2 \frac{dD}{D} \qquad \ldots(60)$$

$$\therefore \frac{dD}{D} = \frac{\gamma f}{4} \frac{dx}{D} \frac{V^2}{\gamma R g T} \qquad \ldots(61)$$

$$D_1'' - D_1 = \frac{\gamma f}{4} \frac{x}{D_1} M_1^2$$

$$\frac{P_{t_1}''}{P_{t_1}} = \frac{P_1''}{P_1} = \left(\frac{D_1}{D_1''}\right)^2 = \frac{1}{\left(1 + \frac{\gamma f}{4} \frac{x}{D_1} M^2\right)^2} \qquad \ldots(62)$$

For a given flight velocity, there will be an optimum for each L/D ratio. This is due to the fact that the amount of pulse compression will increase with $M_d$ while the frictional losses in the duct will also increase with $M_d$. The ratio of final static pressure $P_2''$ over the inlet total pressure $P_{t_1}$ for various L/D ratios is plotted against $M_d$ in Figure 36. Similarly, the ratio of final static pressure $P_2''$ to inlet static pressure $P_o$ is shown in Figures 37, 38 and 39, for flight Mach Numbers $M_o$ = 0.25, 0.50 and 0.75 respectively.

Note that for L/D = 40, $P_2''/P_{t_1}$ has the maximum value at about $M_d$ = 0.52 and thus, if the free stream velocity is less than 0.52 it does not pay to expand the flow above $M_d$ = 0.52. The same thing is true if the free stream velocity is above 0.52.

It should be noted that the shock compression has the same pressure ratio regardless of its position in the tube, but since the initial pressure is different from front to rear, the absolute pressure in the tube after shock compression is not constant but varies from front to rear, that is $P_2 > P_2''$. This greater pressure in front of the tube is helpful during the expulsion phase in building up a flow towards the exit and helping overcome the exit flow losses. If the area of the duct to the exhaust nozzle is adjusted to the correct ratio then this pressure difference will give $M_d$ = 0.52, and assist in exhausting the tube.

There is a further loss due to the flow through the inlet valves. One type of inlet valve which has been explored consists of long slots around the circumference of the tube. The air will flow through the

| | | |
|---|---|---|
| CHECKED BY AB | AERONUTRONIC DEVELOPMENT CORPORATION<br>P.O. BOX 237 PACIFIC PALISADES CALIFORNIA | 2000-1-R1<br>DATE Jan 24 1953 |

FIGURE 36

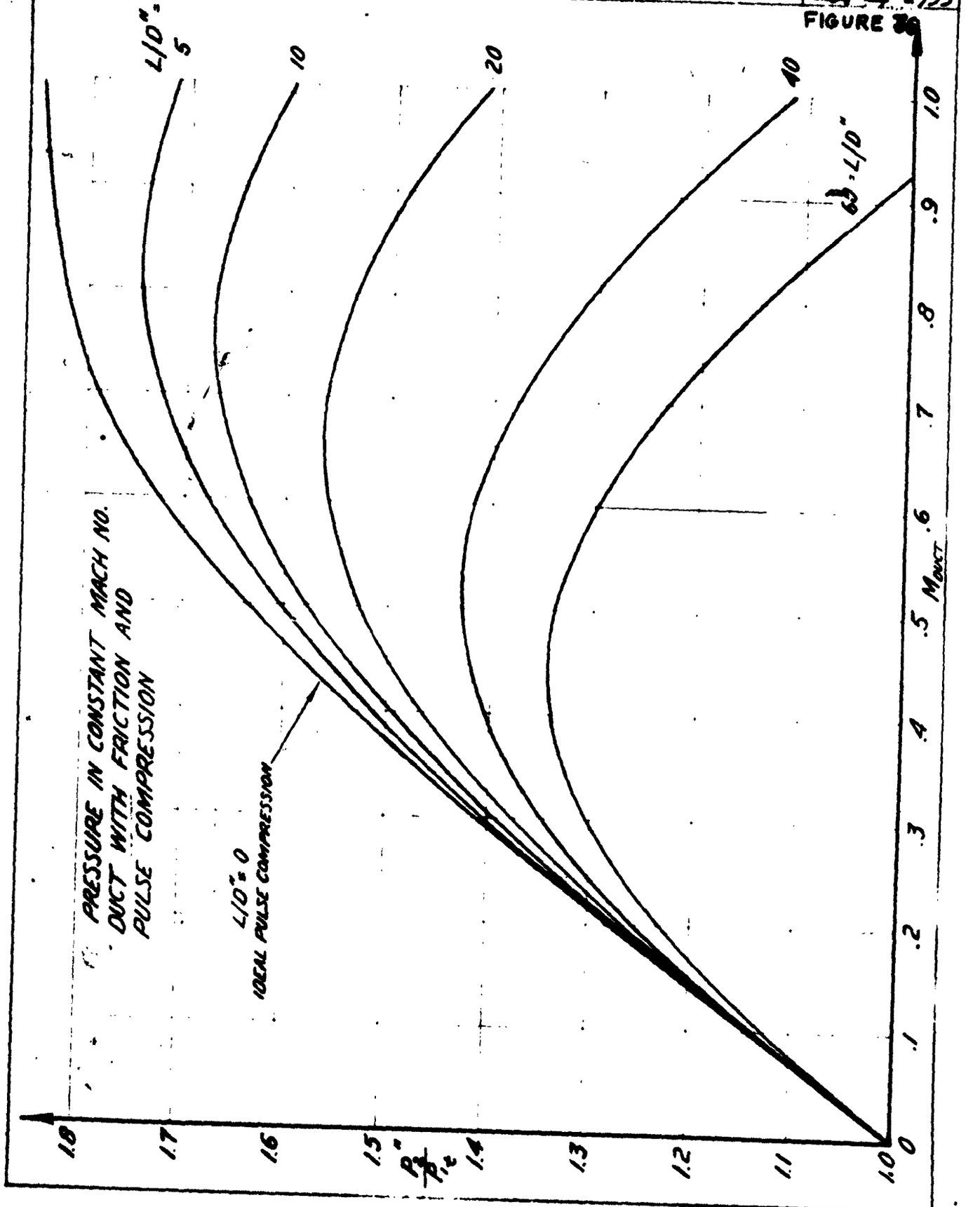

| PREPARED BY | AEROPHYSICS DEVELOPMENT CORPORATION | REPORT NO 2000-1-R1 |
|---|---|---|
| CHECKED BY | PACIFIC PALISADES, CALIFORNIA | DATE Jan 24 1953 |

STATIC PRESSURE IN CONSTANT MACH NO. DUCT WITH FRICTIONAL LOSSES

FIGURE 37

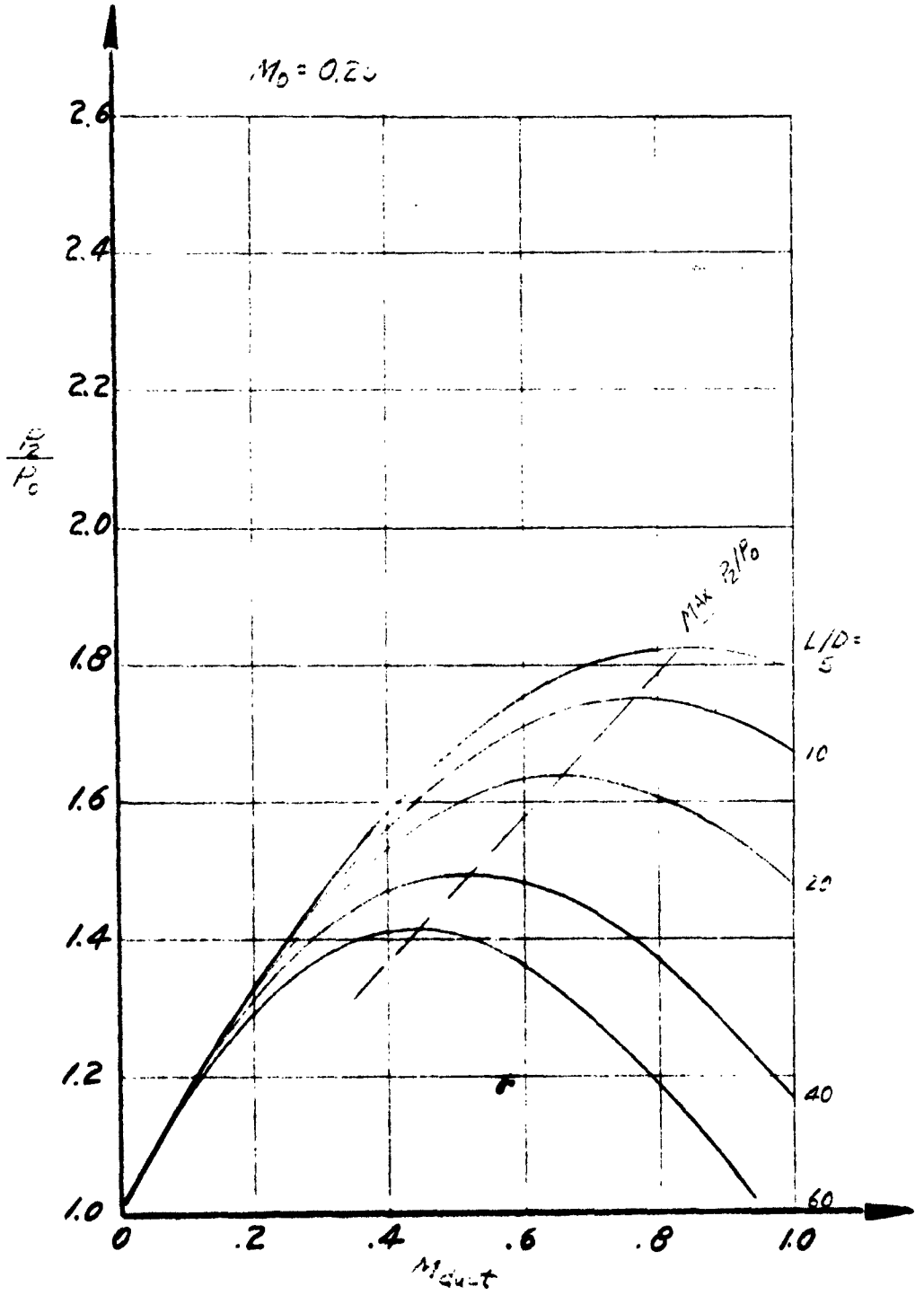

| PREPARED BY | AEROPHYSICS DEVELOPMENT CORPORATION | REPORT NO. 2000-1-R1 |
|---|---|---|
| CHECKED BY | PACIFIC PALISADES, CALIFORNIA | DATE Jan 2[illegible], 1953 |

STATIC PRESSURE IN CONSTANT MACH NO. DUCT WITH FRICTIONAL LOSSES

FIGURE 38

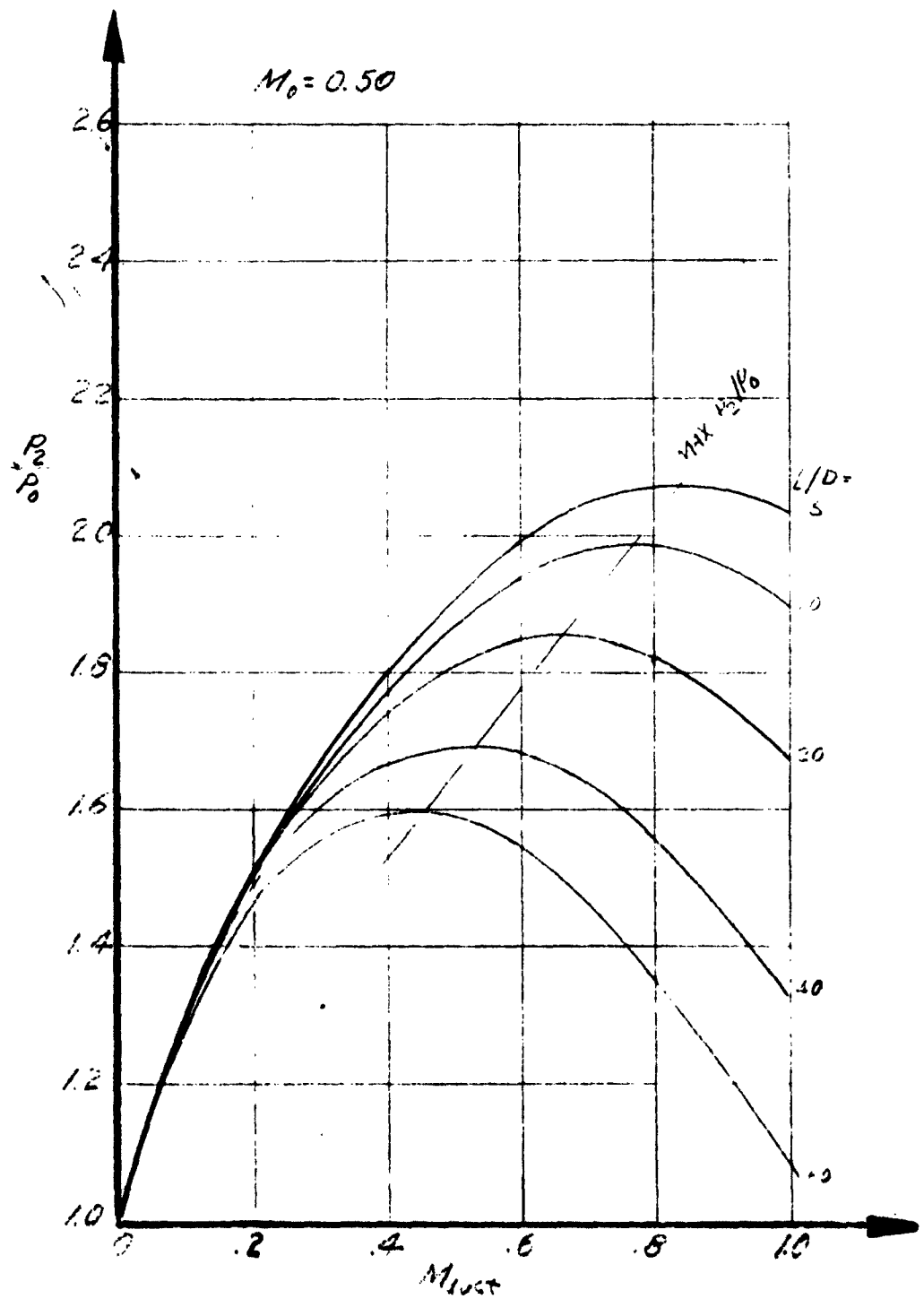

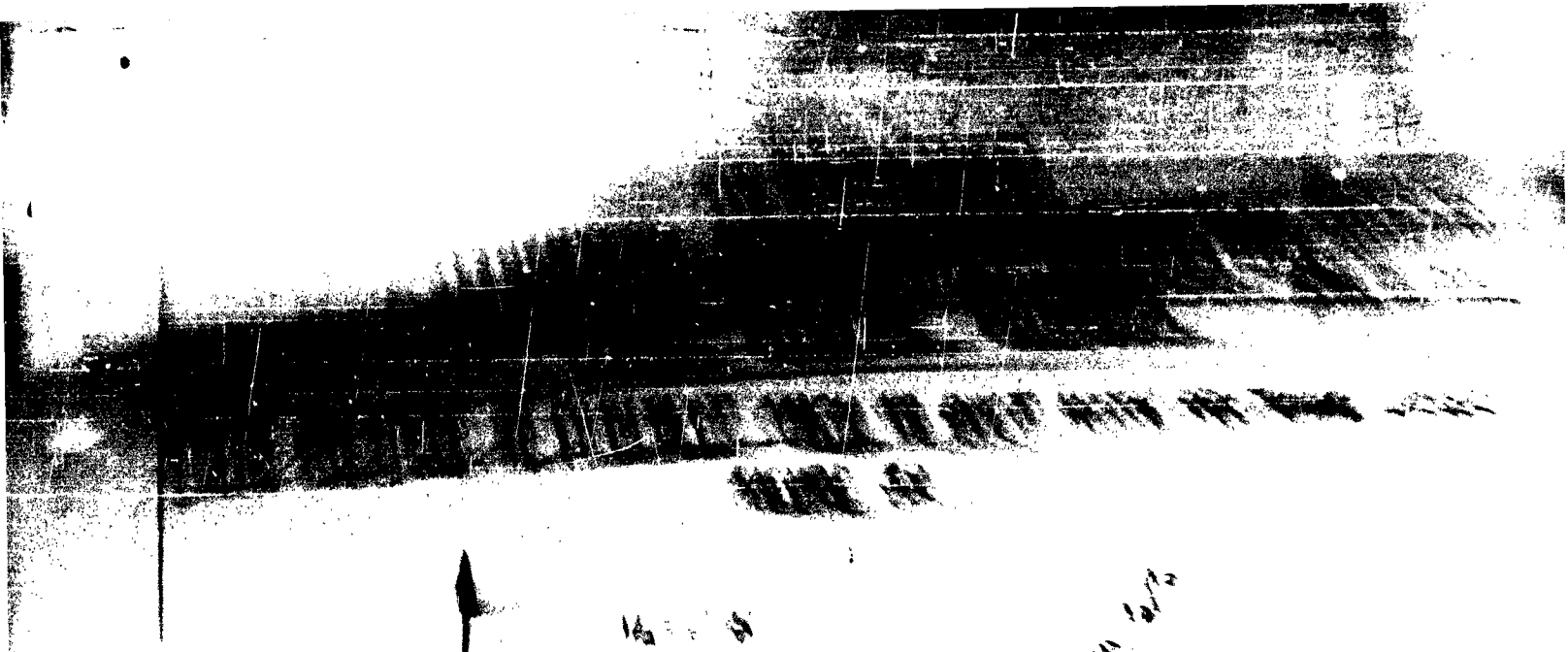

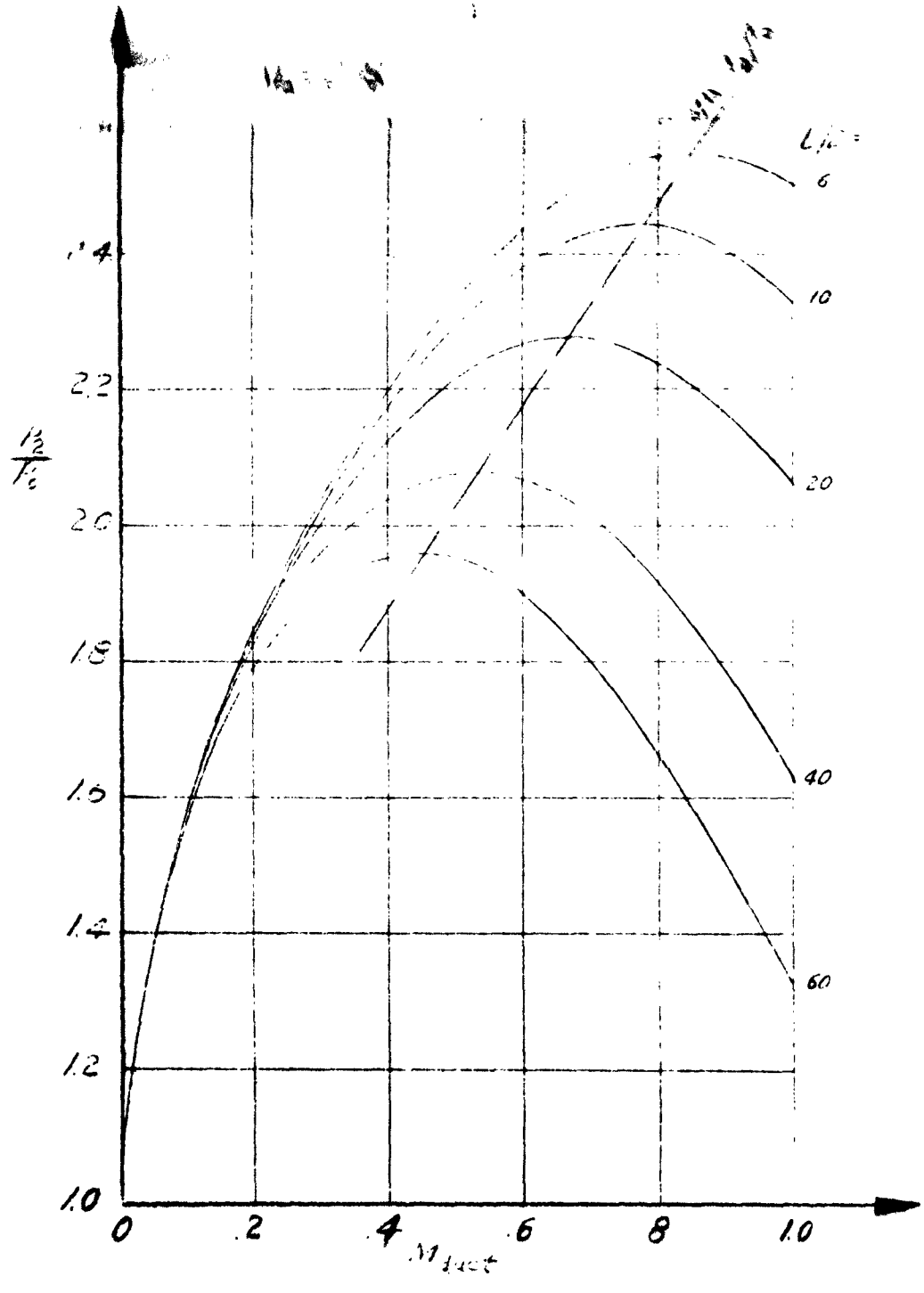

| PREPARED BY | AEROPHYSICS DEVELOPMENT CORPORATION | REPORT NO. 2000-1-R1 |
|---|---|---|
| CHECKED BY | PACIFIC PALISADES, CALIFORNIA | DATE Jan 2[illegible] 1953 |

STATIC PRESSURE IN CONSTANT MACH NO. DUCT WITH FRICTIONAL LOSSES

FIGURE 39

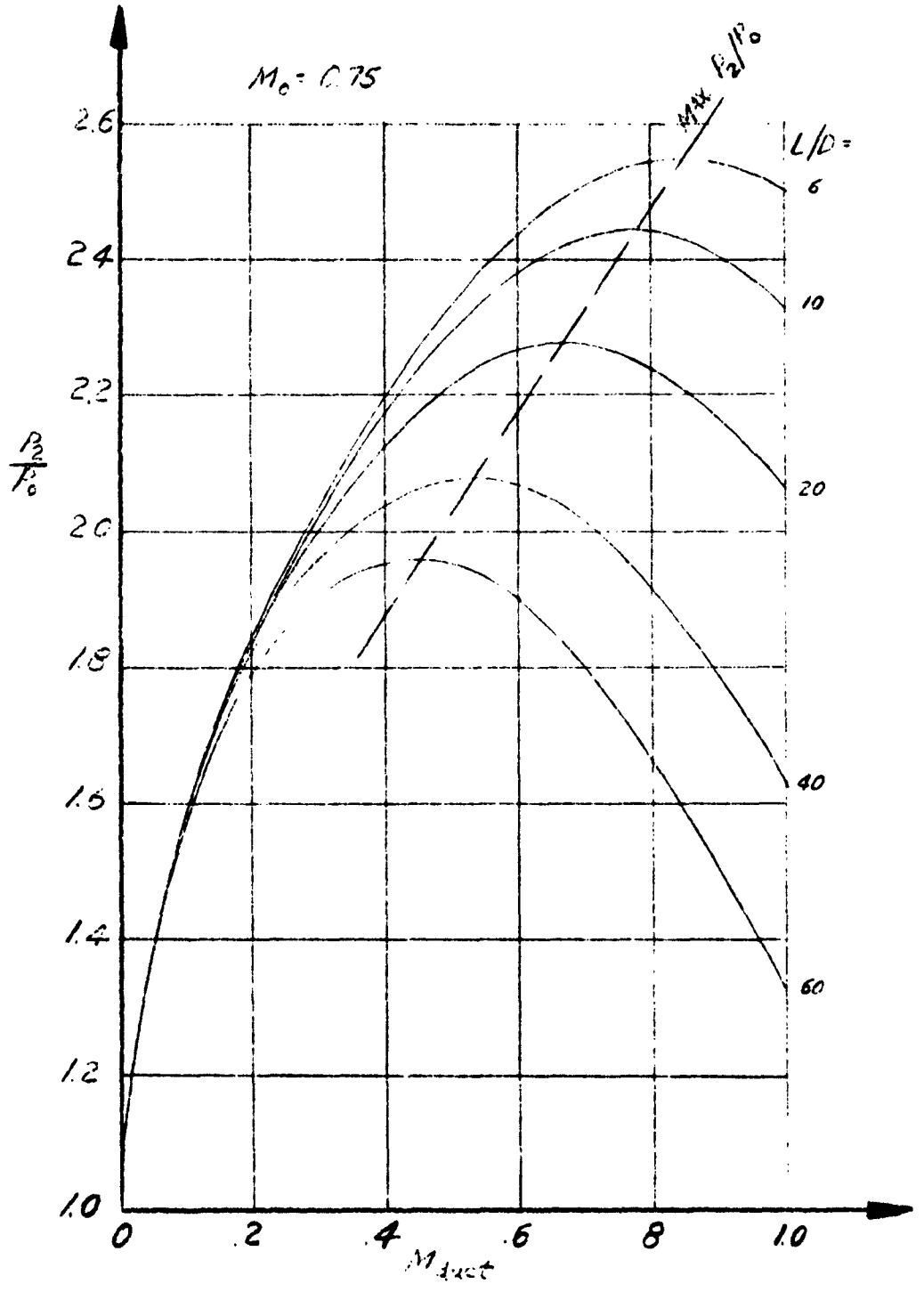

slots at an oblique angle and the area of opening will be such that the normal component of Mach Number = 0.2. Assuming the slots are 0.5" wide, spaced at intervals of 0.60" (see sketch on this page) the pressure loss is computed from the loss upon sudden enlargement.

Loss in head

$$h_L = \left[1 - \frac{A_x}{A_Y}\right] \frac{u_x^2}{2g} = 0.55 \frac{u_1^2}{2g} \quad \ldots(63)$$

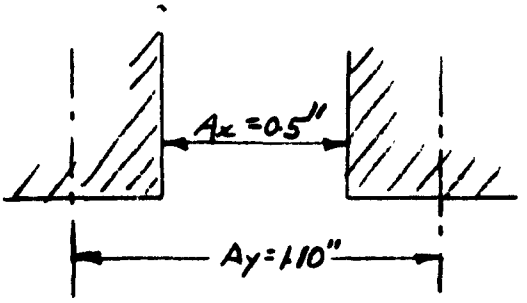


Configuration of Slots

$$\Delta P = \rho g h_L = 0.55 \frac{\rho u^2}{2} \quad \ldots(64)$$

$$\frac{\Delta P}{P} = 0.55 \frac{\gamma M_x^2}{2} = 0.385 M_x^2 \quad \ldots(65)$$

For $M_x = 0.2$

$$\frac{\Delta P_t}{P_t} = 0.0154 \quad \ldots(66)$$

## 4.4 Performance Computations of an Actual Cycle

Before the performance analysis of an actual cycle is carried out, it is necessary to define the following concepts: (1) Effective exit velocity (2) Actual mass flow per cycle.

4.4.1 Effective Exit Velocity. The impulse due to the discharge of a jet with varying exit velocity $u_N$

$$I = \int_{P_0}^{P_3} u_N \, dm \quad \ldots(67)$$

Define an effective exit velocity $\bar{u}_e$ such that

$$\bar{u}_e = \int_{P_0}^{P_3} u_N \frac{dm}{m_{TOT}} \quad \ldots(68)$$

$$m_{TOT} \bar{u}_e = I \quad \text{or} \quad \frac{\bar{u}_e}{a_3} = \frac{I}{P_3 a_3 V_{OL}} \quad \ldots(69)$$

This is obtained from Figure 9 and is plotted on Figure 40. Therefore, the average thrust per cycle is

$$F = \frac{w_a}{g}\left[\bar{u}_e - u_0\right] \quad \ldots(70)$$

where $w_a$ = pounds of air per sec.

RESTRICTED

AEROPHYSICS DEVELOPMENT CORPORATION

PACIFIC PALISADES, CALIFORNIA

REPORT NO. 2000-1-R1

DATE Jan 24 1953

FIGURE 40

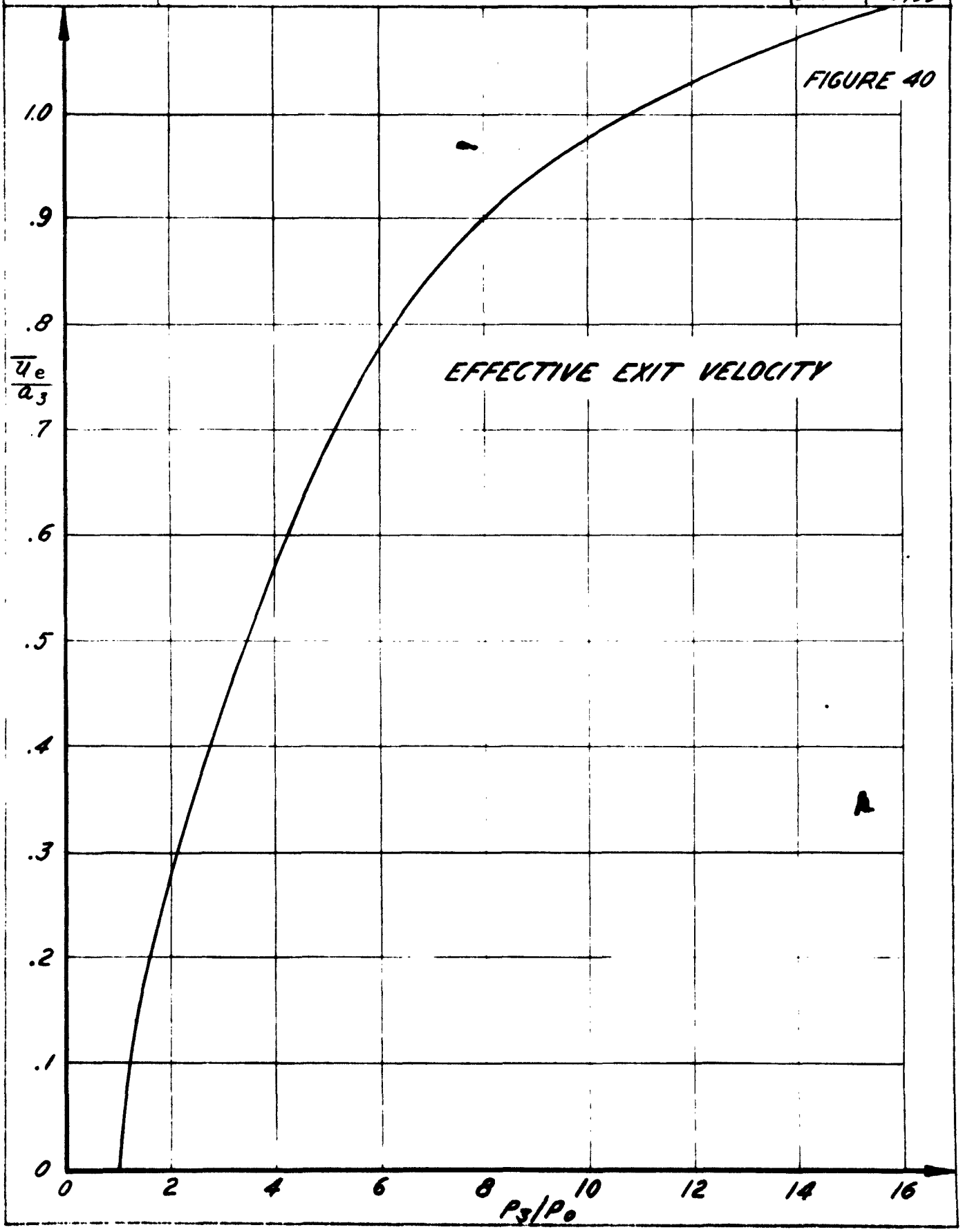






RESTRICTED

$u_o$ = flight velocity

The air specific impulse is given by

$$\frac{I_a}{\sqrt{\theta}} = \frac{F}{w_2\sqrt{\theta}} = \frac{a_{SL}}{g}\left[\frac{u_e}{a_3}\cdot\frac{a_3}{a_o} - M_o\right] \quad \ldots(71)$$

4.4.2 Weight Flow per Cycle. The weight flow per cycle = $\rho_{cyc} \cdot V$ where $\rho_{cyc}$ is the average density in the tube at the instant the valves are closed. In order to calculate this density take the conditions at the instant the front valve has closed. The density will vary from $\rho_2''$ at the rear to $\rho_2$ at the inlet.

$$\rho_{AVG} = \frac{\rho_2 + \rho_2''}{2} \quad \ldots(72)$$

On top of this there is a further reduction of the density at the front end due to the expansion sent out by the inlet valve. Assume the density varies linearly from $\rho_2$ to $\rho_1$ at the valve over a length of $L_1$ (See equation 46).
The mass in the tube is given by

$$m_t = \frac{\rho_2 + \rho_1}{2} L_1 D + \rho_2 (L - L_1) D \quad \ldots(73)$$

This reduces to

$$m_t = \left[1 - \frac{\rho_2 - \rho_1}{2\rho_2}\frac{L_1}{L}\right]\rho_2 V \quad \ldots(74)$$

The average density is then given by

$$\rho_{cyc} = \rho_{AVG}\left[1 - \frac{\rho_2 - \rho_1}{2\rho_2}\frac{L_1}{L}\right]\rho_2 V \quad \ldots(75)$$

where $L_1$ is given by equation (46).

The cycle is made up of four phases-- scavenging, pulse compression, burning and exhausting. The time required for scavenging and pulse compression depends on the length of the duct and the Mach Number and temperature of the flow in the duct.

$$\frac{\tau_3}{L}\sqrt{\theta} = \frac{1}{M_d a_{SL}}\sqrt{\frac{T_o}{T_1}} \quad \ldots(76)$$

$$\frac{\tau_c}{L}\sqrt{\theta} = \frac{1}{M_w a_{SL}}\sqrt{\frac{T_o}{T_1}} \quad \ldots(77)$$

where $M_w = f(M_d)$ and is given in Figure 2.

Equations (76) and (77) are plotted on Figure 41. For no diffusion in the duct $T_1/T_o = 1$ The duration of the exhaust phase is given in Figure 4.

AERO
KED
AEROPHYSICS DEVELOPMENT CORPORATION
PACIFIC PALISADES, CALIFORNIA
REPORT NO 2000-1-R1
DATE Jan. 24 1953

$u_o$ = flight velocity

The air specific impulse is given by

$$\frac{S_a}{\sqrt{\theta}} = \frac{F}{w_a\sqrt{\theta}} = \frac{a_{SL}}{g}\left[\frac{\bar{u}_e}{a_3}\cdot\frac{a_3}{a_o} - M_o\right] \quad \ldots(71)$$

4.4.2 Weight Flow per Cycle. The weight flow per cycle = $\rho_{cyc} \cdot V$ where $\rho_{cyc}$ is the average density in the tube at the instant the valves are closed. In order to calculate this density take the conditions at the instant the front valve has closed. The density will vary from $\rho_2''$ at the rear to $\rho_2$ at the inlet.

$$\rho_{AVG} = \frac{\rho_2 + \rho_2''}{2} \quad \ldots(72)$$

On top of this there is a further reduction of the density at the front end due to the expansion sent out by the inlet valve. Assume the density varies linearly from $\rho_2$ to $\rho_1$ at the valve over a length of $L_1$ (See equation 46).
The mass in the tube is given by

$$m_t = \frac{\rho_2 + \rho_1}{2} L_1 D + \rho_2 (L - L_1) D \quad \ldots(73)$$

This reduces to

$$m_t = \left[1 - \frac{\rho_2 - \rho_1}{2\rho_2}\frac{L_1}{L}\right]\rho_2 V \quad \ldots(74)$$

The average density is then given by

$$\rho_{cyc} = \rho_{AVG}\left[1 - \frac{\rho_2 - \rho_1}{2\rho_2}\frac{L_1}{L}\right]\rho_2 V \quad \ldots(75)$$

where $L_1$ is given by equation (46).

The cycle is made up of four phases-- scavenging, pulse compression, burning and exhausting. The time required for scavenging and pulse compression depends on the length of the duct and the Mach Number and temperature of the flow in the duct.

$$\frac{\tau_3}{L}\sqrt{\theta} = \frac{1}{M_d a_{SL}}\sqrt{\frac{T_o}{T_1}} \quad \ldots(76)$$

$$\frac{\tau_c}{L}\sqrt{\theta} = \frac{1}{M_w a_{SL}}\sqrt{\frac{T_o}{T_1}} \quad \ldots(77)$$

where $M_w = f(M_d)$ and is given in Figure 2.

Equations (76) and (77) are plotted on Figure 41. For no diffusion in the duct $T_1/T_o = 1$ The duration of the exhaust phase is given in Figure 4.

| PREPARED BY | AEROPHYSICS DEVELOPMENT CORPORATION | REPORT NO 2000-1-R1 |
|---|---|---|
| CHECKED BY | PACIFIC PALISADES, CALIFORNIA | DATE Jan 24 1953 |

FIGURE 41

## DURATION OF PULSE COMPRESSION AND SCAVENGING

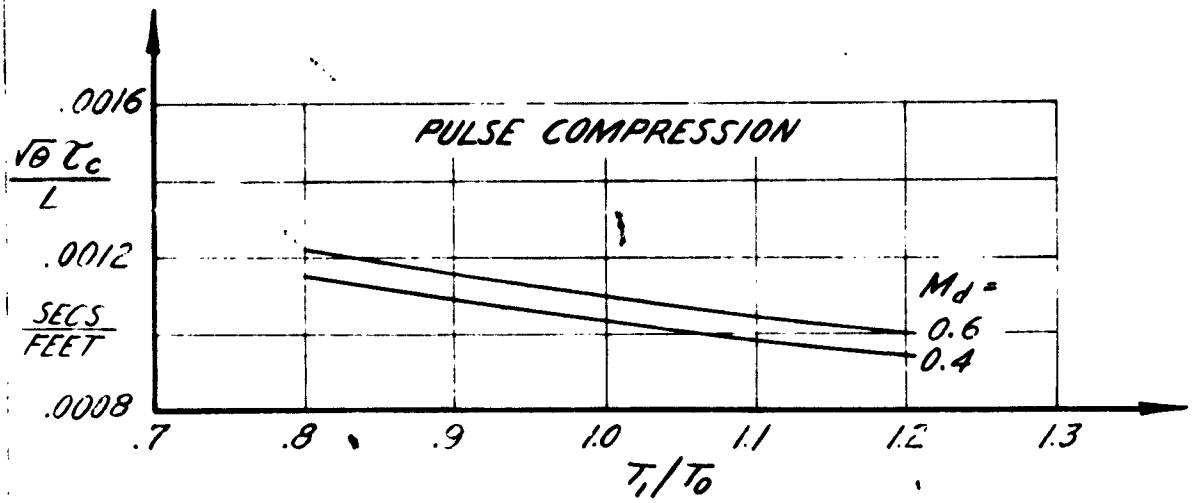


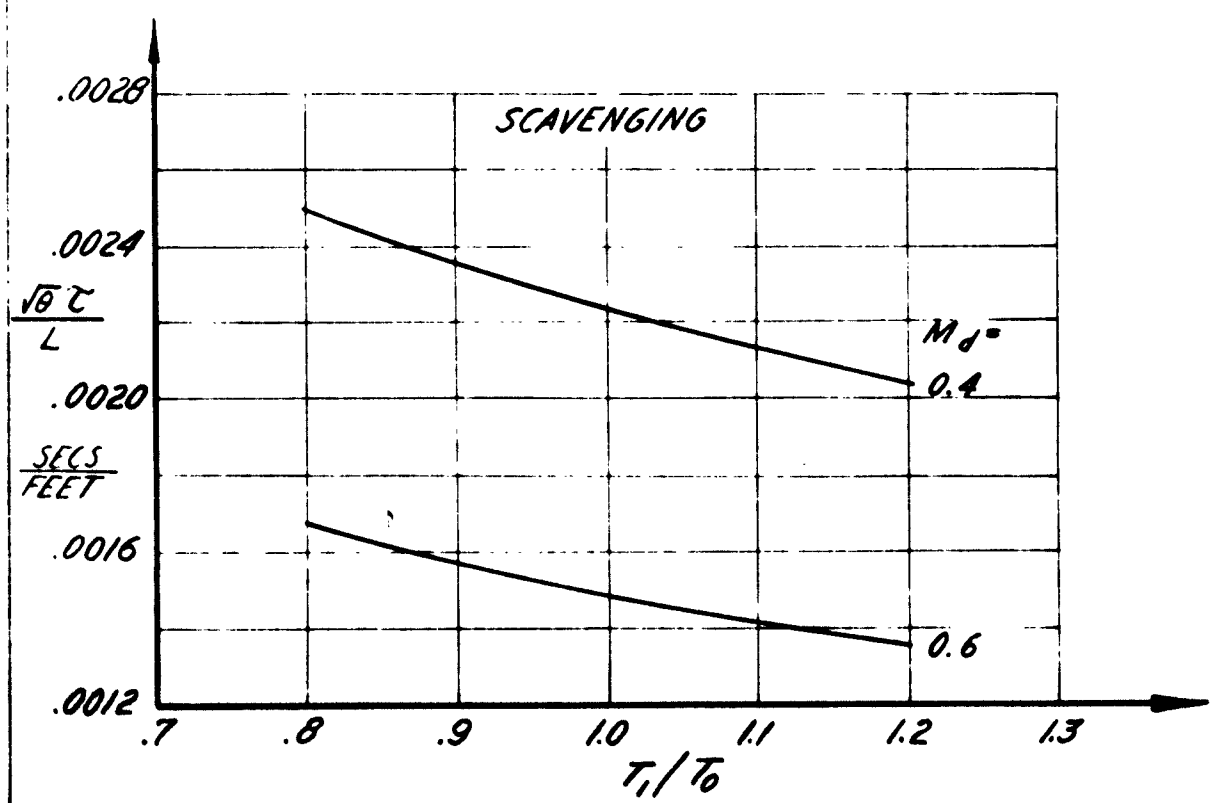

The duration of burning was taken as a constant value for all cases. $\tau_B$ = 0.010 secs.

The fuel-air ratio is obtained from Figure 42. These curves are obtained from the following equations. The enthalpy rise $h_3 - h_2$ due to the burning of a fuel with air is given by

$$\left[\frac{w_a}{w_f} + 1\right](h_3 - h_4) = H_{600°R} - 112 - h_{f\,600°R} \quad \ldots(76)$$

where $\frac{w_a}{w_f}$ = air-fuel ratio

$H_{600°R}$ = heating value of fuel = 18,500 BTU per lb.
112 = average value of $h_{2\,(450\text{ to }750°R)}$ BTU per lb.
$h_{f\,600°R}$ = - 116 BTU per lb.
This curve is plotted on the right hand side of Figure 42. The curves on the left hand side of Figure 42 are obtained by interpolating the tables from Keenan and Kaye. (Reference 5)

The specific fuel consumption is given by the following equation

$$\frac{f}{\sqrt{\theta}} = 3600\ \frac{w_f}{w_a}\ \frac{1}{S_a} \quad \ldots(77)$$

The thrust coefficient is given by

$$C_T = \frac{F}{A}\ \frac{1}{\delta} \quad \ldots(80)$$

and is based on combustion tube area.
The characteristic mass flow for a single tube is given by

$$X = \frac{F}{A} \cdot \frac{1}{S_a} \cdot \frac{\sqrt{\frac{T_{oc}}{520}}}{\frac{P_{oc}}{2116}} \quad \ldots(81)$$

4.4.3 Performance Computations. The performance characteristics of a single tube operating under the assumptions as described in Part 4.1 of this Section are given in Figures 43 to 57. The thrust per square foot of frontal area (or combustion tube area), the specific fuel consumption, the air specific impulse, the thrust coefficient (based on the combustion tube areas) and the characteristic mass flow (based on the combustion tube areas are plotted against $L/D$ or $\frac{\text{length}}{\text{diameter}}$ ratios) for various duct diameters. Three flight Mach numbers $M_o$ are used - 0.25, 0.50 and 0.75; two values of duct Mach number - 0.40 and 0.60; two values of the maximum cycle temperature - 2960°R and 1960°R are used; and three duct diameters - 12 inches, 6 inches, and 4 inches. It is assumed that diffusion from $M_o$ to $M_1$ has an efficiency of 100%. Appendix II gives a description of the method of computing the performance for this case.

| PREPARED BY | AEROPHYSICS DEVELOPMENT CORPORATION | REPORT NO 2000-1-R1 |
|---|---|---|
| CHECKED BY | PACIFIC PALISADES, CALIFORNIA | DATE Jan 24, 1953 |

FIGURE 42

## FUEL AIR RATIO

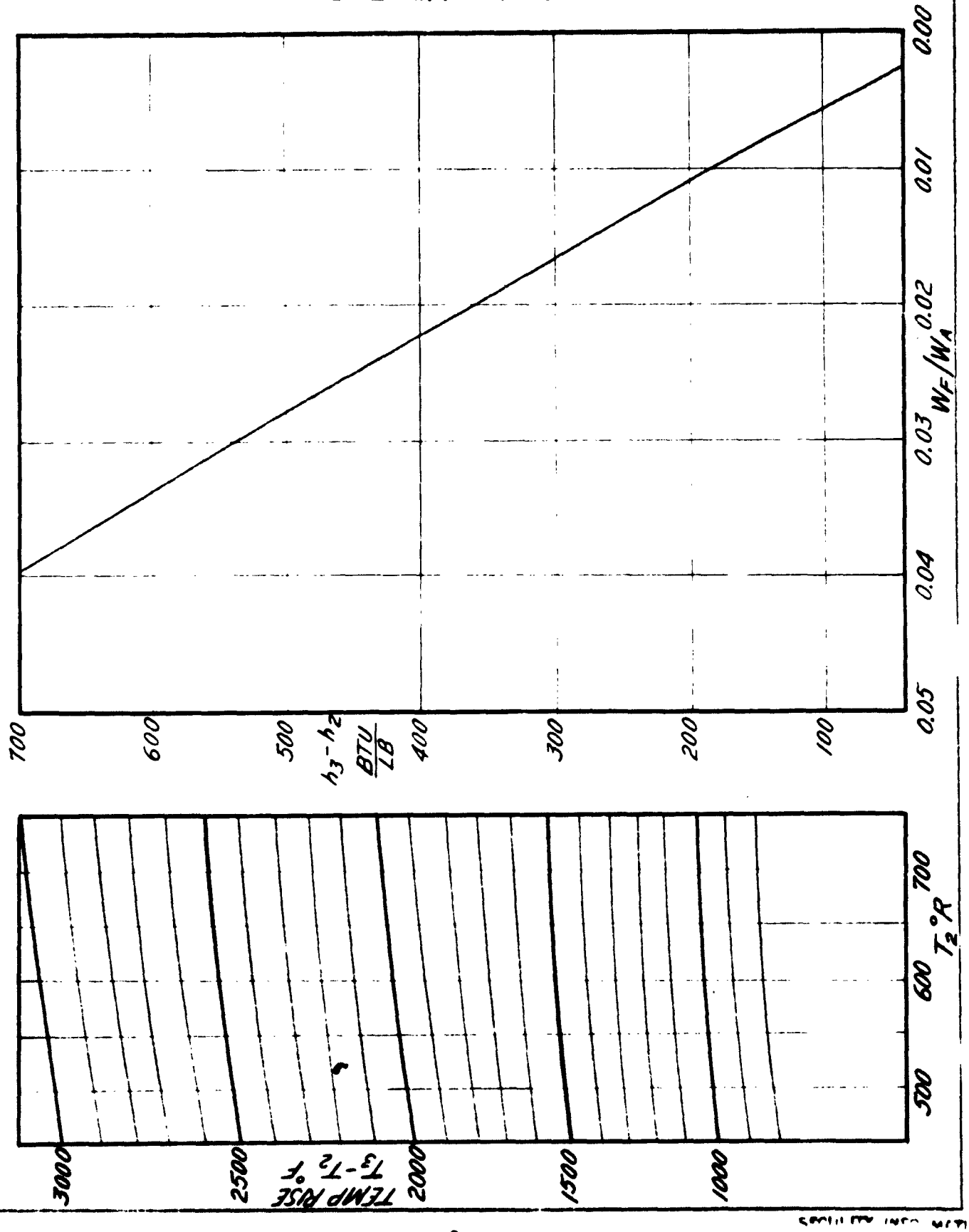

| PREPARED BY | AEROPHYSICS DEVELOPMENT CORPORATION | REPORT NO 2000-1-R1 |
|---|---|---|
| CHECKED BY | PACIFIC PALISADES, CALIFORNIA | DATE: Jan 24 1953 |

FIGURE 43

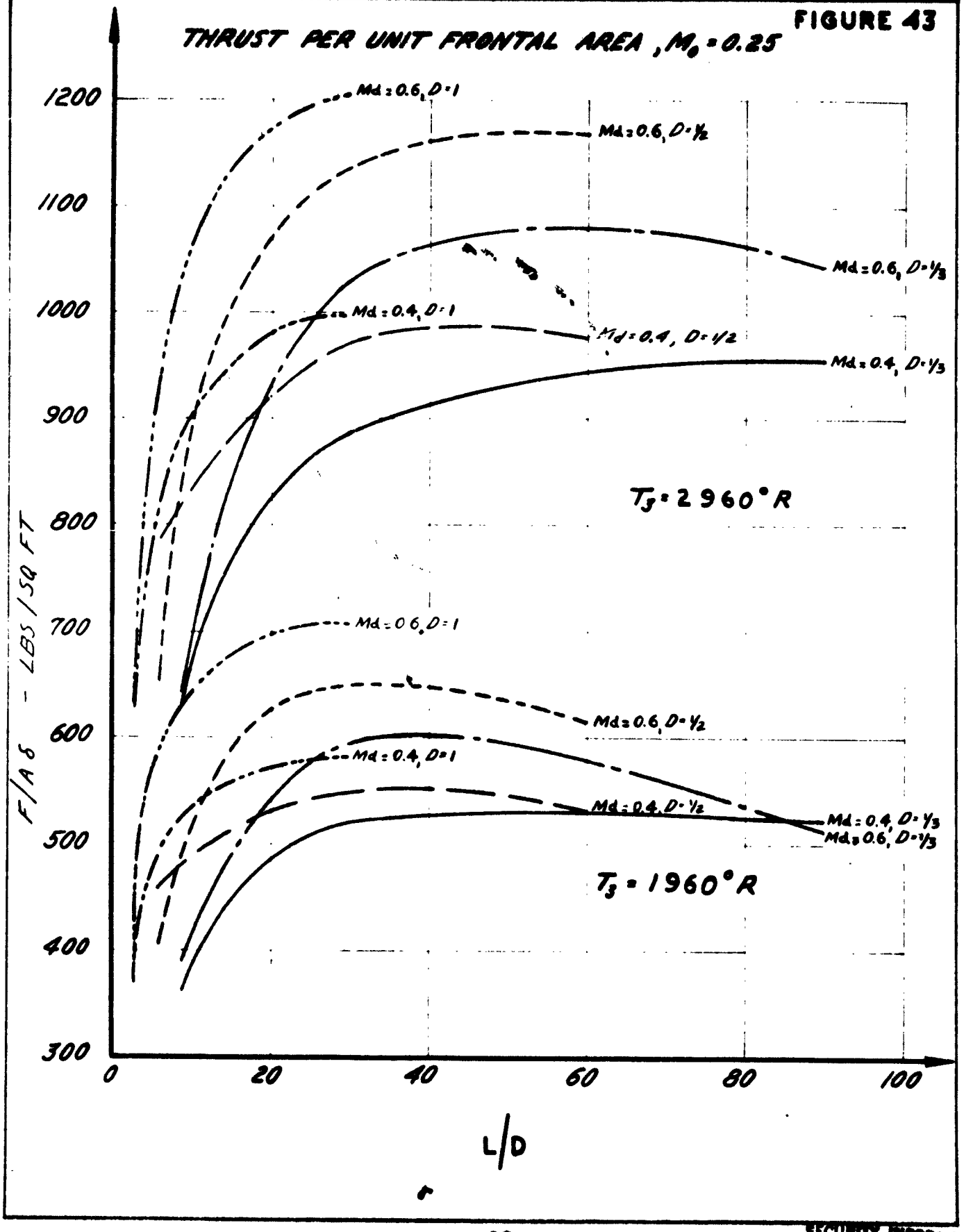

FIGURE 44

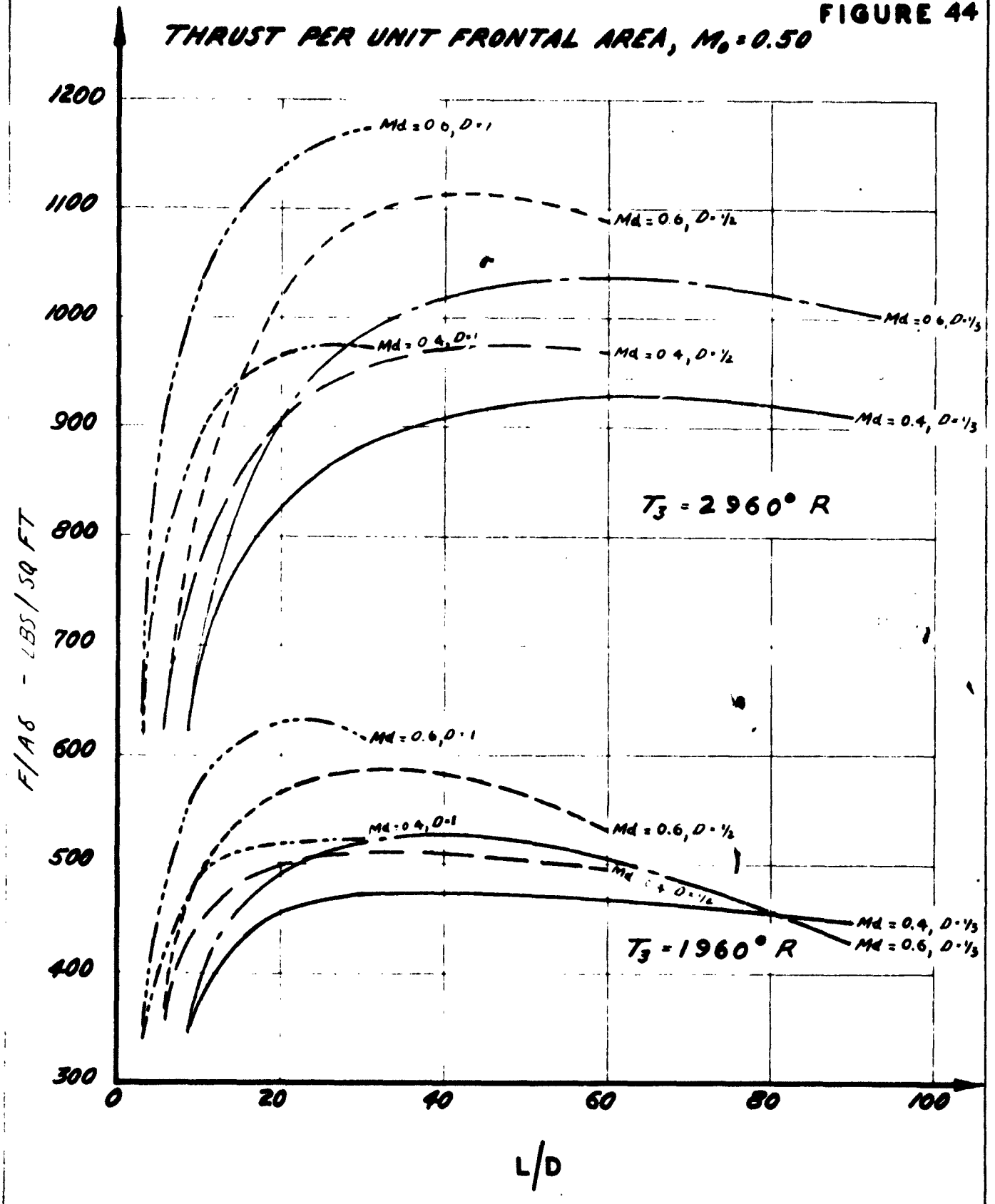

| | | |
|---|---|---|
| PREPARED BY | [redacted] DEVELOPMENT CORPORATION | REPORT NO 2000-1-R1 |
| CHECKED BY | PACIFIC PALISADES, CALIFORNIA | DATE Jan 24 1953 |

FIGURE 45

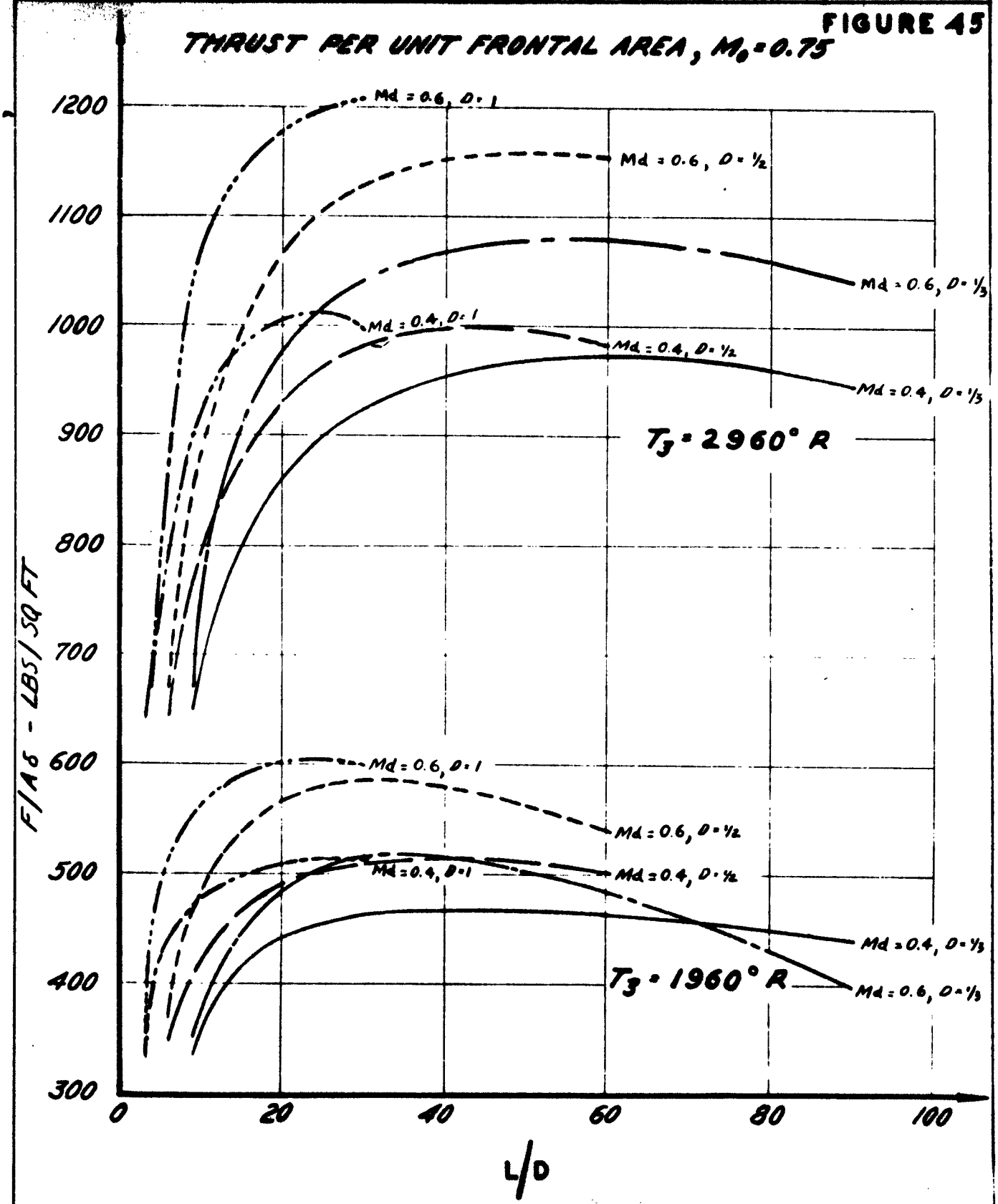

| PREPARED BY | AEROPHYSICS DEVELOPMENT CORPORATION | REPORT NO. 2000-1-R1 |
|---|---|---|
| CHECKED BY | PACIFIC PALISADES, CALIFORNIA | DATE: Jan 24 1953 |

FIGURE 46

## SPECIFIC FUEL CONSUMPTION
## $M_0 = 0.25$

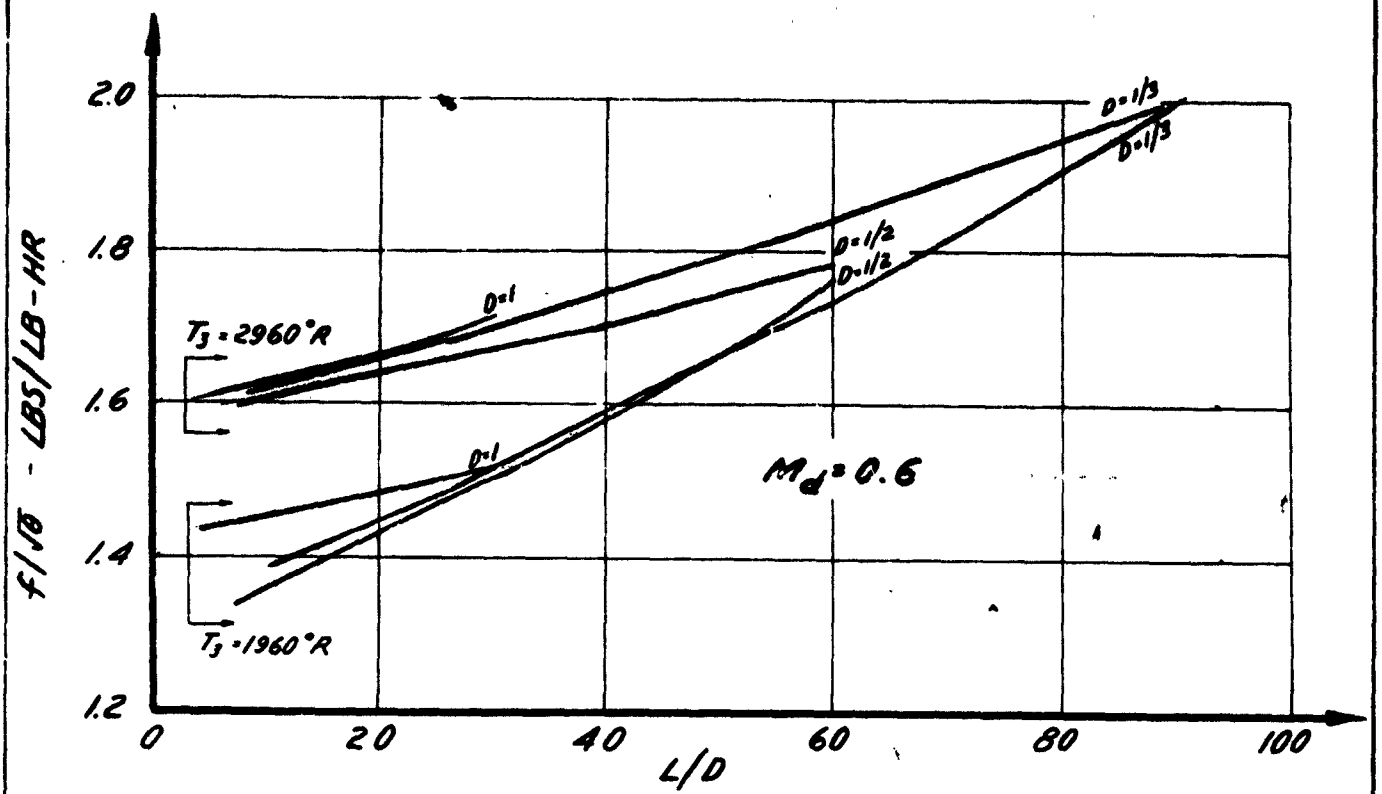


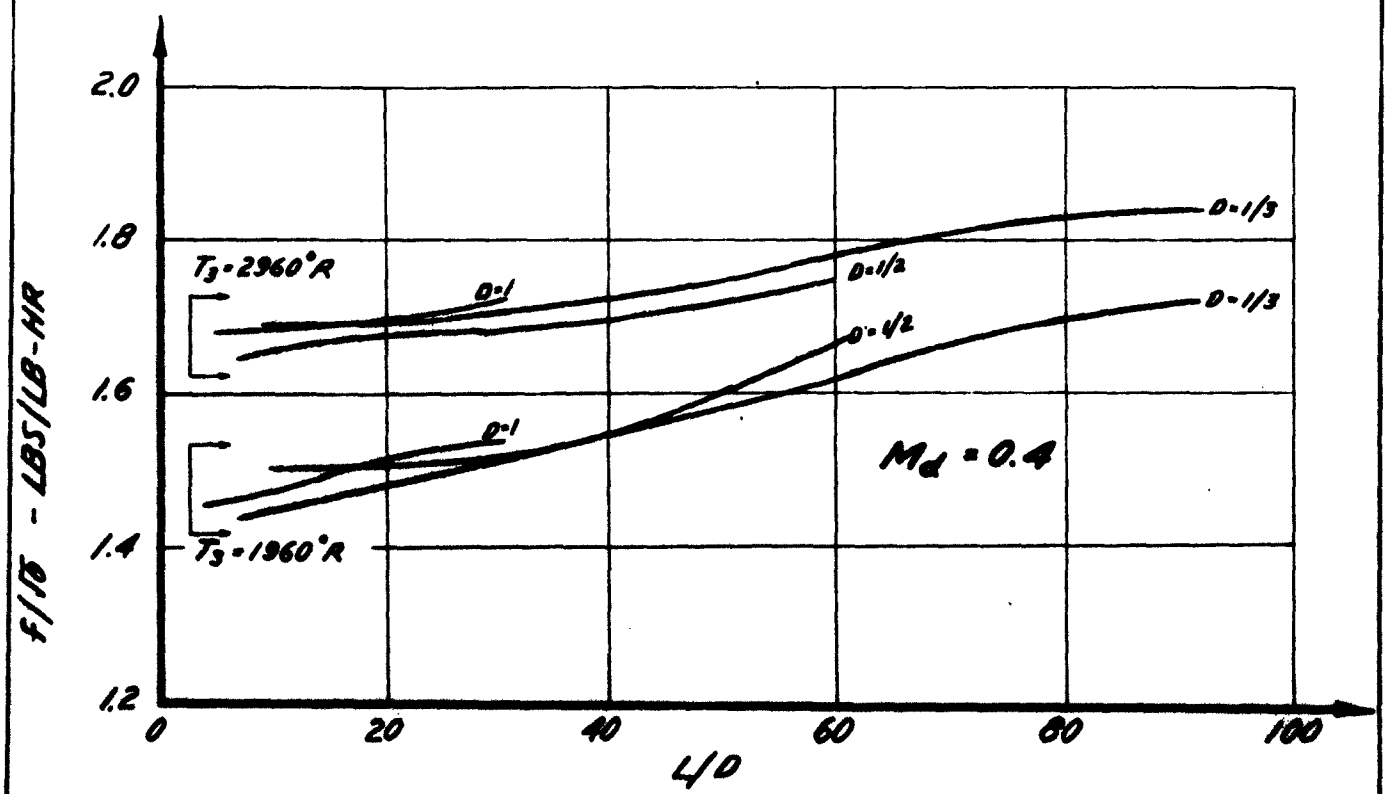

| PREPARED BY | AEROPHYSICS DEVELOPMENT CORPORATION | REPORT NO 2000-1-R1 |
|---|---|---|
| CHECKED BY: | PACIFIC PALISADES, CALIFORNIA | DATE: Jan 21 1953 |

FIGURE 47

## SPECIFIC FUEL CONSUMPTION
$M_\infty = 0.50$

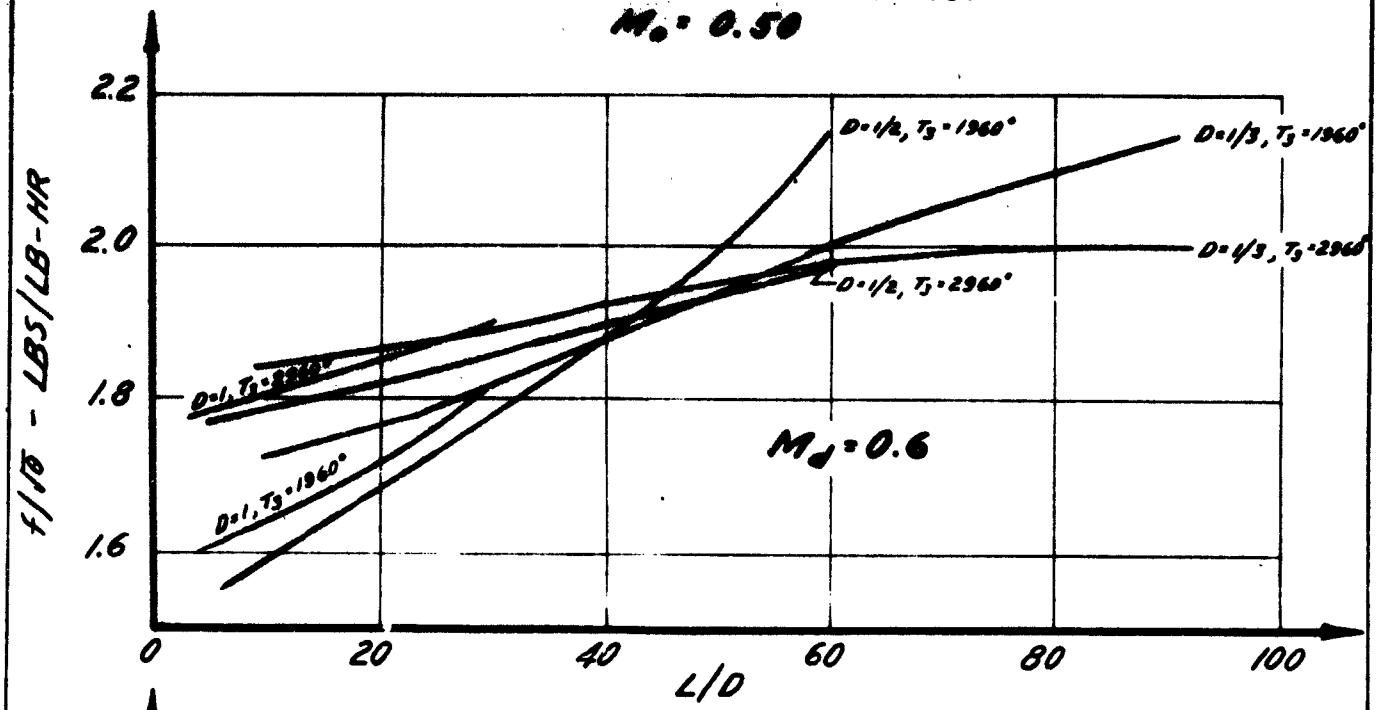


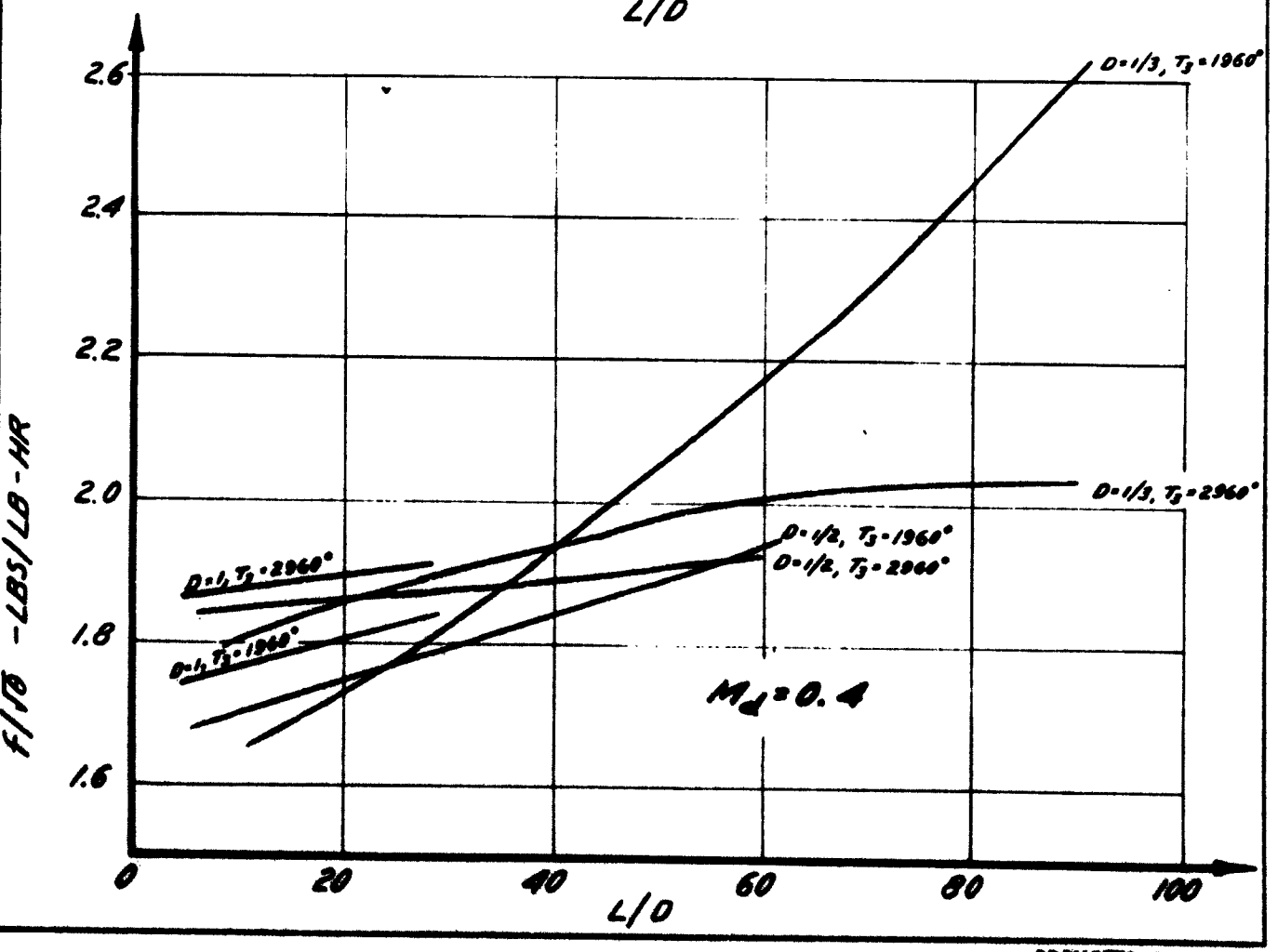

| PREPARED BY | AEROPHYSICS DEVELOPMENT CORPORATION | REPORT NO 2000-1-R1 |
|---|---|---|
| CHECKED BY | PACIFIC PALISADES, CALIFORNIA | DATE Jan 24 1953 |

FIGURE 48

## SPECIFIC FUEL CONSUMPTION
$M_0 = 0.75$

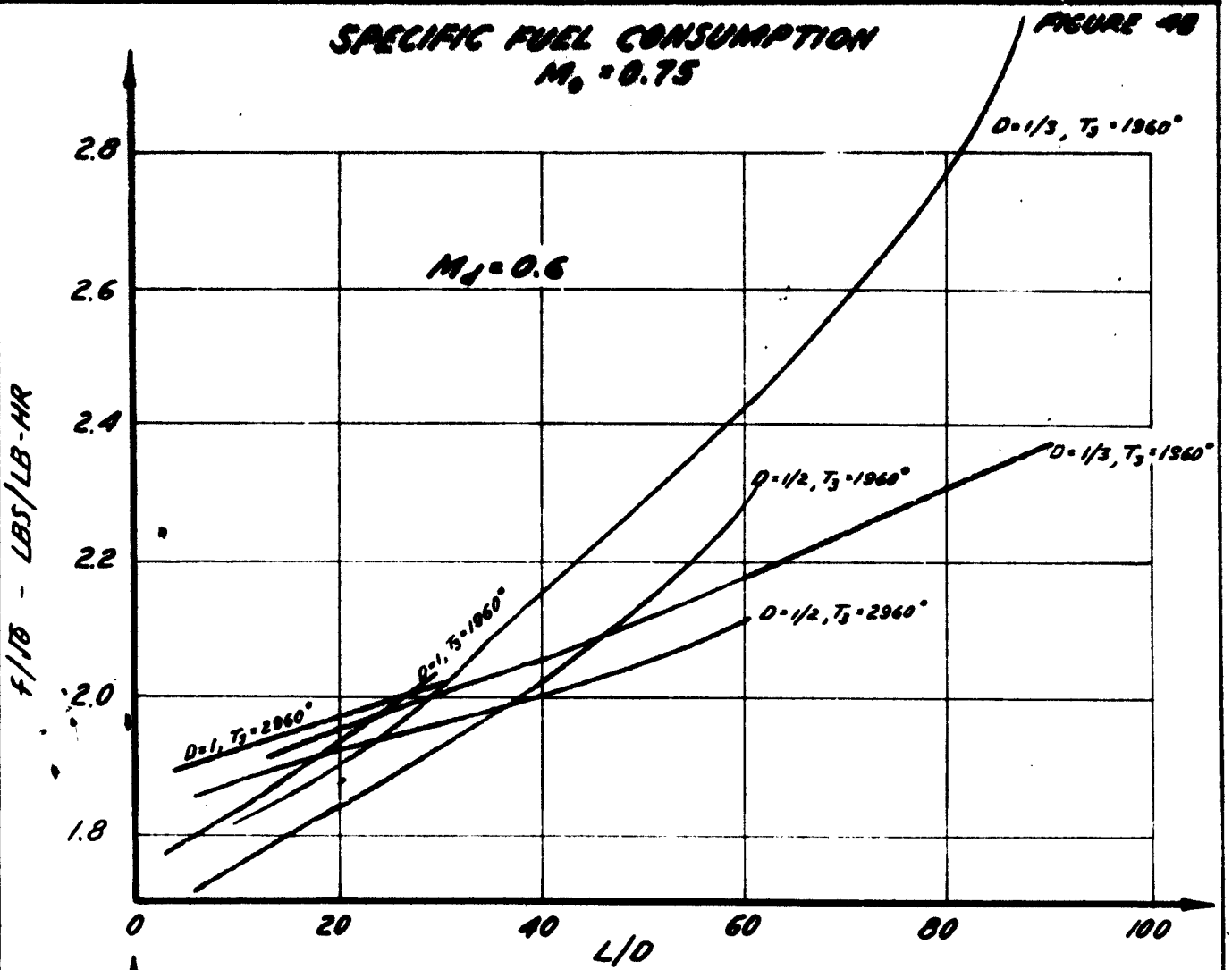


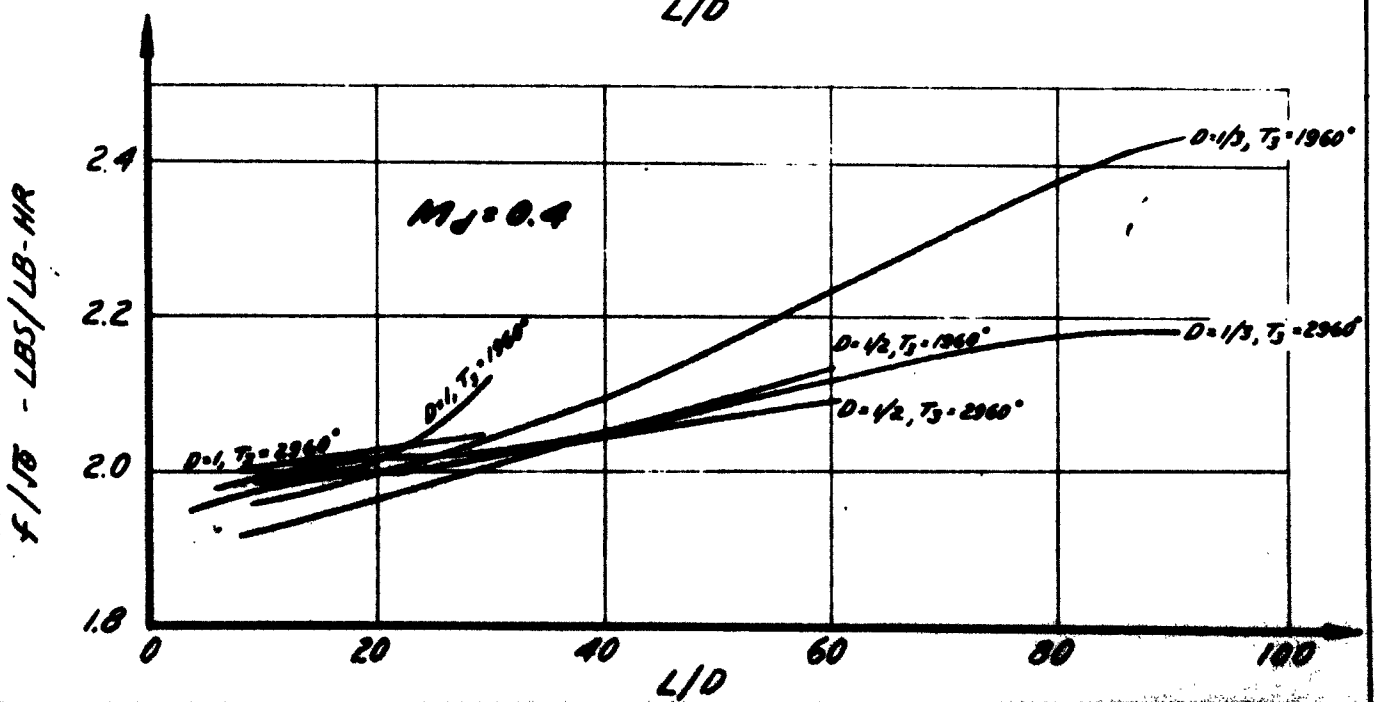

| PREPARED BY | AEROPHYSICS DEVELOPMENT CORPORATION | REPORT NO 2000-1-R1 |
|---|---|---|
| CHECKED BY | PACIFIC PALISADES, CALIFORNIA | DATE Jan 24 1953 |

FIGURE 49

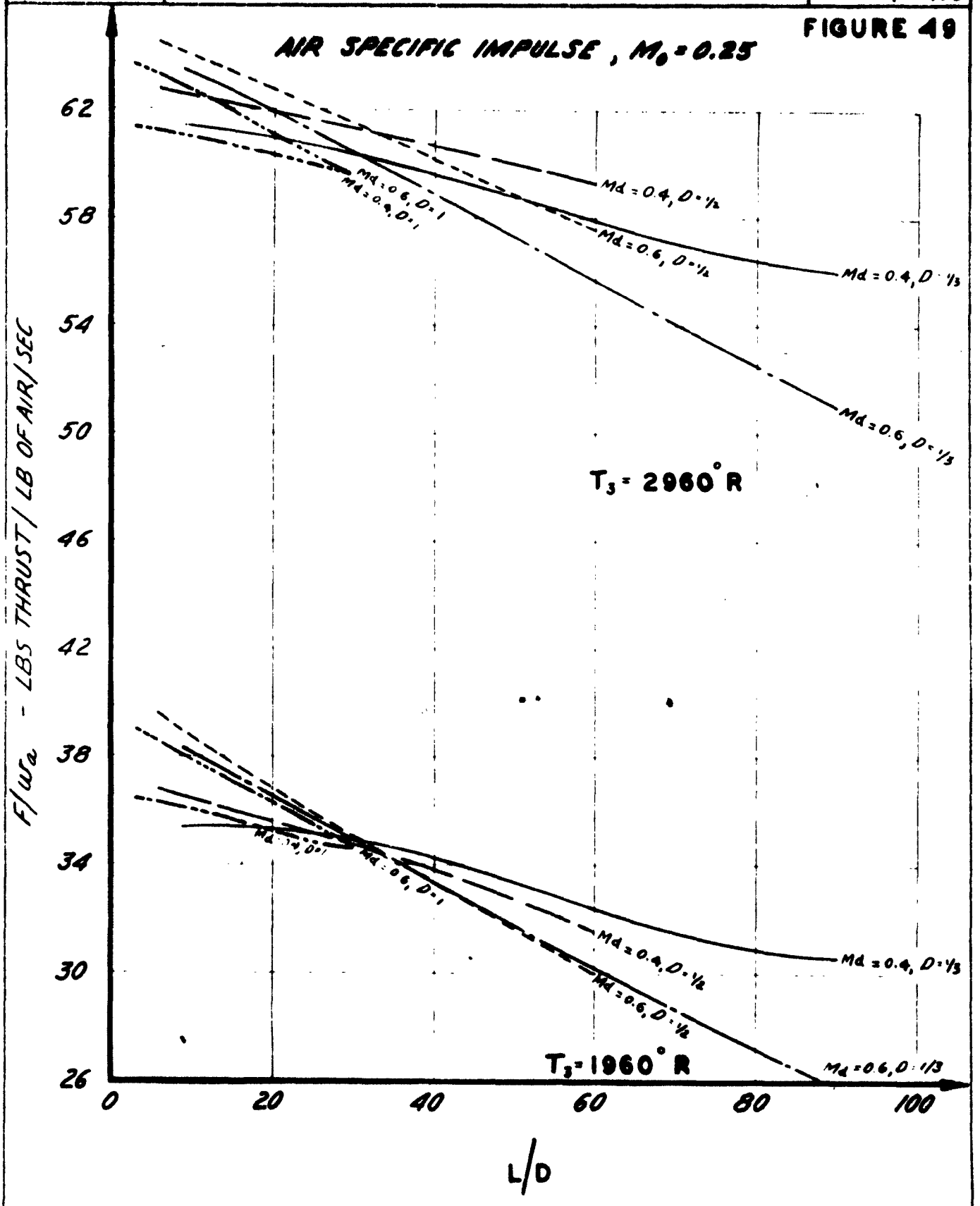

| PREPARED BY | AEROPHYSICS DEVELOPMENT CORPORATION | REPORT NO 2000-1-R1 |
|---|---|---|
| CHECKED BY | PACIFIC PALISADES, CALIFORNIA | DATE Jan 24 1953 |

FIGURE 50

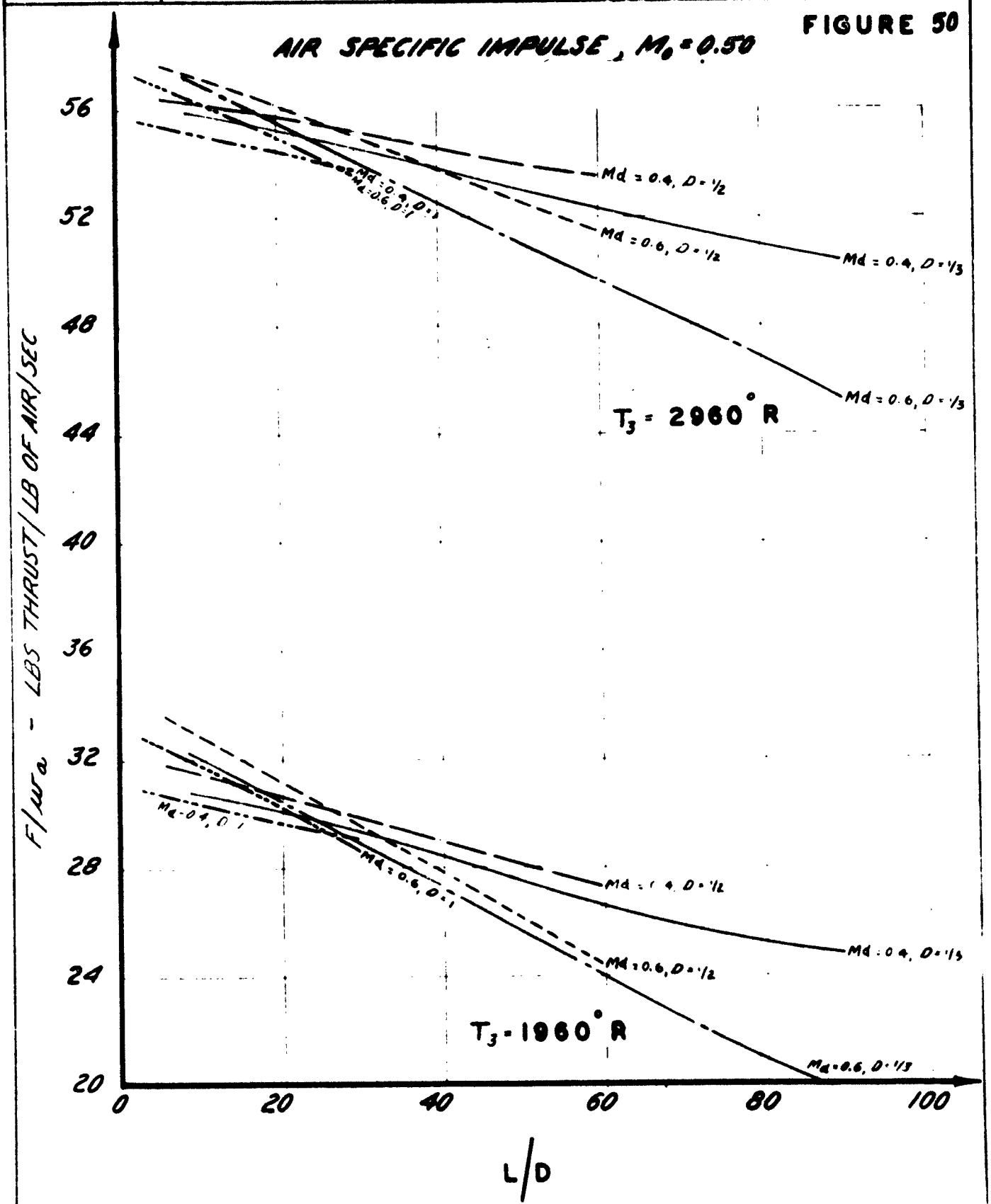

| PREPARED BY | AEROPHYSICS DEVELOPMENT CORPORATION | REPORT NO 2000-1-R1 |
|---|---|---|
| CHECKED BY | PACIFIC PALISADES, CALIFORNIA | DATE: Jan 24 1953 |

FIGURE 51

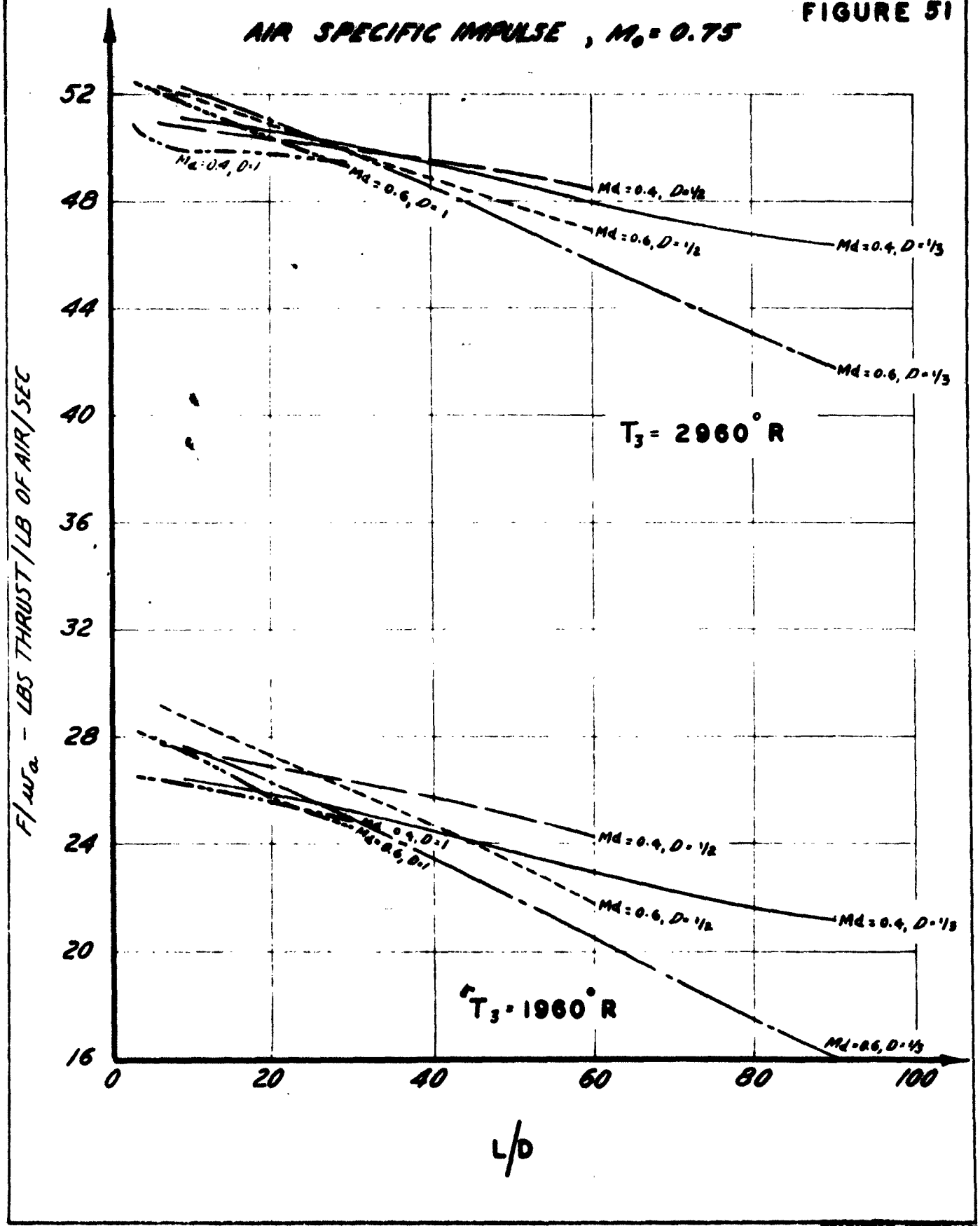

| PREPARED BY | AEROPHYSICS DEVELOPMENT CORPORATION | REPORT NO 2000-1-R1 |
|---|---|---|
| CHECKED BY | PACIFIC PALISADES, CALIFORNIA | DATE Jan 24 1953 |

FIGURE 82

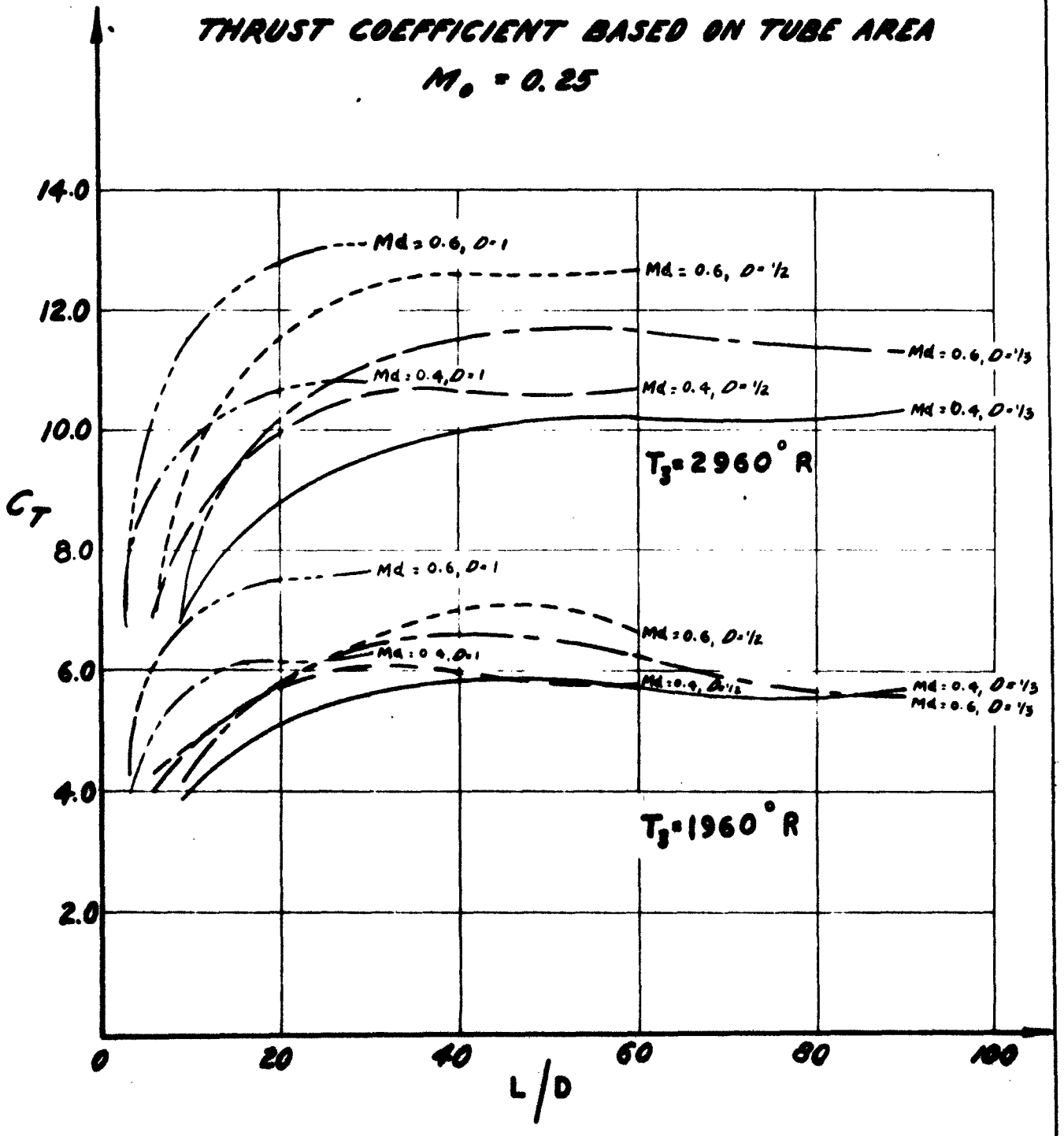

| PREPARED BY | AEROPHYSICS DEVELOPMENT CORPORATION | REPORT NO 2000-1-R1 |
|---|---|---|
| CHECKED BY | PACIFIC PALISADES, CALIFORNIA | DATE Jan 2, 1953 |

FIGURE 53

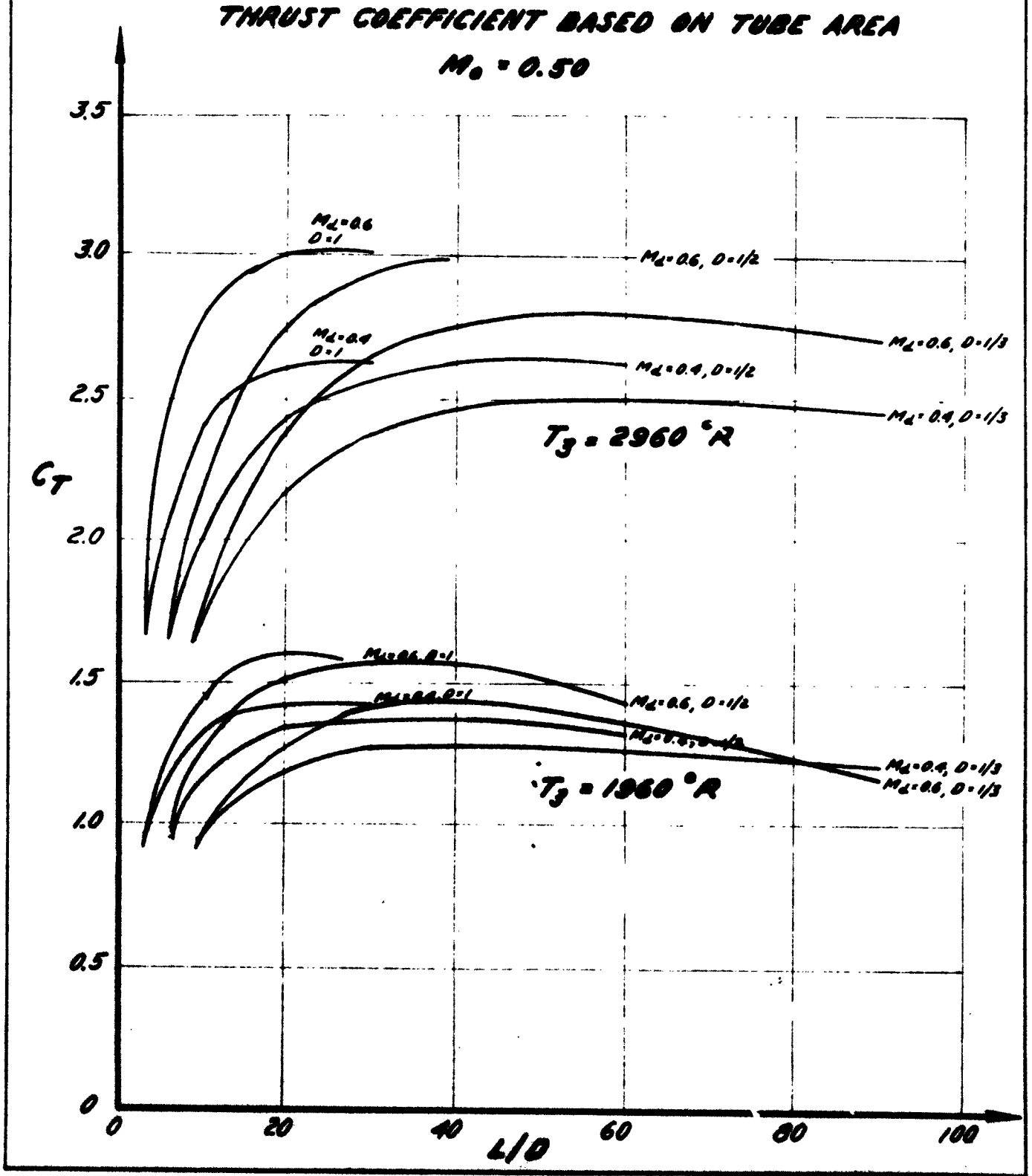

| PREPARED BY: | AEROPHYSICS DEVELOPMENT CORPORATION | REPORT NO. 2000-1-R1 |
|---|---|---|
| CHECKED BY: | PACIFIC PALISADES, CALIFORNIA | DATE: Jan 24 1953 |

FIGURE 54

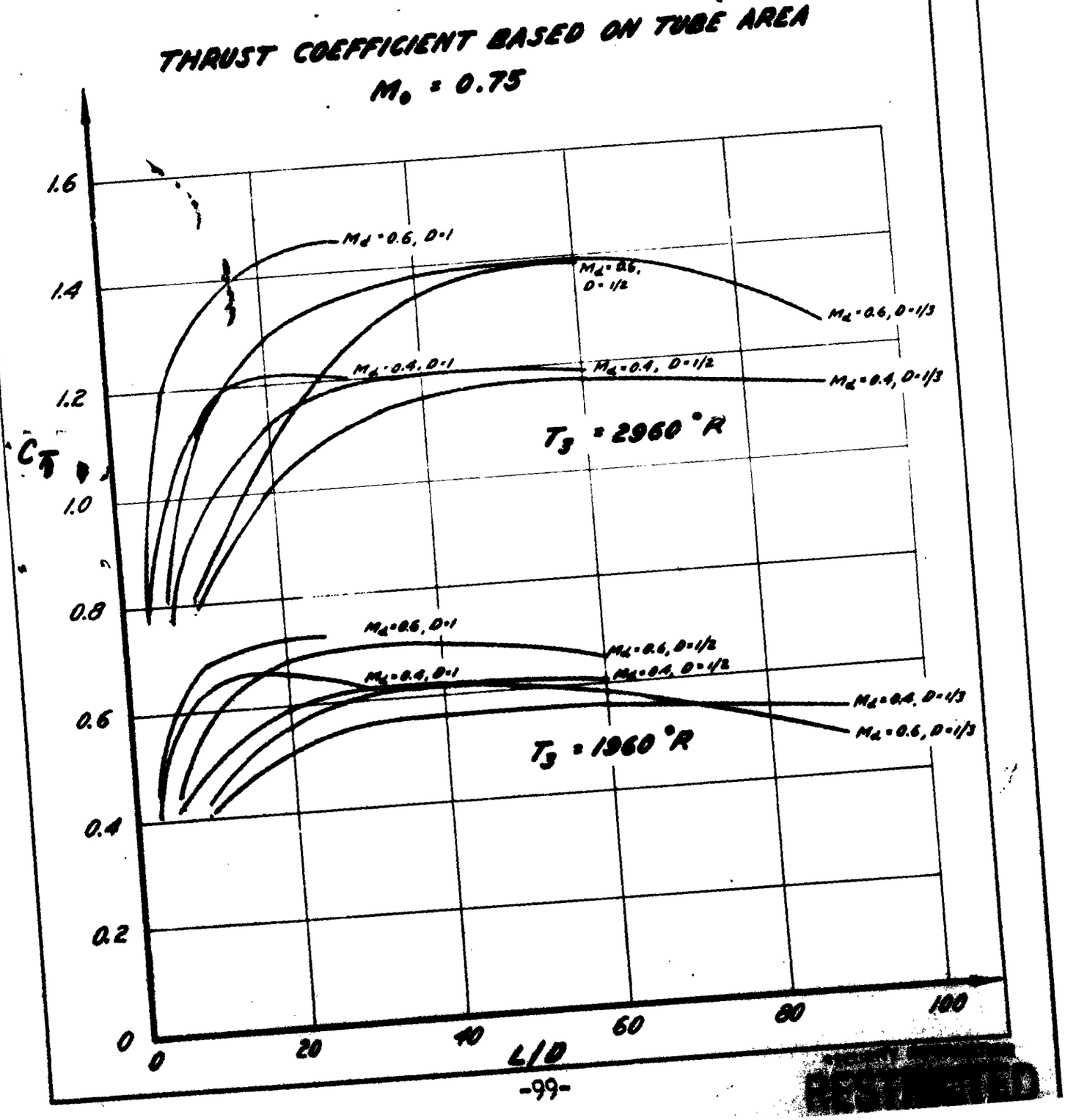

| PREPARED BY | AEROPHYSICS DEVELOPMENT CORPORATION | REPORT NO 2000-1-R1 |
|---|---|---|
| CHECKED BY | PACIFIC PALISADES, CALIFORNIA | DATE Jan 24 1953 |

FIGURE 55

## CHARACTERISTIC MASS FLOW

$M_0 = 0.25$

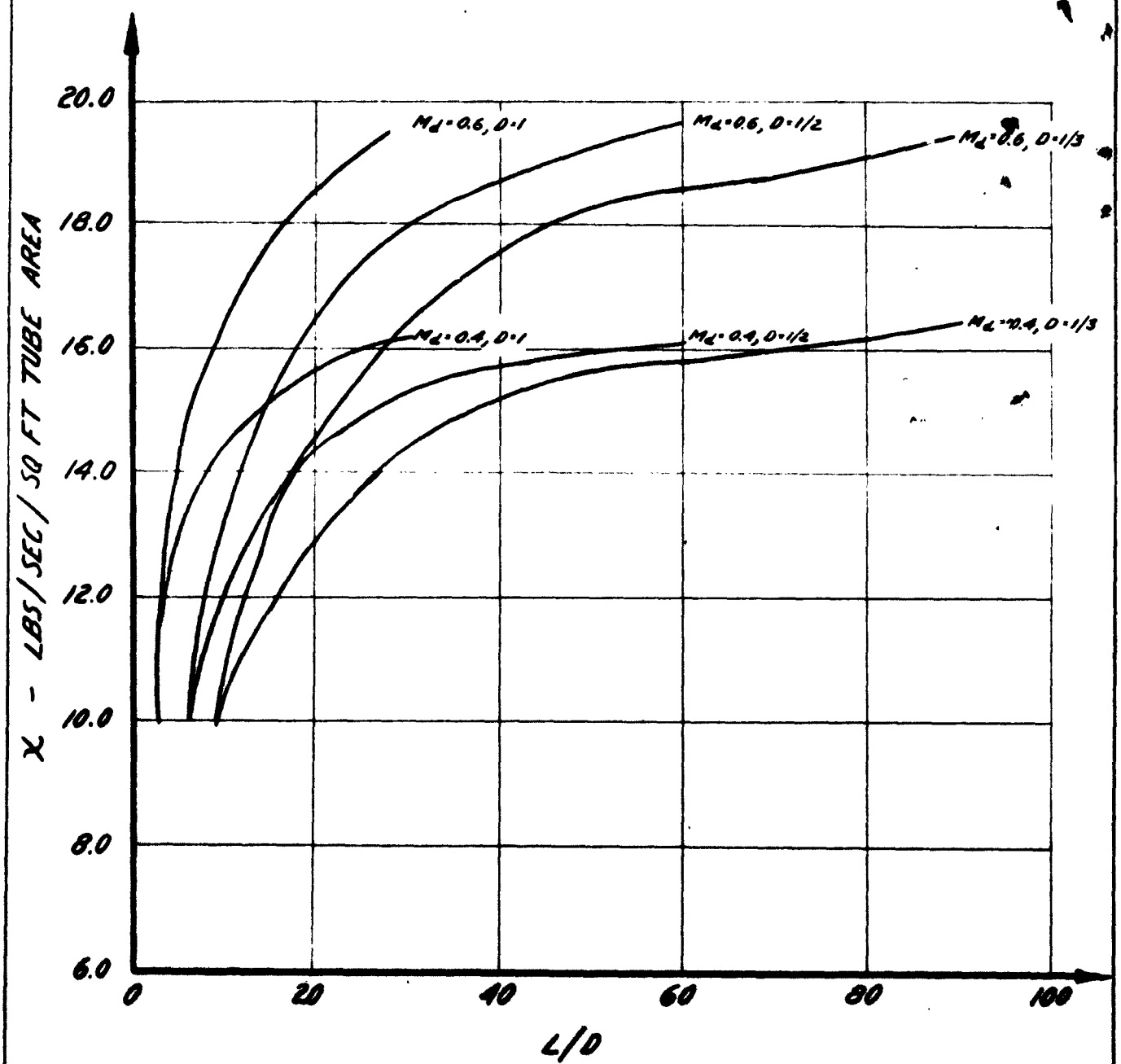

| PREPARED BY | AEROPHYSICS DEVELOPMENT CORPORATION | REPORT NO 2000-1-R1 |
|---|---|---|
| CHECKED BY | PACIFIC PALISADES, CALIFORNIA | DATE: Jan 24 1953 |

FIGURE 56

## CHARACTERISTIC MASS FLOW
## $M_0 = 0.50$

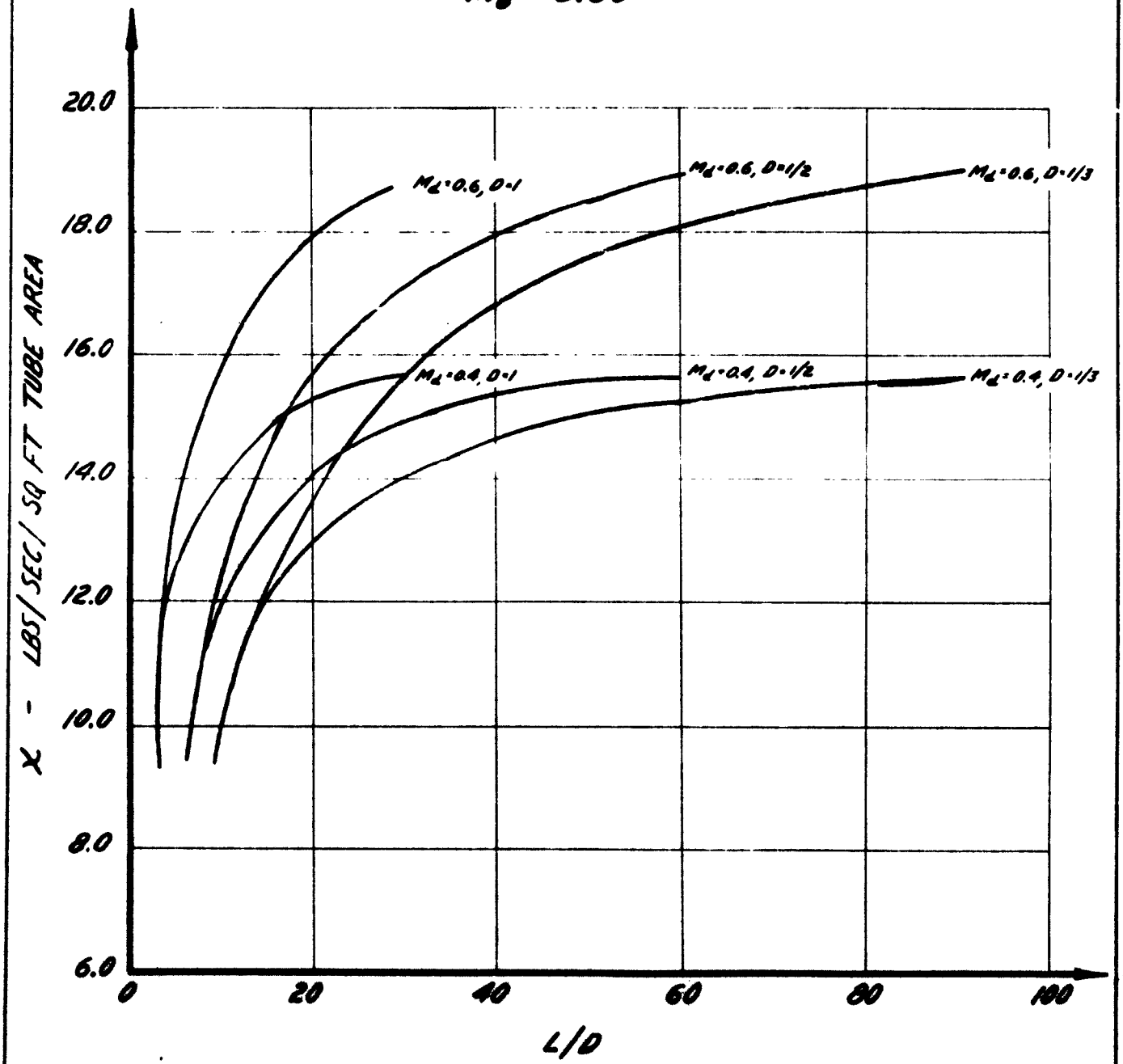

| PREPARED BY | AEROPHYSICS DEVELOPMENT CORPORATION | REPORT NO. 2000-1-R1 |
|---|---|---|
| CHECKED BY | PACIFIC PALISADES, CALIFORNIA | DATE: Jan 24 1953 |

FIGURE 57

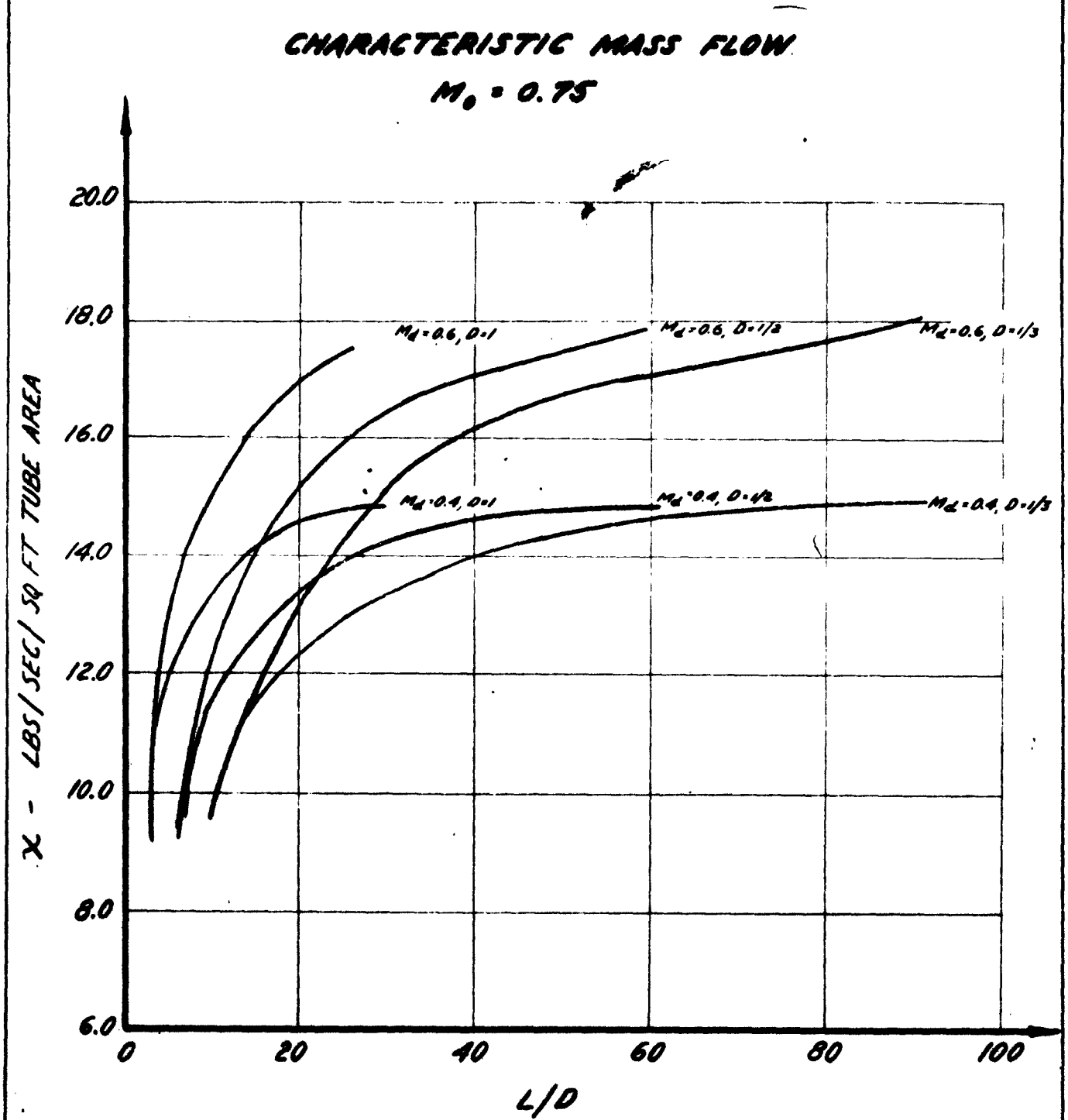

| PREPARED BY | AEROPHYSICS DEVELOPMENT CORPORATION | REPORT NO 2000-1-R1 |
|---|---|---|
| CHECKED BY | PACIFIC PALISADES, CALIFORNIA | DATE Jan 2, 1953 |

It can be deduced from these performance curves that an optimization analysis can be made to determine the best tube length. If the ratio of the weight of the engine to the total thrust is the important parameter, then we can see that by reducing the length of the tubes from the higher $\frac{L}{D}$ ratios we can reach an optimum length where $\frac{\text{weight}}{\text{thrust}}$ is a minimum. This optimum length does not necessarily give the greatest thrust per square foot of frontal area, nor does it give the least specific fuel consumption. A careful design analysis will have to be carried out to determine the optimum engine configuration for a specific application.

SECTION V

PRELIMINARY ANALYSIS OF A 36" DIAMETER ENGINE CONFIGURATION

## 5.1 Application of the Engine

The application of the engine will determine its actual form and performance. It is felt that the applications of this engine will be many and varied. In order to simplify the preliminary performance estimation, a specific type was considered. This permitted an analysis of the valve configuration, the valve characteristics, and the actual effect of the valve on the performance.

Promising applications of this engine appear to be as follows:

(1) Power Pack

(2) Guided Missile Power Plant with Static Thrust
  (a) Subsonic Flight
  (b) Supersonic Flight

(3) Aircraft Powerplant
  (a) Subsonic Flight
  (b) Supersonic Flight

(4) Helicopter Propulsion

(5) Combustion Chamber or Afterburner for a Turbo-Jet

(6) Burner for a Ram-Jet

(7) Stationary Engine as an Auxiliary Power Plant or heating unit

It was decided to make a preliminary design analysis of an engine capable of propelling a missile or aircraft from zero flight speed to a cruising Mach Number of 2.00. The choice of these flight speeds does not preclude that these are the limits, but only sets down a definite application, the configuration will have to be modified to suit the requirements.

## 5.2 Preliminary Design Layouts

The mechanical design layouts of a typical engine embodying the pulse detonation cycle had to be considered in order to determine if there were any obvious mechanical problems that could not be solved. The mechanical design was not considered in detail, but only generally. This was also necessary so that more realistic valve characteristics could be determined and their effect on the cycle could be calculated. The mechanical grouping of the tubes was also a factor affecting the efficiency of the discharge and scavenging phases. As is shown in a

FIG 58
PG 105
MISSING

FIGURE 59

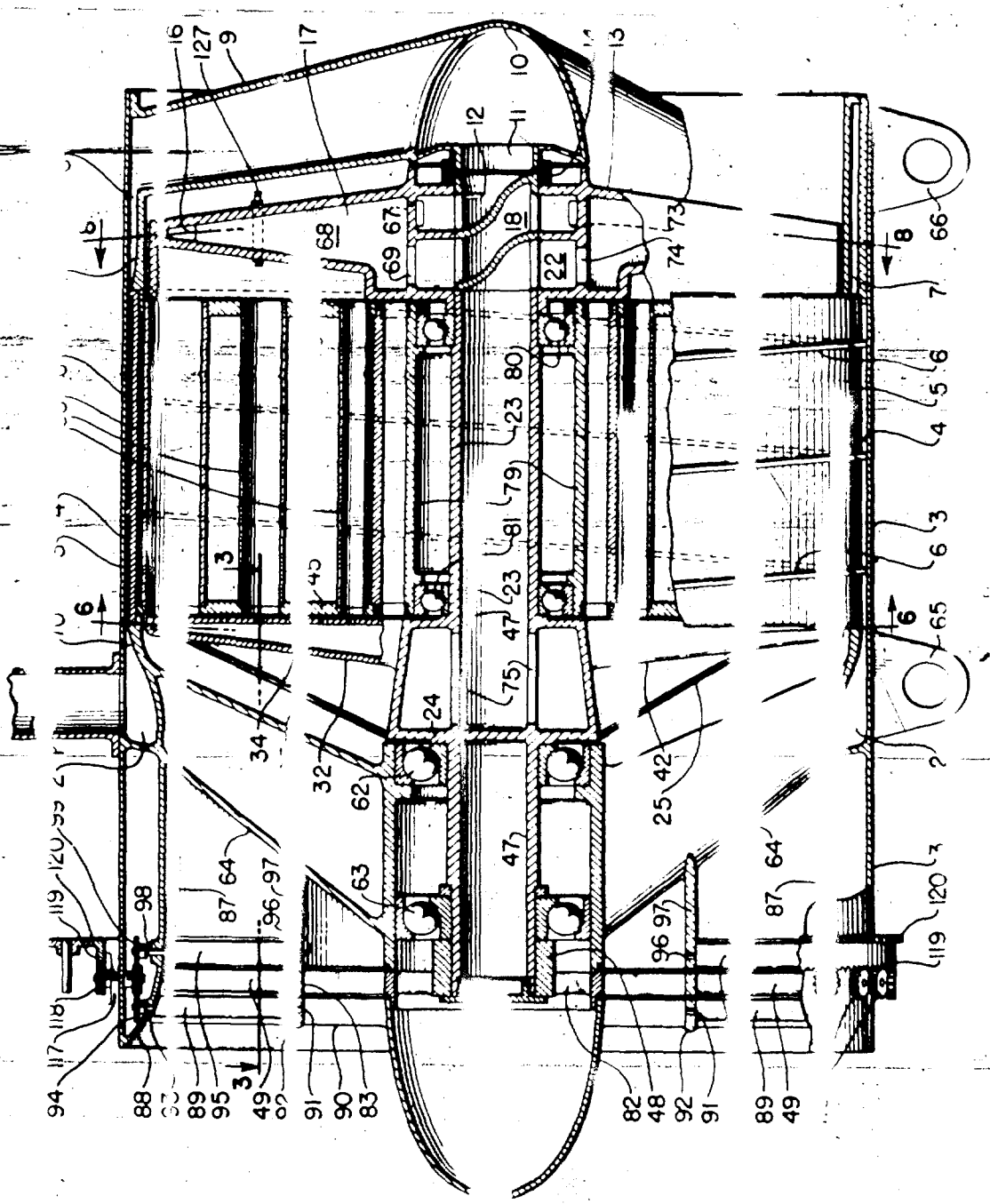

SECTIONAL VIEW OF THE 36" MULTI-JET

later section, these preliminary design considerations have indicated that the heat transfer problem in the cooling of the tubes and the whole engine is a major one for an engine of high specific thrust, and that the most promising solution is to construct the tubes from ceramic materials or coated graphite.

Consideration on the preliminary design layouts went along hand-in-hand with the preliminary performance calculations. Many designs were considered for the valves, including flap, butterfly, venetian blind, sleeve, rotating drum and rotating plate types. At first it was decided that each individual tube be used to power a helicopter rotor, but when a certain application requires a number of tubes to be nested in a group, the mechanism of operating and timing each single valve becomes too cumbersome and complicated.

It has been noted in a previous discussion that short closing and opening times are mandatory for efficient operation and therefore vibratory motions were considered for the valves. On the other hand, the large accelerations required for opening and closing necessitated the use of very heavy and cumbersome springs. The continuously rotating sleeve-type valve on a single tube with inlet and discharge openings arranged in slots on the tube wall, required high rotational speeds and presented too large a bearing surface.

The drum type valve with the tubes arranged around its periphery and discharging through slots perpendicular to the tube axes showed the most promise. This configuration was soon discarded due to its inherent disadvantage of limiting the arrangement of the tubes to one row. The ratio of the total cross sectional area of the tubes to the maximum frontal area of the engine was too small (i.e. 26%).

This led to a second design configuration (See Figures 58 and 59) where the air flowed straight through the tubes and each valve took the form of a rotating disc with cutouts. With this arrangement, up to 50% of the maximum cross sectional area of the engine could be utilized as combustion chamber area.

Due to centrifugal considerations the maximum tip speed of the rotating valves was limited to 750 ft-sec. The cutouts in the valves were arranged so that diametrically opposite tubes were discharging at the same time, producing a force balance about the center line of the engine. Each tube cycles twice for each revolution of the valve. The length of the tubes required then is 15 inches. The diameters of the tubes were kept as small as possible in order to keep the cut-off times as short as possible.

The speed of the valve and the number of cycles for each valve revolution determines the duration of a cycle. The duration of a cycle determines the length of the detonation tubes. For a two-cycle valve (each tube cycles twice for each valve revolution) and a given tube length, the angle subtended by each tube determines the time required for the tube to open and to close. The ratio of the time the

tube is opening and closing to the time the tube is fully opened determines the percentage of air that actually flows into the tube.

Preliminary heat transfer calculations show that approximately eight times the surface area of the tube is required for fins on the outside of each tube to cool the wall to 1500° F when the maximum cycle temperature is 3500° F. This leads to a very heavy construction for each tube, and it also necessitates moving the tubes farther apart, giving a poorer nesting arrangement. Liquid cooling required a very large radiator and a large mass flow of liquid. It was decided, therefore, to consider ceramic materials for the tubes, such as stabilized zirconium oxide or graphitar. Section VIII gives a complete discussion on the cooling problem. The allowable maximum pressure level in the tubes, based on the stress considerations, will determine the maximum Mach number for each altitude.

The valves, on the other hand, must be cooled and, since the fuel must be heated in order for it to vaporize on injection into the combustion tubes, cooling by means of the fuel is used on the valves. The fuel will be brought into a header at the front of the engine, where it will be allowed to flow spirally around, and towards the rear of, the engine. It then will be ducted through struts to the axial shaft by means of a rotating seal, then into the rear valve. It will then flow forward through the shaft into the front valve and then to the fuel nozzles. The pressure in the fuel system will be such that the fuel will remain in the liquid form throughout its passage. As soon as the pressure of the fuel is reduced upon its injection into the air stream, the fuel will vaporize. Vaporized fuel will probably be necessary to support detonation. Figure 59 shows a cut-away drawing of a practical configuration.

The source of power with which the valves are to be driven has not been definitely decided upon. The following methods have been considered:

1. Turbine driven by some of the exhaust gases.
2. Turbine driven by the inlet air.
3. Auxiliary turbine driven by a gas generator.
4. Auxiliary powerplant either internal combustion or electrical.

The method finally selected will be determined partially by the system used to govern the speed of valves. Figure 59 shows a turbine driven by the inlet air. It will be necessary to control the valve speed reasonably accurately. The calculations so far have indicated that the valve speed is a function of the square root of the inlet total temperature.

The solid portion of the exhaust valve is hollowed out to permit

the feed-back of the high pressure and temperature gases. The duct in the exhaust valve is positioned such that it inter-connects the tubes which are at a high pressure to the tubes that are ready to be ignited. In this way, a very strong shock wave is formed and propogated through the fuel-air mixture. Spot calculations show that a pressure ratio of about 4 to 5 can be obtained across the shock wave with this cross-feed.

Figures 58 and 59 shows an artist's conception of the engine. With this postulated configuration a performance analysis of this engine can now be carried out. This 30" diameter engine or a number of these engines can be used to power a missile or aircraft. An analysis of such a system is carried out in a later section.

### 2.3 Cycle of Operation

The basic cycle has been described in a previous Section. The actual cycle of operation is only slightly modified due to finite cut-off times. Figure 60 shows the wave diagram on a time-distance plot. The pressure in the tube is allowed to drop during the discharge phase to a predetermined value, less than the inlet total pressure. When the inlet valve opens (start of scavenging) a compression wave is formed which travels down the tube accelerating the burnt gases to the required Mach Number. The fresh fuel-air mixture is admitted at the front end, while the burnt mixture is ejected axially out the back.

The shock wave produced during the pulse compression will be used to ignite or detonate the fuel air mixture. Actually, this wave is relatively weak (pressure ratio $\approx 2.0$) and therefore an easily detonable fuel will have to be injected into the front end of the tubes while the remainder will contain the regular fuel. An alternate method of detonating the fuel was studied. Briefly, this method uses the hot high pressure gases from a tube that has been previously fired and ducts them back through the exhaust valve into a tube which is ready to be fired. This produces a very strong shock (pressure ratio $\approx 4$ or 5) and also produces a much higher maximum cycle pressure. However, this full pressure is not realized for the discharge, or thrust phase, since the gases are fed back to ignite another tube. The first preliminary calculations showed that the thrust is not changed from the basic cycle and the specific fuel consumption is only slightly increased, but the advantage gained by having a strong shock present makes this type of cycle preferable over the basic cycle described previously.

### 2.4 Non-stationary Flow Processes

Investigation of the non-stationary flow processes was necessary in order to determine the actual duration of a cycle and the effect of the valves on the mass flow per cycle, and the maximum pressure for the cycle.

| PREPARED BY | AEROPHYSICS DEVELOPMENT CORPORATION | REPORT NO. 2000-1-R1 |
|---|---|---|
| CHECKED BY | PACIFIC PALISADES, CALIFORNIA | DATE Jan 24 1953 |

FIGURE 60

## WAVE DIAGRAM FOR STATIC CONDITIONS

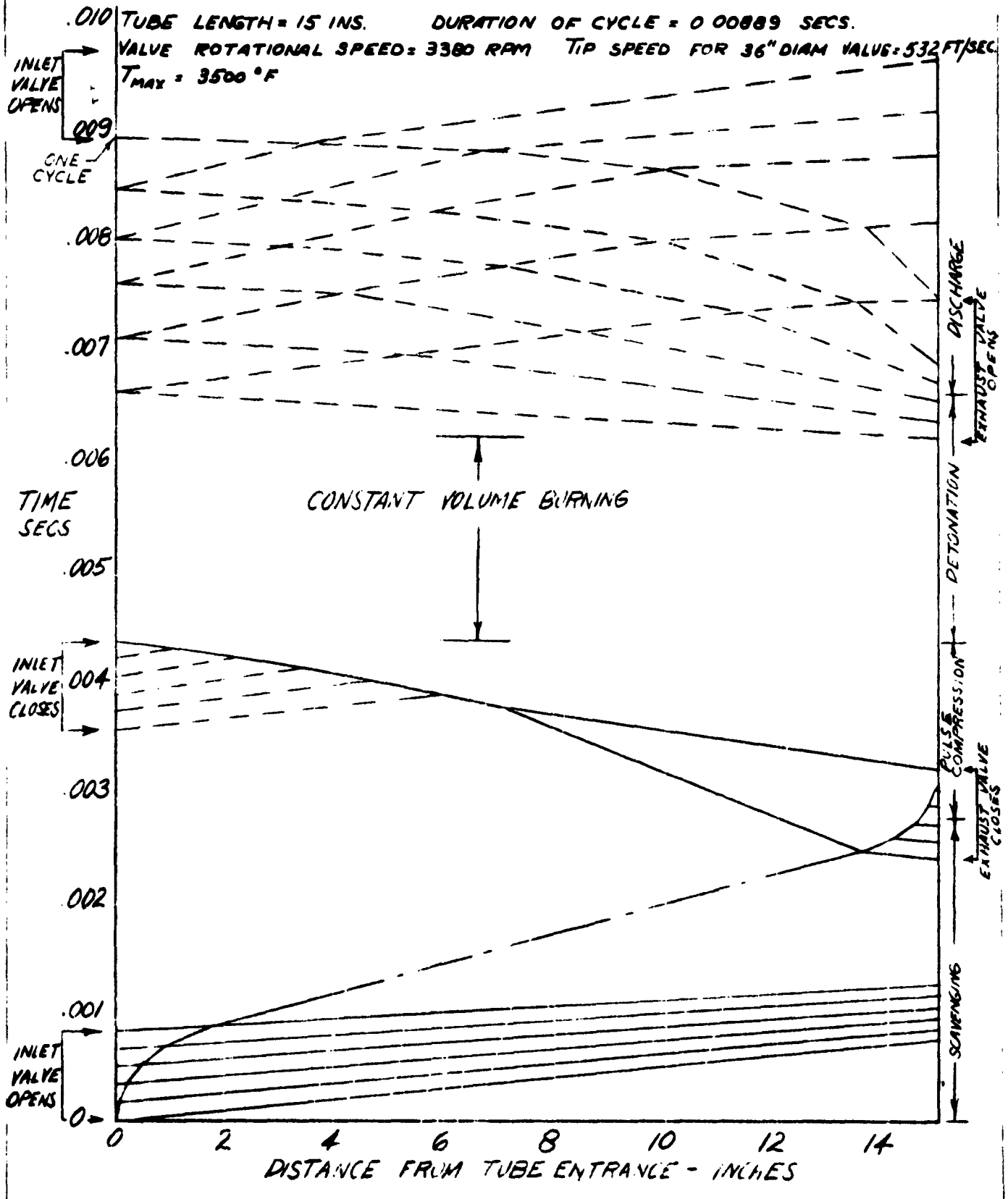

5.4.1 Discharge Phase. The duration of discharge was computed in a previous section using steady flow principles. The duration is given in Figure 4. As was previously mentioned, as the tube is discharging, the pressure is allowed to drop to a certain value before the inlet valve is opened. The duration of the discharge phase can also be computed from non-stationary flow principles. It was decided to make this analysis in order to compare the two results. In order to simplify the computations it was assumed that the exhaust valve opens instantaneously. The procedure followed for the calculations was that given by Duderley in Reference 7. The analysis was carried out under the following assumptions.

1. The exhaust valve is opened instantly.
2. One-dimensional flow is considered only (i.e. constant area duct fore and aft of the exhaust valve).

Along the $C^+$ characteristics

$$\frac{dx}{da_3 c} = \frac{u}{a_3} + \frac{a}{a_3} \qquad \ldots(82)$$

$$\frac{2}{\gamma-1}\left(\frac{a}{a_3} - 1\right) + \frac{u}{a_3} = \lambda = \text{CONST.} \qquad \ldots(83)$$

Along the $C^-$ characteristics

$$\frac{dx}{da_3 c} = \frac{u}{a_3} - \frac{a}{a_3} \qquad \ldots(84)$$

$$\frac{2}{\gamma-1}\left(\frac{a}{a_3} - 1\right) - \frac{u}{a_3} = \mu = \text{CONST.} \qquad \ldots(85)$$

where **a** = velocity of sound
**u** = particle velocity

and the conditions in state (3) are those existing in the tube just before the exhaust valve is opened.

By the use of the above equations, the values for $\lambda$ and $\mu$ can be found for each point on the characteristic net.

The inlet valve (which is closed) is located at position **A**; the exhaust valve (which is opened) is located at position B. (See Figure 61). Along the inlet valve the $C^-$ characteristics are reflected and they become the $C^+$ characteristics and therefore $\lambda = \mu$ at the inlet valve. For any state during the discharge phase, solving

the previous equations, we get

$$\frac{a'}{a_3} = \left[\frac{\lambda+\mu}{4}(\gamma-1)+1\right] \qquad \ldots(86)$$

and $$\frac{P'}{P_3} = \left(\frac{a'}{a_3}\right)^{\frac{2\gamma}{\gamma-1}} \qquad \ldots(87)$$

and $\lambda = \mu$ in our case

$$\therefore \frac{P'}{P_3} = \left[\frac{\mu}{2}(\gamma-1)+1\right]^{\frac{2\gamma}{\gamma-1}} \qquad \ldots(88)$$

Table 11 gives the value of $\mu$, $P'/P_3$ for each point of reflection. The numbering of each point on the characteristic net is self explanatory.

For given conditions in the combustion chamber just prior to the discharge phase and for a given final pressure in the combustion chamber, the time required for discharge down to this pressure can be found from Figure 61 and Table 11. The distance A-B is scaled off to equal the length of the combustion tube. Using the same scale, the distance from the origin to the correct index point measured along the time axis is found. This number is then divided by $a_3$ (using consistent units) to give the time required for the pressure to drop from $P_3$ to P' at the inlet valve. The duration of the discharge phase in $t_3$ is compared with the value of the time computed by steady flow methods.

Typical case for $\gamma_0 = 2.00$, $T_3 = 3900^\circ$ R. and $a_3 = 2955$ ft/sec.

$P'/P_3 = .2337$

$\mu = 1.4$

$\tau_e$(steady) = 0.00157 secs.
$\tau_e$(non-Stat.) = 0.00156 secs.

This comparison has shown that the steady flow considerations are sufficiently accurate for the analysis carried out in this report.

The pressure at the end of the discharge phase will be determined by the flow velocity required for scavenging. It will be assumed that the inlet valve opens instantaneously. The pressure ratio across the inlet valve will be such that when the inlet valve opens a wave configuration is formed which accelerates the new fuel-air mixture to $u' = a'$. The pressure in front of the valve is the total pressure of the inlet air. ($P_{1t}$). The wave configuration formed by the opening of the inlet valve is shown on Figure 62. The valve is located at point A. The valve opens at $t = 0$. The typical case is shown for

| PREPARED BY | AEROPHYSICS DEVELOPMENT CORPORATION | REPORT NO 2000-1-R1 |
|---|---|---|
| CHECKED BY | PACIFIC PALISADES, CALIFORNIA | DATE Jan 24 1953 |

FIGURE 61

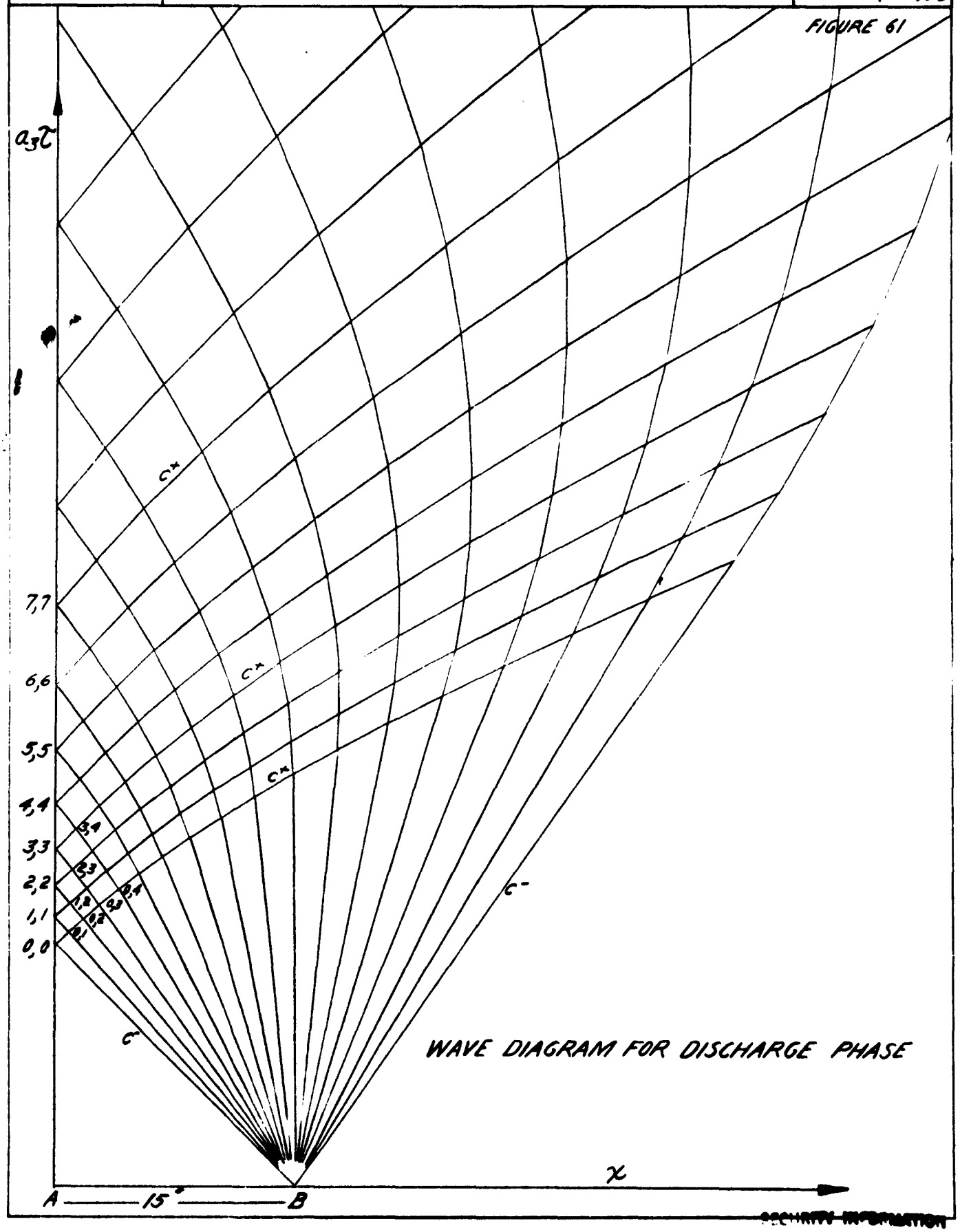


WAVE DIAGRAM FOR DISCHARGE PHASE

| PREPARED BY | AEROPHYSICS DEVELOPMENT CORPORATION | REPORT NO. 2000-1-R1 |
|---|---|---|
| CHECKED BY | PACIFIC PALISADES, CALIFORNIA | DATE Jan 24, 1953 |

$M_B = 2.00.$

$$u_B = u' - \left(\frac{P_B}{P'} - 1\right)\sqrt{\frac{2a'^2}{\gamma\left[(\gamma+1)\frac{P_B}{P'} + (\gamma-1)\right]}} \qquad \ldots(89)$$

$$\frac{P_B}{P'} = 1.70 \qquad \therefore \quad \frac{P_{1t}}{P'} = 2.17 \qquad \ldots(90)$$

$u' = 0$

$u_1 = u_B =$ 1[illegible] ft/sec

$a_1 =$ 1725 [illegible]

$T_1 =$ 124[illegible]

$P_1 = P_B =$ [illegible],700 PSF

$P_{1t} =$ [illegible],000 PSF

$T' =$ 1[illegible]

$\frac{P_B}{P'} =$ 1.70

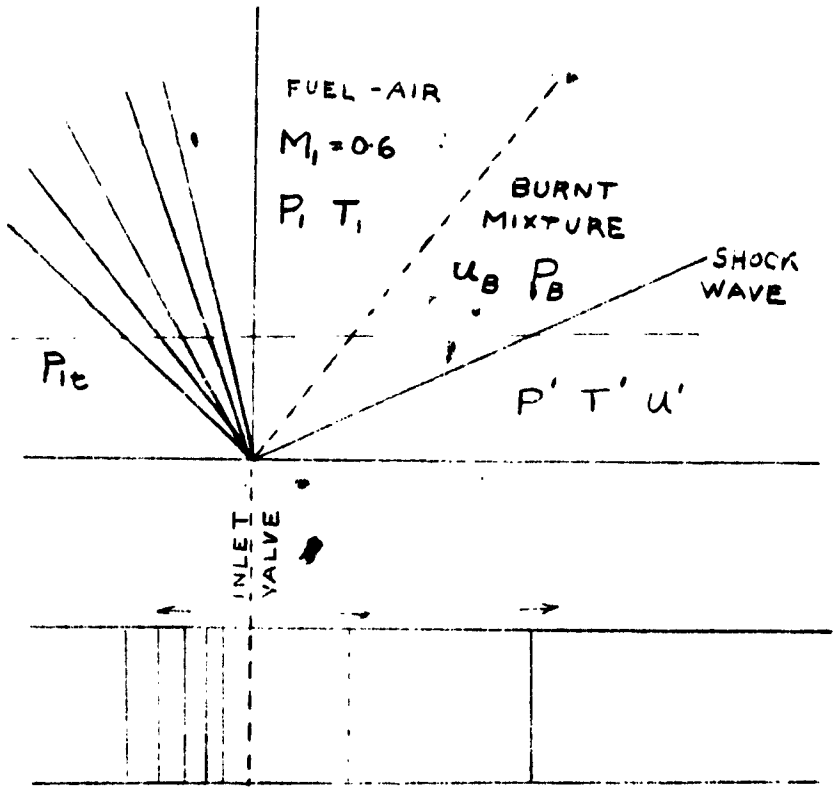


Fig. 62 Wave Configuration Produced When the Inlet Valve Opens

5.4.2. ave diagram for a full cycle. The non-stationary wave diagrams were drawn by using the assumption of linear variations as the valves opened. The acceleration of the interface between the burnt and new mixtures were assumed to take place through a compression wave having a pressure ratio of 1.10. This strength of wave was chosen since it produces a flow Mach Number in the tube of 0.6 (See previous paragraph and equation 90). The compression wave was divided into five parts (or characteristics), each characteristic increasing the interface velocity by 1/5 of the final velocity to give a final Mach Number of 1.0 in the new mixture. The stopping of the fluid particles and the formation of the shock wave by the exhaust valve is computed in the same way. For these computations and for tubes of 15 inches in length, the time for constant volume burning was assumed to be 0.0015 secs., for $M_o$ = 2.00. For any of the other flight Mach Numbers ($M_o$), the rotational speed of the valve was allowed to vary according to the value computed from the scavenging and the pulse compression phases of the cycles. By making the opening and closing times of the valves coincide with the arrival of the waves in these phases, the duration of the total cycle was obtained. This is automatically determined $\tau_B$ and $\tau_E$, and it was found that the latter very nearly coincided with the theoretical computed duration of the phases. The actual time available for discharge was a few percent longer than that determined by theoretical calculation. Since this would determine the final pressure in the tube after discharge, and since it meant that this pressure was lower than that required in the tube to initiate scavenging, it was felt that this would be detrimental to the cycle of operation. At the same time, this simplified the valve timing greatly. The time required for burning, of course, varies with the valve speed, but since the time required for burning was only an assumption, it was felt that the variation with Mach Number could be tolerated. Therefore, the physical valve configuration remained the same, while only the valve speed varied in accordance to the time of arrival of the interface of the new mixture to the exhaust valve and the pulse compression wave. (See Figures 60, 63, 64 and 65). Since these wave speeds depend on the velocity of sound of the incoming air, then the rotational speed of the valve depends only on the square root of the inlet total temperature. RPM = const $\sqrt{T_{ot}}$

The wave diagrams shown on Figures 60, 63, 64 and 65 were computed from the conditions of the incoming air and the tube lengths, using the method described above. Figure 66 shows the valve timing diagrams which give the angular dimensions of the open and closed portions of the inlet and exhaust valves.

5.4.3. Effect of Finite Opening and Closing Times for the Valves

(a) Effect on the Mass of Air per Cycle

If the valves require a time $\tau_V$ to open and close (see Figure 67) then the mass that will flow into the tube while the inlet valve is

AEROPHYSICS DEVELOPMENT CORPORATION
PACIFIC PALISADES, CALIFORNIA

REPORT NO. 2000-1-R1
DATE Jan 2[illegible], 1953

WAVE DIAGRAM FOR $M_o$ = 1.00 FIGURE 63

TUBE LENGTH = 15 INCHES DURATION OF ONE CYCLE = 0.00814 SECS.
VALVE ROTATIONAL SPEED = 3680 RPM TIP SPEED FOR 36" DIAM. VALVE = 578 FT/SEC.
$T_{MAX}$ = 3500 °F

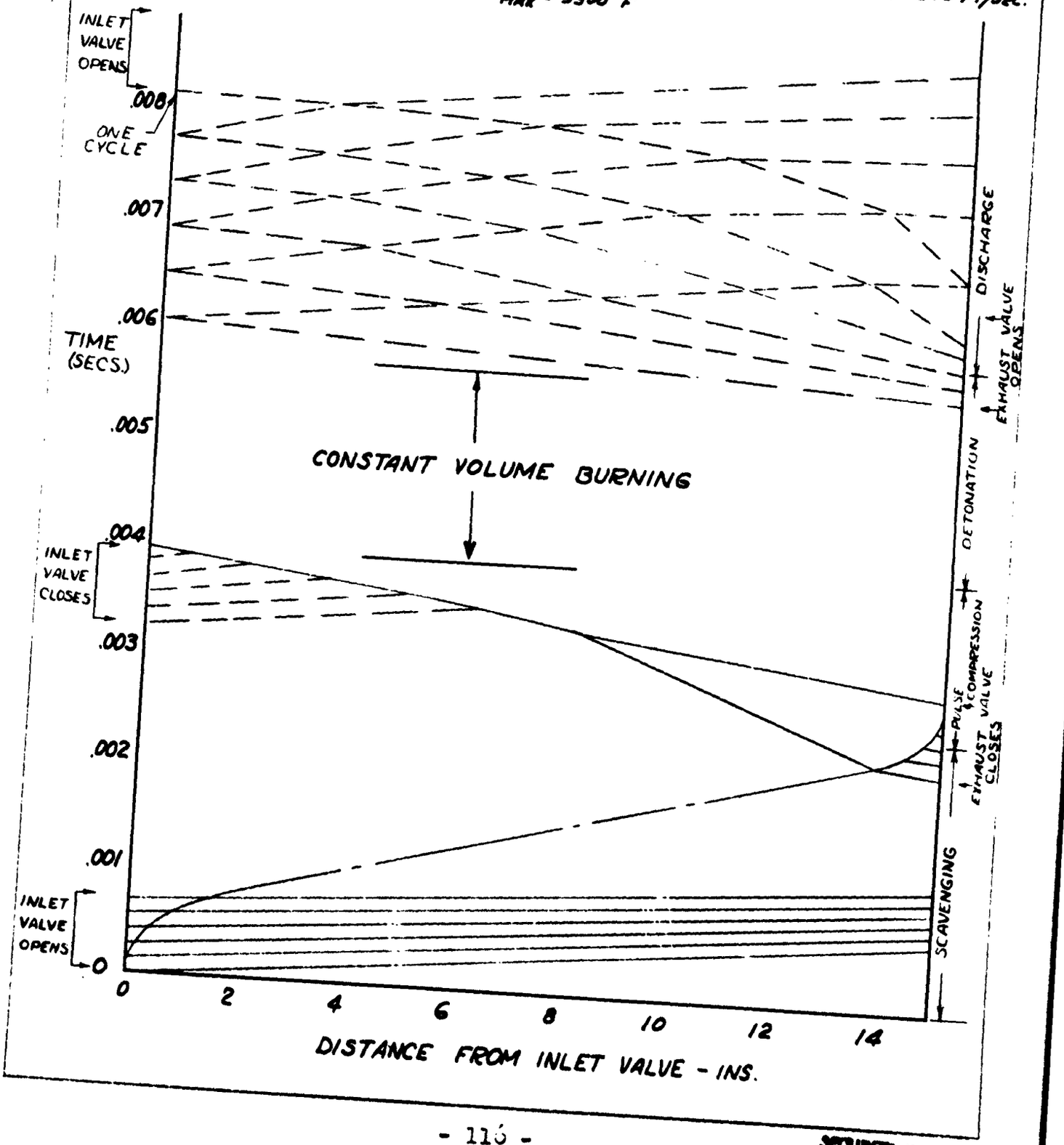

| | | |
|---|---|---|
| PREPARED BY | AEROPHYSICS DEVELOPMENT CORPORATION | REPORT NO 2000-1-R1 |
| CHECKED BY | PACIFIC PALISADES, CALIFORNIA | DATE Jan 24 1953 |

FIGURE 64

## WAVE DIAGRAM FOR $M_o = 2.00$

TUBE LENGTH = 18 INS  DURATION OF ONE CYCLE = 0.00681 SECS.

VALVE ROTATIONAL SPEED = 4410 RPM  TIP SPEED FOR 36" DIAM. VALVE = 685 FT/SEC

$T_{MAX}$ = 3500 °F

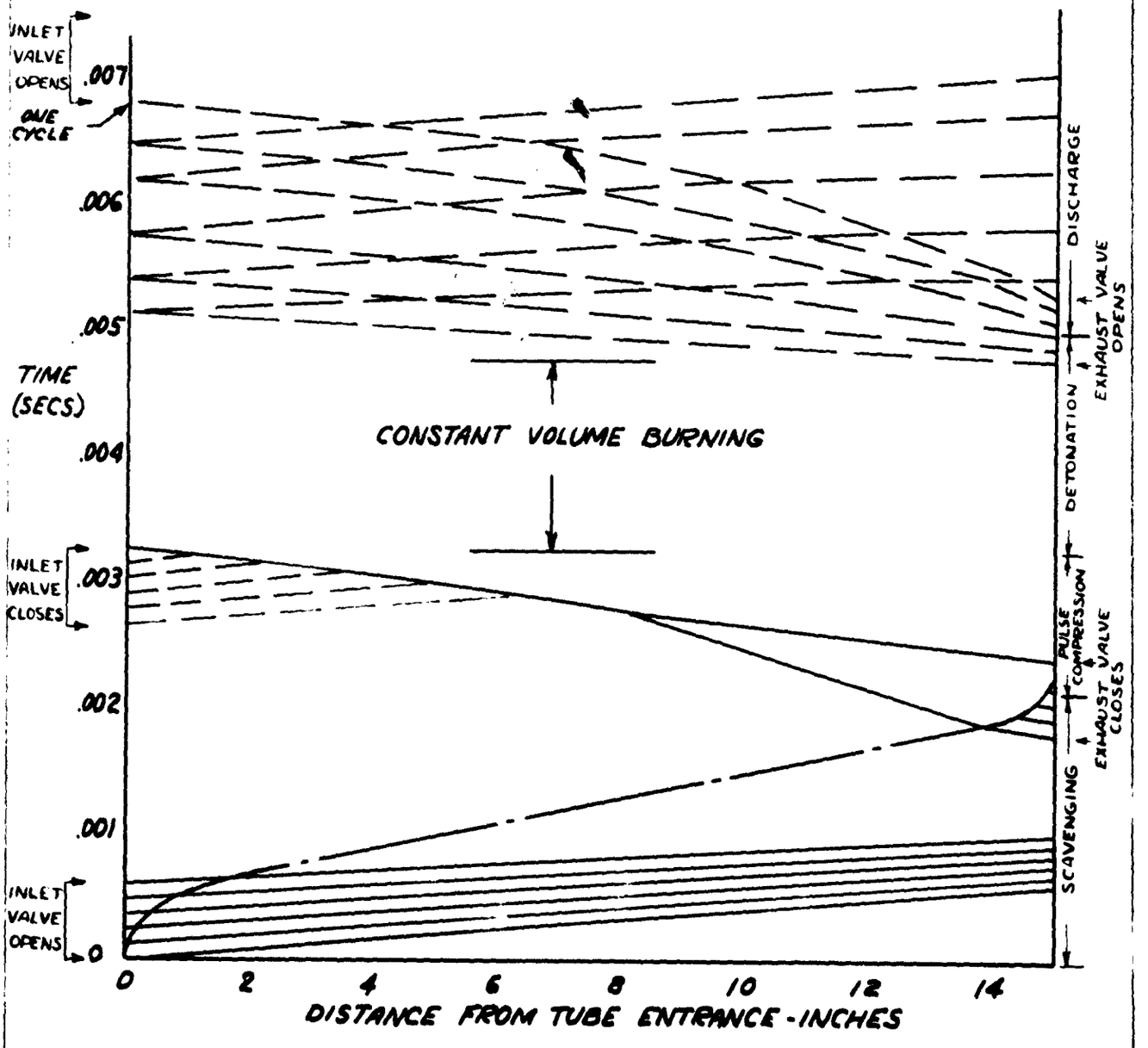

PREPARED BY

CHECKED BY

AEROPHYSICS DEVELOPMENT CORPORATION
PACIFIC PALISADES, CALIFORNIA

REPORT NO. 2000-1-R1

DATE Jan 2[illegible], 1953

FIGURE 65

WAVE DIAGRAM FOR $M_o = 2.80$

TUBE LENGTH = 15 INS. DURATION OF CYCLE = 0.00589 SECS.

VALVE ROTATIONAL SPEED = 5100 RPM TIP SPEED FOR 36" DIAM VALVE = 800 FT/SEC

$T_{MAX} = 3500\,^{\circ}F$

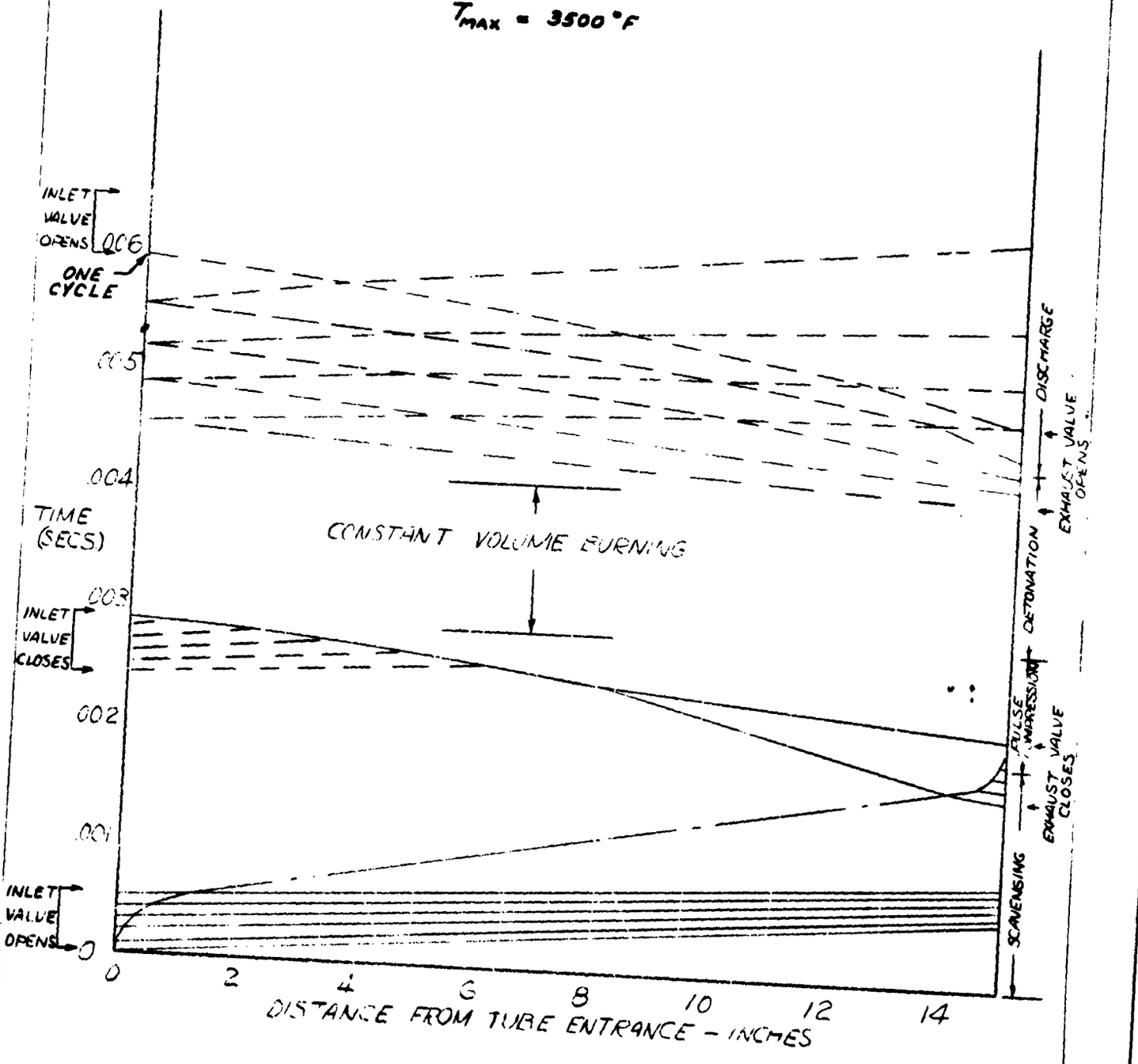

| PREPARED BY | AEROPHYSICS DEVELOPMENT CORPORATION | REPORT NO. 2000-1-A1 |
|---|---|---|
| CHECKED BY | PACIFIC PALISADES, CALIFORNIA | DATE Jan 24, 1953 |

VALVE TIMING DIAGRAMS

FIGURE 66

LENGTH OF TUBES = 15"
DIAMETER OF VALVES = 36"

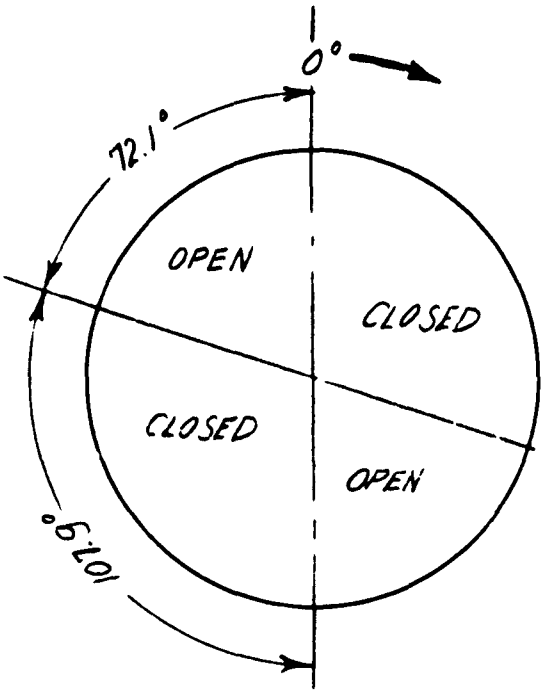


INLET VALVE

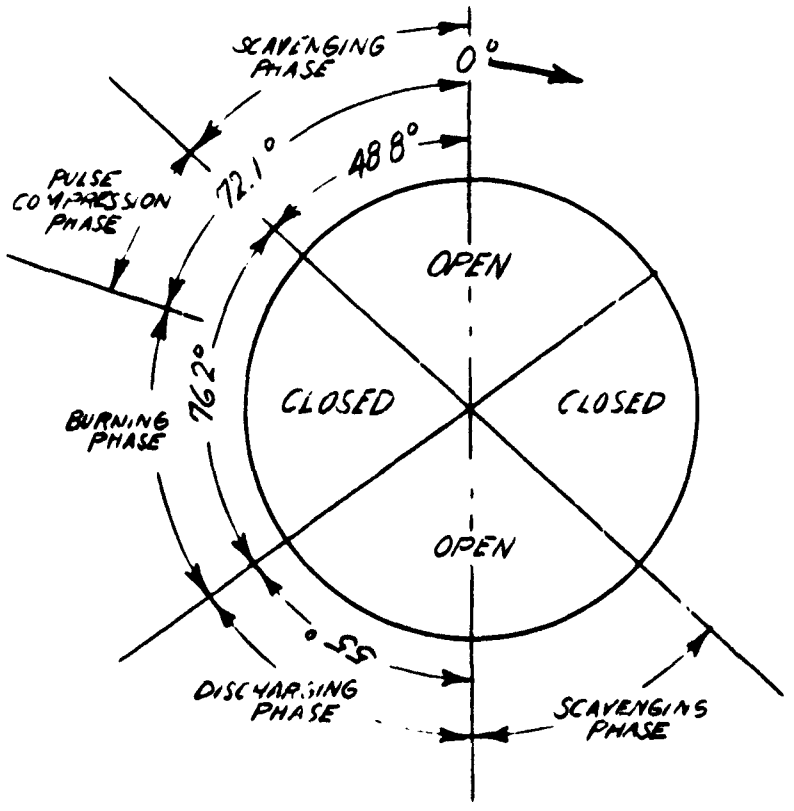


EXHAUST VALVE

open will be reduced from that of the ideal cycle. The reduction in thrust is directly proportional to the reduction in mass per cycle. The reduction in maximum pressure is also directly proportional to the reduction in mass per cycle. The reduction in maximum pressure also causes a reduction in thrust.

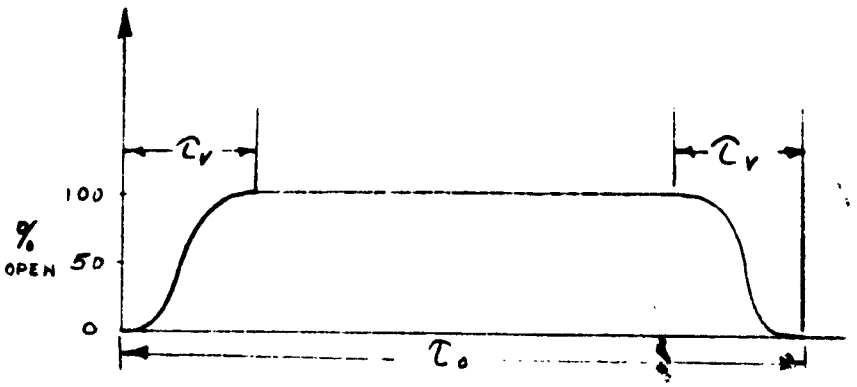


Figure 67 Valve Diagram

In Figure 67 $\tau_o$ is the actual time the inlet valve is opened. This time is determined from the characteristic diagrams given in Figures 60, 63, 64 and 65. It is assumed that if the inlet valve was fully open for the period of time $\tau_o$ then the ideal mass would have entered the tube. Then the ratio of the actual mass per cycle to the ideal mass per cycle would be

$$\frac{W_{ACT}}{W_{IDEAL}} = \frac{\tau_o - \tau_v}{\tau_o} = 1 - \frac{\tau_v}{\tau_o} \qquad \ldots(91)$$

The percentage decrease in thrust due to the reduction of mass flow is then

$$\frac{\Delta F_1}{F} = \frac{\tau_v}{\tau_o} \qquad \ldots(92)$$

The percentage decrease in maximum cycle pressure due to the decrease in mass per cycle is then $\tau_v/\tau_o$ , and the further percentage decrease in thrust due to the decrease in maximum cycle pressure is

$$\frac{\Delta F_2}{F} = K \frac{\tau_v}{\tau_o} \qquad \ldots(93)$$

where K is given in Figure 66. The value of K is obtained by differentiation of the impulse in Figure 9. Since the average thrust is given by $I/\tau_{TOT}$ , assuming that $\tau_{TOT}$ does not vary with $P_3/P_o$ ( $\tau_{TOT}$ does not actually vary more than 2% with $P_3/P_o$ over the range $4 \leq P_3/P_o \leq 24$ ) the slope of the curve of Figure 9 gives the percentage variation of the thrust against $P_3/P_o$ .

FIGURE 68

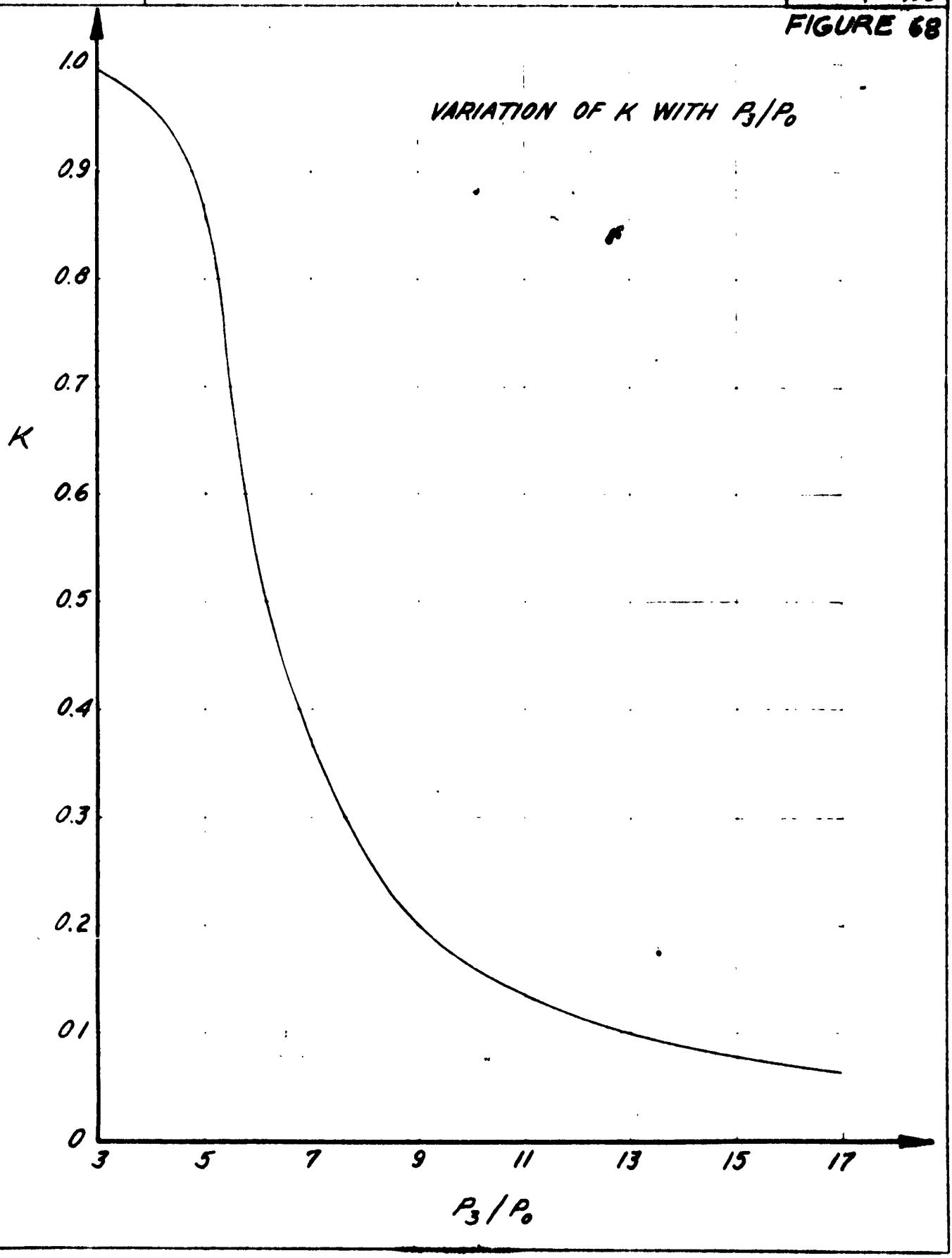
VARIATION OF K WITH $P_3/P_0$
K
1.0
0.9
0.8
0.7
0.6
0.5
0.4
0.3
0.2
0.1
0
3
5
7
9
11
13
15
17
$P_3/P_0$

The ideal thrust then is reduced by the fraction

$$1-\frac{\Delta F}{F}=1-\frac{\Delta F_1}{F}-\frac{\Delta F_i}{F}=\left(1-\frac{\tau_v}{\tau_o}\right)\left(1-K\frac{\tau_v}{\tau_o}\right) \quad \ldots(94)$$

The specific thrust is reduced by the fraction

$$\left(1-K\frac{\tau_v}{\tau_o}\right) \quad \ldots(95)$$

The specific fuel consumption is increased by the fraction

$$\left(1-K\frac{\tau_v}{\tau_o}\right) \quad \ldots(96)$$

## 5.5 Performance Analysis of the Supersonic Engine

5.5.1. General. In computing the performance of the engine as described, various assumptions were made. These were:

(1) Burning time was 0.0015 seconds

(2) A Mach Number of 1.0 was assumed for the scavenged gases as they are discharged.

(3) The following diffuser efficiencies were used:

| Speed | Total Pressure Ratio - $\frac{P_{it}}{P_{ot}}$ |
|---|---|
| $0 \leq M_o \leq 1.0$ | 1.00 |
| $M_o = 2.0$ | 0.95 |
| $M_o = 2.8$ | 0.85 |

(4) The thrust was computed from the impulse obtained from (a) the high pressure sonic discharge of the burnt gases through the open end of the tubes with no nozzle expansion considered, (b) from the discharge of the remaining burnt gases during scavenging.

The impulse of the intake air was subtracted from the above impulses to give the net impulse. The flow during the discharge or expansion phase was assumed to issue at a Mach number of 1.0 and no expansion was considered. Any reaction of the pressures on the solid portions between the tubes was neglected. It is expected that a pressure greater than static pressure is obtained in the outlet duct of the whole engine. A more careful study of these assumptions is made below.

5.5.2. Assumptions. It was felt that the burning time used was as good an assumption as can be made at this time. It is hoped that future experimental results in the literature will throw more light on this phase of the cycle.

The following consideration for the scavenge flow is given for the lower or subsonic flight Mach numbers. For this case it was felt that the exit velocity for the remainder of the burnt gases was assumed to be too high and therefore gave an impulse that was too great. It will be assumed that this flow is discharged at a velocity equal to the inlet velocity of the fresh fuel-air mixture entering the tube at the front end. This would be true for the lower Mach numbers $0 \leq M_o < 1.0$.

Consider a tube just at the end of the discharge or expansion phase. The pressure in the tube drops to or below the total pressure of the inlet flow $M_o$ at which time the inlet valve is opened. The inlet flow traveling at a Mach number $M_o$ has been brought to rest at the mouth of the tube while it was closed. Meanwhile, at the exit of the tube, the ambient static pressure is lower than the pressure in the tube, which is equal to the total pressure of a flow of Mach number $M_o$. The conditions here are similar to the subsonic flow surrounding an airfoil, i.e. total pressure at the stagnation point on the leading edge and static pressure at the trailing edge. Therefore, in the tube the remainder of the burnt gases continue to flow out of the tube. This flow may be compared to the steady flow of air in a stream tube towards a stagnation point and then away from the stagnation point.

In computing the impulse produced by the ejection of the remainder of the burnt gases during the scavenging phases the exit velocity is assumed to be the same as the inlet velocity of the new fuel-air mixture. This will be true for the subsonic flight Mach numbers, i.e. $0 \leq M_o < 1.0$.

For the supersonic Mach numbers it will be seen that the total pressure in the tube will be sufficiently high to produce sonic exit velocity during scavenging. At supersonic flight speeds the pressure in the tube during scavenging and immediately after the discharge phase will be, at first, low, then after the pressure wave from the opening action of the inlet valve arrives, the pressure is increased. This can be seen in Figures 60 and 63.

The performance computations are carried out in Appendix III and are tabulated in Tables 6 and 7. The curves for the thrust, specific fuel consumption, air specific impulse, thrust per unit maximum frontal area, thrust coefficient and characteristic mass flow are given in Figures 69, 70, 71, 72, 73, and 74.

The drag coefficient of a typical large missile is plotted on Figure 75. This missile has a ground launch weight of 52,000 pounds with a wing area of 425 square feet. Four engines are required, each

| | AEROPHYSICS DEVELOPMENT CORPORATION | 2000-1-82 |
|---|---|---|
| | [illegible] PACIFIC PALISADES CALIFORNIA | Jan 24 1953 |

FIGURE 60

ACTUAL THRUST OF A 36" DIAMETER MULTI-JET

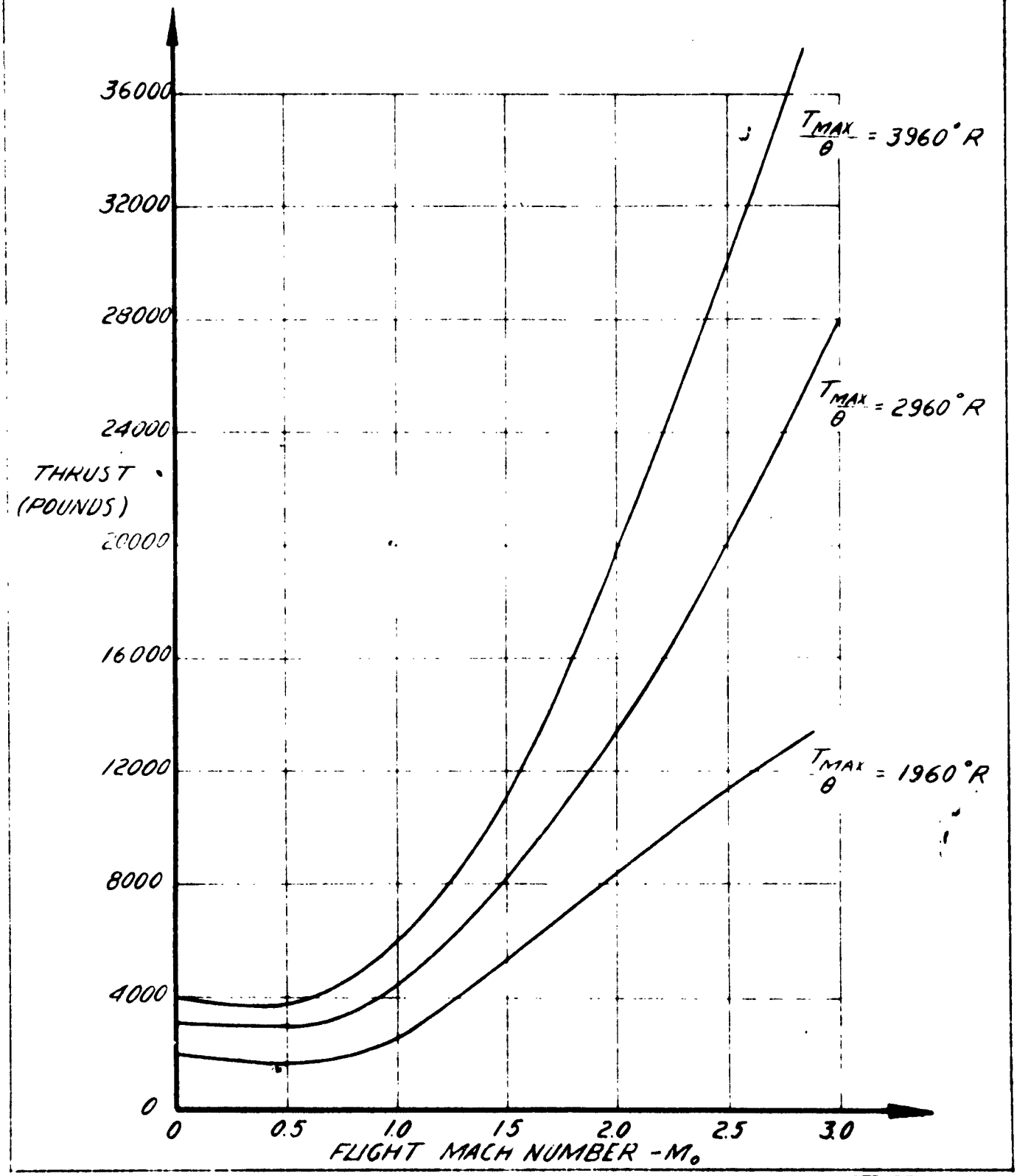

AERODYNAMICS DEVELOPMENT CORPORATION
[illegible] SANTA BARBARA, CALIFORNIA

NO. 2000
DATE Jan 24 1953

FIGURE 70

AEROPHYSICS DEVELOPMENT CORPORATION

P.O. BOX 657 BALTER PALM SPRINGS CALIFORNIA

2000-1-[illegible]

DATE Jan 24 1953

FIGURE 71

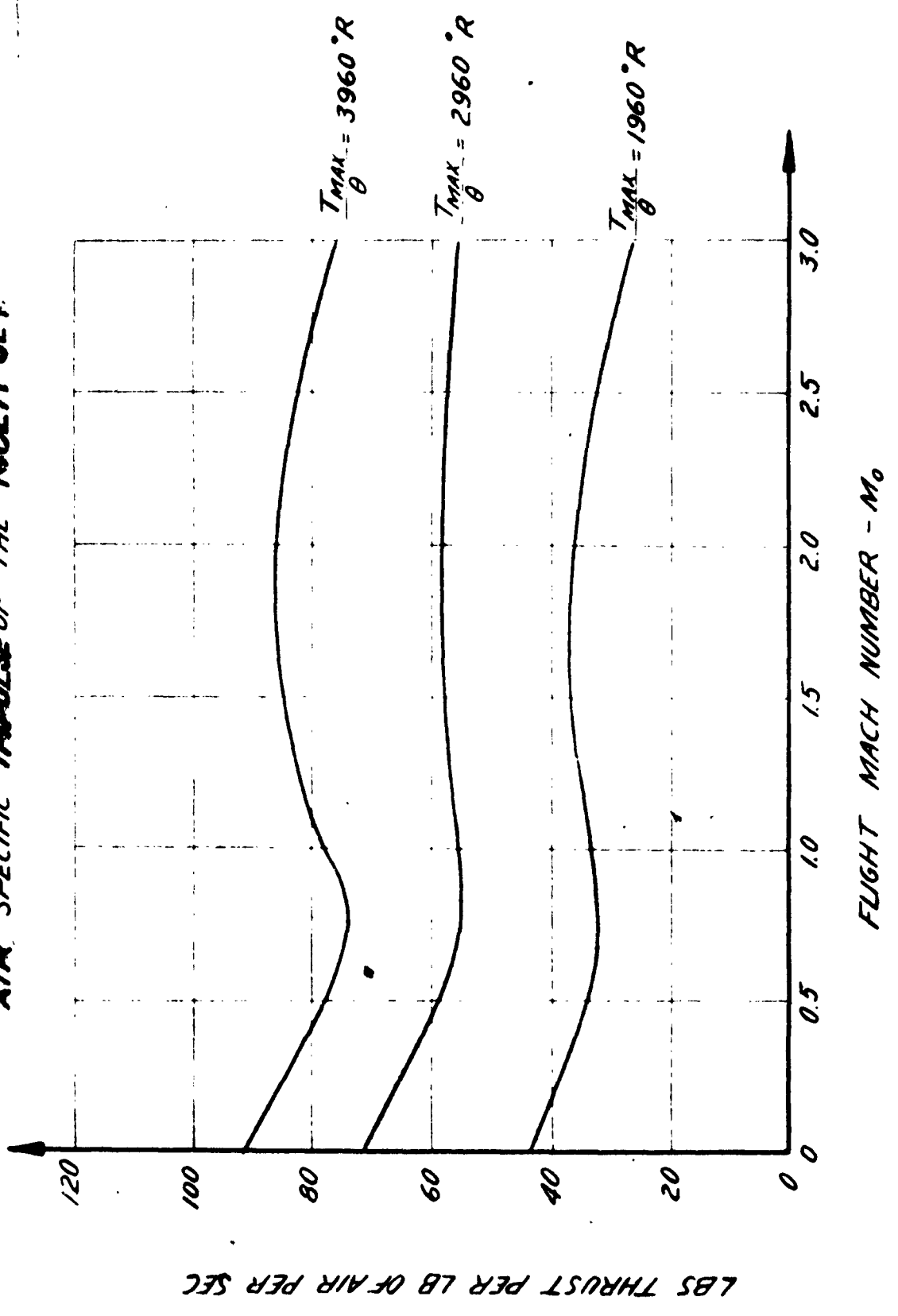

AEROPHYSICS DEVELOPMENT CORPORATION
P.O. BOX 657 PALM SPRINGS CALIFORNIA

REPORT 2000-1-R1
DATE Jan 24, 1953

FIGURE 72

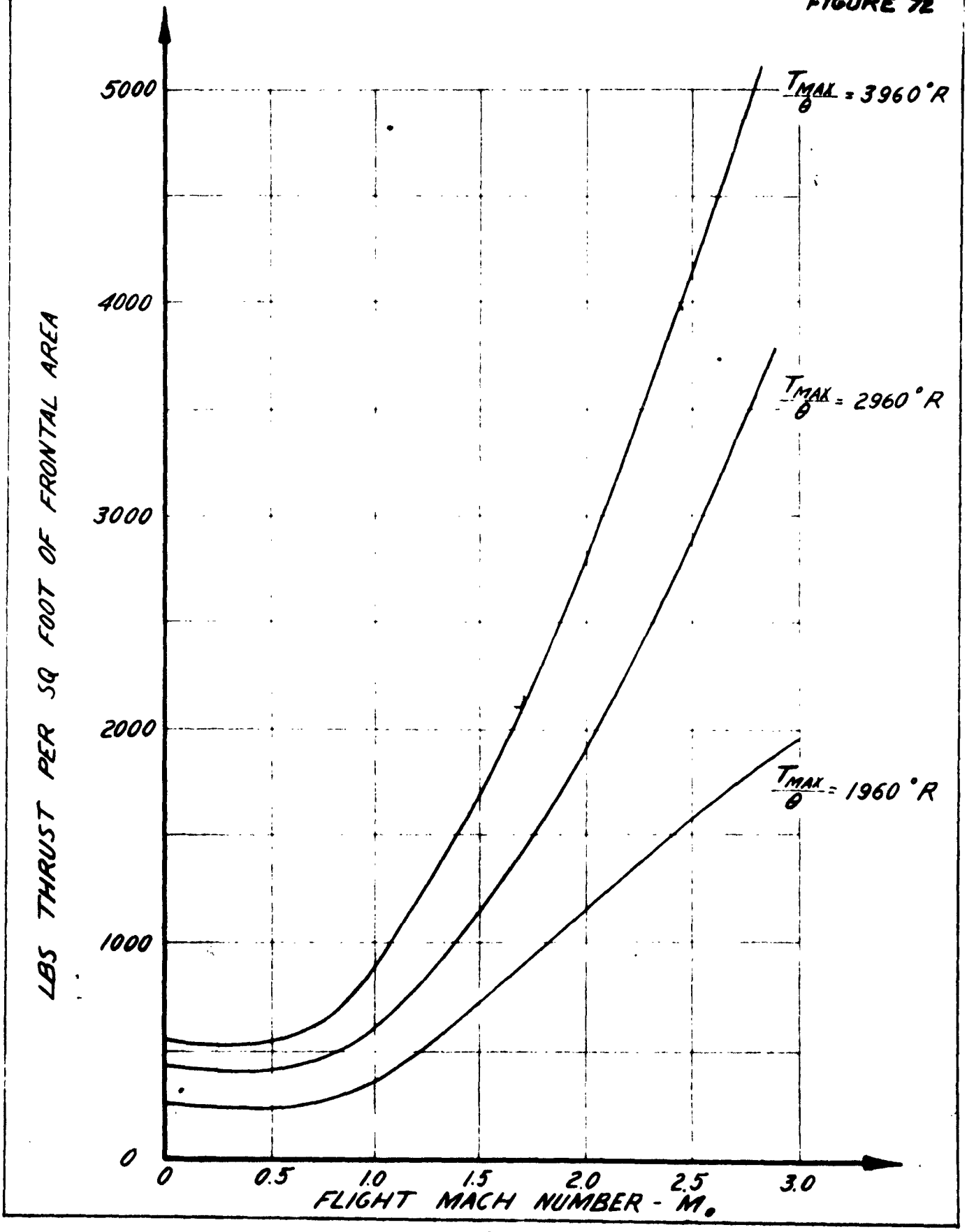

| | AEROPHYSICS DEVELOPMENT CORPORATION | REPORT NO. 2000-1-R1 |
|---|---|---|
| | PACIFIC PALISADES, CALIFORNIA | DATE Jan 24 1953 |

FIGURE 73

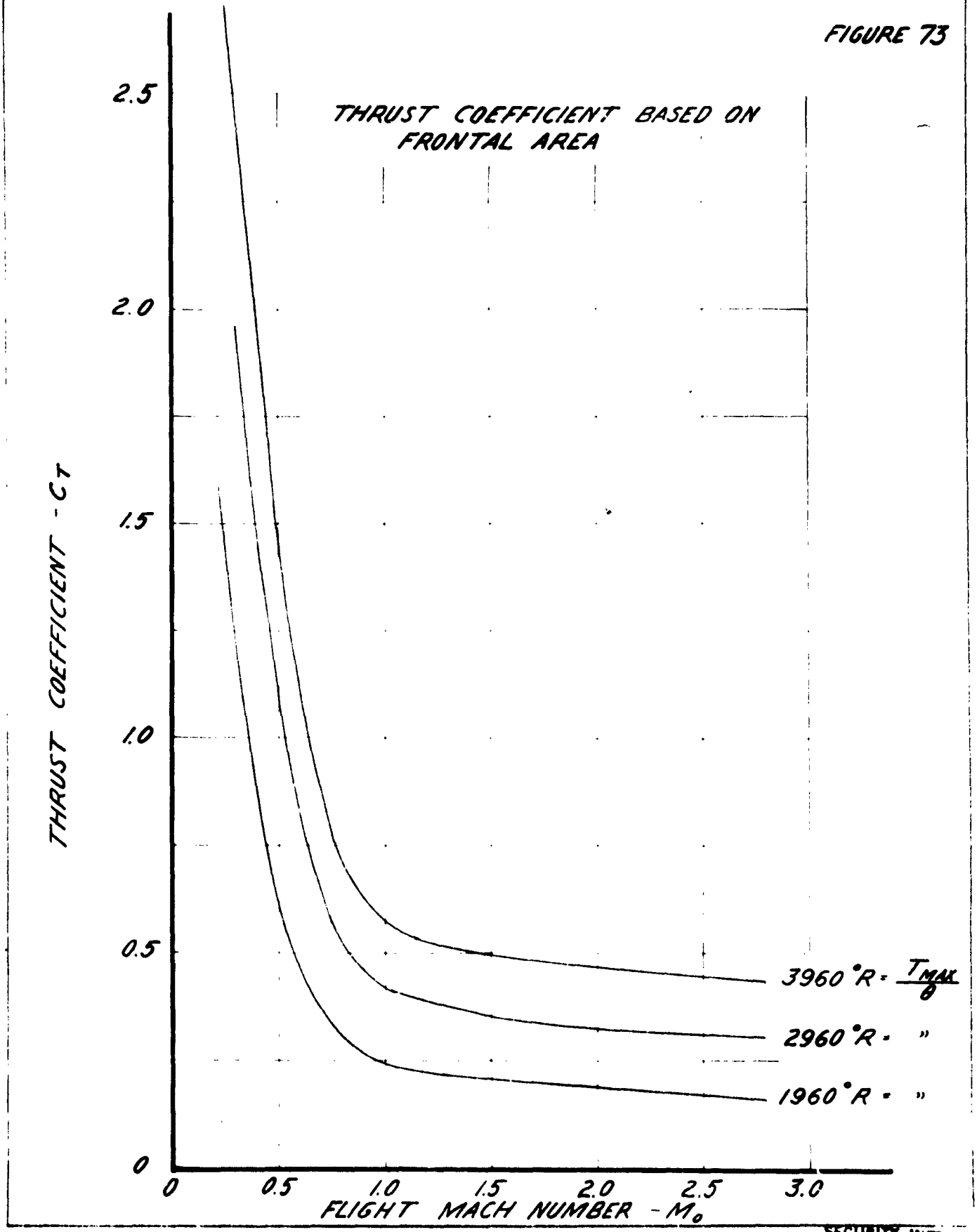

| PREPARED BY | AEROPHYSICS DEVELOPMENT CORPORATION | REPORT NO 2000-1-R1 |
|---|---|---|
| CHECKED BY | PACIFIC PALISADES, CALIFORNIA | DATE Jan 24 1953 |

FIGURE 74

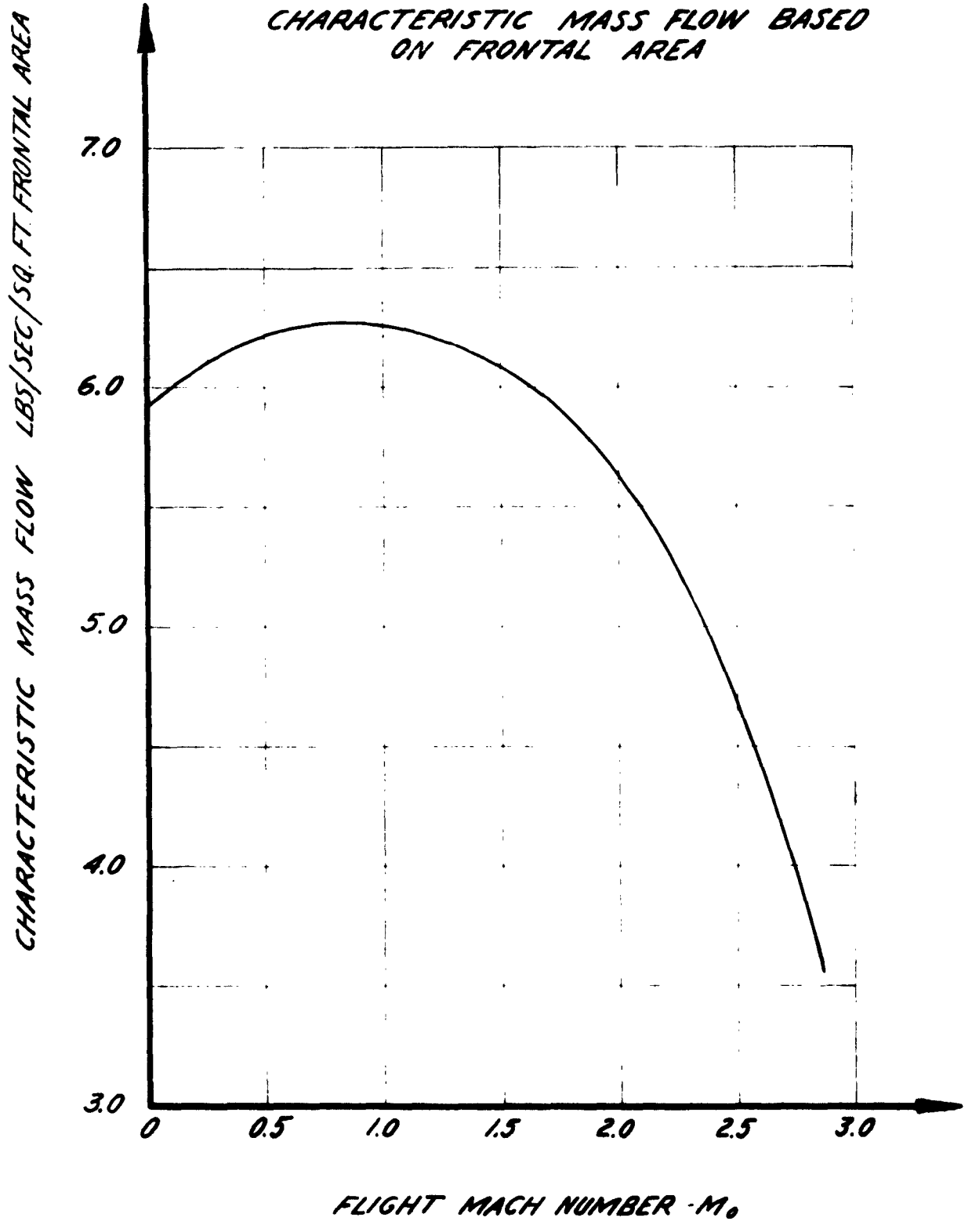

| PREPARED BY | AEROPHYSICS DEVELOPMENT CORPORATION | REPORT NO 2000-1-R1 |
|---|---|---|
| CHECKED BY | PACIFIC PALISADES, CALIFORNIA | DATE Jan 24, 1953 |

FIGURE 75

DRAG COEFFICIENT FOR A TYPICAL LONG RANGE MISSILE

WING AREA = 425 SQ. FT.
GROUND LAUNCH WEIGHT = 52,000 #
TAKE OFF VELOCITY = 320 FT/SEC

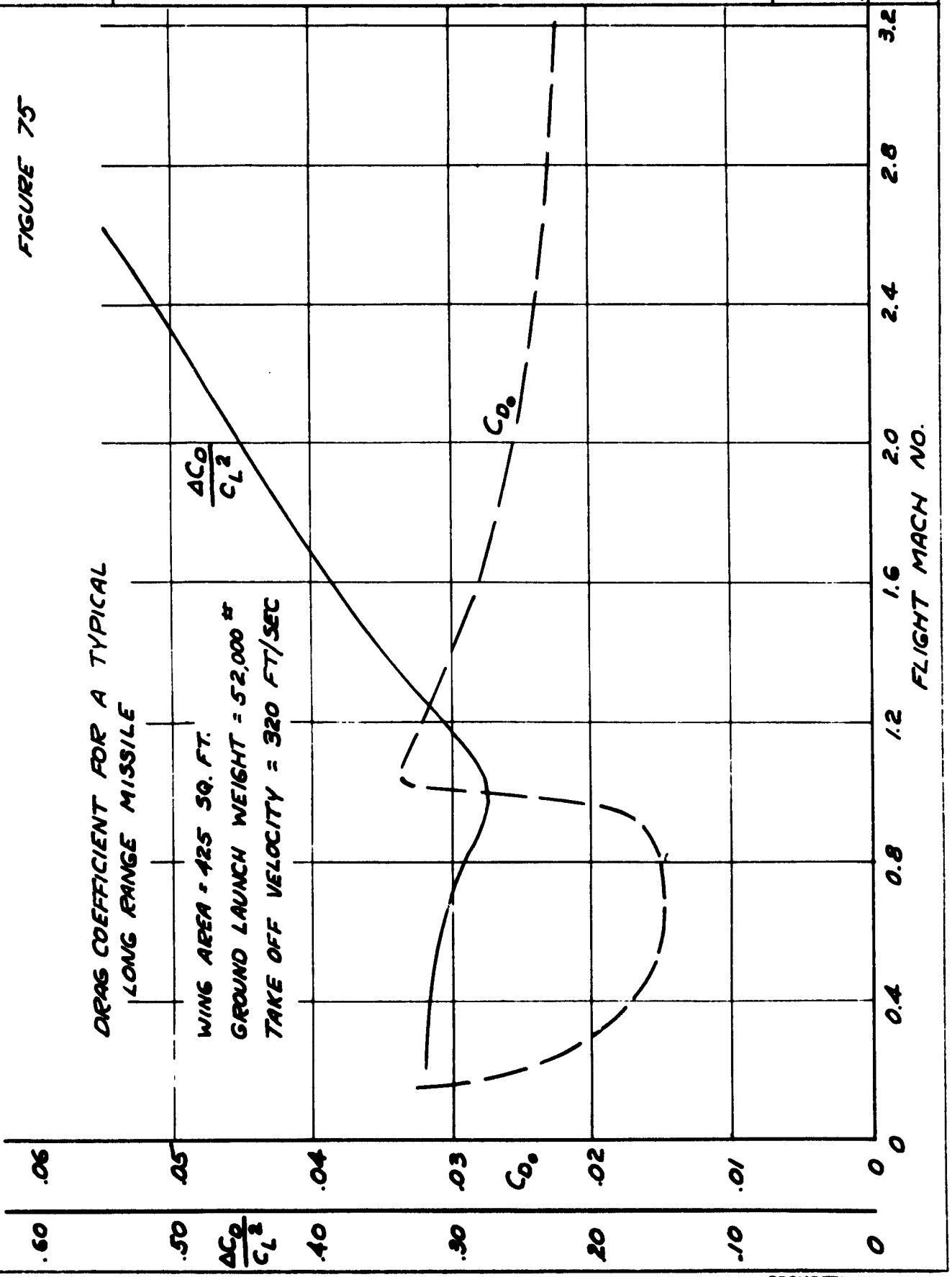

having an outside diameter of 36" and each weighing about 1,000 pounds for a total engine weight of 4,000 pounds. It will be noted in Figure 76 that this system has sufficient excess thrust to accelerate through M = 1.0 at sea level by operating at a maximum cycle temperature of about 3,200° F. The minimum cruising speed (Figure 77) at h = 35,000 feet will be $M_o$ = 1.30 for Tmax = 2540° F. Similarly at 5,000 feet, this system has sufficient thrust to accelerate through M = 1 and accelerate to M = 2.00 by operating at a maximum cycle temperature Tmax = 3350° F. Figure 78 gives the minimum flight velocity (or take-off velocity).

The maximum cross-sectional diameter of the engine is 36 inches, the length is 45 inches without diffuser. The cross-sectional area of the combustion tubes is 506 square inches or 49.5% of the maximum cross-sectional area of the engine. There are six concentric rows of 32 tubes each. The diameters of the tubes decrease from the outer to the inner circle and they are 2.62", 2.22", 1.87", 1.50", 1.23", and 1.02" respectively. The length of the tubes is 15". The total dry weight of the engine is approximately 1,000 pounds.

.. Leakage Losses

Most of the leakage losses will occur when there is a large pressure differential across the valves. These conditions are present during the burning and discharge phases. The only time the exhaust valve is closed is during the pulse compression and burning phases. During the compression phase, the pressure is relatively low in the tubes and, therefore, percentage-wise, very little leakage will occur. During the burning phase, the pressure will rise in the tubes and most of the leakage will occur. Any leakage around the exhaust valve is not all lost, as a collection chamber ducts all gases released by the engine to the exit nozzle to produce thrust. Although this is not as an efficient a process as if there was no leakage, it was assumed that the loss in thrust from this leakage is small.

The inlet valve is closed during the burning and discharge phases. The worst case would occur if the leakage losses were directly ducted to the outside and completely lost. Actually, there will be an interflow from one tube to another, and the only losses will occur at the outer edges of the inlet valve. The pressure surrounding the inlet valve will be very nearly the total pressure of the incoming air. Actually, during the latter part of the discharge phase, the leakage will be reversed and air will flow into the tubes.

A hypothetical case under the worst conditions will have the following assumptions:

(1) The leakage flow is completely lost to the atmosphere by each individual tube.

(2) The leakage area will be that formed at the periphery of each tube at a valve clearance of 0.005".

PREPARED BY

CHECKED BY

**AEROPHYSICS DEVELOPMENT CORPORATION**

**PACIFIC PALISADES, CALIFORNIA**

REPORT NO 2000-1-R1

DATE Jan 24 1953

FIGURE 76

## DRAG AND THRUST COEFFICIENTS

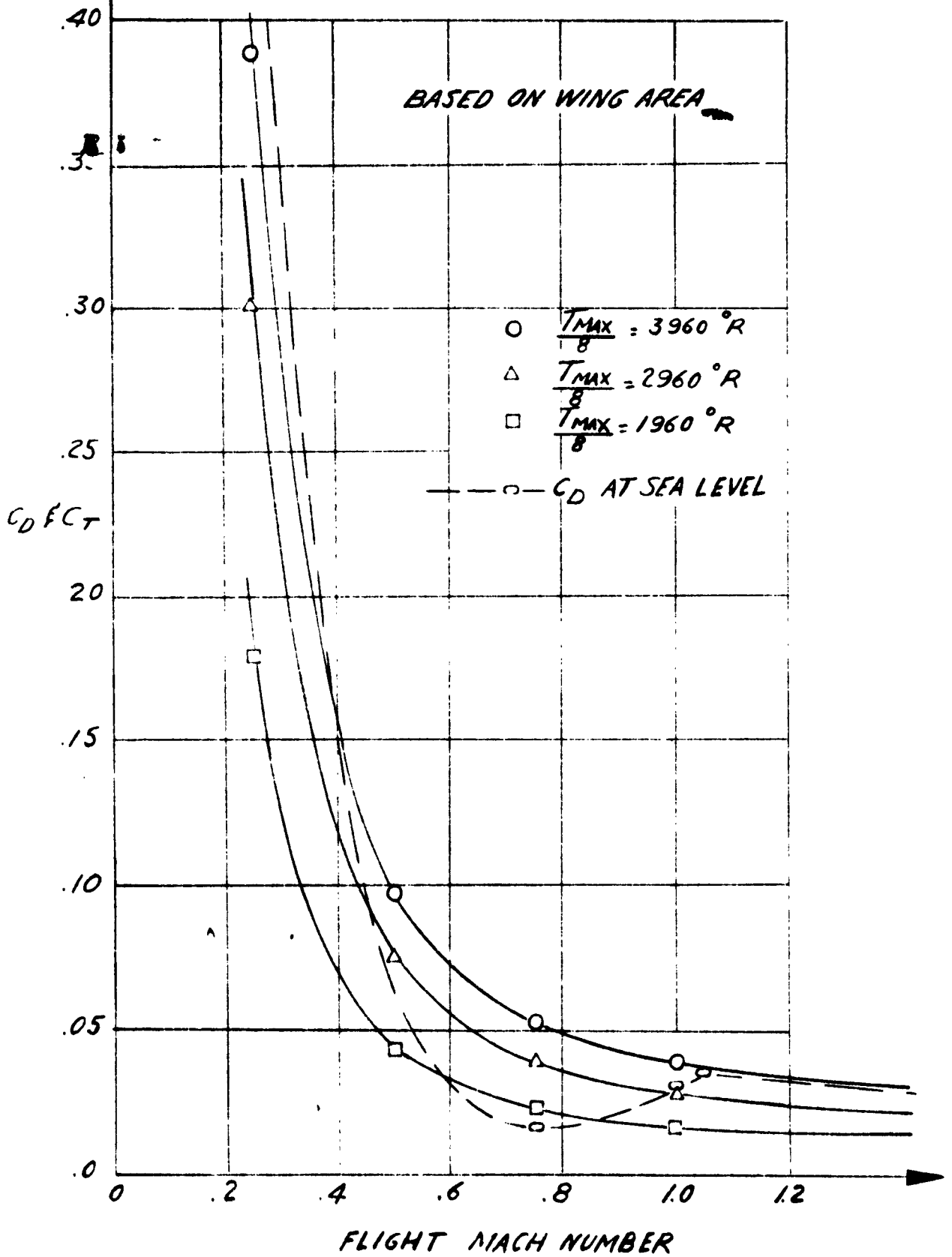

| PREPARED BY | AEROPHYSICS DEVELOPMENT CORPORATION | REPORT NO 2000-1-R1 |
|---|---|---|
| CHECKED BY | PACIFIC PALISADES, CALIFORNIA | DATE Jan 24 1953 |

FIGURE 77

| ALTITUDE FEET | $\frac{T_{MAX}}{\theta}$ | $T_{MAX}$ |
|---|---|---|
| 0 | 3960°R | 3500°F |
| | 2960°R | 2500°F |
| | 1960°R | 1500°F |
| 5000 | 3960°R | 3350°F |
| | 2960°R | 2380°F |
| | 1960°R | 1425°F |
| 15000 | 3960°R | 3080°F |
| | 2960°R | 2190°F |
| | 1960°R | 1290°F |
| 25000 | 3960°R | 2800°F |
| | 2960°R | 1980°F |
| | 1960°R | 1155°F |
| 35000 | 3960°R | 2540°F |
| | 2960°R | 1780°F |
| | 1960°R | 1020°F |

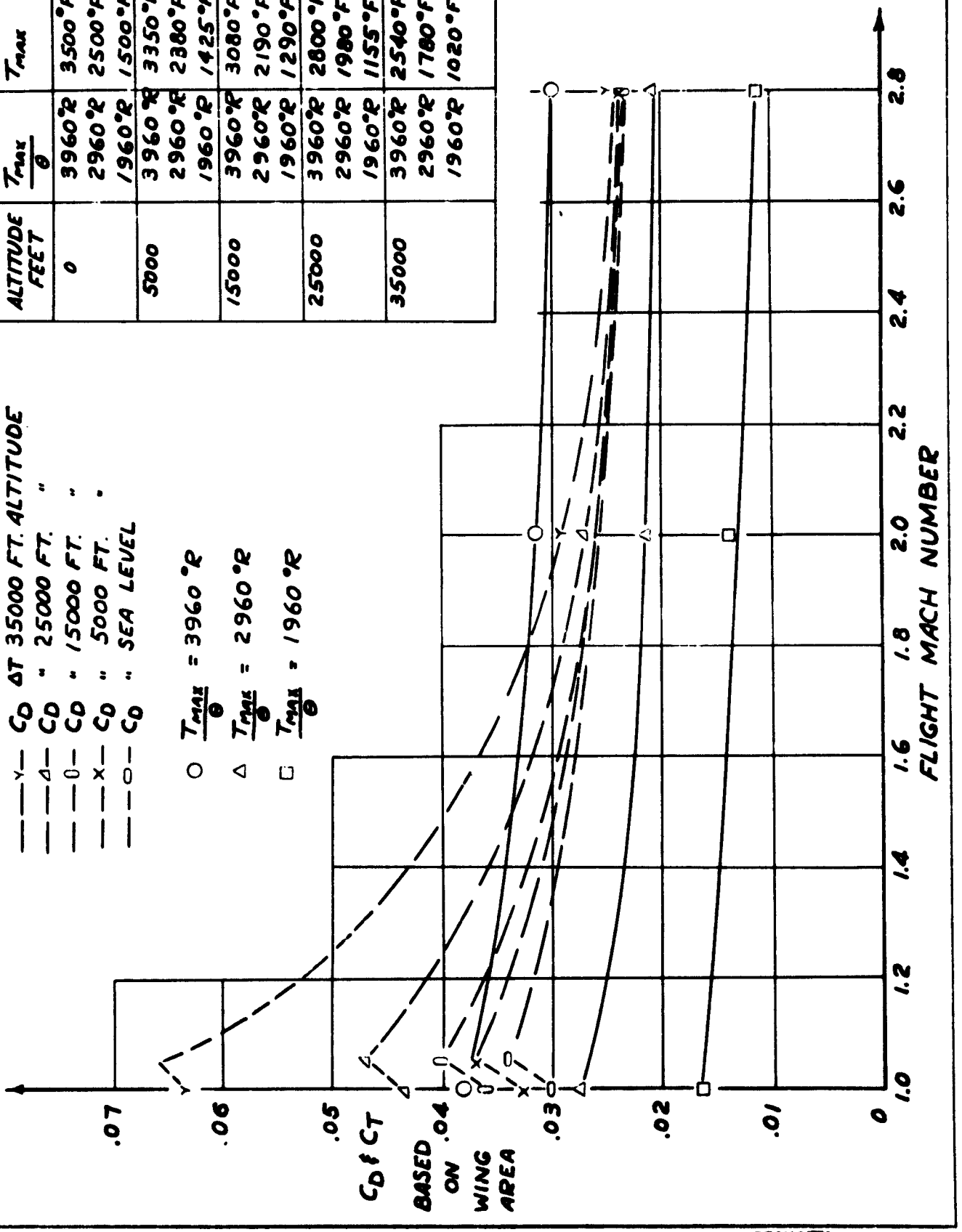

| | | |
|---|---|---|
| | AEROPHYSICS DEVELOPMENT CORPORATION | 2000-1-R1 |
| | P.O. BOX 452 PALO ALTO CALIFORNIA | Jan 24 1953 |

FIGURE 78

## DRAG AND THRUST AT SEA LEVEL

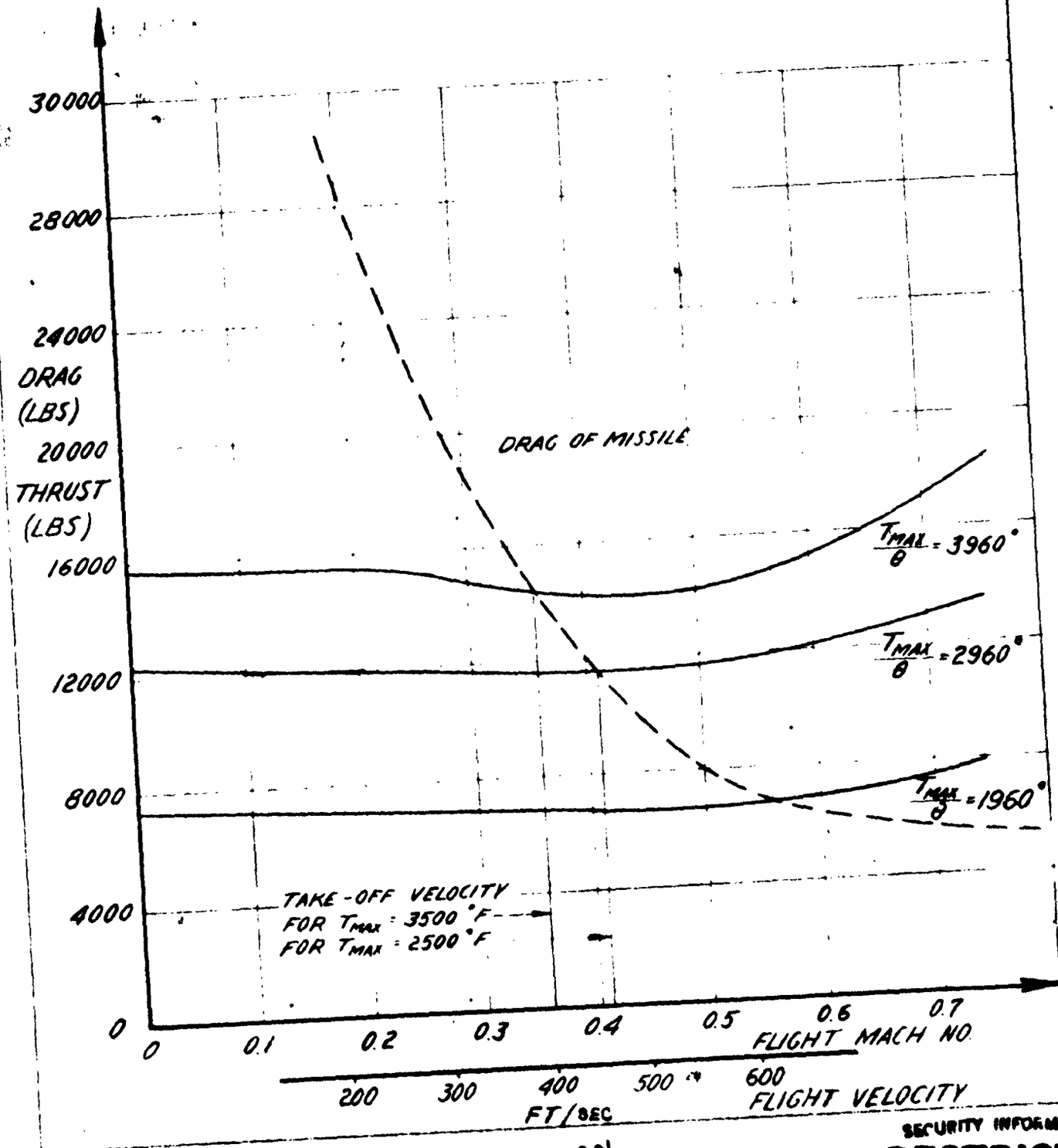

(3) The amount of flow loss due to leakage during the discharge phase will be given by the amount of flow discharged at the exit multiplied by the ratio of leakage area to discharge nozzle area of each tube.

For the smallest tubes (diameter = 1.02 inches), the percentage of the discharged flow lost through leakage to that discharged during the thrust phase is ,

$$\frac{\text{Area of leakage}}{\text{Area of discharge}} = \frac{\pi \times 1.02 \times 0.005 \times 100}{\pi/4 \times 1.02^2} = 1.96\%$$

For the largest tubes (diameter = 2.62 inches), this loss is

$$\frac{\text{Area of leakage}}{\text{Area of discharge}} = \frac{\pi \times 2.62 \times 0.005 \times 100}{\pi/4 \times 2.62^2} = 0.76\%$$

The above figures indicate that 2% to 3/4% of the air discharged (depending on the tube diameter), during the exhaust phase, is lost through leakage through the inlet valve. Since a greater percentage of the discharge area is composed of the larger diameter tubes then the weighted mean of the leakage losses at the inlet valve during discharge is 1.1% of the total mass flow through the engine. Further leakage will occur during the burning phase both at the inlet and exhaust valves. We will make the following assumptions:

1. Duration of burning = duration of discharge

2. Average pressure in the tube during burning = the average pressure in the tube during discharge

From the above assumptions we can conclude that leakage losses at (1) the inlet valve during burning, (2) the exhaust valve during burning, each equal the leakage losses at the inlet valve during the discharge phase. The total leakage losses during burning and exhaust then amount to 3.3% of the mass flow per cycle. There remains then to determine the leakage losses at the exhaust valve during pulse compression. Since the duration of pulse compression is approximately the same as for the discharge phase, and since the pressure in the tube is less than the average pressure during discharge, a conservative estimate of these losses would be 1.1%.

The total leakage losses for the cycle is then 4.4% of the mass flow per cycle. Very simply, a conservative estimate of the leakage losses is four times the losses at the inlet valve during the discharge phase. These losses were not included in the computations.

## 5.7 Performance of the Multi-Jet using Surface Combustion

The above performance analysis of the 36 inch diameter engine depended on the assumption for the duration of burning. The duration of the burning phase was determined from the information obtained on

detonation from the various investigations reported in the literature. This is described in more detail in Section IX .

Preliminary heat transfer calculation show that approximately eight times the tube surface area is required for fins on the outside of each tube to cool the wall to 1500° F when the maximum cycle temperature is 3500° F. This leads to a very heavy construction for each tube, and it also necessitates moving the tubes farther apart, given a poor nesting arrangement. Liquid cooling required a very large radiator and a large mass flow of liquid. It was decided, therefore, to consider ceramic materials for the tubes, such as stabilized zirconium oxide or graphitar. Section IX gives a complete discussion on the cooling problem and on the high temperature materials.

Since ceramic tubes must be used in the engine the phenomenon of surface combustion can be used to ignite the fuel-air mixture for each cycle. This type of ignition system is used in the small 8" diameter subsonic unit and the cycle is described in detail in the following section. Actually the durations used for the burning phase have been only assumptions and the question still remains whether the duration of burning is substantially different for the two methods of ignition. From the present state of the investigations carried out in detonation and surface combustion, there isn't sufficient information to make a fair comparison of the two systems. The only comparison that can be made now is between the two assumptions. The two methods proposed for the ignition of the fuel-air mixture are described in more detail in Section IX and the justification for the assumptions used, is given there.

It is interesting on the other hand to see what effect this new method of ignition has on the performance of the Multi-Jet. We will assume that the engine configuration remains the same as described previously. Section VI describes the method used to calculate the duration of burning but for continuity it will be repeated here.

If the assumption is made that the burning is completed by means of a radially traveling flame an equivalent flame velocity can be computed. This equivalent flame velocity is of such a magnitude that as the mixture flows longitudinally through the length of the tube the flame travels radially through the radius of the tube. In reference 10 mass flows of up to 60 lbs/sec/sq ft of burner cross sectional area were burned in an 18 inch long burner of 3 inch internal diameter. Thermal choking of the exit flow was caused at this high mass flow. A low conservative estimate of the velocity of the fuel-air mixture at the entrance of the burner in the above experiments would be about 300 ft/sec or $M_1 = 0.27$. To traverse the 18" length it takes $\frac{18}{12 \times 300} = 0.00500$ seconds. The flame meanwhile travels from the walls to the center of the tube or a distance of 1.50". The equivalent flame speed then is $\frac{1.50}{12 \times .00500} = 25$ ft/sec.

The maximum tube diameter in the Multi-Jet is 2.62". The time required for burning then is the time required for the flame to travel radially or

$$\tau_B = \frac{2.62}{2 \times 12 \times 25} = 0.00436 \text{ secs.}$$

The time assumed previously was 0.0015 secs. and therefore this increases the total cycle time by approximately 0.0030 seconds if the above assumptions are true. The total cycle time for the $M_o = 2.80$ case (see Figure 60) was 0.006 seconds; now with the new type of ignition it is increased to 0.009 seconds. Here we see the main difference between the two cycles. This results in the reduction of the average thrust by 1/3 or the thrust in this case is 66 2/3% of the thrust computed with the detonation type engine. The specific fuel consumption and the air specific impulse remain the same, since Tmax and Pmax remain the same. The characteristic mass flow, however, is reduced.

The above analysis applies only if the combustion tubes are kept at the length of 15 inches. By making a careful study of Figure 60 we see that the reduction of the thrust is due to the relative increase of the duration of the burning phase with respect to the duration of the other phases. If we could increase the durations of the other phases in the same ratio as the burning phase was increased, then as long as the impulse increased in the same ratio we can obtain the same performance for our surface combustion engine as we had computed for our detonation engine. Here we note the disadvantage of an engine operating on the constant volume cycle -- that is, the decrease in average thrust due to an increase in the duration of constant volume combustion. However, in the present design a very important principle makes it very convenient to increase the average thrust by adjusting the duration of the burning phase with respect to the rest of the phases. This is most simply done by adjusting the length of the combustion tubes. The duration of each of the phases of scavenging, pulse compression and discharge varies directly as the length of the combustion tubes. The impulse also varies directly with the length of the combustion tubes. Therefore, by increasing the length of the combustion tubes by the same ratio as the burning time was increased then we will obtain the same thrust per square foot of frontal area as we obtained for the detonation engine. This, of course, would increase the weight/thrust ratio, due to the longer tubes. The increase of this parameter may or may not be too critical and will depend on the application of the engine. The longer tube engine would weigh approximately 1½ times the weight of the engine described at the beginning of this section. Preliminary weight studies indicate that this engine would weigh 1600 lbs.

The longer tubes do present a problem due to their greater $\frac{L}{D}$ ratio making the frictional flow losses greater and requiring a greater pressure to move the flow in the tube. Again the frictional losses are not bordering on the critical stage and can be absorbed without

reducing the performance not more than 2 to 4%.

The lengthening of the tubes is not the only solution. The tube diameters can be decreased so that the burning time can be reduced to 0.0015 seconds as before. This solution does not increase the engine weight nor its length, and it has a further advantage in that it reduces the valve closing and opening times (due to the fact that the valve does travel at the same speed while the tube diameters have been reduced).

We are now beginning to see that we must arrive at a compromise and that an optimization analysis must be made in order to obtain the most efficient engine. The duration of burning was computed by using the diameters of the largest tubes. The engine consists of several concentric rows of tubes each with tubes of different diameters, and, therefore, we must compromise on the burning time. It was felt that since the burning time is only an assumption that a detailed optimization analysis should not be made at this time. From the considerations of this section we have a clear picture of the overall design of the Multi-Jet, and we can see its potentialities and its most important parameters.

The present analysis is only limited by the lack of information on the burning phase, either for the detonation or for the hot wall method of ignition. Some experiments were carried out in order to find some of the answers and these are reported in a later section. When the actual burning times are determined then a definite tube length can be found which will give the most efficient engine.

| PREPARED BY | AEROPHYSICS DEVELOPMENT CORPORATION | REPORT NO 2000-1-R1 |
|---|---|---|
| CHECKED BY | PACIFIC PALISADES, CALIFORNIA | DATE Jan 24 1953 |

SECTION VI

PERFORMANCE ANALYSIS OF AN 8" DIAMETER ENGINE

## 6.1 Performance of a Typical Unit Operating on the Ideal Cycle

The cutaway perspective view of Figure 79 shows the general configuration of the Multi-Jet engine.

The combustion chambers are arranged as a set of parallel cylindrical tubes in a drum-like cylinder whose outside diameter is 8¼ inches. This drum-like cylinder contains two end walls between which are mounted the combustion tubes. The tubes are arranged in a set of six circles with the tubes on the outer circle having the larger diameter, and gradually decreasing in diameter to the inner circle of tubes of smallest diameter. The inside diameter of each of the tubes from the outer to the inner circles is 0.51", 0.47", 0.40", 0.29" 0.29" and 0.25" respectively. There are 32 tubes in each row. The length of all the tubes is 8 inches. The cross-sectional area of the combustion tubes is 25.0 square inches and the total volume of the combustion chambers is 0.0369 cubic feet. The tubes are surrounded and packed with Fiberfrax insulation material. This material resembles cotton wool and can be packed with various densities around the tubes. The material will withstand temperatures up to 3000°F.

The inlet valve consists of four flat vanes with a cut 50% of the area open. The exhaust valve has the same configuration. (See Figure 79). The valves can be rotated by a number of methods; the two most promising are:

1. Electrically driven by a small motor.
2. Hydraulically driven by the high pressure fuel traveling up the helicopter blade.

A more detailed description of the valve drive system and the fuel system is given in a later section.

With the above physical dimensions of the Multi-Jet, the ideal performance can be calculated. The computations are given in Table 8 and are described in detail in Appendix IV. The curves of ideal thrust, specific fuel consumption, air specific impulse, thrust per unit maximum frontal area, weight/thrust ratio, thrust coefficient and characteristic mass flow are given in Figures 80, 81, 82, 83, 84, 85 and 86.

## 6.2 Burning Phase

The combustion chambers are composed of ceramic materials which

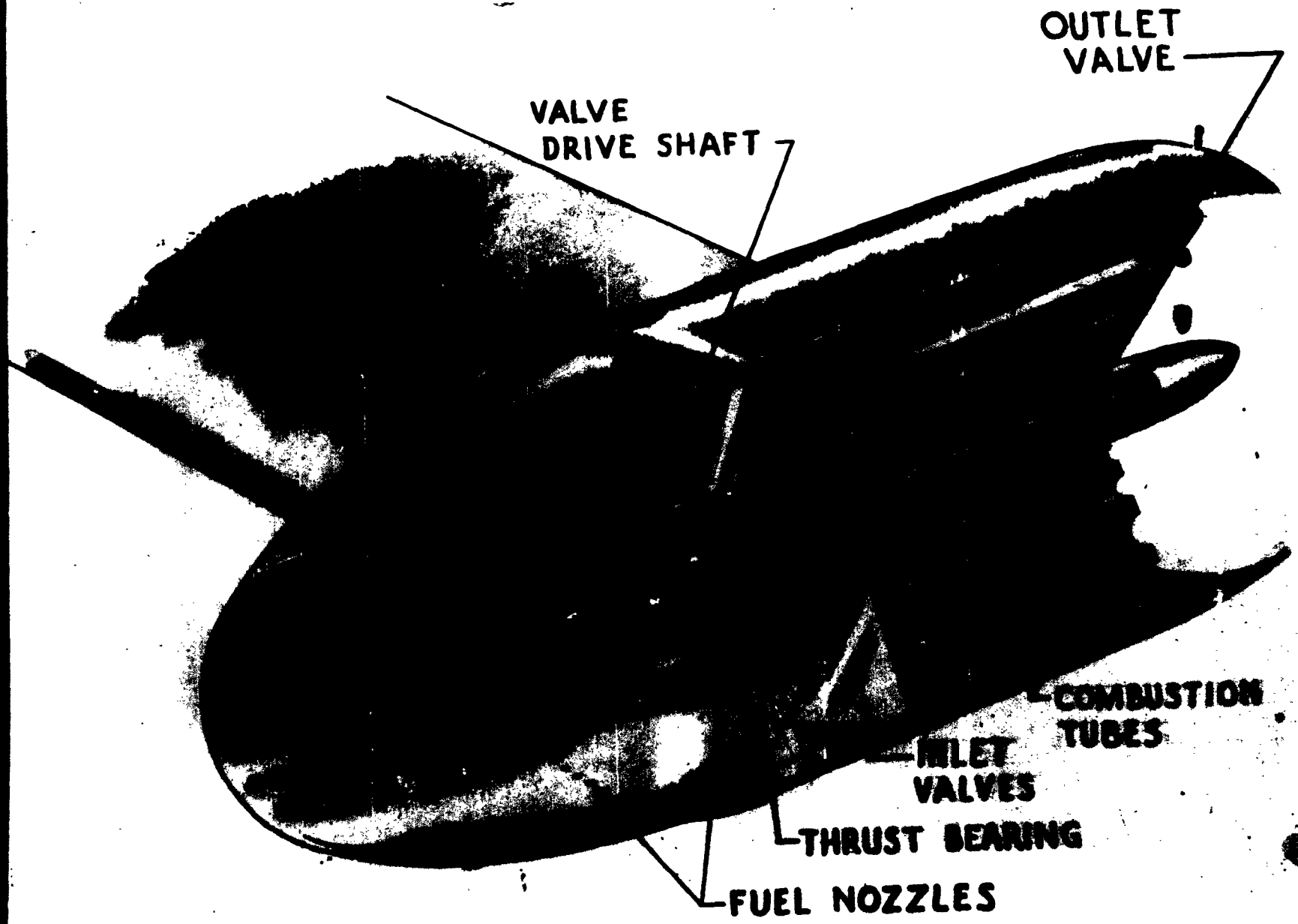


PERSPECTIVE VIEW OF THE MULTI - JET

| PREPARED BY | AEROPHYSICS DEVELOPMENT CORPORATION | REPORT NO 2000-1-R1 |
|---|---|---|
| CHECKED BY | PACIFIC PALISADES, CALIFORNIA | DATE Jan 24 1959 |

FIGURE 80

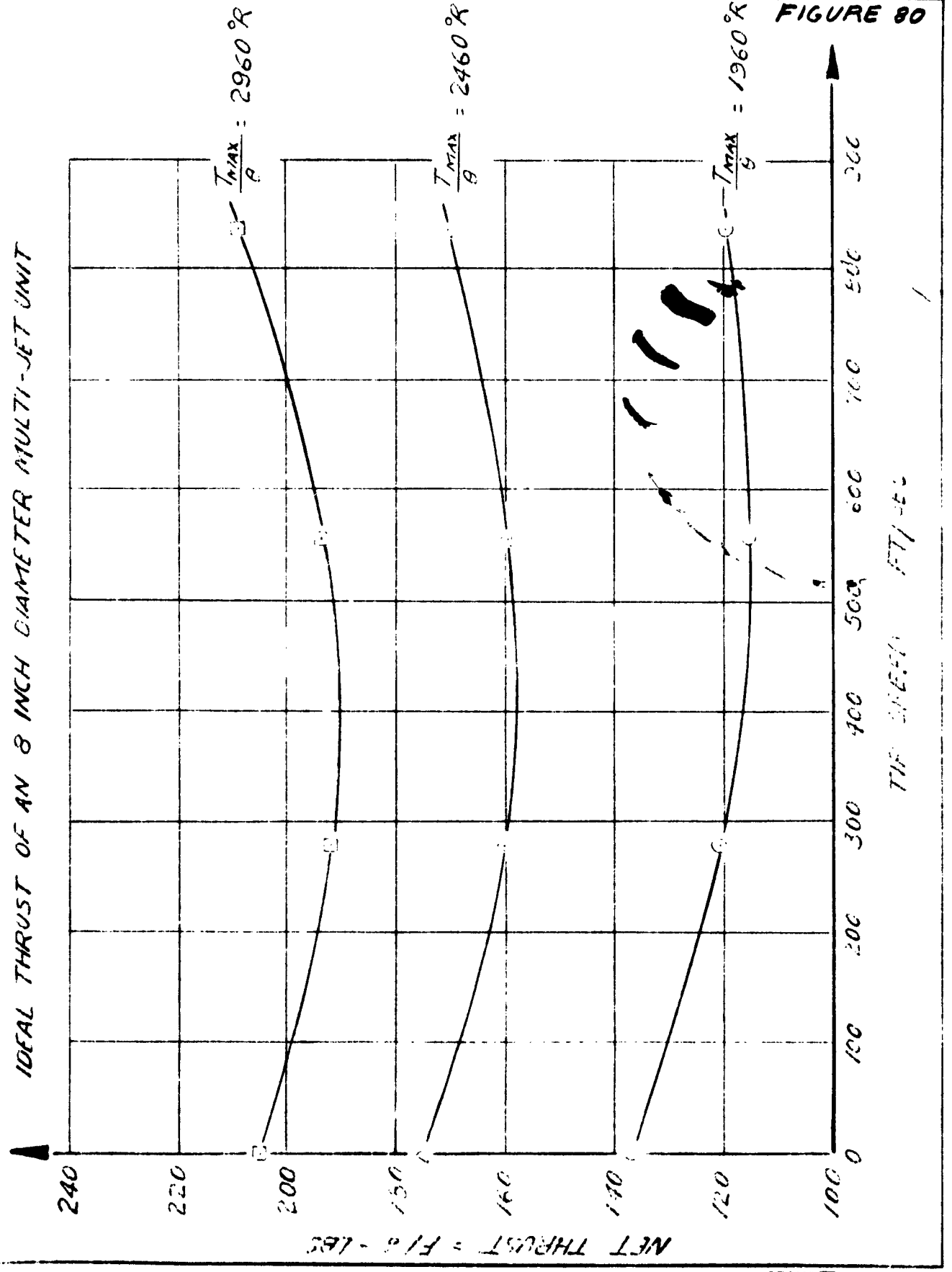

| PREPARED BY | AEROPHYSICS DEVELOPMENT CORPORATION | REPORT NO 2000-1-R1 |
|---|---|---|
| CHECKED BY | PACIFIC PALISADES, CALIFORNIA | DATE Jan 24 1953 |

FIGURE 81

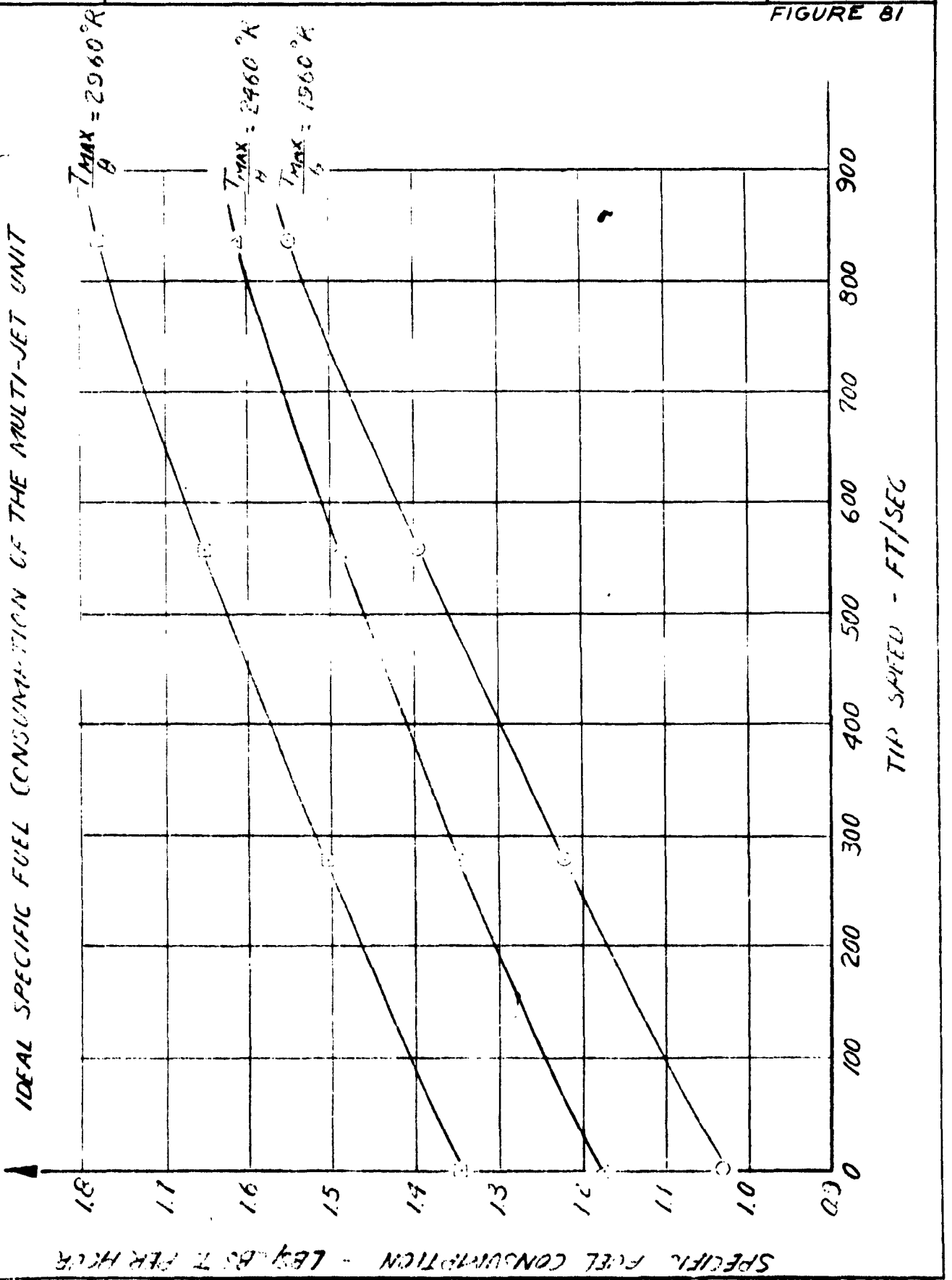

AEROPHYSICS DEVELOPMENT CORPORATION
P.O. BOX 657 PACIFIC PALISADES CALIFORNIA

2000-1-R2

DATE Jan. 24, 1953

FIGURE 82

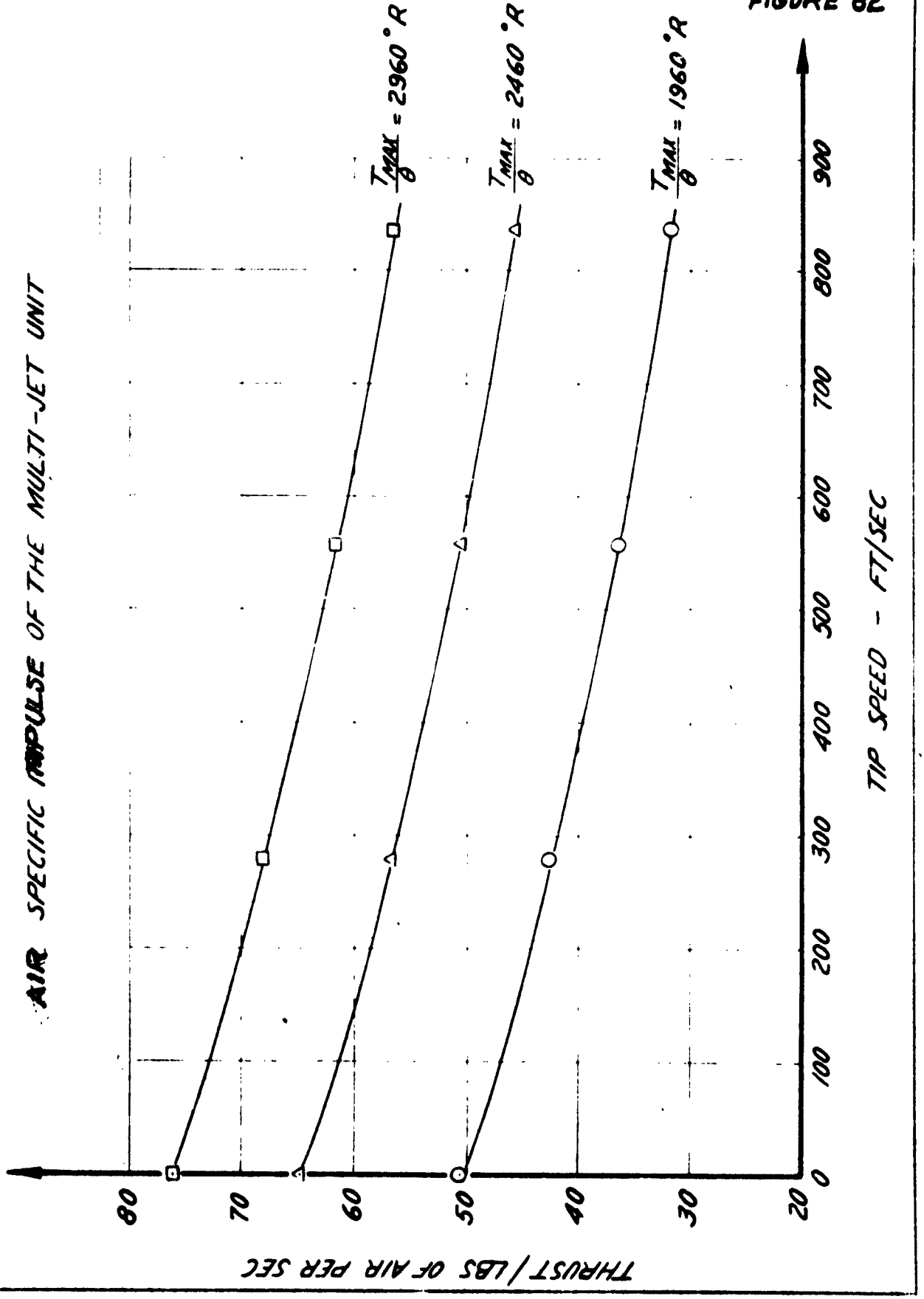

AEROPHYSICS DEVELOPMENT CORPORATION
P.O. BOX 657 PACIFIC PALISADES CALIFORNIA

2000-1-R1

DATE Jan 24 1953

FIGURE 83

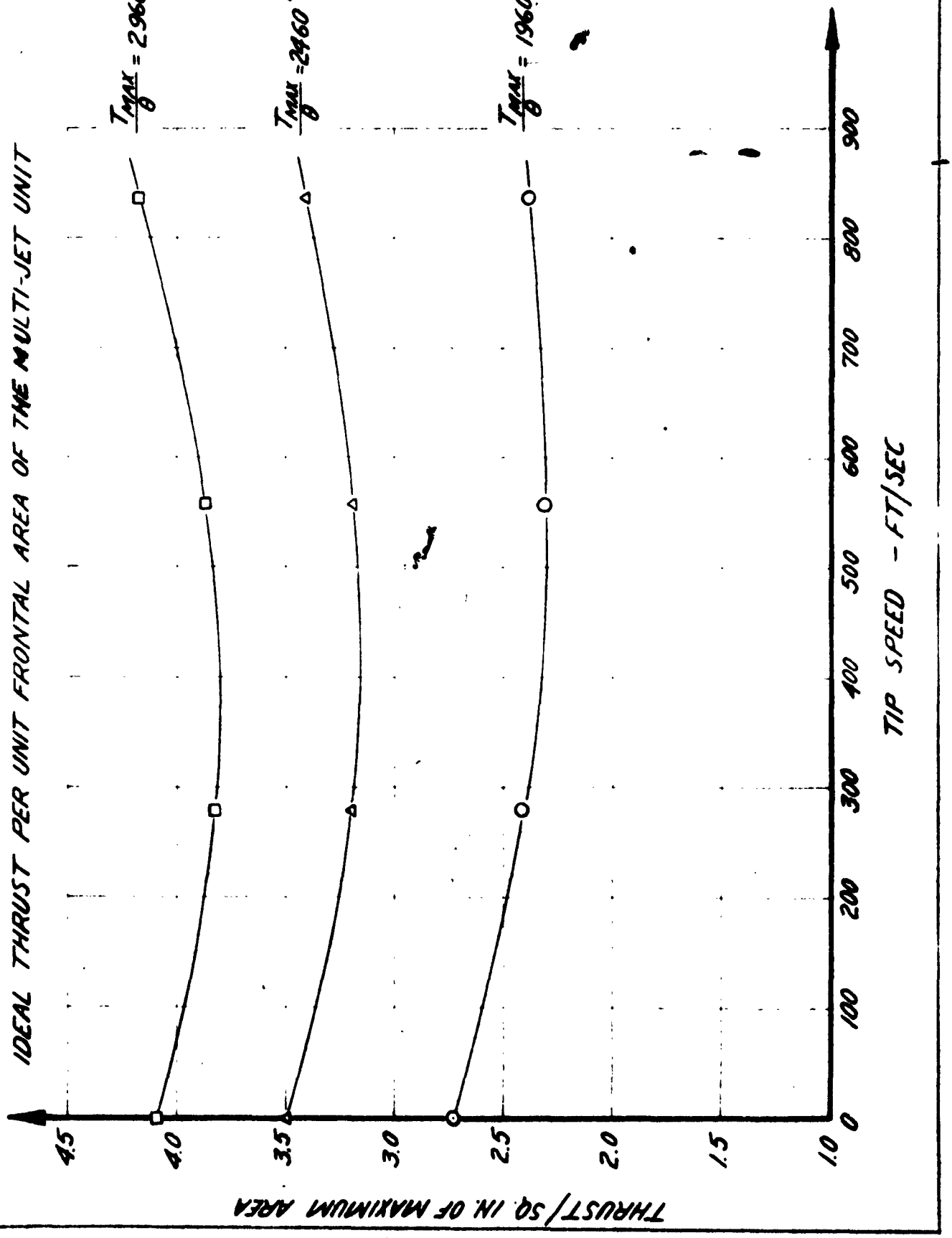

| PREPARED BY | AEROPHYSICS DEVELOPMENT CORPORATION | REPORT NO 2000-1-R1 |
|---|---|---|
| CHECKED BY | PACIFIC PALISADES, CALIFORNIA | DATE Jan 24 1953 |

FIGURE 84

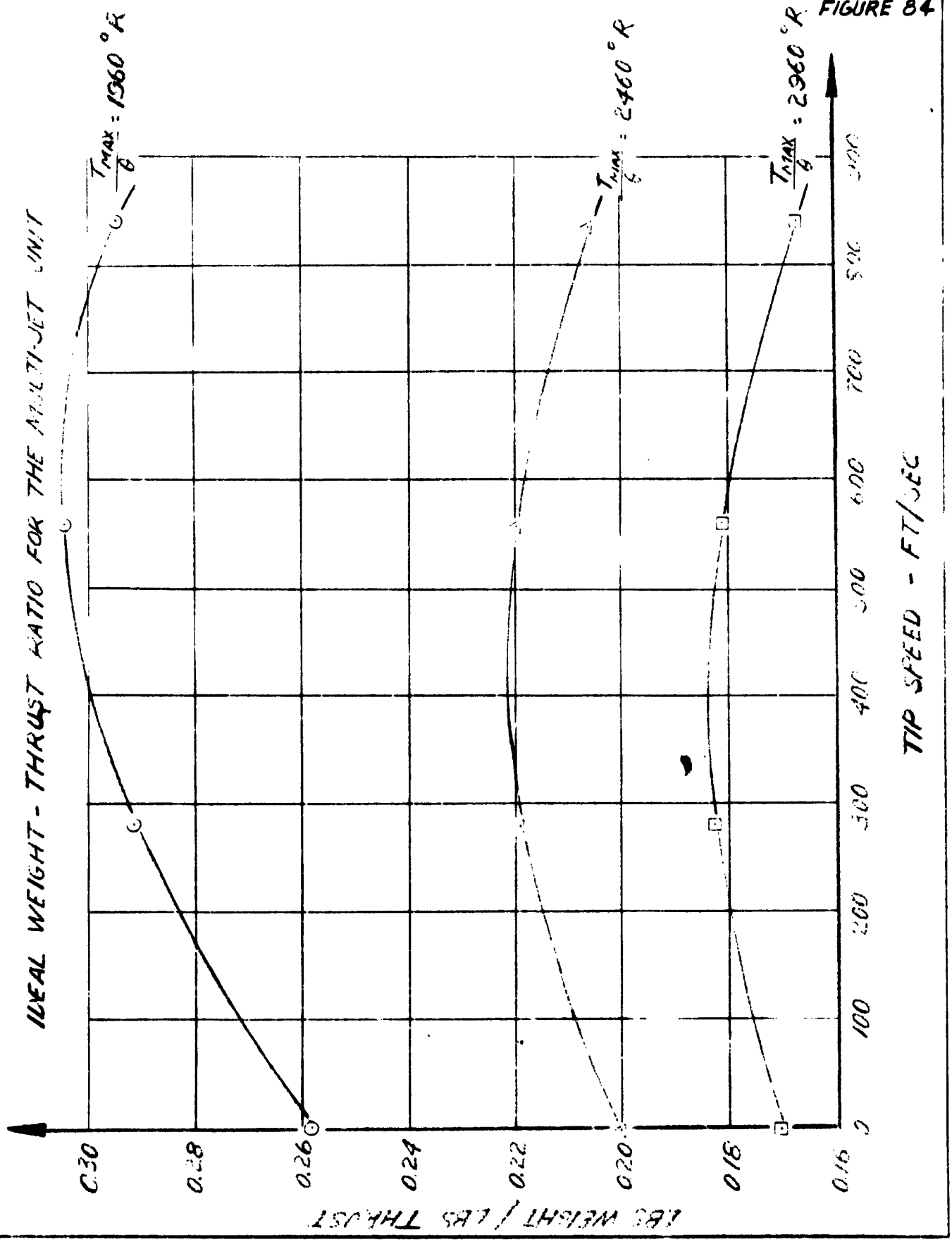

| PREPARED BY | AEROPHYSICS DEVELOPMENT CORPORATION | REPORT NO 2000-1-R1 |
|---|---|---|
| CHECKED BY | PACIFIC PALISADES, CALIFORNIA | DATE Jan 24 1953 |

FIGURE 85

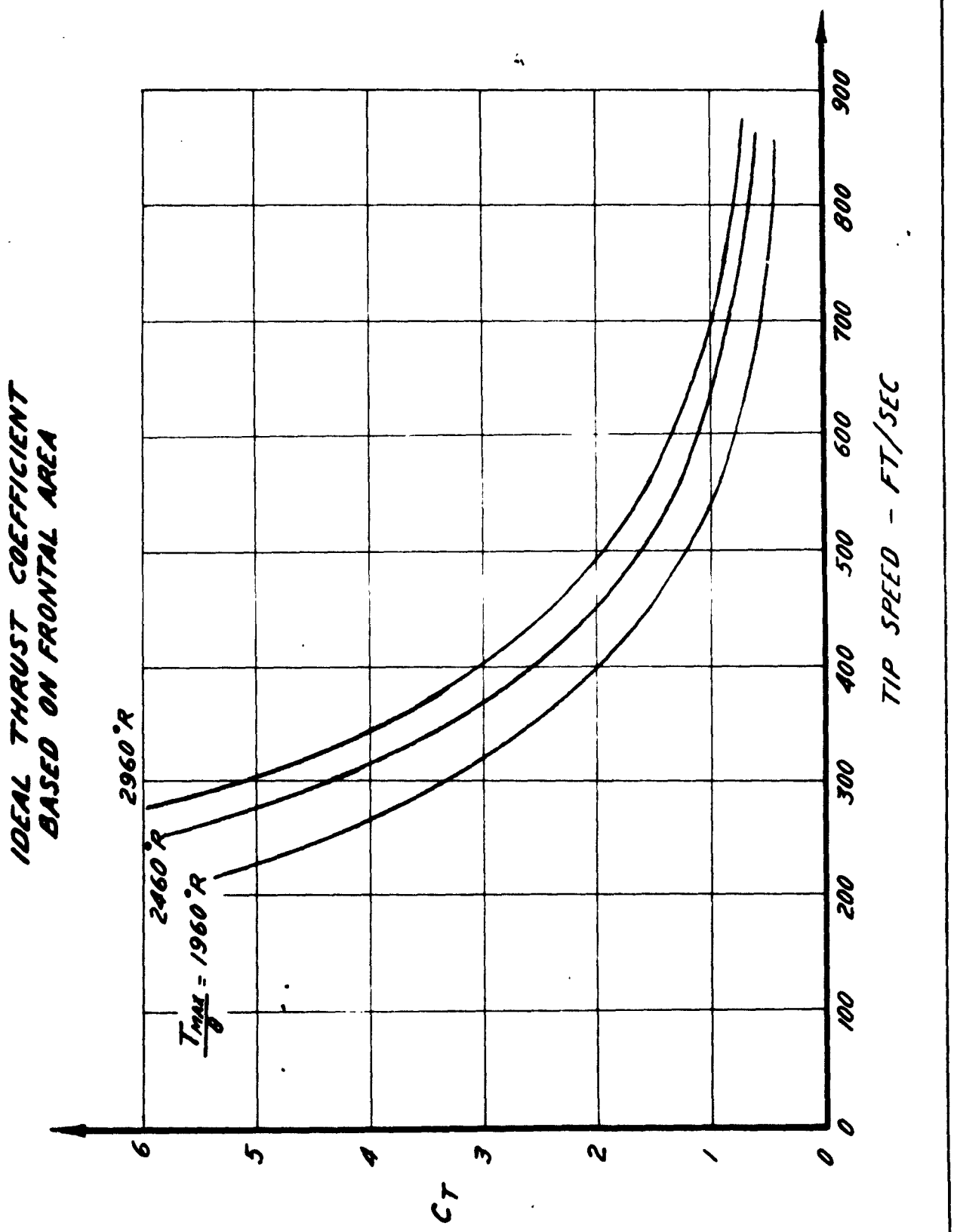

| PREPARED BY | AEROPHYSICS DEVELOPMENT CORPORATION | REPORT NO 2000-1-R1 |
|---|---|---|
| CHECKED BY | PACIFIC PALISADES, CALIFORNIA | DATE Jan 24 1953 |

FIGURE 86

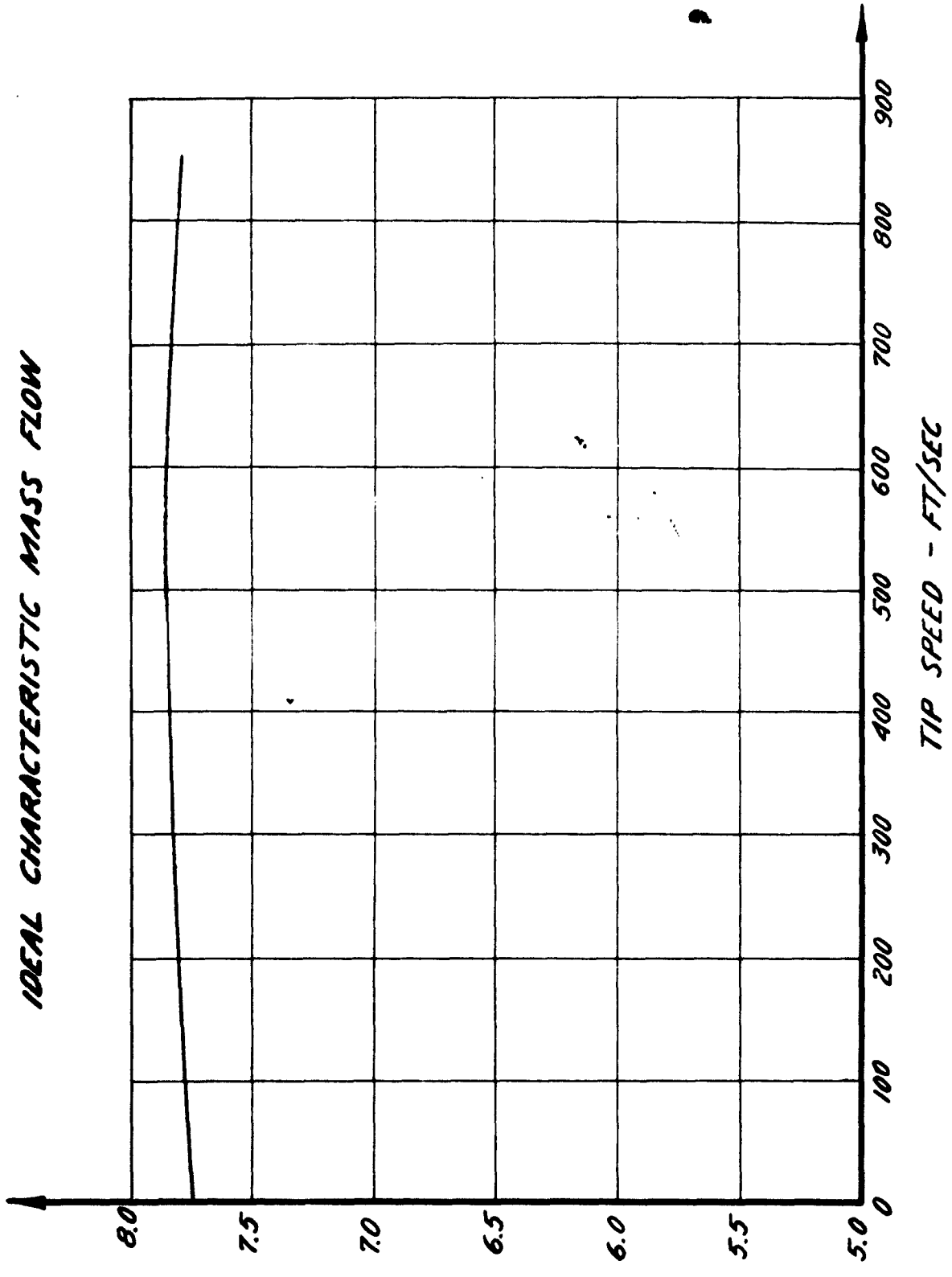

will withstand high temperatures and high pressures. The tubes will be allowed to heat up to very high temperatures (approx. 2000°F) so that each successive charge of fuel-air mixture is ignited by the hot walls. The surface combustion of fuel-air mixtures has been studied by a number of investigators. References (10) and (11), for example, deal with the surface combustion of fuel-air mixtures in ceramic tubes. Both references indicate that very high mass flows can be burned efficiently in ceramic tubes with hot walls. The fundamentals of surface combustion are at present being studied by Dr. Fiock of the Bureau of Standards under an Air Force Contract.

As the fuel-air mixture enters a tube and flows toward the rear, the mixture nearest the walls ignites and the flame travels radially in the tube. Reference 10 shows that for a 3" diameter tube, the fuel-air mixture is completely burned while flowing at high velocities through a tube 18" long. The length and diameter of the tubes of the Multi-Jet will be adjusted so that when the mixture arrives at the rear of the tube it is not completely burnt but only ignited along the boundary layers. This can be seen in Figure 87. The exhaust valve then closes, forming a normal shock wave which travels upstream, stopping the inflowing gases. (See Figure 87 (b)). This shock wave travels upstream through the central core of unburnt gases and through the boundary layers of burnt gases. After the passage of the shock wave, the pressure and temperature of the fuel-air mixture has been

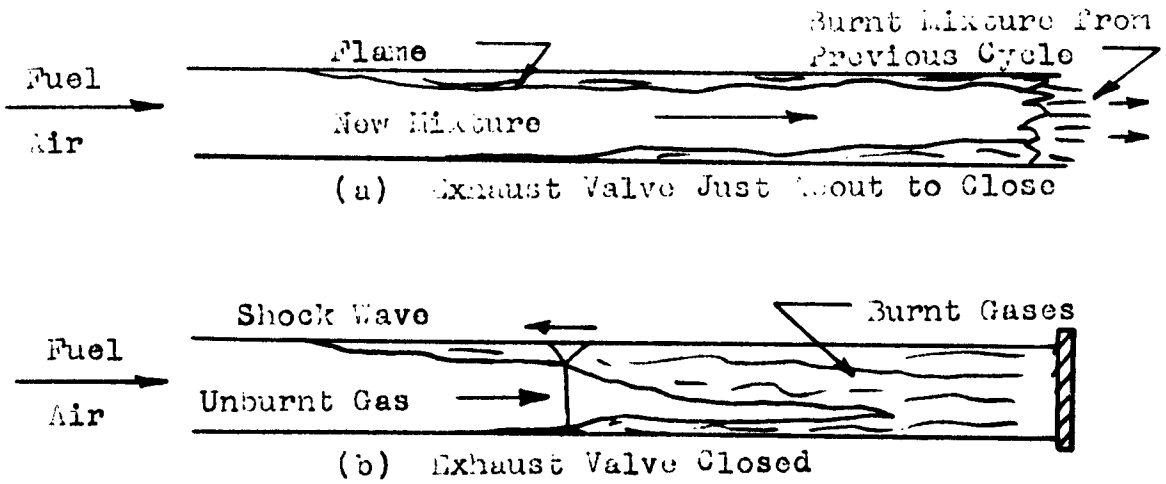


FIGURE 87

raised so that the radial flame accelerates raising the pressure and temperature further and the burning proceeds at an accelerating rate. When the shock wave arrives at the front of the tube, the inlet valve is closed and the burning is completed at constant volume.

If the assumption is made that the burning is completed by means of a radially traveling flame, an equivalent flame velocity can be computed. This equivalent flame velocity is of such a magnitude that, as the mixture flows longitudinally throughout the length of the tube, the flame travels radially through the radius of the tube. In Reference 10, mass flows of up to 60 lbs/sec/sq ft of burner cross-sectional area were burned in an 18" long burner of 3" diameter; thermal choking of the exit flow was caused at this high mass flow. A conservative estimate of the velocity of the fuel-air mixture at the entrance of the burner, in the above experiments, would be about 300 ft/sec or $M_1 = 0.27$. To traverse the 18" length, it takes

$$\frac{18}{12 \times 300} = 0.0050 \text{ seconds (approximately)}$$

The flame meanwhile travels from the walls to the center of the tube or a distance of 1.50". The hypothetical equivalent flame speed then is

$$\frac{1.50}{12 \times 0.0050} = 25 \text{ ft/sec}$$

The maximum tube diameter in the Multi-Jet is 0.50". The time required for the flame to traverse radially would be

$$\tau_B = \frac{0.25}{12 \times 25} = 0.00083 \text{ seconds}$$

A conservative estimate on the duration of the burning phase would be 0.001 seconds.

More extensive research will have to be carried out on this type of combustion in tubes of various diameters and lengths. The phenomenon as described by Howland and Simmonds in Reference (11) indicates that the combustion is taking place in a series of explosions while in Reference (10) the only indication of rough burning is shown in the longer burner lengths. It must be noticed on the other hand that in Reference 11 the fuel-air mixture was introduced into the ceramic tubes through an orifice whose diameter was smaller than the tube diameter, while in the tests of Reference 10, a smooth flow nozzle preceeded the ceramic burner.

The fact that non-steady burning may be achieved even with a steady supply pressure promises to simplify the application to the

present engine, for the length of the tube may be easily adjusted to produce burning or explosion frequencies equal to the frequency of operation produced by the valves. The opening and closing phases produced by the valves may be adjusted to the frequencies of explosions.

C.2.1 Frictional Flow Losses. In order to reduce the losses in the duct during the induction phase due to friction and heating, the diameter of the combustion tube is allowed to increase toward the rear. The equations for the area increase were developed in Section V. For this case, for a given flight velocity, there will be an optimum $M_d$ for each $L/D$ ratio. This is due to the fact that the amount of pulse compression will increase with $M_d$ while the friction losses in the duct will also increase with $M_d$. The ratio of final static pressure $P_2''$ over the inlet total pressure $P_{ot}$ for various $L/D$ ratios is plotted against $M_d$ in Figure 36.

C.2.2 Effect on the Total Duration of the Cycle. The non-stationary wave diagrams were drawn by making use of the assumption of linear variations as the valves opened. The acceleration of the interface between the burnt and new mixtures was assumed to take place through a compression wave having a pressure ratio of 1.70. (See equation 90). This strength of wave was chosen since it produces a flow Mach Number in the tube of 0.6 as the scavenging starts. The compression wave was divided into four parts (or characteristics) each characteristic increasing the interface velocity by $\frac{1}{4}$ of the final velocity to give a final Mach Number of 0.6 in the new mixture. The stopping of the fluid particles and the formation of the shock wave by the exhaust valve is computed in the same way. For these computations and for tubes of 6 inches in length, the time for constant volume burning was assumed to be 0.0010 secs at $M_o = 0.75$. (See Section C.2). For any of the other flight Mach Numbers the rotational speed of the valve was computed from the scavenging and the shock compression phases of the cycles. By making the opening and closing times of the valves coincide with the arrival of the waves in these phases, the duration of the total cycle was obtained. This automatically determined $\tau_B$ and $\tau_E$; for the other Mach Numbers ($M_o = 0.50$, 0.25 and 0) and it was found that the latter very nearly coincided with the theoretical duration of the phases at these Mach Numbers. The actual time available for discharge was a few percent longer than that determined by theoretical calculation. Since this would determine the final pressure in the tube after discharge, and since it meant that this pressure was lower than that required in the tube to initiate scavenging, it was felt that this is a conservative assumption. At the same time, this simplified the valve timing considerably. The time available for burning, of course, varied with the valve speed, but, since the time allowed for burning was sufficient enough, it was felt that the variation with Mach Number could be tolerated. Therefore, the physical valve configuration remained the same, while only the valve speed varied in accordance to the time of arrival of the interface of the new mixture to the exhaust valve and the arrival of the pulse compression wave to the inlet

valve. This was determined by the simplified characteristics diagramed in Figures 89 and 90. Since these wave speeds depend on the velocity of sound of the incoming air, then the rotational speed of the valve depends only on the square root of the inlet total temperature.

$$RPM = CONST \sqrt{T_{ot}}$$

The wave diagrams shown on Figures 89 and 90 were computed from the conditions of the incoming air and the tube lengths, using the method described above. Figure 91 shows the valve timing diagrams which give the angular dimensions of the open and closed portions of the valves.

6.2.3 Leakage Losses. The computations for the leakage losses were carried out in detail in Subsection 5.6 for the 36" diameter engine. For the smaller engine the only difference will be the smaller diameter of the combustion tubes and the smaller clearance between the valves and the tube openings. It will be assumed that for this case a clearance of 0.002" can be maintained in the engine.

For the smallest diameter tubes (D = 0.25 inches) the percentage of the discharged flow lost through leakage to that discharged during the thrust phase is

$$\frac{\text{Area of leakage}}{\text{Area of discharge}} = \frac{\pi \times 0.25 \times 0.002 \times 100}{\pi/4 \times 0.25^2} = [illegible]$$

For the largest tubes (D = 0.51 inches) this loss is

$$\frac{\text{Area of leakage}}{\text{Area of discharge}} = \frac{\pi \times 0.51 \times 0.002 \times 100}{\pi/4 \times 0.51^2} = 1.57\%$$

The weighted mean of the above losses is 2.1%. Using the criterion of Subsection 5.6 we then determine the total leakage losses to be 2.1 X 4 = 8.4%. These losses are included in the actual performance characteristics computed for the Multi-Jet.

6.3 Performance Analysis of the Multi-Jet

The curves for thrust, specific fuel consumption, air specific impulse, thrust per unit frontal area, weight/thrust ratio, thrust coefficient and characteristic mass flow are given in Figures 92, 93, 94, 95, 96, 97 and 98 respectively. The computations for these curves are given in Table 9 and are described in detail in Appendix V.

The actual specific fuel consumption given in Figure 93 shows that it does not monotonically decrease with the maximum cycle temperature. The specific fuel consumption decreases as the temperature decreases from 3000°F to 2000°F then it begins to increase again.

PREPARED BY
CHECKED BY DB
AEROPHYSICS DEVELOPMENT CORPORATION
P.O BOX 657, PACIFIC PALISADES, CALIFORNIA

REPORT NO. 2100-182
DATE Jan 28 1951

Figure 89

## WAVE DIAGRAM FOR $M_o = 0.75$

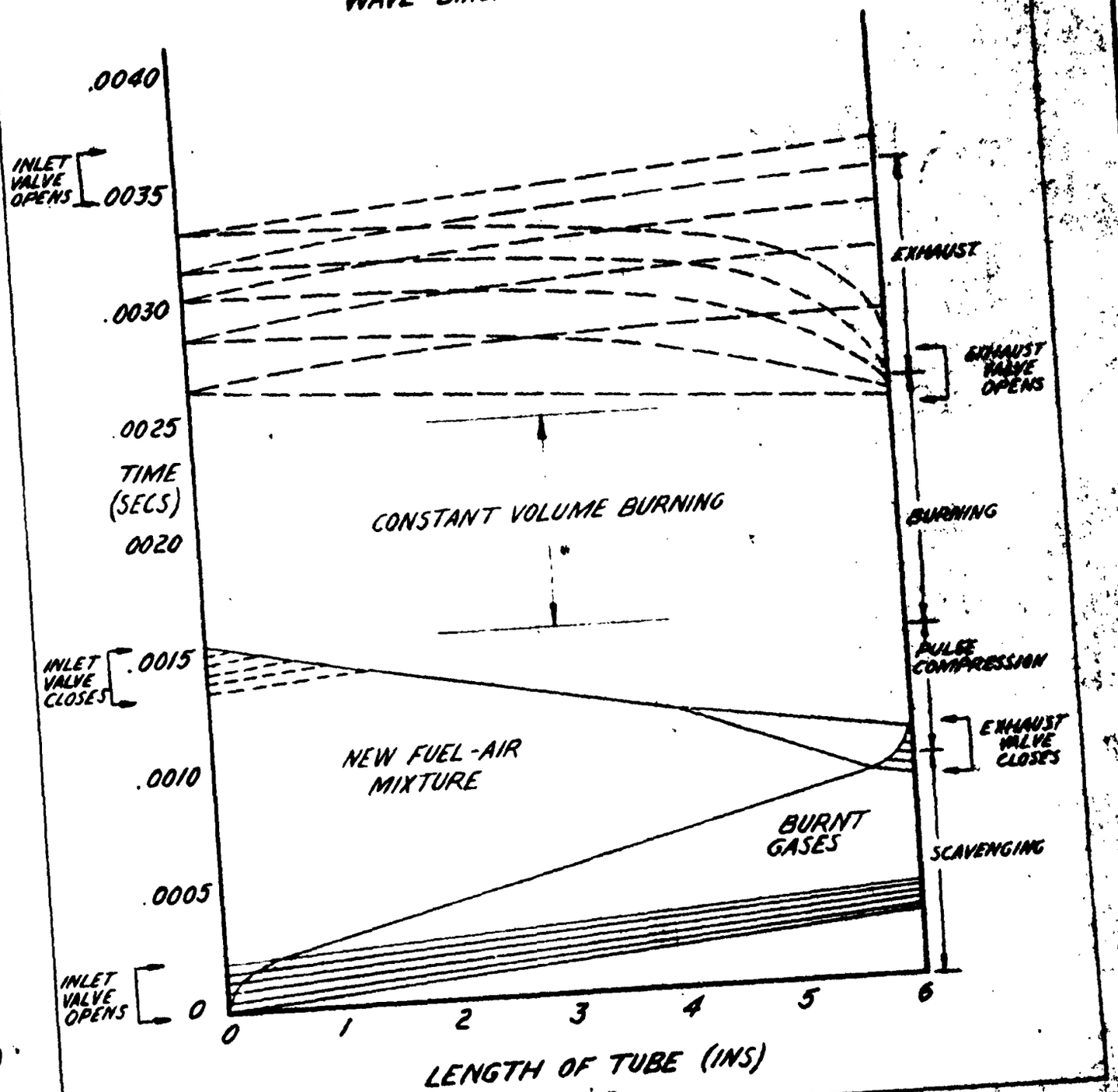

PREPARED BY

CHECKED BY

AEROPHYSICS DEVELOPMENT CORPORATION
P.O BOX 657 PACIFIC PALISADES CALIFORNIA

REPORT NO. 2000-1-R1

DATE Jan 24 1953

FIGURE 90

WAVE DIAGRAM FOR $M_o = 0$

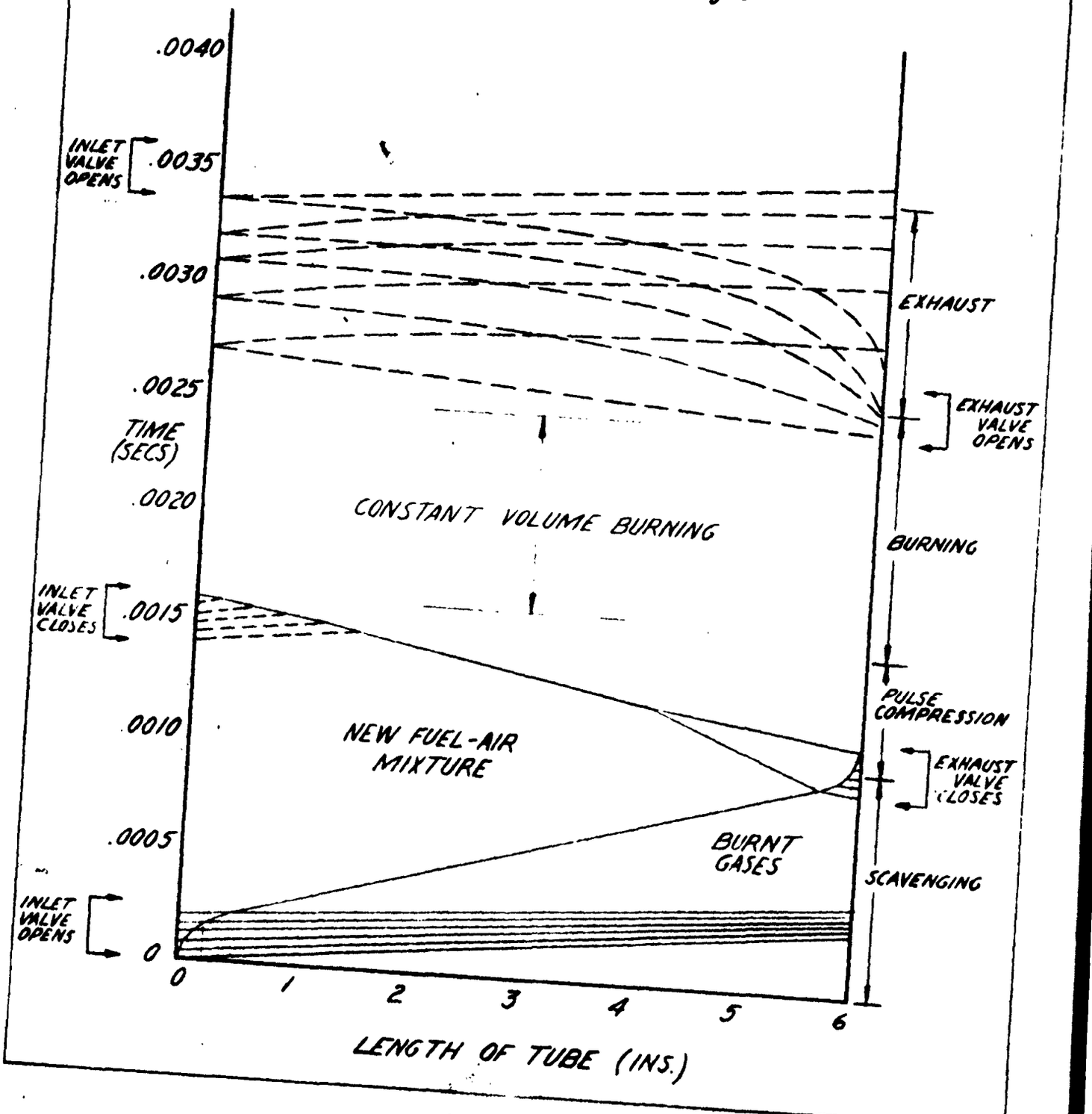

AEROPHYSICS DEVELOPMENT CORPORATION
P.O. BOX 657 PACIFIC PALISADES CALIFORNIA

2000-1-R1
Jan 21 1953

FIGURE 91

## VALVE TIMING DIAGRAMS

LENGTH OF TUBES = 6"
DIAMETER OF VALVES = 8"

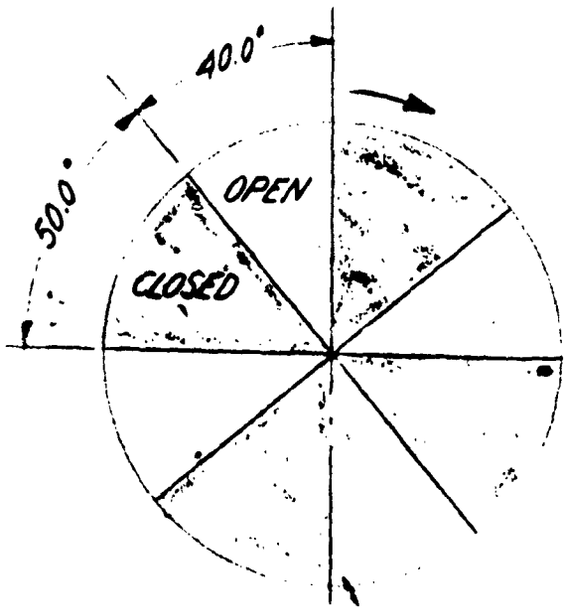


INLET VALVE

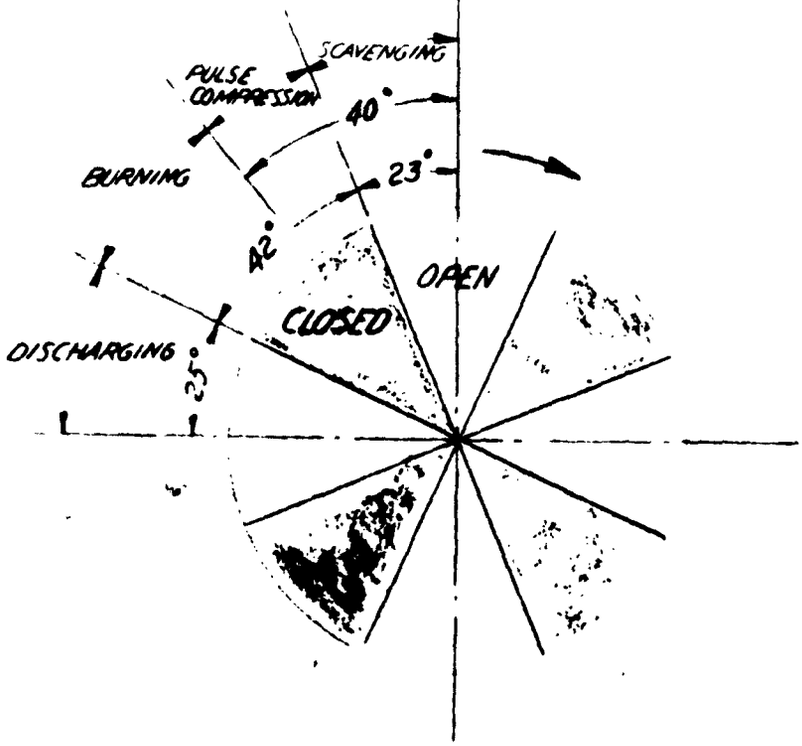


EXHAUST VALVE

PREPARED BY

CHECKED BY

AEROPHYSICS DEVELOPMENT CORPORATION
PACIFIC PALISADES, CALIFORNIA

REPORT NO. 2000-1-R1

DATE Jan 24 1953

FIGURE 92

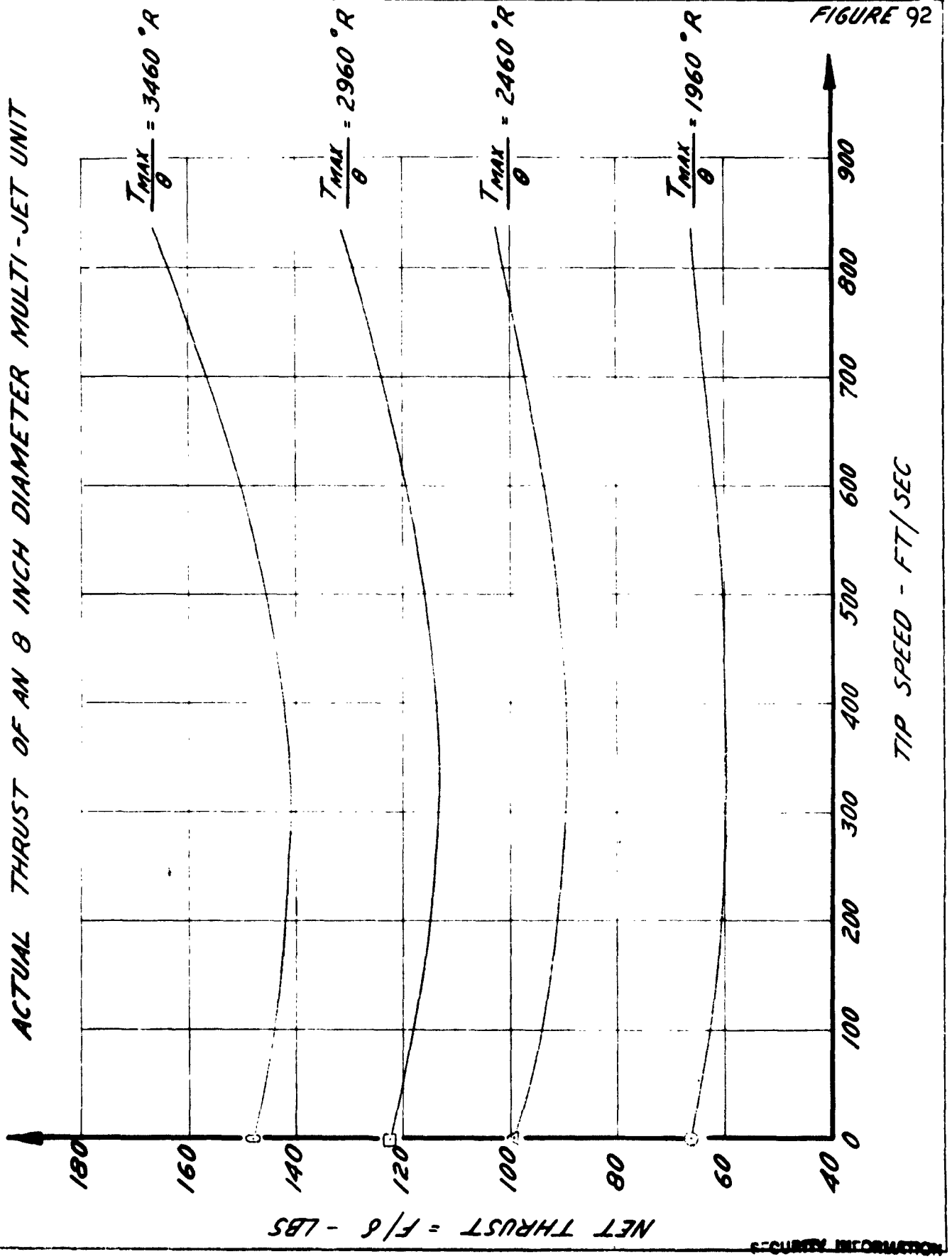

AEROPHYSICS DEVELOPMENT CORPORATION
PACIFIC PALISADES, CALIFORNIA

REPORT NO 2000-1-R1
DATE Jan 24 1953

FIGURE 93

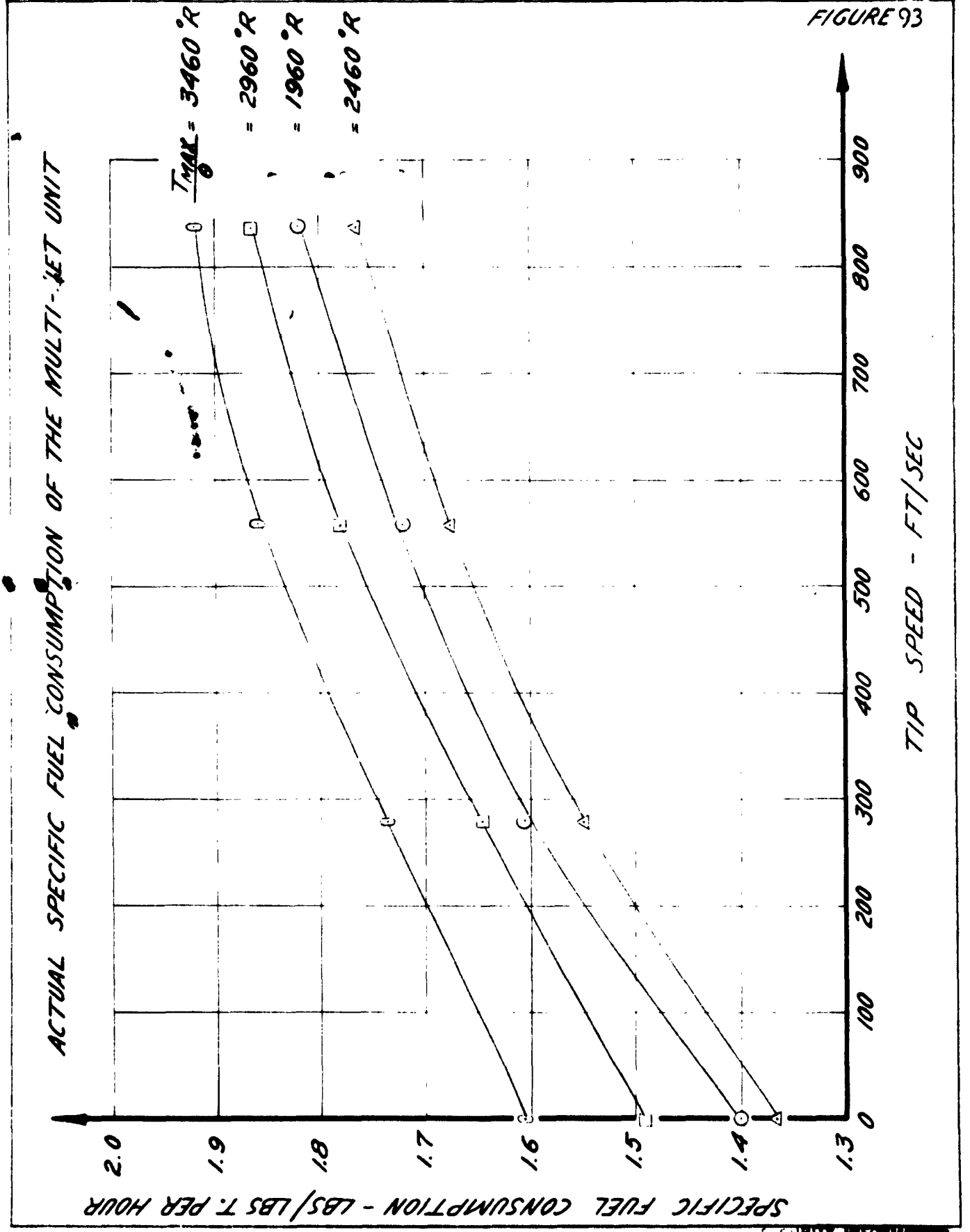

| PREPARED BY | AEROPHYSICS DEVELOPMENT CORPORATION | REPORT NO 2000-1-R1 |
|---|---|---|
| CHECKED BY | PACIFIC PALISADES, CALIFORNIA | DATE Jan 24 1953 |

FIGURE 94

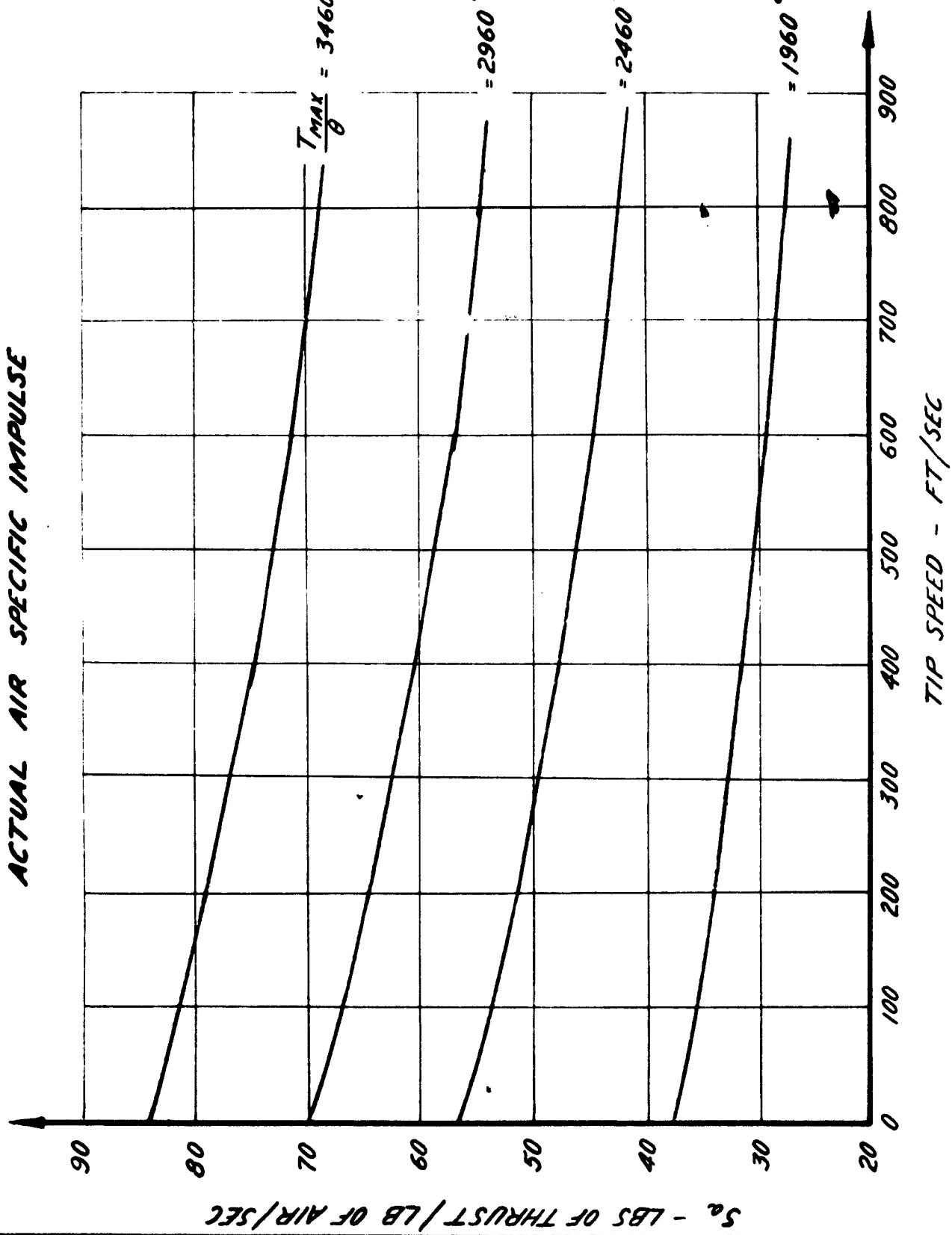

| PREPARED BY | AEROPHYSICS DEVELOPMENT CORPORATION | REPORT NO 2000-1-R1 |
|---|---|---|
| CHECKED BY | PACIFIC PALISADES, CALIFORNIA | DATE Jan 24 1953 |

FIGURE 95

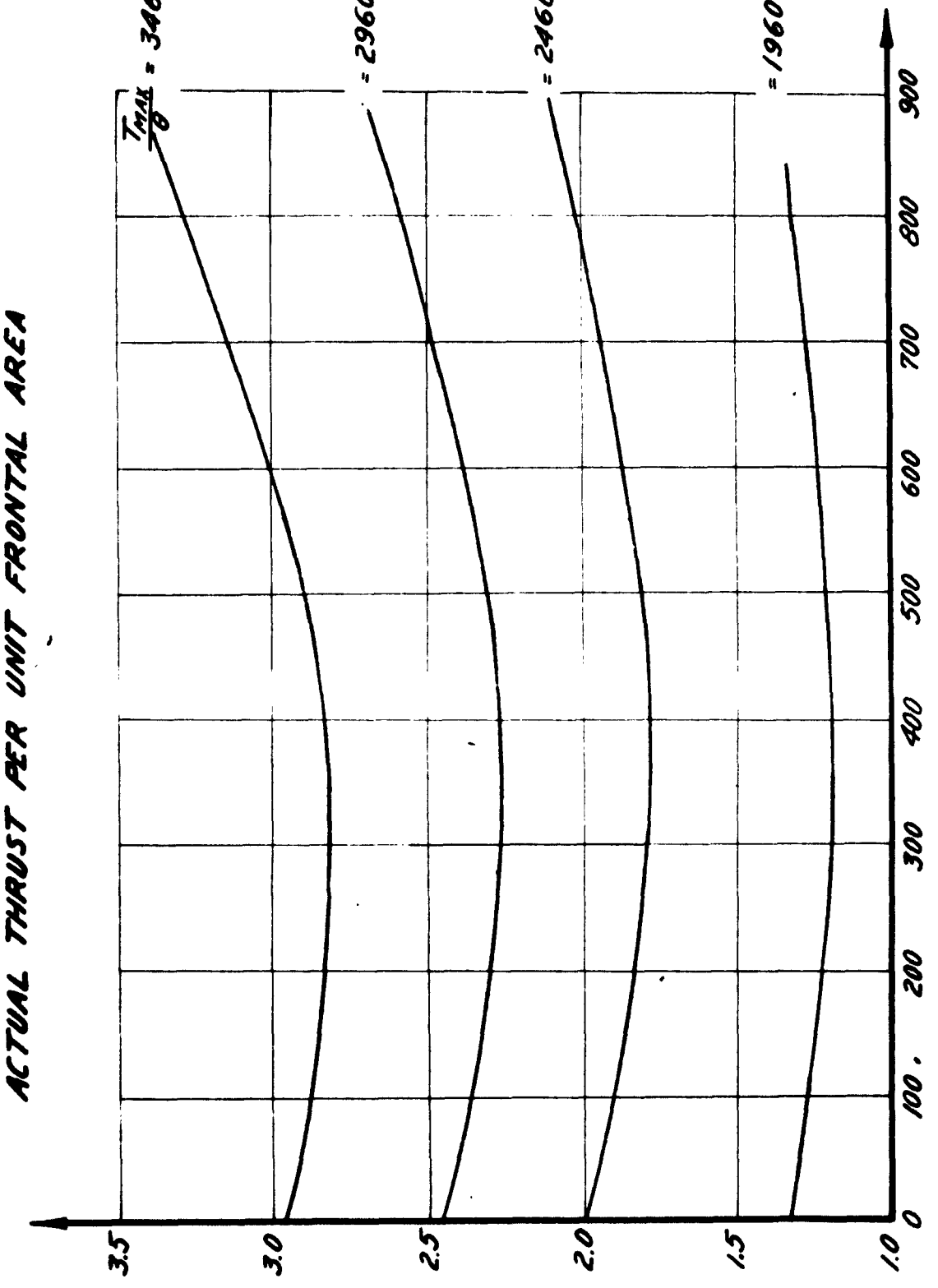

| PREPARED BY | AEROPHYSICS DEVELOPMENT CORPORATION | REPORT NO 2000-1-R1 |
|---|---|---|
| CHECKED BY | PACIFIC PALISADES, CALIFORNIA | DATE Jan 2, 1953 |

FIGURE 96

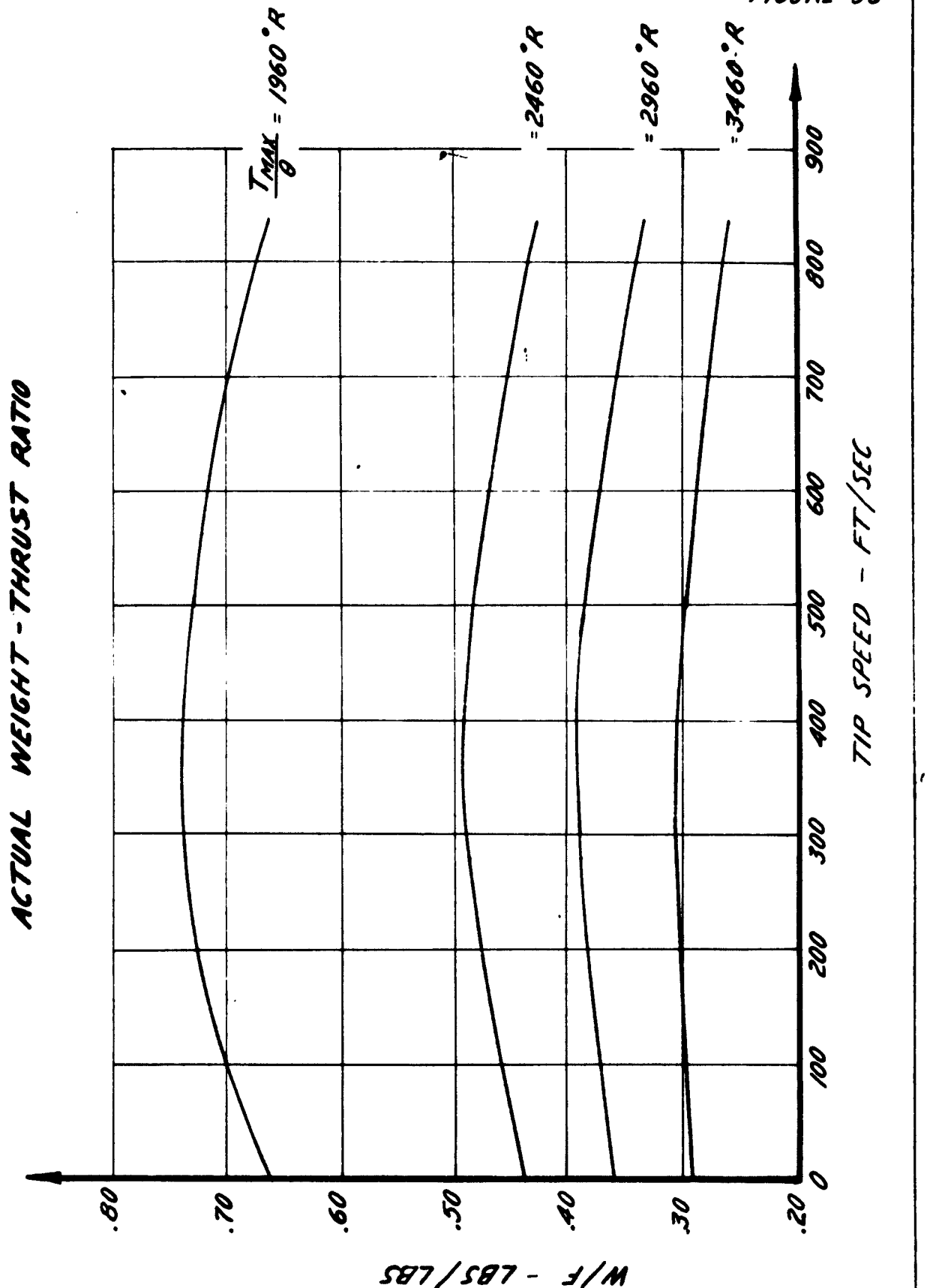

| PREPARED BY | AEROPHYSICS DEVELOPMENT CORPORATION | REPORT NO. 2000-1-R1 |
|---|---|---|
| CHECKED BY | PACIFIC PALISADES, CALIFORNIA | DATE. Jan 24 1953 |

FIGURE 97

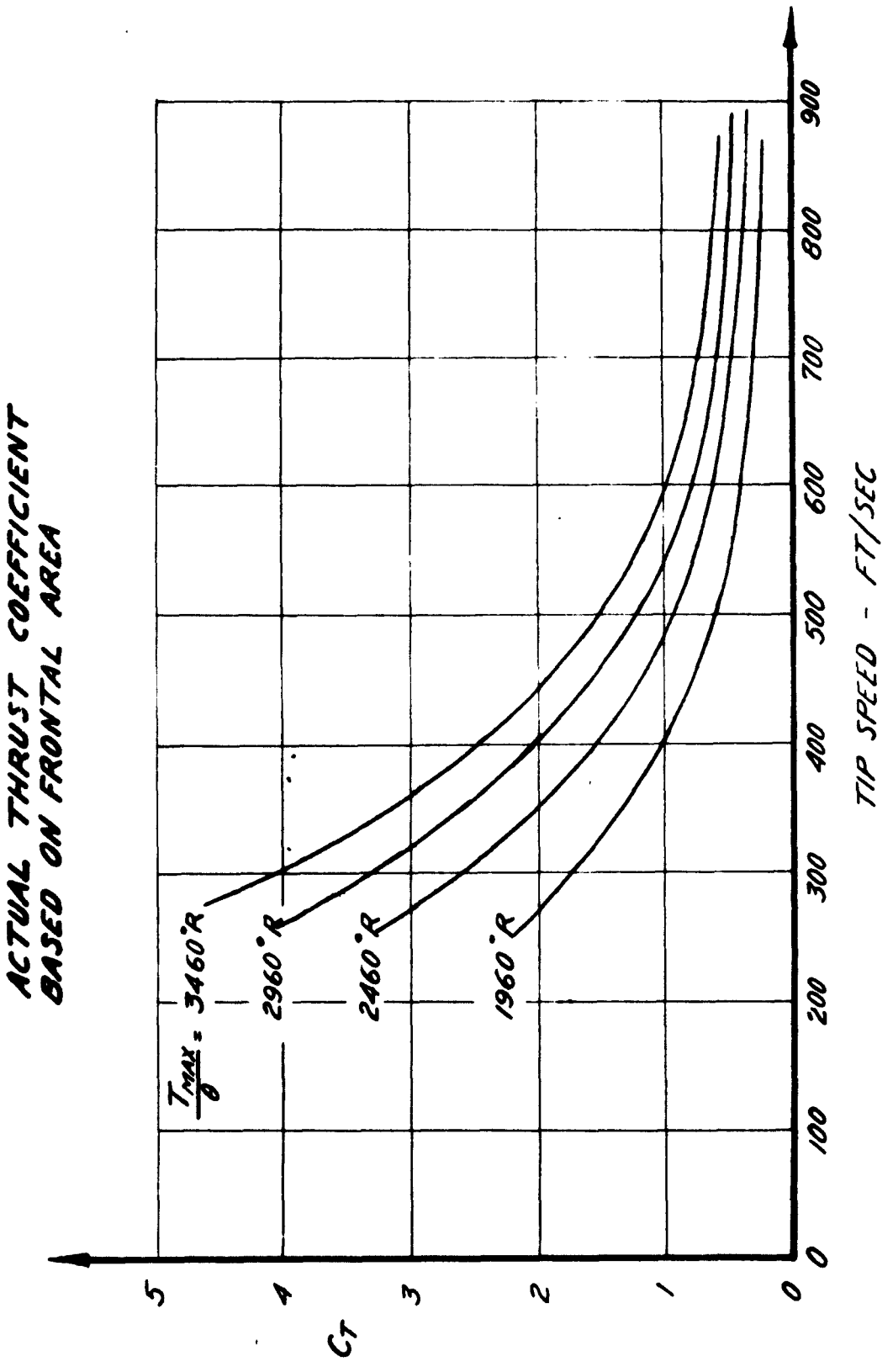

| PREPARED BY | AEROPHYSICS DEVELOPMENT CORPORATION | REPORT NO 2000-1-R1 |
|---|---|---|
| CHECKED BY | PACIFIC PALISADES, CALIFORNIA | DATE Jan 24 1953 |

FIGURE 98

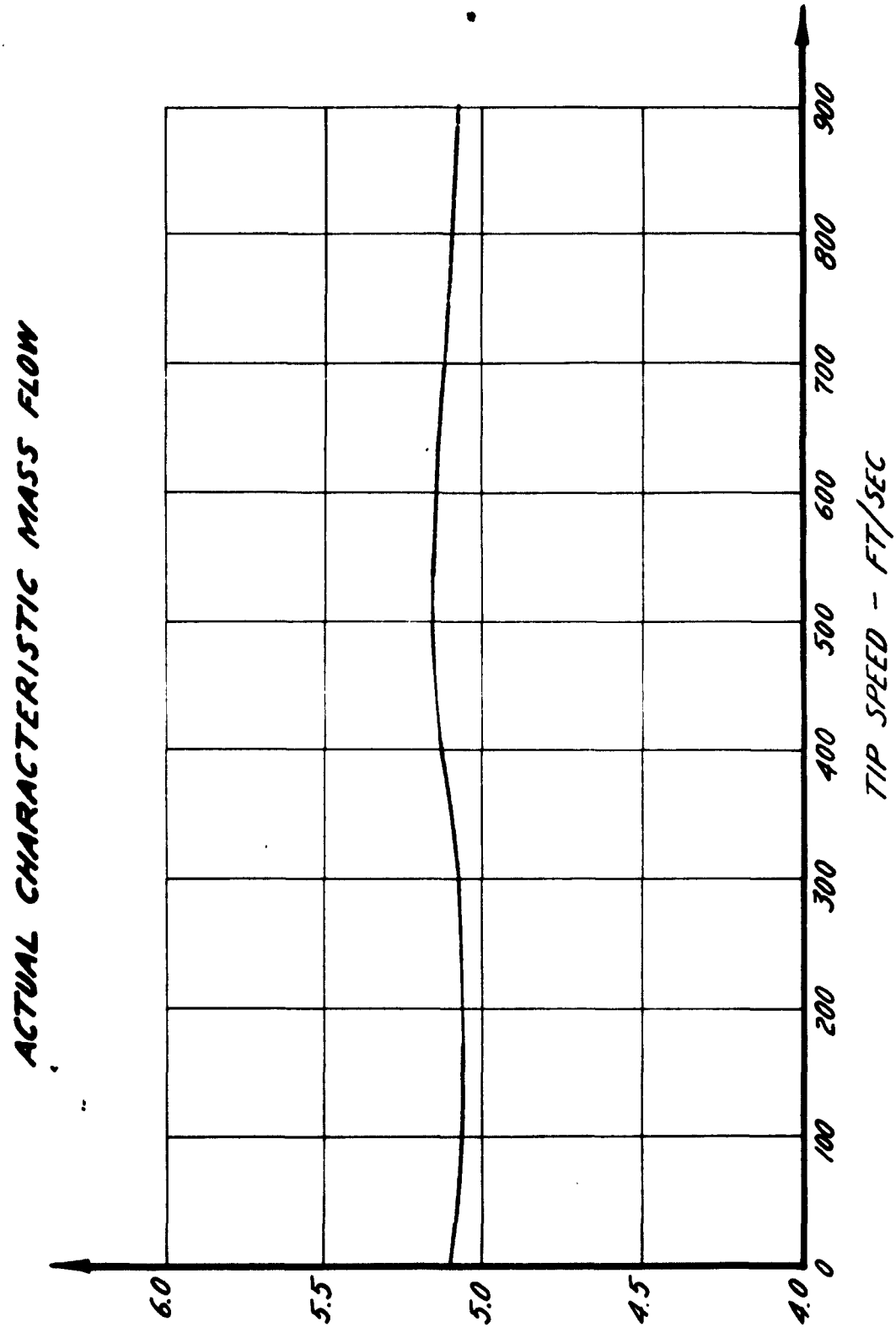

The ideal values of the specific fuel consumption on Figure 81 do not exhibit this same trend but do decrease monotonically with temperature. The reason for the reversal in the actual values is due to the reduction factor obtained from the loss in mass flow in the actual case. The reduction factor, for the specific fuel consumption, is a function of the reduction in maximum cycle pressure ratio. This function is given by equation 96. It will be noticed that for the lower temperatures (and therefore lower maximum cycle pressures) the value of K is large and therefore there is a greater percentage increase in the specific fuel consumption at the lower temperatures than at the high temperatures for a given loss in mass flow. This greater increase causes the reversal shown in Figure 93.

These performance curves include the following losses

1. Flow Viscosity.
2. Corrected Duration of Cycle for a practical engine.
3. Loss in mass flow due to slow opening and closing actions of the valves.
4. Leakage losses at the inlet and exhaust valves due to a clearance of 0.002 inches.

## 6.4 Preliminary Design Considerations

6.4.1 Blade Root Stress. The inlet valve configuration is shown in Figure 99. The thickness at the root is 0.335" while the thickness at the tip is 0.125". The thrust of the Multi-Jet will be transmitted through the inlet valve. The 120 lb jet thrust will be divided equally between the 4 vanes or 30 lbs per vane. The stress at the root will be due to two forces

1. The bending moment due to the thrust on the valve face.
2. The tension due to the centrifugal force.

The average thickness of the blade is

$$\frac{0.335 + 0.125}{2 \times 1.50} = 0.150$$

The average thickness is reduced by the factor $\frac{1}{1.50}$ due to the fact that the blade has an aerodynamical shape. The area of the blade is 5.40 square inches. Assuming the blade is made of solid steel and has a density of 0.28 lbs/cu inch, the total weight of the blade is then

$$W = 0.510 \times 5.4 \times 0.28 = 0.227 \text{ lbs}$$

| PREPARED BY | AEROPHYSICS DEVELOPMENT CORPORATION | REPORT NO. 2000-1-31 |
|---|---|---|
| CHECKED BY | PACIFIC PALISADES, CALIFORNIA | DATE Jan 24 1953 |

FIGURE 99

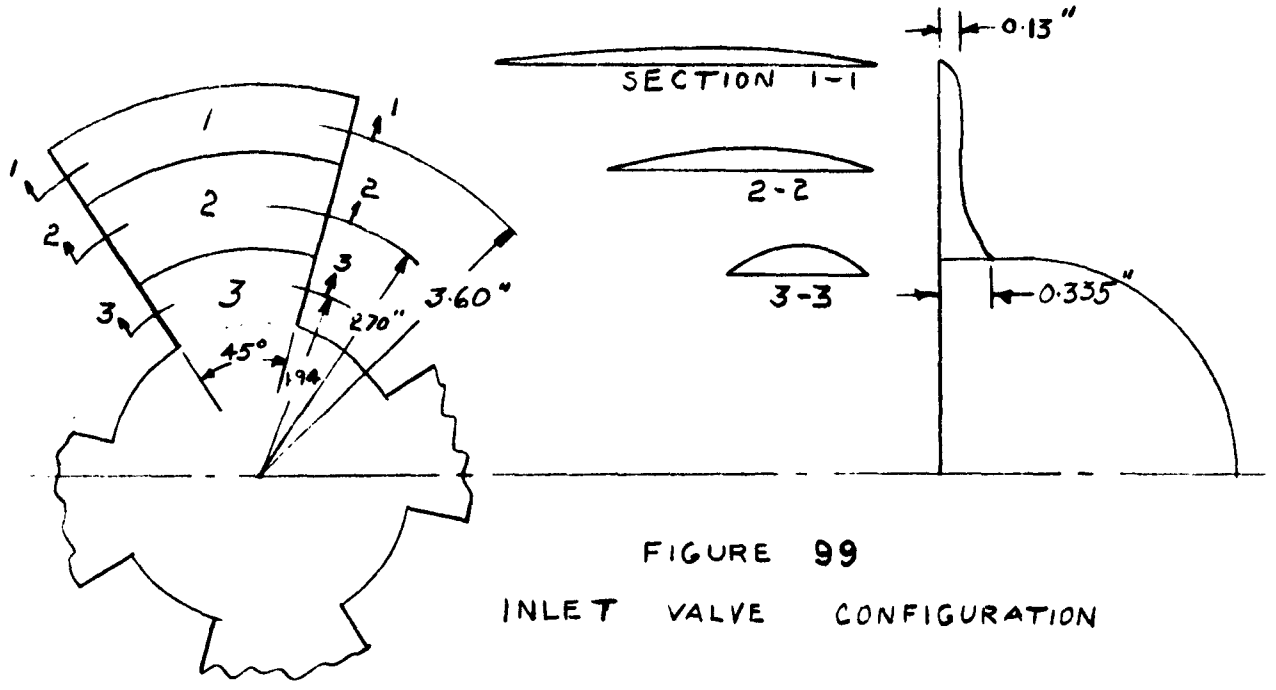


FIGURE 99

INLET VALVE CONFIGURATION

The center of gravity of the blade is located at about 2.65" radius. The maximum angular velocity of the valve is 3600 RPM.

The centrifugal force due to the rotation is

$$C.F = \frac{W}{g}\left(\frac{2\pi\ RPM}{60}\right)^2 \ell_{c.g.}$$

$$= \frac{0.227}{32.2}\left(\frac{2\pi \times 3600}{60}\right)^2 \frac{2.65}{12} = 227 \text{ lbs.}$$

Length of blade at the root = 1.18"

Area at the root = $\frac{0.335 \times 1.18}{1.50} = 0.265$ sq in

Stress at the root = 900 lbs/sq in

Thrust force on blade = 30 lbs at about 1.5" from the root of the blade

Bending moment at the root of the blade = 30 X 1.5 = 45 inch lbs

Fibre Stress = $\frac{Mc}{I}$ $\qquad I = \frac{1.18 \times 0.335}{12} = 0.00369 \text{ in}^4$

where $C = \frac{0.335}{2} = 0.168$

Stress = $\frac{45 \times 0.168}{0.00369} = 2050$ psi

| PREPARED BY | AEROPHYSICS DEVELOPMENT CORPORATION | REPORT NO. 2000-1-R1 |
|---|---|---|
| CHECKED BY | PACIFIC PALISADES, CALIFORNIA | DATE Jan 24 1953 |

The maximum fibre stress at the root of the blade is 2950 psi.

3.4.2 Aerodynamic Drag of the Revolving Blades. The blade is divided into three sections as shown on Figure 99. The computations are given in Table 10. The drag coefficient of column 8 was estimated for the various sections of different thickness/chord ratios taking into account the frictional drag on the surface and the pressure drag on the curved surface. The drag of the revolving fairing would add a torque of about 0.0545 in.lbs. The total torque of the revolving valves due to aerodynamic drag is 0.228 in.lbs.

The power required is then = torque X R.P.S.

or $= 1.14 \frac{\text{ft lbs}}{\text{sec}}$

$= 0.0021$ H.P.

Assuming a friction coefficient for the thrust bearing of 0.0025, with a thrust load of 120 lbs, the bearing friction is = 0.30 lbs. Assume the races are at a radius of 1.50" the power required to overcome bearing friction is

$$= \frac{0.30 \times 1.50}{12} \times 60 = 2.25 \text{ ft lbs/sec or } 0.0041 \text{ HP}$$

Total horsepower to drive the valves then is 0.0062 HP.

3.4.3 Valve Drive Mechanism. Various methods have been considered that would be suitable to drive the valves. Some of these are

1. Electric motor
2. Hydraulic motor driven by the pressurized fuel or pressurized air
3. Reaction of the jet exhaust driving a turbine
4. Reaction of the inlet air driving a turbine

Using the reaction of the jet exhaust or the inlet air to drive a turbine presents the problem of speed regulation. A mechanism will be required to adjust the torque produced by the turbine to drive the valves at the correct speed. The complexity of an air driven turbine can be seen from the drawing of such a system in Figure 58. On the other hand, the electric motor with a speed control makes it a very easy problem to control the valve speed either manually from the cockpit or automatically. The hydraulic motor driven by the fuel is also a good solution since it incorporates the fuel feed and control system which is needed in any case. A description of this system is given in Appendix VI.

6.4.4 Starting Mechanism. There are four functions which must be provided for, while starting the Multi-Jet.

1. Rotation of the valves.
2. Induction of fuel-air flow through the combustion tubes.
3. Pumping of fuel to the rotor tips.
4. Ignition sources in each combustion tube.

If the electric motor method is used to drive the valves a storage battery will be needed to rotate the valves while the helicopter rotor is at a standstill. Also a small propeller which induces an air flow through the whole unit will be mounted at the duct entrance. At normal cruising velocities this propeller will free-wheel. Another method of supplying air for starting is by means of a compressed air bottle in the main body of the helicopter. In order to supply fuel for the starting phase an accumulator separated into two compartments by a rubber diaphragm will be used. One compartment is filled with fuel while the other is pressurized with compressed air. The fuel is driven out to the rotor blades where it is ejected into the intake duct of the Multi-Jet. Since an ignition source in each tube would require a large network of wiring, a simple solution would be to ignite the fuel-air mixture before it enters the tubes. The mixture burns partially, expands through the engine and develops a small amount of thrust and also heats the combustion tubes. When the tube walls are sufficiently heated to cause auto-ignition of the incoming fuel-air mixture, the thrust will increase, the blades will accelerate until the flame in the intake duct will be blown out and the Multi-Jet will operate under its own cycle. As the rotors begin to rotate, the fuel pressure increases and the pressurized accumulator can be by-passed. Appendix VI also describes a starting system that can be used in conjunction with an hydraulically driven valve system. The considerations for fuel feed and control given in Appendix VI would apply for any case.

6.5 General Structural Design Consideration

Preliminary structural studies indicate that gyroscopic moments can be easily resisted by the helicopter rotor blade without any penalties and therefore it will not be necessary to use a pair of engines on each blade for the sake of counteracting gyroscopic forces. However, it appears that certain reinforcing will be necessary in the helicopter blades to take care of the centrifugal forces caused by the engine. The valves are subjected to (a) two types of centrifugal forces (b) to bending stress (c) are exposed to high temperatures. It is felt however that by careful design a reliable unit can be easily obtained. There appears to be no fundamental difficulties which cannot be overcome in actual design of the valve, bearing and shaft combination.

| PREPARED BY | AEROPHYSICS DEVELOPMENT CORPORATION | REPORT NO. 2000-1-R1 |
|---|---|---|
| CHECKED BY | PACIFIC PALISADES, CALIFORNIA | DATE Jan 24,1953 |

## SECTION VII

## EFFECT ON HELICOPTER DESIGN AND PERFORMANCE

The development of a helicopter may be subdivided into five parts as follows:

1. Powerplant Selection
2. Rotor Design and Performance
3. Stability and Control
4. Vibration and Noise
5. Structural Design

These parts will be amplified somewhat in the following paragraphs in order to show how the present development effects the general problems of helicopter design.

### 7.1 Powerplant Selection

The type of power unit which is used to drive the rotor has a controlling influence on the configuration and performance of the helicopter. Numerous authors have mentioned the inherent advantage of propelling the rotor by means of thrust units at the tips of the blades, which impose very little torque on the body of the machine; in contrast to propelling the rotor at the hub, which transmits the full rotor torque to the body. The hub propulsion method then requires a powerful means to counteract the rotor torque, in the form of a tail rotor or counter-rotating main rotor; whereas, the tip propulsion method may use a vertical fin attached to the body to overcome the small hub bearing friction during powered flight when the air flow is downward, or during gliding flight when the air flow is upward.

At present, the inherent simplicity of the helicopter equipped with tip propulsion is somewhat offset by the following disadvantages: First, the available power units for supplying thrust at the blade tips are only in the developmental stage, and have higher fuel consumption than the engine-in-body configurations; second, means for transferring fuel from tanks in the body to the rotor tips is more complicated than from tank to engine; third, the development of a thrust unit subject to centrifugal effects offers an additional problem; and, fourth, the problem of starting several tip units is more difficult than one engine, and may involve extra weight.

However, in spite of these drawbacks, the weight-empty savings which accompany the tip propulsion method seem to permit the simpler

jet powered helicopter to have range, endurance and carrying capacity comparable to that of the internal combustion engine powered helicopter. The mechanical problems of fuel transfer and centrifugal force are not serious. Furthermore, improvements in fuel consumption of the tip propelled rotors may be expected while the reciprocating engines have reached close to their limits in fuel economy.

The present development of a Multi-Jet powerplant, as discussed in this report, offers the possibility of the lowest fuel consumption than any other tip propulsion unit yet devised. This feature, in addition to its simplicity and low cost would appear to make it probably the most promising propulsion system for the helicopter of the future.

## 7.2 Rotor Design and Performance

Assuming the availability of a tip propulsion unit capable of developing a thrust of T pounds at the rotor tip, the number of rotor blades, the diameter of rotor, and other details may be worked out by well established methods of aerodynamic analysis.

Preliminary calculations for the Multi-Jet unit having a thrust of F = 90 pounds each operating at a cycle maximum temperature of 2000°F mounted on a three-blade rotor, with a tip speed of 600 ft/sec would be capable of delivering a total of 300 HP suitable for a helicopter of gross weight 3600 lbs with a rotor of about 41 feet diameter. With these 8" diameter units operating at higher cycle temperatures, the available power is increased and therefore the gross weight and size of the helicopter can be increased substantially. These proportions give a disc loading of 2.7 lb/sq ft and a power loading of 12 lb/HP. The proposed helicopter would be a six-passenger transport with the following weight summary:

| | | |
|---|---|---|
| Weight Empty | 35% $W_o$ | = 1260 lbs |
| Pilot and Payload | 6 X 200 | = 1200 |
| Fuel | | = 1140 |
| Gross Weight = $W_o$ | | = 3600 lbs |

The endurance of this machine would be 3.0 hours hovering at 6000 feet with 85 percent full power or 240 hp at full load, and with a specific fuel consumption of 1.65 lb/hr/lb thrust. The helicopter would be capable of a range of about 320 miles at 100 mph with full load. By operating at a cycle temperature of 3000°F the Multi-Jets could develop a thrust of 160 lbs each or 520 hp at 600 ft/sec rotor tip speed. This extra power would be available for take-off, climbing, hovering and other special manoeuvers.

If the payload were replaced by additional fuel, the hovering endurance would be approximately 6.20 hours and the range 630 miles. This is almost as good range and endurance as to be expected of the piston-engine powered helicopter (See Figure 100). The values of Figure 100 were obtained from Reference 12. On the recent trans-Atlantic flight of S-16 helicopters, the longest hop was 800 miles from Greenland to Iceland. It was assumed that allowances were made on this flight for 25 percent fuel remaining in the tank and for 25 mph favorable winds. Without these allowances, it is estimated that these machines have a maximum no-wind range of about 850 miles. The Multi-Jet helicopter is expected to attain range and endurance performance within 20 percent of the piston type machines.

The curves of Figure 101 give a better comparison of the different types of propulsive devices. The curves give the endurance of the helicopters plotted against the permissible payload. These curves are a cross plot of those of Figure 100. The curves show that the Multi-Jet system is unsurpassed except for the two extreme ends of the endurance scale. Even for the long endurances, the piston engine driven helicopter is only carrying a small percentage of its gross weight as payload. It must be realized that the curves of Reference 12 represent average values of many existing and proposed helicopters and therefore represent only approximate trends and magnitudes.

## 7.3 Stability and Control

The use of a directional trim fin for counteracting the hub bearing friction of the tip-propelled rotor is the principal change from the piston engine type of helicopter. A simpler control system is thus attained with lower weight and less power required than the tail rotor or counter-rotating main rotors. Methods of rotor control and stability as developed for the piston engine powered rotor may be used for the jet-propelled helicopter.

## 7.4 Vibration and Noise

Replacement of the tail rotor boom by a thin trim fin is expected to greatly reduce the troublesome vibration due to rotor blade downwash, with an exciting frequency of about 9 cycles per second. Removal of the engine from the body will eliminate this source of vibration. Removal of the engine exhaust noise from a point below the body and replace by jet units at the rotor tips may or may not reduce the noise level in the cabin. The firing frequency of the Multi-Jet with 32 cylinders per row will be 960 cycles per second. Such frequencies are relatively easy to eliminate by light weight sound proofing materials. Lower frequencies should be nearly absent with smoothly running jet units, although some 60 cycle/sec noise may be expected with irregular operation of certain cylinders.

AERODYNAMICS DEVELOPMENT CORPORATION
P.O. BOX 657 PALO ALTO CALIFORNIA

FIGURE 16

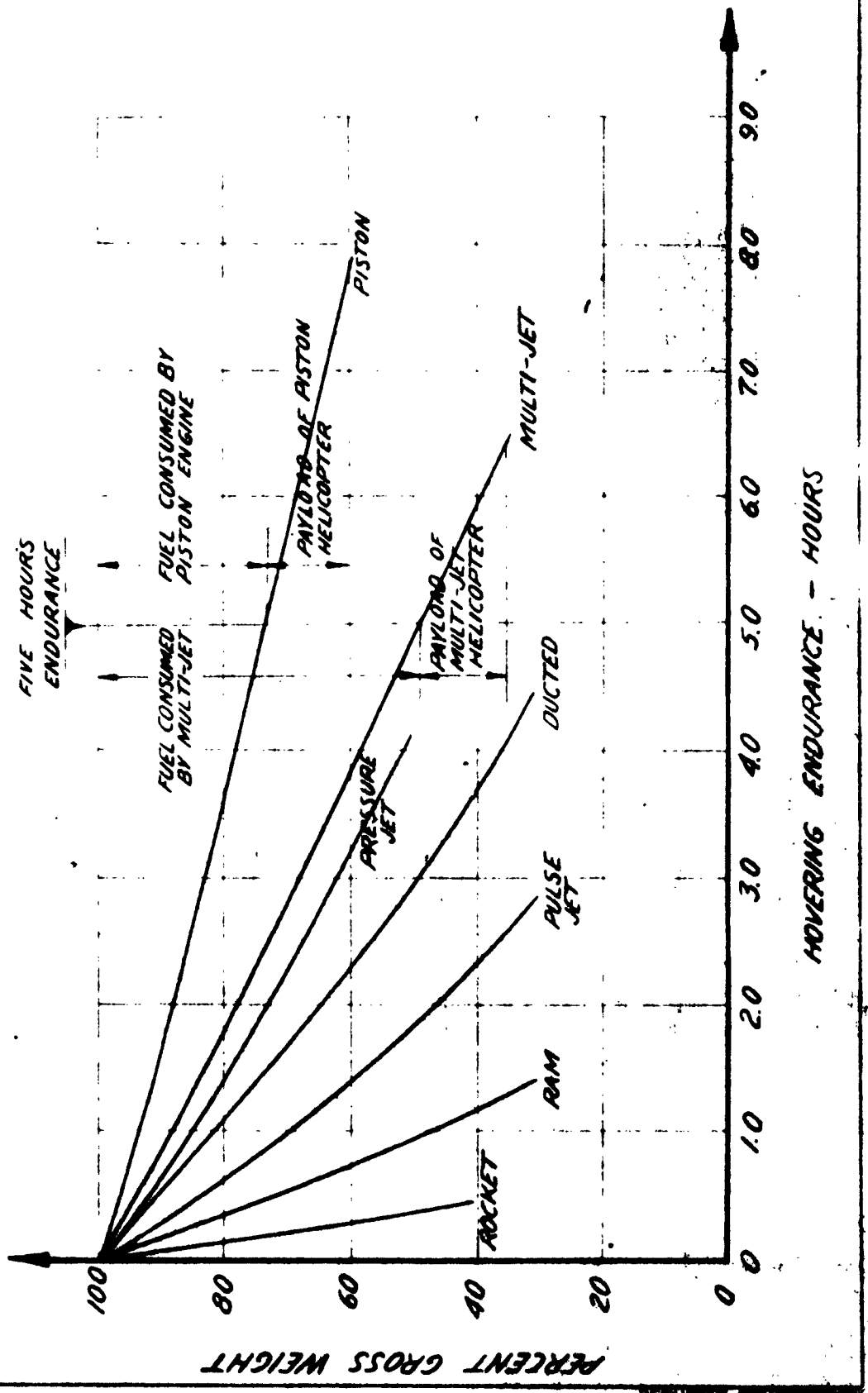

AEROPHYSICS DEVELOPMENT CORPORATION
P O BOX 657 PACIFIC PALISADES CALIFORNIA

REPORT NO. 2000-1-R1
DATE Jan 24 1953

FIGURE 101

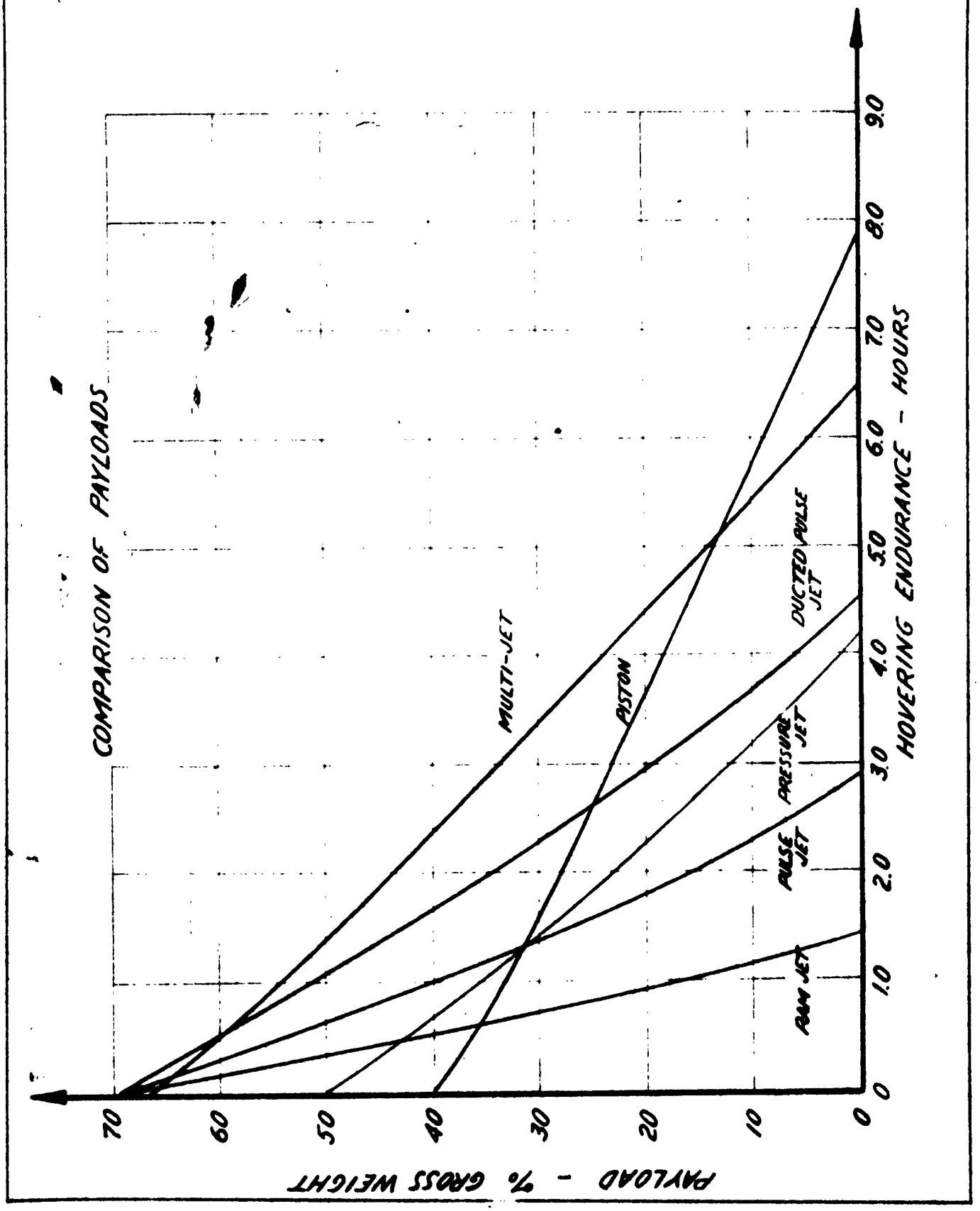

It is expected that the Multi-Jet machine will have less vibration than the piston machines, with comparable noise level in the cabin and a noise level in the external field about 1/20 of that of a 6000 pound thrust turbojet. Due to the fact that the three jets are not simultaneously pointing directly at the observer, the average noise at a given point is probably even less than this amount. Further studies may be expected to reduce this external noise still further with some weight and fuel penalties.

7.5 Structural Design

The predominant change in structural design is the addition of the mass of the Multi-Jet units at the rotor blade tips. This tends to reduce the natural frequency of the blades, requiring some adjustments to the rotor and/or landing gear details to avoid ground resonance. Since a number of methods have been developed for correcting ground resonance by kinematics and damping, this problem is not expected to be a serious disadvantage.

New developments in rotor blade design should, as they become available, be considered for the jet-propelled rotor. The trend toward a thick, tough skin with low density core material seems to be in the right direction for the helicopter of the future.

In modifying an existing helicopter to serve as a flight test machine for the Multi-Jet, a 3-blade single rotor machine could be selected, having a gross weight of 3000-4000 lbs. The main rotor would need to be redesigned to accommodate the jet units. The tail rotor could be driven from the main rotor shaft, or replaced by a vertical fin. The body, landing gear and flight controls could be used with little change. A considerable saving in the development time for a flight proven jet unit is expected to result from this plan. On the other hand, a complete redesign would be necessary to provide a serviceable helicopter.

| PREPARED BY | AEROPHYSICS DEVELOPMENT CORPORATION | REPORT NO. 2000-1-R1 |
|---|---|---|
| CHECKED BY | PACIFIC PALISADES, CALIFORNIA | DATE Jan 24,1953 |

## SECTION VIII

## ANALYSIS OF THE DESIGN OF COMBUSTION TUBES

### 8.1 Tube Structures

During most of the contract period of the work on the Multi-Jet engine, it was not known whether it would be necessary to have a cooled or uncooled tube structure. However, it was realized that the possibility existed that an uncooled tube structure may prove desirable.

Possible cooled structures were analyzed simultaneously with uncooled structures to estimate comparative advantages and disadvantages and optimize the theoretical design as rapidly as possible. As volume and weight are critical and an inexpensive structural material is desirable, the field of present possible structural materials for an uncooled structure is limited. In uncooled structures, the following materials were considered:

(1) Zirconium Boride plus Nickel (American Electro Metals Corporation)

(2) Metamic - LT - 1 (Haynes Stellite Div., Union Carbide

(3) Graphite - EBP (National Carbon Company)

(4) Graphitar (The United States Graphite Company)

(5) Stabilized Zirconium Oxide (The Norton Company)

(6) Silicon Carbide (The Carborundum Company)

(7) Stupalith (Stupakoff Ceramic and Manufacturing Co.)

(8) Alumina (96%) (Coors Porcelain Company)

(9) Kentanium K151-A (Kennametal Inc.)

(10) Molybdenum (Fanstell Metallurgical Corporation)

(11) Enameled Steel Tubes (Solar Aircraft Company) Solaramic (California Enameling Co.) A418 Coating

(12) Quartz (Fused) (General Electric Company)

| PREPARED BY | AEROPHYSICS DEVELOPMENT CORPORATION | REPORT NO 2000-1-R1 |
|---|---|---|
| CHECKED BY | PACIFIC PALISADES, CALIFORNIA | DATE Jan 24,1953 |

The following materials were considered for possible use in cooled structures:

(1) SAE 4130 Heat Treated

(2) Stainless 19-9 DL

(3) Haynes Alloy No. 25 (Haynes Stellite Division)

(4) Kentanium K151A (Kennametal, Inc.)

Initial calculations were made to determine the equilibrium temperature of the uncooled tube exit considering only the flow through the tube. The local tube heat transfer coefficients were calculated, using turbulent flow heat transfer formula for tubes. (See Reference 14).

$$h = \frac{k}{D} \frac{0.0396 \ (Re_d)^{3/4}}{\frac{1}{Pr} + 1.5 \ Pr^{-1/6} \ Re_d^{-1/8} \left(1 - \frac{1}{Pr}\right)}$$

h = heat transfer coefficient = BTU/hr/sq ft/$^{o}$F

k = thermal conductivity of gas = BTU/hr/ft/$^{o}$F

D = tube diameter = feet

$Re_d$ = Reynolds Number of flow with respect to the tube diameter (dimensionless)

Pr = Prandtl Number of gas (local) (dimensionless)

The most recent extrapolations of thermal conductivity and viscosity of air by Keyes (See Reference 15) were used.

At a maximum combustion chamber temperature and pressure of 3000$^{o}$F and 400 psi, respectively, it was found that the equilibrium tube wall temperature would be 2700$^{o}$F. This high cooled tube wall temperature results from the exhaust flow heat transfer coefficients being about twice the scavenge flow heat transfer coefficients and from the applied durations (the scavenging portion of the engine cycle amounts to only one-third the duration of the exhaust flow condition at the tube exit). The uncooled equilibrium tube wall temperature decreases along the tube from the exit to the forward end of the tube in a fashion substantially proportional to the duration of hot exhaust flow at the place involved in the tube. It was found that longitudinal heat transfer through the metal or ceramic wall could be neglected in comparison to the convective surface heat transfer. An equilibrium wall temperature only a few hundred degrees above the total inlet air temperature should exist at the forward end of the tube.

## 8.2 Cooled Tube Structures

The required heat transfer in an externally air cooled tube designed for high Mach number low altitude operation was then calculated assuming a mean tube temperature of 1100°F and a tube material of heat treated 4130 steel. Although an average flow of only 5% of the total air flow passing through the tubes is required to absorb the required heat flow from the surface of the combustion tubes (temperature rise of only 130 degrees in this external air flow), the external surface area of the combustion tubes is far too small to transfer the required heat flow. Designs considering tube finning and special cross flows failed by a large margin to allow external air cooling of a simple metal tube to be considered (particularly in the region of the tube exits).

Regenerative fuel cooling of the 4130 tubes was then considered. The maximum allowable wall temperature is low as local fuel vaporization must be prevented. Under this condition, the required heat absorption by the fuel is about three times the amount that may be absorbed by the fuel without vaporization at reasonably high pressures ($\approx$350 psi). Recirculation of the fuel to an inlet air heat exchanger was not attractive on the basis of the trapped fuel and heat exchanger weights as well as the large pump requirements and general design engineering complexity.

Composite metal-ceramic structures were considered in order to reduce the required heat flow to an external cooling air flow. A fundamental difficulty exists in the proper distribution of stresses with large changes in operating temperature. The mean expansion of the metal tube surrounding a ceramic liner could be matched (at least in theory) for one temperature profile but not for another. Enamel-type coatings appear to be temperature limited to about 1800°F top operational temperature at the present, and are consequently unsuitable in this application.

A structure containing both a cooled and uncooled portion was given some thought. As compressive strengths of many materials are much greater than their tensile strengths (particularly at high temperature), an uncooled combustion tube was considered to be externally pressurized by high pressure air contained in a surrounding metal tube. The surrounding metal tube was cooled by a small external air flow as the heat flow to the metal from the uncooled inner tube may be shown to be quite small. The buckling strength of the inner uncooled tube was computed by formulae given by R. G. Sturn (Reference 16) or S. B. Batdorf (Reference 17). Such a composite structure actually gave minimum total tube weights, but the scheme appears undesirable on the basis of the mechanical attachment complexity of pressurizing lines and difficulty of insuring reasonable stable leakproof operation on the high pressure air. In addition, some source of high pressure air or gas is required.

Other materials considered for the proposed cooled structure present fundamentally the same problems as in the case of 4130. Since it is desired to have very high combustion chamber temperatures, improvement in the material properties at 2000°F level does not mean too much in this design.

3.3 Uncooled Tube Structures - General

A combustion tube structure composed of uncooled tubes capable of taking the required pressure loads at high temperature would be desirable. A review of the material properties of uncooled tube material follows and is given in Table 12.

Zirconium Boride plus nickel (Borolite) appears to be the most suitable material except that it is presently being made on only a small scale. (Reference 18). However, it is oxidation-resistant at very high temperature, has the excellent rupture strength of 100,000 psi at 2400°F, and is very thermal-shock-resistant. Rupture strength represents a combined effect of compressive and tensile strengths, and it may be that the tensile strength is considerably less than the rupture strength. However, even 20,000 psi tensile strength at 2400°F would be most excellent. The thermal conductivity of Zirconium boride is in the range of the alloy steels and its density is only two-thirds that of steel. Experiments which plunge samples heated to 4710°F into water with no material fracture demonstrate its excellent thermal shock properties. This material is presently limited to a thickness to diameter ratio of ¼ for a one-half inch I.D. tube five inches long but thinner wall thicknesses may be possible in the future. Presently lacking, is information on its elastic modulus, expansion coefficient, specific heat, and creep strength data up to high temperatures.

Metamic (LT-1), (Reference 19) although possibly quite weak at 3000°F, shows good tensile strength at 2400°F of about 3200 psi. In addition, the thermal and mechanical shock stability of Metamic appears to be quite good. Dimensional tolerances of cast pieces are quite poor, however, and tubes of this material used in the Multi-Jet engine would have to be cast oversize and machined to the correct size. Cost of this material is low, however, in comparison to Borolite, Coated Molybdenum, or Kennametal and machining may be easily accomplished by carbide tools. Allowance must be made in any assembly for an appreciable thermal expansion. Metamic will oxidize at high temperature but the oxide is adherent and protects the base structure. The stress-rupture time curves for this material are not known but with the ceramic-metal composition should be reasonably good.

Graphite has excellent thermal shock properties, but is low in thermal strength and oxidizes in air above 700°F. However, graphite increases in tensile strength and in elastic modulus with an increase in temperature up to about 4500°F, (See References (20), (21). In addition, it is known that graphite can be coated with molybdenum

disilicide or silicon carbide to form a thin, oxidation-resistant coating which is adherent over a wide temperature range. The molybdenum disilicide coating is less rough than the silicon carbide coating. A design tensile strength of 3000 psi may be considered at high temperatures for a graphite structure similar to EBP of the National Carbon Company. Such a structure appears theoretically feasible for the design of the Multi-Jet engine. The required wall thickness to diameter and length ratios are less than those easily available, but thicker pieces could be molded and turned down to the required thickness. The coatings on individual tubes and their strength could be tested before assembly and defective tubes discarded.

Graphitar is the trade name of the U. S. Graphite Company for their graphite-carbon mixtures. A wide range of material properties may be achieved, but the largest values of tensile strength are obtained on the purest graphite samples. Lower thermal conductivity may be obtained by the addition of carbon with a sacrifice in thermal strength. Graphite-carbon bodies offer no theoretical advantage for use as uncooled combustion tubes as compared to pure graphite bodies.

Stabilized Zirconium Oxide of the Norton Company (Reference 22) apparently has many desirable properties for use at high temperatures, but it is dubious that it is sufficiently thermal shock resistant as its thermal conductivity and specific heat are low. In addition, it seems that it would be difficult to obtain thin wall tubes.

Carbofrax (85% Silicon Carbide) (Reference 23) has an excellent thermal conductivity although its maximum modulus of rupture is only 3125 psi at 2460°F. Consequently, its tensile strength must be less than one-half of this value as the compressive strength of carbofrax is known to be much higher than the tensile strength. Nevertheless, Carbofrax does not oxidize and its coefficient of thermal expansion is quite low.

Stupalith (A-2417) is lithium alumno-silicate material with a coefficient of thermal expansion lower than even quartz. It is a low cost material that can be made dimensionally accurate. Although it does not oxidize, its strength is not very high and it melts at about 2450°F.

Alumina has fair strength up to high temperatures, but its thermal shock properties are quite poor.

Kentanium appears to be a very useful material at 2000°F and lower, but the stress-rupture time curves preclude its consideration at 2400° and above.

Molybdenum has been successfully coated with molybdenum disilicide to give a protection from oxidation of 100 to 200 hours at 2500°F.

However, in addition to being a very heavy material, again, stress-rupture time curves are not known for this material at high temperatures. However, there is a possibility if some increase in combustion tube weight may be tolerated that coated molybdenum tubes may be used in Multi-Jet.

Quartz tubes are quite economical and could be used as combustion tubes except that their tensile strength is very poor.

The strength of some of the refractory cements available are quite remarkable. Adamant Fire Brick Cement has a bonding strength of 1270 psi at 2000°F with fire brick. This cement and chrome based cements are available which show good strengths bonding to metal surfaces at temperatures even above 2000°F.

A new synthetic fiber, Fiberfrax, appears to be useful for thermal insulation and packing to rigidly hold high temperature tubes up to temperatures of 2500°F. A resilient shock absorbing material which may be used to allow thermal expansion and contraction of solid pieces is a welcome addition to the materials available for high temperature work above 2000°F. Refrasil of H. I. Thompson Co. and a fiber in Johns Manville blankets show less thermal conductivity for a given packing density than Fiberfrax, but these materials are limited to a maximum continuous operating temperature of 1800°F. Figure 102 gives a comparison of the thermal conductivity versus temperature insulating materials.

## 3.4 Thermal Shock Considerations

As thermal shock properties often appear to be critical in the design of the uncooled combustion tubes for the Multi-Jet engine, a review was made of existing thermal shock or stress theory. An article by C. M. Cheng (Reference 24) shows good correlation between theory and experiment concerning the thermal shock failure of flat plates. Timoshenko (Reference 25) gives a thermal stress analysis for tubes as well as flat plates that does not analyze in detail the temperature gradients that result as a consequence of the resistance factor ($R = k/hb$) as shown by Cheng, but formulates the thermal stress equation to allow the determination of stresses for any assumed or calculated temperature gradient. Now transient heat transfer charts (Reference 26) allow the temperature profile in a material to be determined readily so that an approximate conservative temperature difference is obtained for use in Timoshenko's formula for thin wall tubes:

$$\sigma_t = \frac{\epsilon E \Delta T}{2(1-\nu)}$$

$\sigma$ = thermal stress = psi

$\epsilon$ = thermal expansion coefficient = inches/inch/°F

$E$ = Modulus of elasticity = psi

AEROPHYSICS DEVELOPMENT CORPORATION
PACIFIC PALISADES, CALIFORNIA

2000-1-R1

DATE Jan 24 1953

FIGURE 102

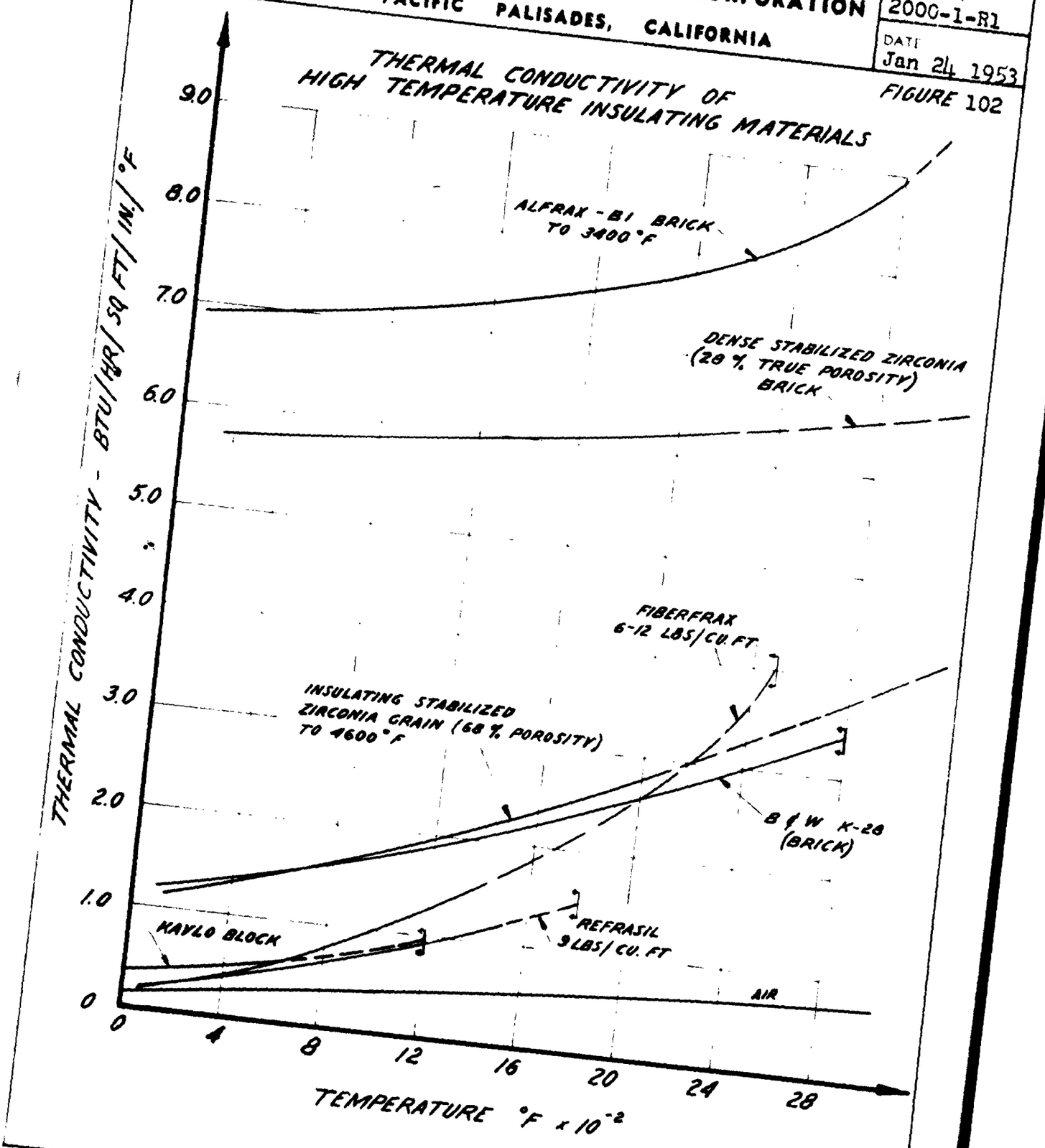

$\Delta T$ = Temperature difference = $^{o}F$

$\nu$ = Poisson's Ratio = dimensionless

The tube tensile strength at the local temperature must be greater than the thermal stress to prevent fracture.

Figure 103 gives representative temperature and stress profiles in an uncooled tube wall as determined by the flight condition. It may be perceived that the most critical thermal stress will exist in a tube wall at the cessation of combustion at the highest flight speed and lowest altitude. The thicker the tube wall, the larger may be the maximum internal tube pressure, as given by the conventional hoop stress formula for thin tubes:

$$\sigma = \frac{rP}{t}$$

$\sigma$ = Tensile stress = psi

$r$ = Tube radius = inches

$t$ = Tube thickness = inches

$P$ = Pressure differential across tube wall = psi

However, the thicker the tube wall, the greater will be the temperature difference, $\Delta T$, upon starting and stopping combustion with resulting greater thermal stresses. Upon cessation of combustion in an uncooled tube, the outer tube fibers at high temperature are put into compression as the inner tube fibers seek to contract upon cooling and are prevented because of adherence to the outer tube fibers. Thus the inner tube fibers are put into tension at an initially high temperature. Upon heating the tubes initially by the combustion, the inner tube fibers are put into compression, the initially cold outer tube fibers in tension. The difference in the material temperature level should make the cessation of combustion case the most critical.

Table 12 summarizes available information on various high temperature materials. It is obvious that more information is required to accurately evaluate combustion tube material on a theoretical basis as to thermal stressing. However, using this information and making educated guesses of the unknown quantities, the calculation of approximate required tube thickness and thermal stress as a stringent cooling requirement is allowed. The results of these calculations are presented in Table 13. Charts for transient heat transfer in flat plates were used to determine the maximum thermal stress in the tube wall. (See Reference 26). For the present wall thickness to diameter ratios used, this is a good approximation. The temperature profile versus radius was then plotted and the temperature difference obtained. Timoshenko's formula was then used to obtain the maximum stresses (Reference 25). It is believed that the

AERONAUTICS DEVELOPMENT CORP.
REPORT NO. 2000-1-R1
FIGURE 103

REPRESENTATIVE TEMPERATURE AND STRESS PROFILES IN TUBE WALL

INITIAL COMBUSTION CONDITIONS AT LOW MACH NO.

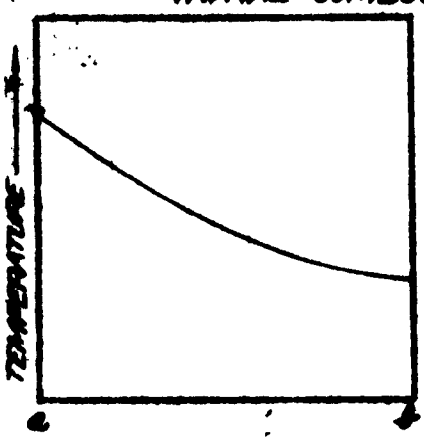


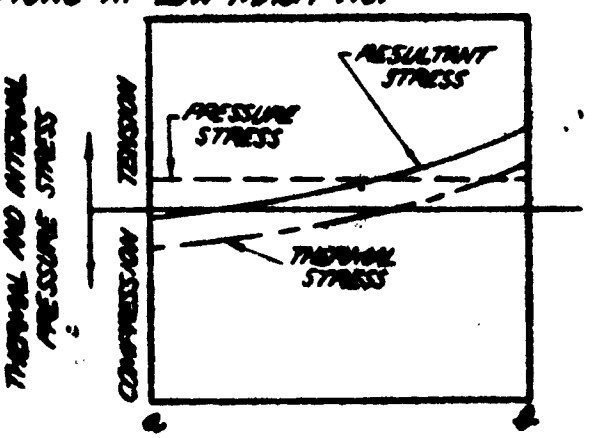


STEADY STATE COMBUSTION CONDITIONS AT HIGH MACH NO. AND LOW ALTITUDE

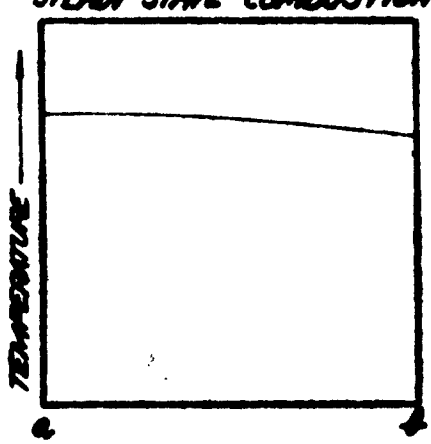


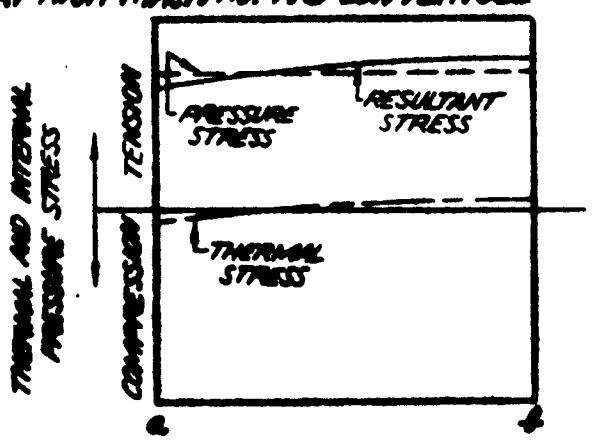


FLAME OUT AT HIGH MACH NO. AND LOW ALTITUDE

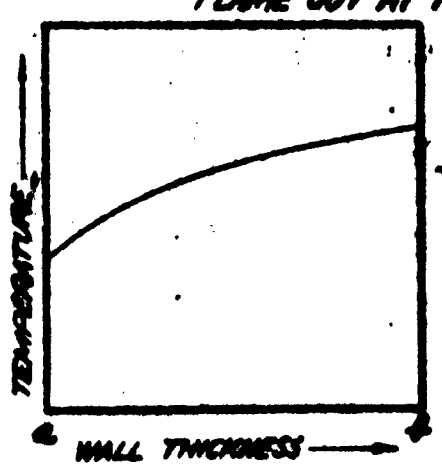


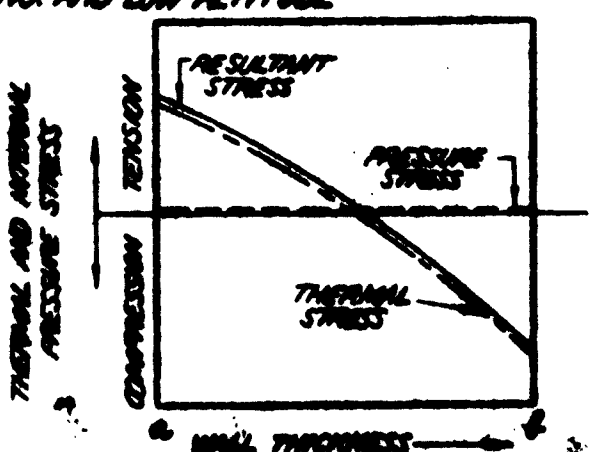

| PREPARED BY | AEROPHYSICS DEVELOPMENT CORPORATION | REPORT NO 2000-1-R1 |
|---|---|---|
| CHECKED BY | PACIFIC PALISADES, CALIFORNIA | DATE Jan 24, 1953 |

calculations are conservative, by a rather large factor, as some material variations in specific heat and thermal conductivity with temperature gradients caused by preheating of boundary layer air by the preceeding tube areas and an intermittent air flow (flow occurs only 50% of the time, whereas steady state flow has been assumed in the thermal stress calculation). From Table 13, it is perceived that only graphite or Zirconium Boride plus nickel may be considered in this application on the basis of the thermal shock calculations. Thermal shock calculations for silicon carbide, Metamic LT-1, and Kentanium K-151A were not made at 3000°F, as their properties are not sufficiently good to warrant serious consideration at such a high temperature.

As a sample of the calculations that were made, the following, using Metamic LT-1 tube material, are representative. Determine the thermal stress in one inch I. D. Metamic tube upon cooling from a tube temperature of 2400°F with cessation of combustion at the maximum helicopter rotor flight Mach Number of .75.

Maximum tube pressure $M_0 = 0.75$ and a combustion temperature of 2500°F if (12.3 po) = (12.3) (14.7) = 180 psia, $\Delta P$ = 165 psig.

Considering a design tube tensile strength of 725 psi at 2400°F (a combustion gas temperature of 2500°F corresponds to a maximum possible mean wall temperature of 2400°F at the tube exit--lower wall temperatures are obtained at the tube inlet and short time tensile strength of Metamic LT-1 is 5200 psi @ 2400°F)

$$t = \frac{Pr}{\sigma} = \frac{165(0.5)}{725} = 0.114 \text{ inches}$$

The average heat transfer coefficient of the wall to the cooling air must be determined.

$$h = \frac{k_a}{D} \frac{0.0396 \, (Re_d)^{3/4}}{\left[1/Pr + 1.5 \, Pr^{-1/6} \, Re_d^{-1/8} (1 - 1/Pr)\right]}$$

Consider inlet air temperature = 120°F @ $M_0$ = .75

exit air temperature = 800°F

Average Pr = .68

Average $k_a$ = .024 BTU/hr/ft/°F

Now under combustion conditions, the inlet flow velocity is higher than without combustion due to the under-pressurization of the tube caused by the momentum of the exit flow when started initially at the high combustion pressure level. The design inlet flow velocity is $M_2 = 0.6$ under combustion conditions. Without combustion, it may be conservatively assumed

$M_2 = 0.3$ or $u_2 = (0.3)(1250) = 375$ ft/sec.

| PREPARED BY | AEROPHYSICS DEVELOPMENT CORPORATION | REPORT NO 2000-1-R1 |
|---|---|---|
| CHECKED BY | PACIFIC PALISADES, CALIFORNIA | DATE Jan. 24 1953 |

$$Re_d = \frac{UD}{\nu} = \frac{375}{12}\,\frac{10^5}{20} = 1.56 \cdot 10^5$$

Therefore

$$h = \frac{(.024)(12)(.0396)(1.56\cdot 10^5)^{.75}}{\left[\frac{1}{.68} + 1.5(0.68)^{-\frac{1}{6}}(1.56\cdot 10^5)^{-1/8}\left(1-\frac{1}{a_{68}}\right)\right]}$$

$$h = 62 \text{ BTU/hr/sq. ft./°F}$$

considering the flow for 50% of the time, the mean value is h = 31

Therefore $R = k/hs = \frac{1}{bs} = \frac{50}{12}\,\frac{12}{.114}\cdot\frac{1}{31} = 14.1$

Using Figure 13 to 18 p. 288 of Reference 26

$$\theta/\theta_0 = .97$$

$$\theta = .97\ (2400 - 100) = 2230$$

$$\Delta T = 2300 - 2230 = 70^\circ F$$

From Timoshinko

Maximum $\sigma_t = \frac{E \epsilon \Delta T}{2(1-\nu)} = \frac{10^7 \cdot 7 \cdot 10^{-6} \cdot 70}{2\,(.75)}$ = 3270 psi

This is approximately the short time tensile strength of Metamic LT-1 at 2400°F. However, a number of conditions would exist in actual operation which make the above calculation quite pessimistic. The assumed flight Mach Number would decrease rapidly if combustion should cease in an engine on a helicopter rotor. Also, no allowance was made for the longitudinal temperature variation that would normally exist in the tubes in regular operation--this would make the inlet end of the tube much cooler than the exit end. In addition, the boundary layer heating of the inlet flow would decrease the maximum temperature differential between the cooling air and the tube. Thus, it is concluded that the Metamic LT-1 material could be safely used on the basis of thermal shock in the helicopter rotor application $M_o$ = .75 at the 2500°F combustion gas temperature level.

## SECTION IX

## EXPERIMENTAL RESULTS

### 9.1 Purpose of Surface Combustion Tests

It was necessary in the preliminary Multi-Jet engine design to make a number of educated guesses or assumptions on certain material properties and cycle operational techniques. A small scale effort appeared necessary to prove these assumptions or indicate more appropriate designs. In particular, more information on what materials in the form of tubes could be used at very high temperatures was required, what minimum surface ignition temperatures are possible, what range of fuel-air ratios are possible in a rotary valve engine, and some idea of the minimum combustion tube length, minimum combustion time and rotary valve speed to obtain efficient combustion. Consequently, an apparatus was constructed for steady state and pulsating (rotary valve) combustion and was tested during the last three months of the contract. It was not intended that this apparatus give precise quantitative measurements of thrust and fuel consumption to be applied to the Multi-Jet. (The contractual studies consisted mainly of preliminary design and analysis of the cycle of operation.) However, operation of this simple apparatus did allow a greater appreciation of the problems involved in rotary valve engines and should enable the test engineers to design and test, in a less time and money consuming fashion, a rotary valve engine.

### 9.2 Description of Test Apparatus:

The air supply consisted of a small air compressor and storage tank of 15 cu.ft. capacity which held air at a maximum pressure of 175 psig. This air was throttled by a manual control valve (as shown in Figure 104 and discharged into a twenty foot length of two inch pipe. Here the inlet air temperature, pressure, and flow was measured. The flow measurement was made by means of a standard orifice plate with flange taps and a water manometer. A mercury thermometer was used to measure the air temperature and was held in the pipe by means of a packing gland and nut. The inlet air total pressure was measured by either a water manometer, an acetlyene tetrabromide manometer or a pressure gauge.

Ethylene was used as fuel in these tests and had the following composition:

| | |
|---|---|
| 96% | $C_2H_4$ |
| 1% | $C_2H_2$ |
| 1 to 2% | $C_2H_6$ |
| 1% | $CH_4$ |

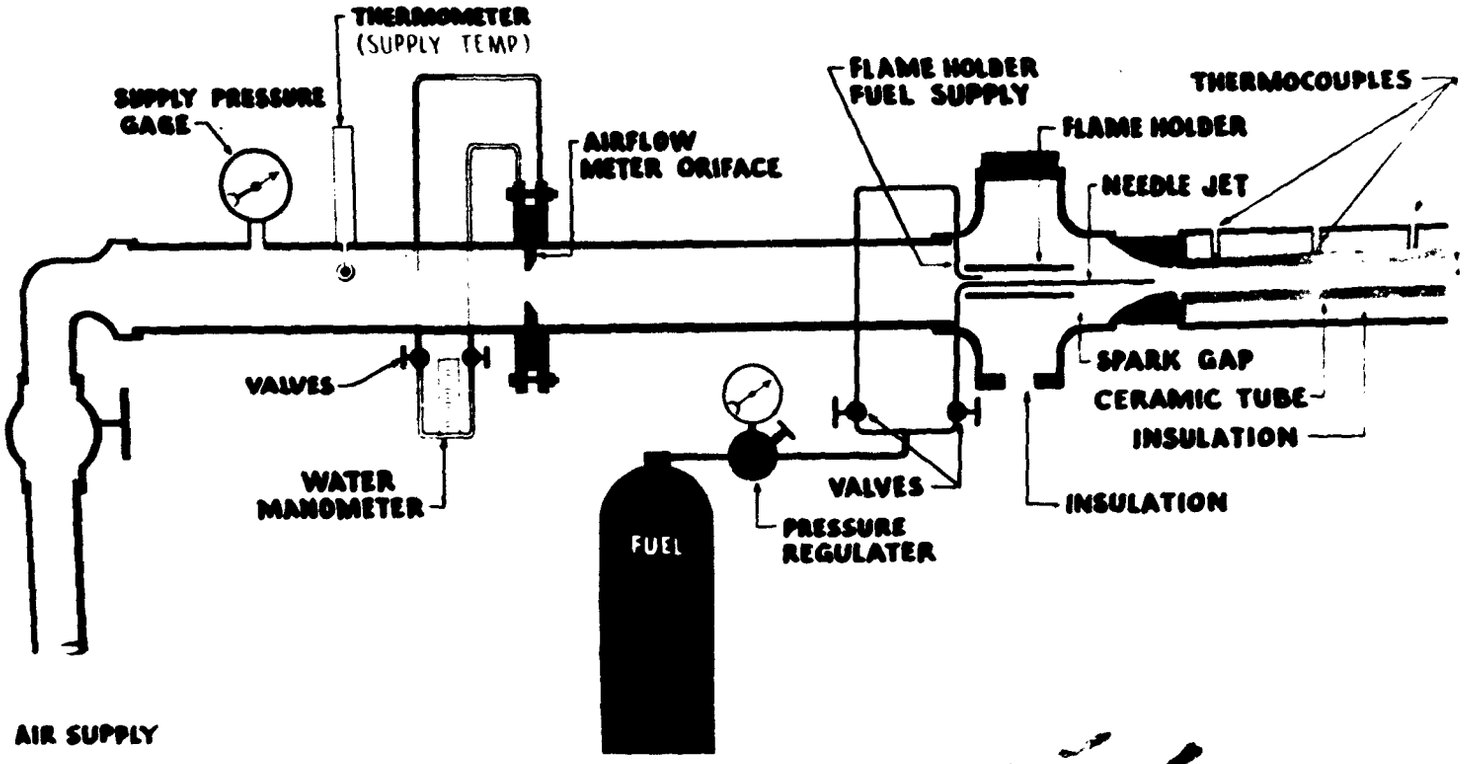


AEROPHYSICS DEVELOPMENT CORPORATION
PACIFIC PALISADES, CALIFORNIA

DATE

FIGURE 104

STEADY FLOW SURFACE COMBUSTION FLOW DIAGRAM

| PREPARED BY | AEROPHYSICS DEVELOPMENT CORPORATION | REPORT NO 2000-1-R1 |
|---|---|---|
| CHECKED BY | PACIFIC PALISADES, CALIFORNIA | DATE Jan 24 1953 |

A length of capillary tubing (marked needle jet on Figure 104) was used as a flow measuring device on the fuel flow. The capillary pressure differential and absolute upstream pressure of the fuel was used to calibrate the capillary tubing by measuring the volume displacement of a brine solution at various flow rates. A home-made tube preheater was constructed in a two inch pipe tee. This consisted of an additional ethylene jet, a small flameholder and spark ignitor as shown in Figure 104. A model airplane ignition coil, dry cells, switch, and ceramic lead in plug were used in the ignitor. The preheater functioned over a wide range of inlet air velocities to the combustion tube as the velocities in the two inch tee were quite low. A picture of the tee and the two fuel valves is shown on Figure 120. When it was desired, the preheater was closed off by closing the valve on its line and the calibrated fuel flow through the needle jet was used in the experiments. The preheater flame holder and the calibrated needle jet is shown on Figure 121 (new) Figure 104 shows schematically the arrangement used on the steady state surface combustion tests. The combustion tube was generally mounted in a holder and held in place by ceramic cement and a high temperature fiber insulation. Platinum and platinum with 13% Rhodium thermocouples were used along the wall and in the exhaust stream with the temperatures taken from calibrated millivoltmeters. The thermocouple used in the exhaust gas stream was corrected for the radiation and conduction error using charts given in Reference 27. A smooth convergent nozzle was used which had the same outlet I.D. as the combustion tube being tested. The internal diameter of the tubes tested was approximately $\frac{1}{2}$ inch in diameter.

Figure 105 shows schematically the rotary valve combustion tube arrangement. Figure 106 shows the actual test layout. The air and fuel inlets remained essentially the same as in steady state combustion (a greater mixing length was allowed before the rotary valve), and the combustion tube was inserted in a rigid fashion between two rotary valve plates. An exploded view of the rotary valve is given in Figure 107. The rotary valves consisted of four slots at the same radius having openings slightly larger than the internal diameter of the tube being tested. The inlet and exit rotary valve plates are keyed to the same shaft which is driven by a 3/4 horsepower motor through a variable speed drive. The operating rpm could be varied from 2300 to 5500 by this arrangement. All the plates were milled flat and valve clearances were obtained by the use of shim stock. The angular position of the slots on the exit valve was set as indicated by theory with respect to the slots on the inlet valve.

Figure 108 shows the rotary valve installation with a crude thrust plate which was used to get approximate exit thrust measurements. The suspended thrust plate was constructed of an empty paint can which essentially changes the direction of exit flow through ninety degrees. A spring balance was moved when taking a measurement to hold the thrust plate in a fixed position. The lever system

| PREPARED BY | AEROPHYSICS DEVELOPMENT CORPORATION | DATE |
|---|---|---|
| CHECKED BY | PACIFIC PALISADES, CALIFORNIA | DATE |

FIGURE 105

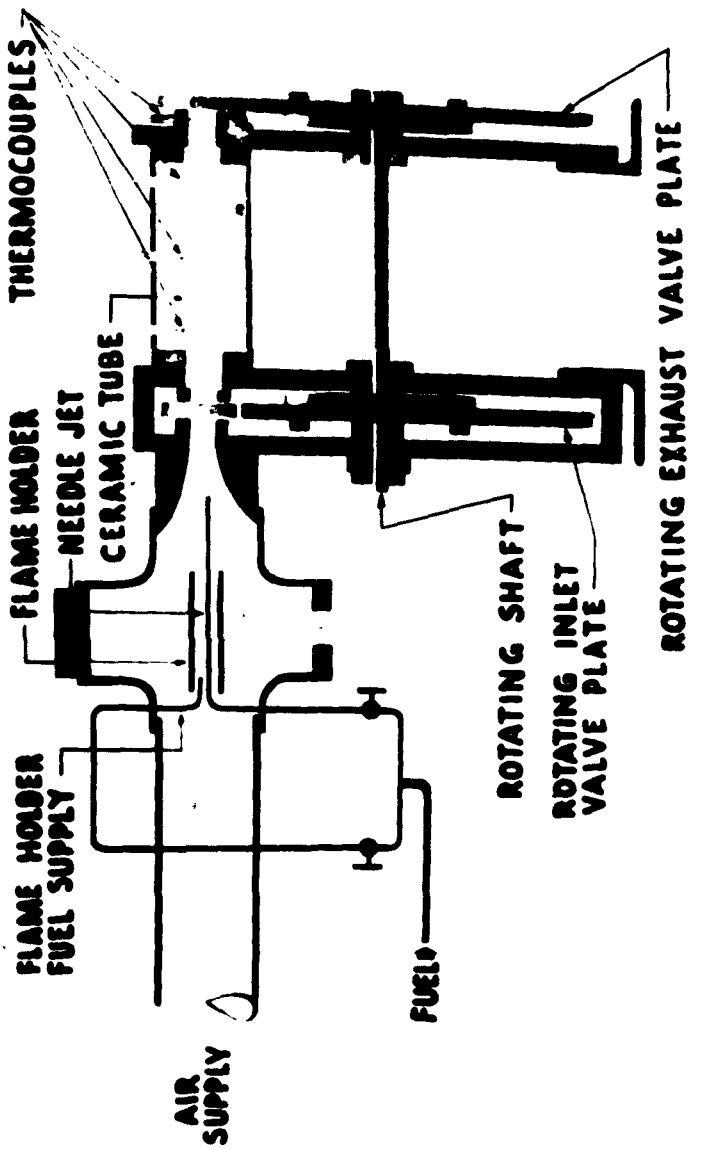


ROTARY VALVE SURFACE COMBUSTION FLOW DIAGRAM

| PREPARED BY | AEROPHYSICS DEVELOPMENT CORPORATION | REPORT NO 2000-1-R1 |
|---|---|---|
| CHECKED BY | PACIFIC PALISADES, CALIFORNIA | DATE Jan 24, 1953 |

FIGURE 106

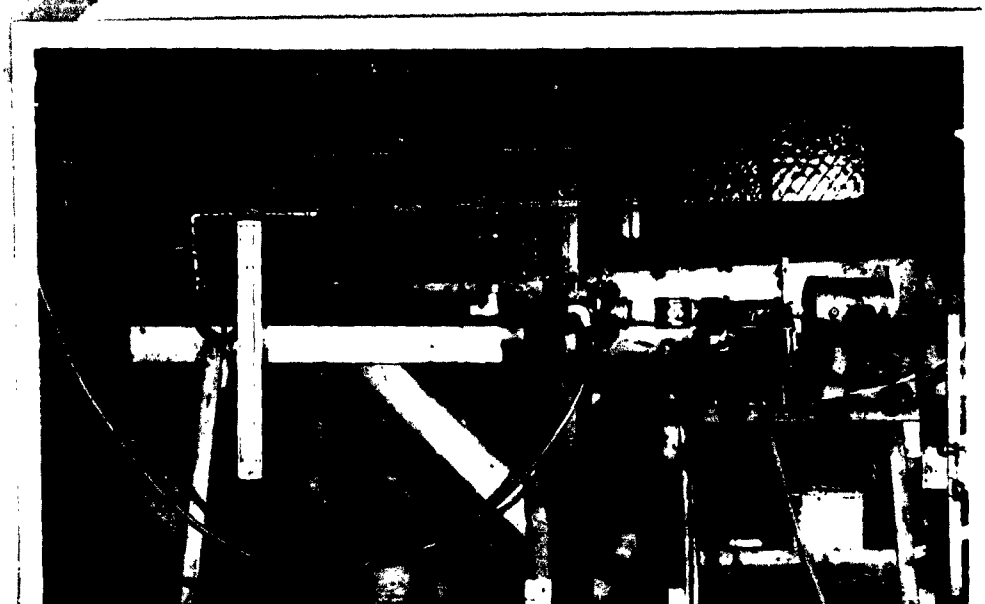

EXPERIMENTAL TEST LAYOUT
ROTARY VALVE TESTS

FIGURE 107

ROTARY VALVE CONSTRUCTION

magnified the thrust obtained by a factor of three. Calibration of the thrust plate with steady flow (no combustion and flow exit velocity calculated from measured chamber pressure) indicated the thrust plate was accurate ±10% over the range of measurement.

9.3 Properties of Tested Materials

The possible delivery dates prevented the testing of tubes of Borolite, Carbofrax, Kentanium K 151-A, Coated Molybdenum, and Fused Stabilized Zirconia. Those materials tested in a tube form were Enameled Steel, Alumina, Fused Translucent Quartz, Stupalith A2417, Graphite, and Metamic LT-1. Figure 109 indicates the installation method used in the steady flow surface combustion tests and Figure 110 shows the insulated quartz tube mounted in place ready for testing.

The enameled steel tubes -- both with the Solar Aircraft and the California Metal Enameling Company coatings were unchanged as long as metal temperatures did not exceed 2000°F. At higher temperatures, the ceramics cracked off easily and the steel oxidized rapidly. The enameled steel tubes cooled off rapidly after preheating and surface ignition and the subsequent combustion could only be maintained in an insulated 12 inch long tube for less than a minute at relatively low inlet flow velocities -- 50 feet per second.

Much longer times were possible for surface ignition and combustion with the high percentage alumina tubes (> 96%). However, this material had to be preheated and cooled quite carefully to prevent cracking due to thermal shock. Figure 111 shows the typical thermal shock fracture obtained in cooling and alumina tube a little too rapidly. Ignition and surface combustion at inlet velocities to 150 feet per second was possible in this tube when the initial tube temperature was 2000°F.

Both translucent and transparent quartz tubes were tested in an insulated as well as a non-insulated condition. These tubes cooled rapidly after preheating and surface ignition and subsequent combustion could be maintained for only a minute or two at low inlet flow velocities (≈50 feet/sec) even in the insulated case. Tests with the transparent non-insulated quartz tubes indicated conclusively that ignition started at the surface of the tube and spread rapidly to the rest of the mixture at a rate chiefly dependent on the inlet flow velocity (to a lesser extent dependent on the fuel-air ratio). The quartz material has low strength and Figure 112 shows a typical expanded quartz tube after a steady flow surface combustion test. A periodic pulsating combustion occurred in this test as well as many others which will be described and explained in more detail later.

A Stupalith ceramic -- A2417 -- was used in a number of the tests with considerable success as long as wall temperatures less than 2300°F were obtained. This material would support surface combustion at high inlet flow velocities up to 150 feet per second for a consid-

| PREPARED BY | AEROPHYSICS DEVELOPMENT CORPORATION | REPORT NO 2000-1-R1 |
|---|---|---|
| CHECKED BY | PACIFIC PALISADES, CALIFORNIA | DATE Jan 24,1953 |

FIGURE 108

ROTARY VALVE WITH THRUST PLATE

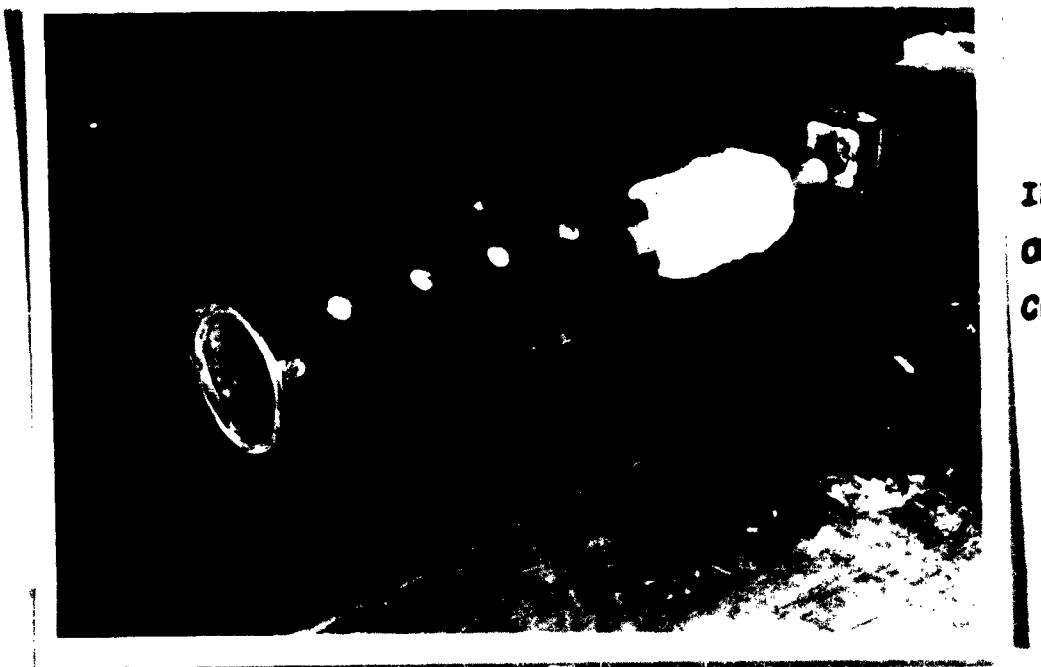

FIGURE 109

INSTALLATION OF THE COMBUSTION TUBE

| PREPARED BY | AEROPHYSICS DEVELOPMENT CORPORATION | REPORT NO 2000-1-R1 |
|---|---|---|
| CHECKED BY | PACIFIC PALISADES, CALIFORNIA | DATE Jan 24,1953 |

FIGURE 110

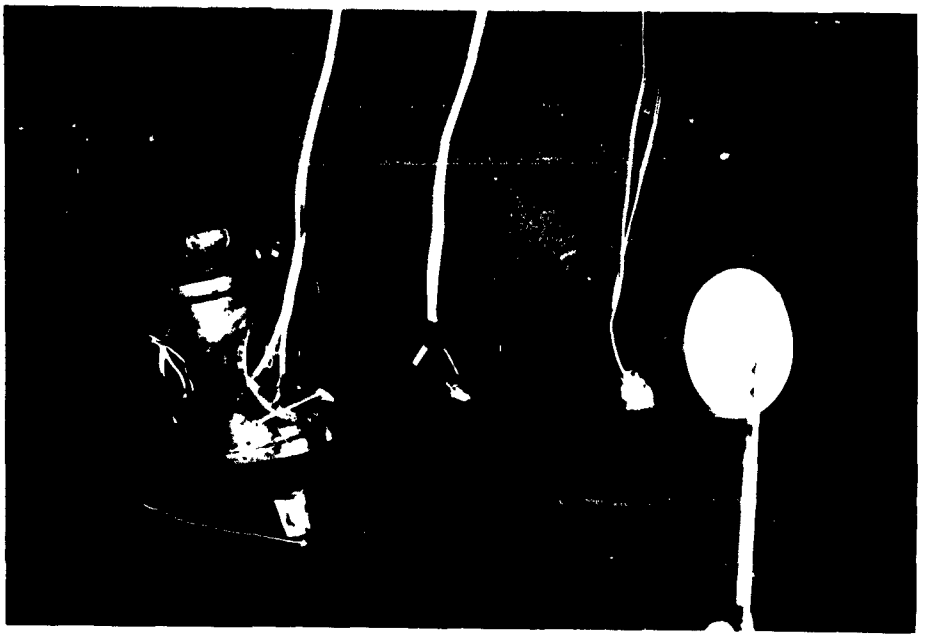

MOUNTED, INSULATED QUARTZ
TUBE READY FOR TESTING

FIGURE 111

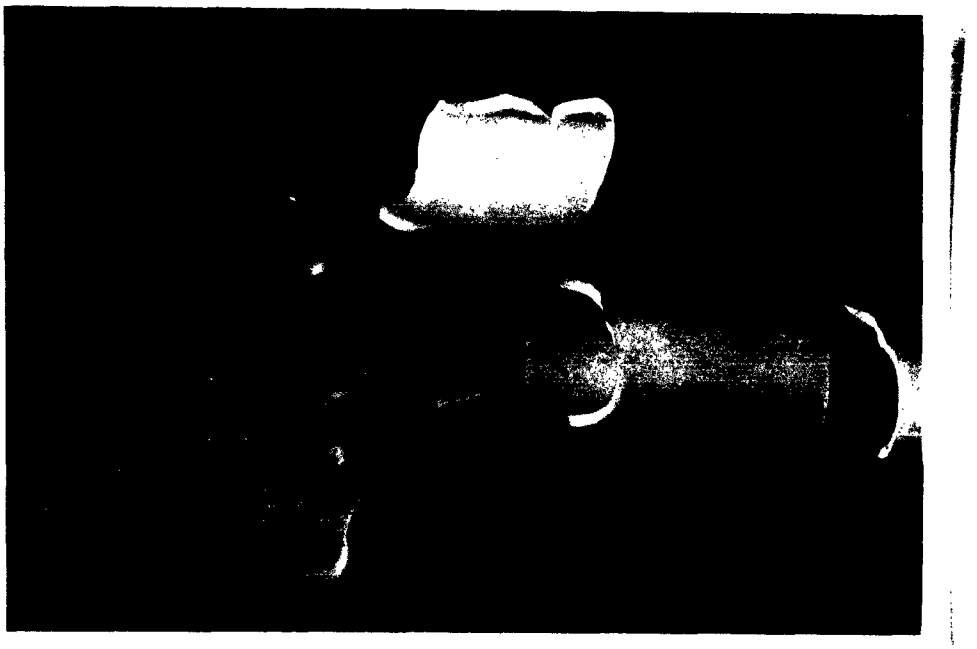

ALUMINA TUBE SHOWING THERMAL SHOCK
(After Steady Flow Surface Combustion)

erable time (several minutes--12 inch length) but would melt easily as shown by Figure 113 if 2300°F was exceeded. This material had excellent thermal shock properties.

Graphite (AGX Grade of National Carbon Co.) was fabricated into tubes from rods by the Aerophysics Development Company. No difficulty was experienced in obtaining a one-sixteenth inch wall with a one-half inch internal diameter. The graphite did not burn appreciably in the air flow even when preheated to 2400°F but upon injecting fuel and using surface combustion, the graphite burned slowly away (5 minutes). See Figure 114. Very high inlet velocities ($\approx$230 ft/sec) were possible with surface combustion in graphite tubes. Thermal choking at the tube exit limited the possible inlet flow velocity to this tube.

An attempt was made to coat several graphite tubes with a layer of silicon carbide to prevent oxidation of the graphite when operating with surface combustion. The two upper tubes on Figure 122 are (PAGE 200 coated, the lower tube is uncoated pure carbon tube. The graphite tubes were dipped into the following composition:

200 parts silicon powder (200 mesh and finer)

450 parts No. 1945 Beckosol Solution (resin)

150 parts Mineral Spirits

The coated tubes were allowed to air dry for 48 hours and then were heated rapidly to 2600°F in a helium atmosphere, and held at this temperature for 15 minutes. These tubes when tested lasted up to one-half hour with surface combustion thus showing a considerable life increase over the uncoated tubes. Time was not available to make additional tests before the end of the current contract. There is good reason to believe that if the tubes were heated more slowly and possibly to a higher temperature that a much more adherent bond would be produced on the tube surface. The resin bond carbonizes easily, but graphitization of this carbon will not ordinarily occur under temperatures of 3100°F (Reference 28). A silicon carbide layer apparently will form at about 2500°F between silicon and carbon. In addition, a stronger finer grade of graphite than AGX may be utilized. Investigators at the Battelle Memorial Institute have succeeded in coating graphite with an adherent layer of molybdenum disilicide. However, after two or three hours at 3000°F, the molybdenum disilicide has been reported to convert to molybdenum carbide which oxidizes quite easily. The possible life of a molybdenum disilicide coating on graphite at the 2500°F temperature level is not known to the authors of this report but should be one of the subjects in further investigation of high temperature combustion tubes.

| PREPARED BY | AEROPHYSICS DEVELOPMENT CORPORATION | REPORT NO 2000-1-R1 |
|---|---|---|
| CHECKED BY | PACIFIC PALISADES, CALIFORNIA | DATE Jun 24, 1953 |

FIGURE 112

QUARTZ TUBE WITH EXPANDED SECTION (Exit End)
(After Steady Flow Surface Combustion)

FIGURE 113

STUPALITH - A 2417
MELTED WALL AFTER TESTED

| PREPARED BY | AEROPHYSICS DEVELOPMENT CORPORATION | REPORT NO 2000-1-F1 |
|---|---|---|
| CHECKED BY | PACIFIC PALISADES, CALIFORNIA | DATE Jan 24 1953 |

Metamic LT-1 material was tested in the form of a combustion tube with excellent results. Under steady flow, surface combustion occurred (after preheating) for several minutes with tube six inches long with inlet velocities up to 100 feet per second. There was apparently no change in the tube dimensions after several hours of testing at various fuel/air ratios and inlet velocities. On some tests, wall temperatures as high as 2900° were indicated. The Metamic tube material as presently made is not dimensionally accurate, the tube is not round and there is a noticeable camber in its length. (See Figure 115) In order to stack a large number of tubes in a given space, such Metamic tubes would have to be machined to size. However, it can be easily worked with carbide tools so that although the machining costs are appreciable, such costs may not be prohibitive.

Two high temperature cements supplied by the Botfield Refractories Company proved highly useful. Adachrome Plastic Super-Cement adhered exceptionally well to metal over a wide temperature range and was used mixed with Fiberfrax as a high temperature sealant between tubes and their holders. It apparently has excellent thermal shock properties and gives no evidence of spalling or erosion in high velocity high temperature gas streams. Adamant Fire Brick Cement has an excellent high temperature bonding strength and was mixed with Fiberfrax and cast to form tubes by the Aerophysics Development Corporation. The strength of the composite structures thus formed was reasonable and it is believed that much greater strengths would be possible by casting with improved techniques. Such composites may provide a very economical material for use in surface combustion tube.

Fiberfrax, a ceramic fiber, has proved to be a very useful insulating and resilient material for use at high temperatures. There is apparently no change in its form at temperatures up to at least 2500°F. At higher temperatures ($\approx$3000°F) it apparently melts and sinters together. For example, it was used as the insulation around the graphite tubes. When the graphite burned away, the cavity formed in the Fiberfrax had the dimensions of the graphite O.D. and graded from a melted sintered material at the internal surface to the unchanged fiberous material a short distance from that surface. The thermal conductivity of Fiberfrax though poorer than other fibers such as Refrasil at low temperature is still quite good at very high temperatures long after Refrasil would have melted.

It appears difficult to obtain most of the high temperature tube materials with wall sections as thin as would be required in the Multi-Jet. While Metamic or graphite may be machined to the desired internal diameter to wall thickness ratio of 8 to 1, most materials considered are so brittle and hard that the only method

| PREPARED BY | AEROPHYSICS DEVELOPMENT CORPORATION | REPORT NO 2000-1-R1 |
|---|---|---|
| CHECKED BY | PACIFIC PALISADES, CALIFORNIA | DATE Jan 14, 1953 |

FIGURE 114

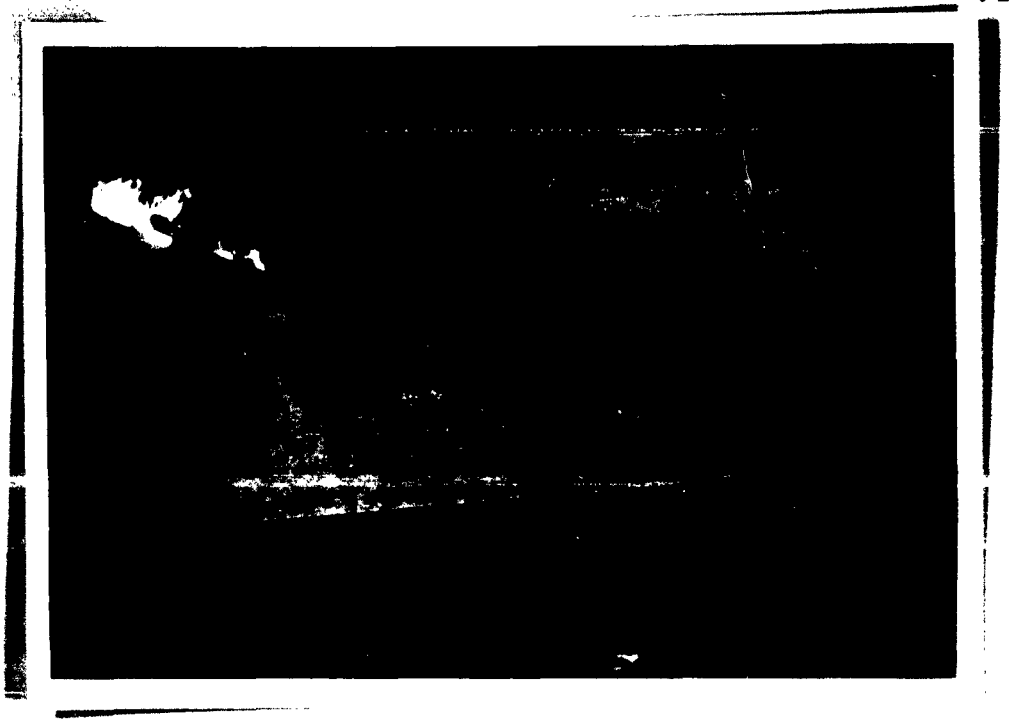

GRAPHITE TUBE AFTER
5 MINUTES OF SURFACE COMBUSTION

FIGURE 115

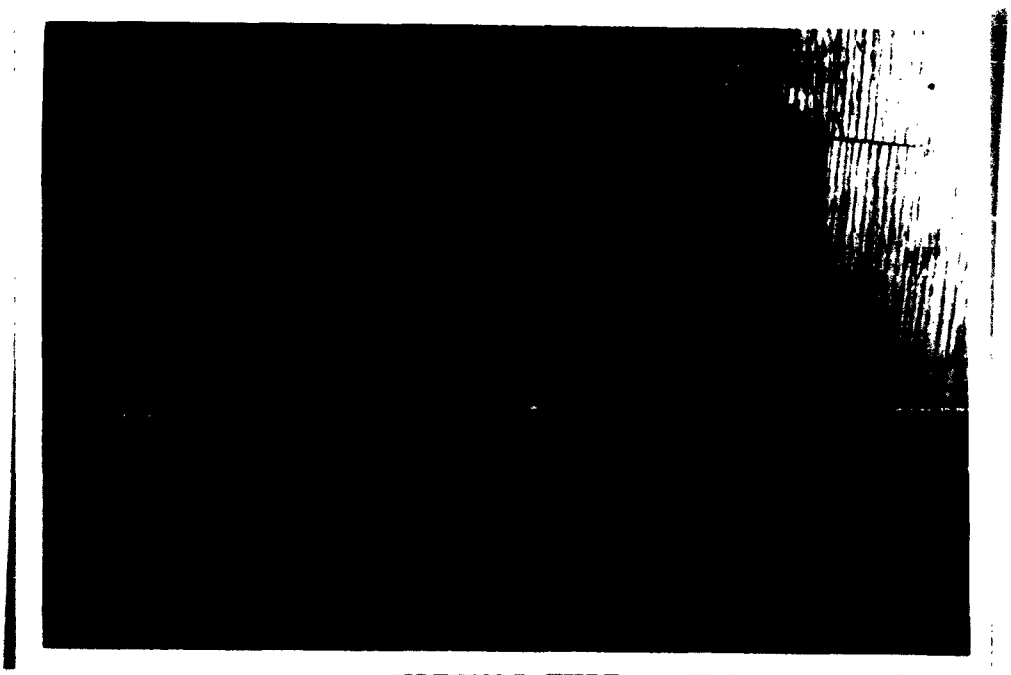

METAMIC TUBE

possible for shaping thin sections would be to use ultrasonic vibration as the ultrasonic carving machine of the Cavitron Equipment Corporation. It is not known how feasible this method would be from a production time and cost viewpoint, but if accurate holes in refractory materials can be made as advertised, the possibility exists of using a single drilled block of refractory material for the engine tube structure. Of course, the possibility also exists of casting a refractory such as Babcock and Wilcox Kromecast or high temperature cements in a mold with suitable hole inserts. A block structure offers important advantages over a tube structure in regard to possible tube capture area per unit frontal area. However, the possibility of a block structure depends critically on the thermal shock properties of a given material.

9.4 Results - Surface Combustion Testing

It was determined that a minimum wall temperature of approximately 1800°F was required to maintain surface ignition of fuel-air ratios of 0.03 and above under steady flow conditions. Combustion with fuel-air ratios below 0.3 would blow out easily at relatively low inlet flow velocities (≈50 ft/sec). Material composition apparently had little or no effect on the minimum surface ignition temperature which was approximately 1800°F for all tube materials tested. A fuel-air ratio of .03 corresponds to a maximum combustion temperature of 2200°F with constant pressure combustion. The maximum possible inlet flow velocities were limited in many cases by thermal choking of the exit flow. The preheater flame is shown on Figure 123. Steady flow surface combustion is shown on Figure 124. (PP 202+203)

An intermittent combustion phenomena of some interest occurred with some of the tubes tested. (Shown schematically in Figure 116). Briefly, with surface combustion occurring, under steady state flow conditions, the surface ignition point in the tube with the tube cooling will gradually recede from the inlet flow end until a significant portion of the mixture is not burned in the tube (indicated by the exhaust flame). Then in the exit flow, an external explosion apparently may take place which causes a flow reversal and secondary combustion of the completely mixed fuel and air in the tube. This allows heating of the walls ahead of the previous ignition point. The resulting combustion pressure causes the flow to exit rapidly until once again an explosion of a combustible mixture at the tube exit may cause a flow reversal and secondary combustion. This appears to the observer as pulsating combustion until suddenly the combustion occurs smoothly once again. The wall thermocouples indicate that during the pulsating combustion, the combustion tube heats up. Evidently, when the ignition of the fuel-air mixture from the tube surface is far enough upstream, the combustion of the mixture is completed before leaving the tube. Thus no pulsation can be obtained from the exhaust gas flow. Such an intermittent combustion technique is of interest as another approach to the problem of

| PREPARED BY | AEROPHYSICS DEVELOPMENT CORPORATION | REPORT NO 2000-1-R1 |
|---|---|---|
| CHECKED BY | PACIFIC PALISADES, CALIFORNIA | DATE Jan 24 1953 |

FIGURE 116

MODEL OF INTERMITTENT & STEADY STATE SURFACE COMBUSTION

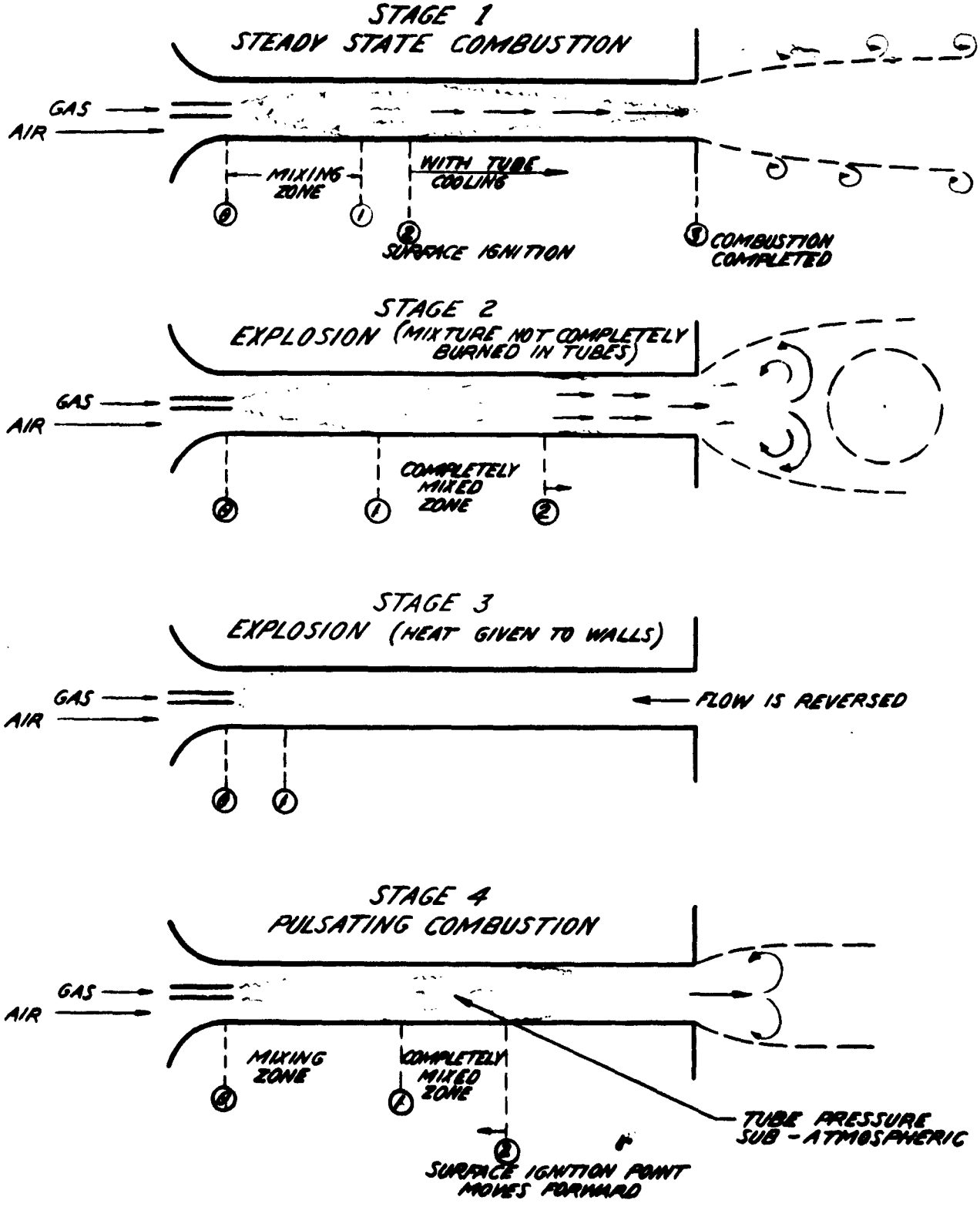

preheating the surface combustion tubes. The mean tube inlet flow velocity varied over a range of about 50 to 100 ft/sec with tests on one-half inch I. D. tubes six and twelve inches long.

A few tests were made with an uncooled rotary valve using surface combustion tubes. (Figure 117). After preheating the tube, the preheater was shut off and the needle jet turned on. Then the motor accelerated the rotary valve to a high rpm. It was found that although the inlet air supply valve was unchanged during this procedure, the differential on the water manometer measuring the air flow (orifice plate and flange taps) increased to a figure three to five times the previous differential reading. The inlet air supply valve is essentially a critical flow orifice (upstream pressure much larger than twice the downstream pressure) so that the actual air flow would decrease as the supply pressure decreased during the run. Consequently, the air flow was determined before and after a combustion test under steady flow conditions, the inlet air supply valve being unchanged over this time. The magnitude of the change in the indicated reading of orifice plate manometer was quite surprising to the authors of this report.

Due to the available time for testing, only six inch long tubes were tested. The tube wall temperature was maintained with rotary valve combustion for durations many times that possible under steady flow combustion under the same inlet conditions. With the six inch long Metamic tube, combustion in one test was maintained at a mean inlet flow velocity of 190 ft/sec, a minimum fuel/air ratio of .022 and a valve rpm of 2300 for a duration of many minutes before the thrust level dropped appreciably (showing tube had cooled sufficiently and could not provide ignition). The maximum inlet velocity for the steady flow surface combustion case with a six inch Metamic tube was about 100 feet per second at a minimum fuel/air ratio of approximately .03. It is interesting to note that a fuel-air ratio of .022 under constant volume combustion gives substantially the same temperature rise as .03 under constant pressure combustion ($\approx 2140^{\circ}F$). Thus, it is apparently possible to operate at significantly lower fuel-air ratios with rotary valve combustion and at much higher mean inlet flow velocities than with steady flow surface combustion. It is believed that somewhat longer tubes would maintain their wall temperatures indefinitely, and of course the percentage heat loss from a multiple tube structure would be much less. Other tubes such as quartz, Stupalith, and enameled steel cooled more rapidly than the Metamic for the same inlet flow rates. A graphite tube functioned well until it burned out and the Stupalith tube was difficult to run since it melted so easily. A transparent quartz tube without insulation when run with the rotary valve showed the combustion to consist of rapid pulsations. (Figure 118)

The rotary valve tubes were preheated for several minutes before running so that appreciable clearances were required on the rotary parts to prevent freezing due to warpage. This prevented an approxi-

| PREPARED BY | AEROPHYSICS DEVELOPMENT CORPORATION | REPORT NO 2000-1-R1 |
|---|---|---|
| CHECKED BY | PACIFIC PALISADES, CALIFORNIA | DATE Jan 24,1953 |

FIGURE 117

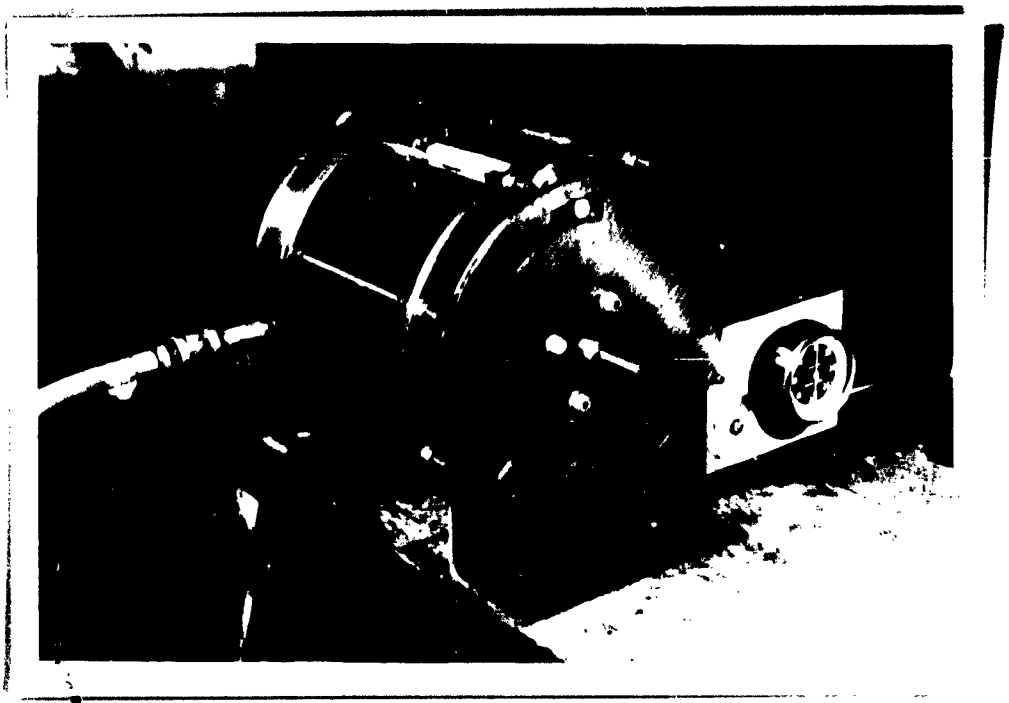

ROTARY VALVE COMBUSTION TESTING

FIGURE 118

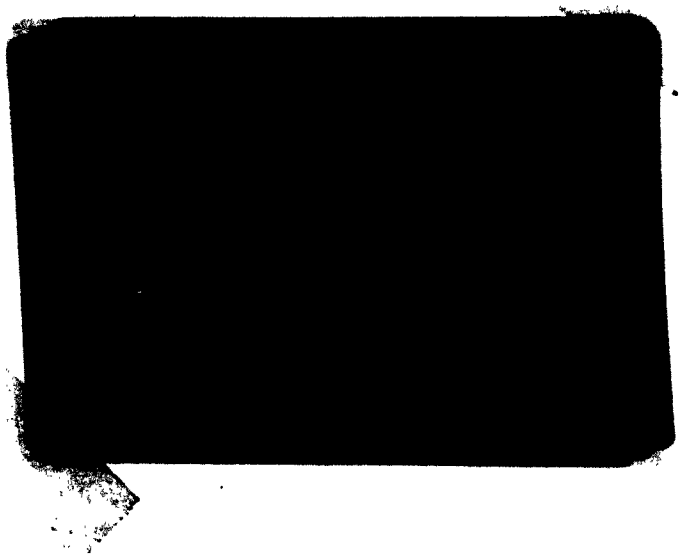

QUARTZ TUBE IN ROTARY VALVE MECHANISM

mate measurement of the possible exit thrust due to the large leakage losses in the clearances between rotor blades and the tube. Fuel cooling of the rotary valves in actual practice will prevent such distortions. Despite these losses, several runs were made which indicated an appreciable net thrust. The inlet air thrust was computed by calculating a "free stream" flow Mach Number which corresponded to the combustion tube inlet total pressure (assuming 100% pressure recovery).

An assembly was then designed and detailed for testing surface combustion tubes with internal diameters up to an inch and for lengths from six to eighteen inches with a rotary valve. (See Figure 119). The rotary valve speed may be varied from 1000 to 6000 rpm by means of a Varidrive motor. Internal water cooling of the rotary valves combustion tube supports have been considered in this assembly so that no distortion due to heat is anticipated. Other features include the translational movement of either rotary valve by increments less than one thousandth of an inch relative to the combustion tube faces and a rotational movement of the exit valve relative to the inlet valve by fine and coarse adjustments on the splined shaft. It is estimated that this precision apparatus would cost not more than $4000 to construct complete with drive motor.

## 9.5 Detonation

A systematic search of the literature has not revealed any experiments on the detonation of commercially available, easy to handle fuels.

The theory governing the detonation wave and the combustion flame has been fully studied by many authors (See References 29, 30, and 31). However, the exact conditions necessary for the formation of a detonation wave from the various sources of ignition still remain to be determined. Many reports were found that described the investigations carried out to determine the limits of detonation for various fuels and fuel/air mixtures. (See References 32 to 36). None of these included any experiments on gasolene or kerosene with air..

It was concluded that the final steady state conditions in the combustion chamber after burning could be estimated on the assumption of constant volume combustion. Actually the detonation wave will develop very high pressures and temperatures, but since it is initiated at a closed end, and expansion wave will immediately follow it reducing these peak pressures. Neglecting heat transfer the final conditions should be very near the conditions after constant volume burning. The principal merit of the detonative combustion is that it proceeds much more rapidly than the deflagration wave. The principal problem will be the initiation of the detonation. Once the detonation is established, it proceeds very rapidly. Thus the time

# ROTARY VALVE TEST ASSEMBLY FOR COMBUSTION TUBES

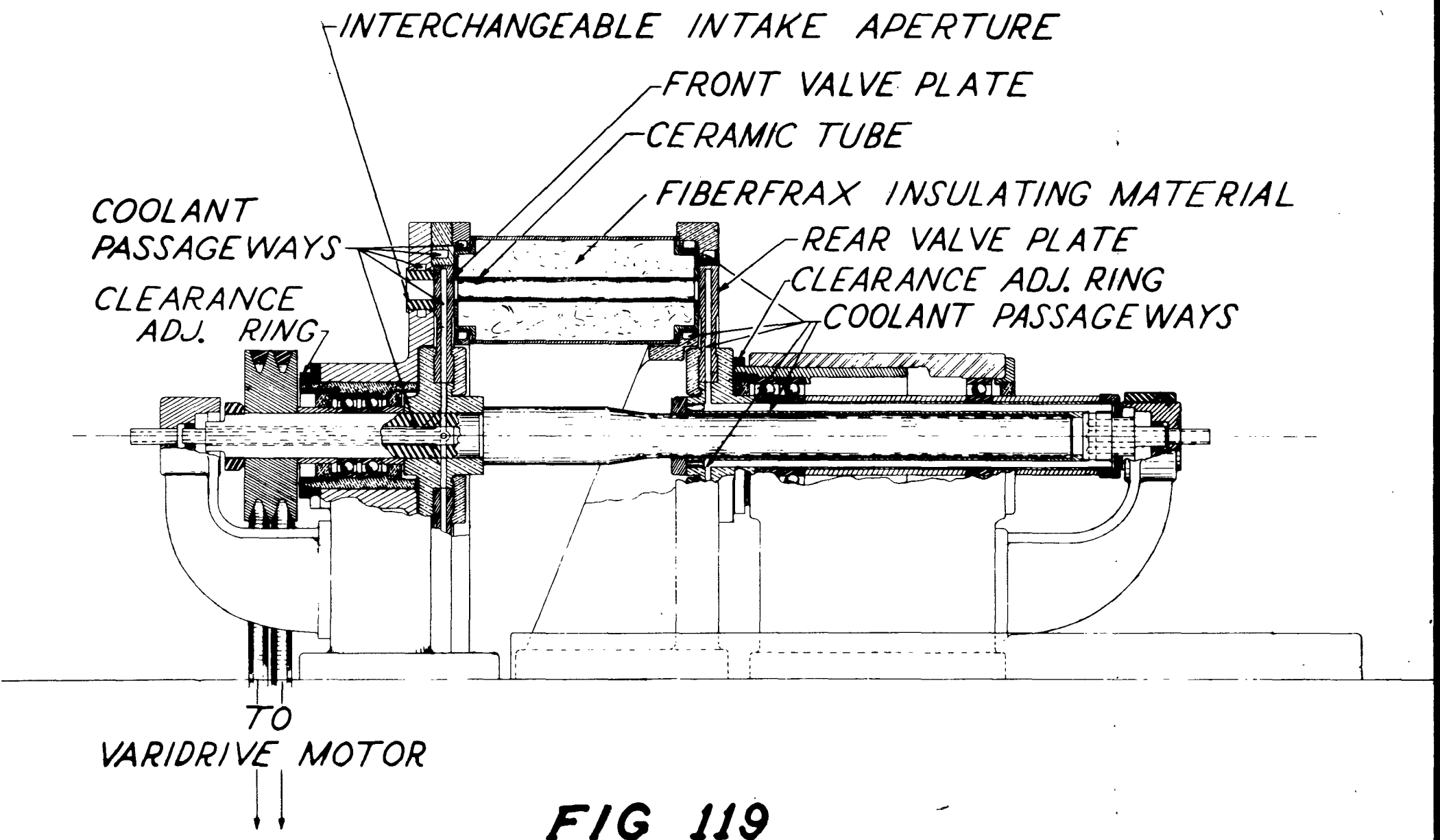


FIG 119

| PREPARED BY | AEROPHYSICS DEVELOPMENT CORPORATION | REPORT NO 2000-1-R1 |
|---|---|---|
| CHECKED BY | PACIFIC PALISADES, CALIFORNIA | DATE Jan 24,1953 |

FIGURE 120

FUEL VALVES AND PREHEATER ASSEMBLY

FIGURE 121

PREHEATER FLAME HOLDER AND NEEDLE JET

| PREPARED BY | AEROPHYSICS DEVELOPMENT CORPORATION | REPORT NO 2000-1-R1 |
|---|---|---|
| CHECKED BY | PACIFIC PALISADES, CALIFORNIA | DATE Jan 24, 1953 |

FIGURE 122

CARBON TUBES

FIGURE 123

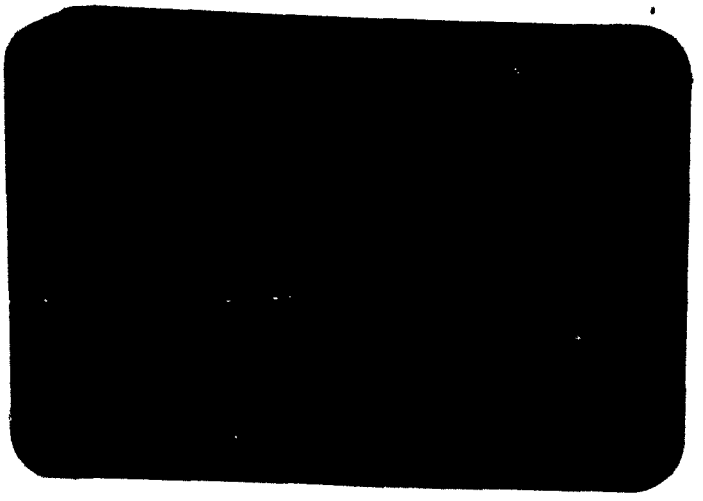

PREHEATER FLAME

| PREPARED BY | AEROPHYSICS DEVELOPMENT CORPORATION | REPORT NO 2000-1-R1 |
|---|---|---|
| CHECKED BY | PACIFIC PALISADES, CALIFORNIA | DATE Jan 24, 1953 |

FIGURE 124

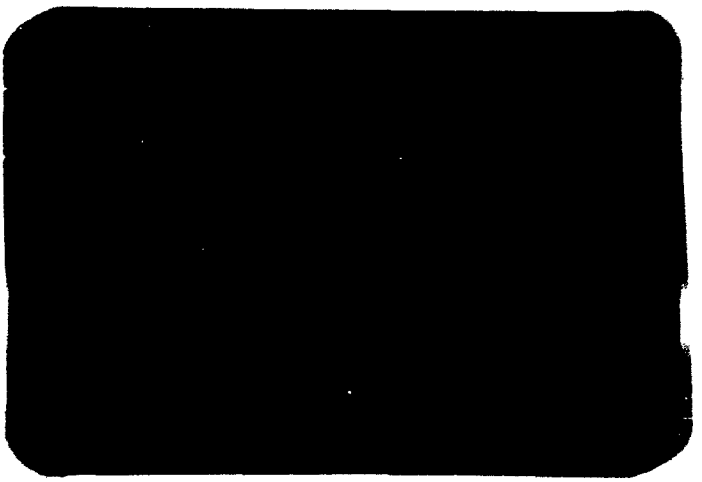

SURFACE COMBUSTION FLAME

required for burning is practically equal to the time for initiation of detonation.

Zeldovich (Reference 37) describes the problem of self-ignition of a mixture and indicates various means of increasing the possibility of the formation of a detonation wave. For example, rough tubes will cause a shock wave to ignite a mixture while if the same wave traveled in a smooth tube, the mixture would not be ignited.

It seems that the two important parameters that will control the formation of the detonation wave will be (a) the local temperature of the ignition source; (b) the presence of discontinuity conditions in the mixture (i.e. a shock wave). Since in the Multi-Jet a shock wave is utilized for the pulse compression, the use of this wave will greatly increase the possibility of detonation. On the other hand this is a relatively weak wave and may not be strong enough to ignite the mixture. This can be overcome by focusing the wave in a cone where high local pressures and temperatures can be obtained causing a detonation to form or by a feedback of hot high pressure gases from a previously fired tube.

## 9.6 Experimental Investigation of Detonation

It was decided that there was great need for an experimental investigation to determine the limits and ease of formation of detonation of common fuels. Shepherd (Reference 36) describes experiments he carried out on ethelene and acetylene in a shock tube. Applying a pressure difference across a copper membrane in a 1" diameter tube and causing the membrane to rupture Shepherd produced shock waves of varying strength that travelled into the fuel-air mixture. By means of a wave speed camera he was able to measure wave velocities before and after detonation and thereby determine if detonation had occurred. He found that certain ethelene/oxygen mixtures could be detonated by shock waves with pressure ratios of two to three.

A shock tube was set up in which the detonation of fuel-air mixtures by means of shock waves could be investigated. A simple layout sketch of the apparatus is shown in Figure 125. This tube is enclosed in a 4-inch pipe casing for safety precautions. The left end of the detonation tube is left open and a window in the 4-inch casing makes it possible to observe the open end of the detonation tube. Pressures up to 100 psi gage have been used in the compression chamber. With this pressure, when the cellophane diaphragm breaks, a shock wave having a pressure ratio of 2.40 is propogated through the detonation tube. The detonation tube is filled with the fuel/air mixture and the observation of a flash at the open end of the detonation tube will indicate that a detonation wave has been initiated by the shock wave. A photograph (Figure 126) of the shock tube is shown with the compression chamber on the right enclosed by the 4-inch diameter casing. The casing over the expansion chamber on the left

| PREPARED BY | AEROPHYSICS DEVELOPMENT CORPORATION | REPORT NO 2000-1-R1 |
|---|---|---|
| CHECKED BY | PACIFIC PALISADES, CALIFORNIA | DATE Jan 24 1953 |

FIGURE 125

LAYOUT OF PRESENT SHOCK TUBE FOR DETONATION EXPERIMENTS

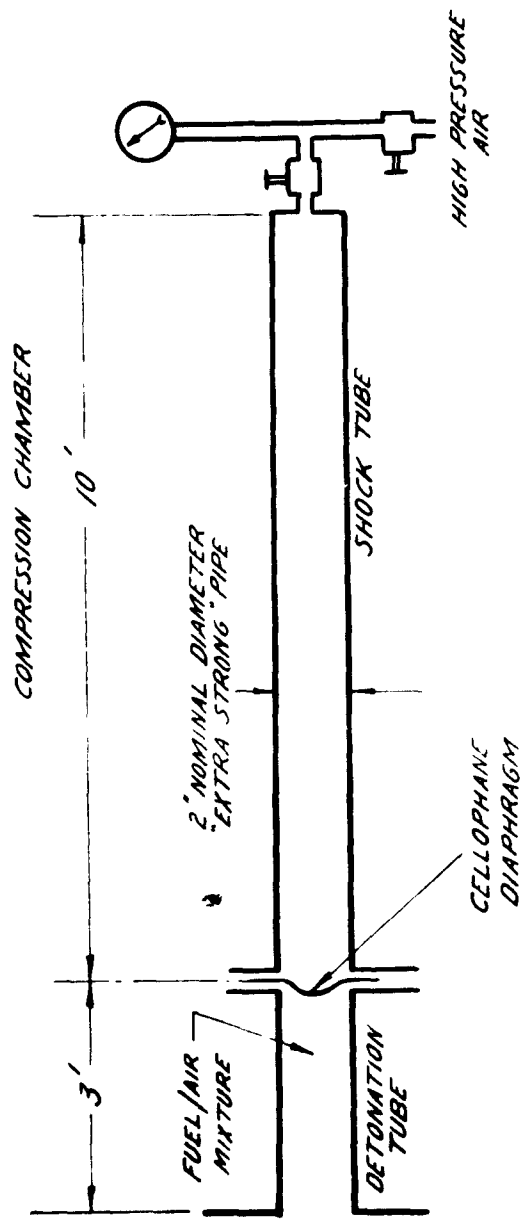

| PREPARED BY | AEROPHYSICS DEVELOPMENT CORPORATION | REPORT NO. 2000-1-R1 |
|---|---|---|
| CHECKED BY | PACIFIC PALISADES, CALIFORNIA | DATE Jun 24, 1953 |

FIGURE 126

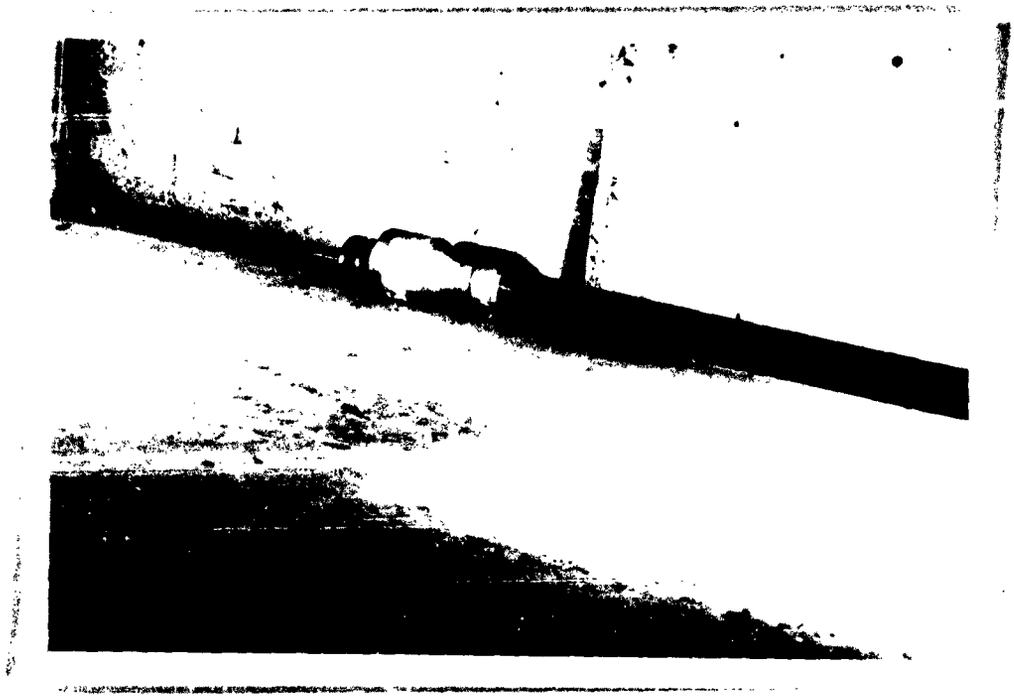

SHOCK TUBE

FIGURE 127

DIAPHRAGM JOINT

has been removed. A close-up view of the diaphragm joint is seen on Figure 127.

## 9.7 Detonation Experiments

Various ethylene-air mixtures were introduced into the expansion chamber and their combustability or ignitability was proved by their ignition by means of a spark. This spark was obtained by means of a small ignition system used on the small model airplane gas engines. The ethylene and air were introduced separately into the expansion chamber and were thoroughly mixed by means of a plunger which was passed through the tube a few times. When the mixture was ignited with the spark a very weak, muffled pop was heard and a very dull, blue flame, tinged with orange, was noticed issuing from the end of the tube. During these ignition tests, a single cellophane diaphragm was placed in its usual position in the shock tube and a single sheet was tied to the end of the expansion tube. The pressure obtained due to the ignition was barely able to blow off the piece of cellophane on the end of the tube, while the diaphragm was unbroken. After each ignition the tube was blown out by allowing compressed air to pressurize the compression chamber and rupture the single sheet of cellophane clamped in the diaphragm position.

The next step was to determine which of the above mixtures that proved to be ignitable by means of a spark could be detonated by means of a shock wave. The fuel-oxygen in the ethylene-air mixture was in the same range of ratios as those used by Shepherd in his experiments on ethylene-oxygen reported in Reference 36. These fuel-air mixtures could not be detonated by means of a shock wave. Pressures up to 100 psi were used in the compression chamber producing shock waves with a pressure ratio of 2.5. It was deduced then that the shock waves were not strong enough to detonate the ethylene-air mixtures. Since it was impossible to obtain higher pressures with the present air supply, stronger waves were not produced.

It was then decided that the experiments of Shepherd (Reference 36) should be repeated. He found that an 18% mixture of ethylene and oxygen could be detonated by means of a shock wave having a pressure ratio of 1.80 (produced in a shock tube having a compression chamber pressure of 65 psi.)

In our experiments the air in the expansion chamber was displaced by allowing the oxygen to flow through the tube for a few minutes. The tube was then closed and the ethylene was allowed to flow into the expansion chamber. The gases were then thoroughly mixed. Again shock waves up to a pressure ratio of 2.50 did not detonate the ethylene-oxygen mixtures. It was not clear why

Shepherd's results could not be duplicated. To determine if the mixture was combustible, the spark was again used to ignite the mixture.

On ignition with the spark the mixture ignited and burned with explosive violence. It was deduced that detonation had occurred.. The expansion chamber was 3½ feet long and 2 inches in diameter. A tube 4" in diameter surrounded the end of the expansion chamber to collect the exhaust gases and duct them out of the room. This 4" tube which was made of galvanized sheet iron was blown apart by the explosion. It was from this observation that it was deduced that detonation had occurred.

The detonation experiments were discontinued at this time due to the difficulty of obtaining higher compression chamber pressures in order to produce stronger shocks. It was also during this period that it was felt that since the combustion tubes had to be manufactured from ceramic compositions that the ignition by the hot walls should be investigated. It is hoped that with more information on detonation that the detonation type of combustion can be utilized in this engine.

Actually as the shock wave travels through the boundary layers of burnt and burning gases in the surface combustion type engine, the pressure and temperature behind the wave are increased thereby increasing the wave velocity. This process can accelerate to the point where a detonation wave will be developed.

9.8 Conclusions:

The use of hot surface ignition appears to be a practical method of obtaining combustion in tubes contained in a rotary valve engine. Further work is required to optimize the combustion tube and rotary valves construction. From a material viewpoint, a Multi-Jet engine for a helicopter rotor blade could be theoretically designed now at the top combustion gas temperature of 2500° F and have a reasonable life expectancy. Many methods appear promising that may allow the use of higher gas combustion temperatures with lighter weight structures and greater characteristic inlet mass flows. Experimentally, there was no indication that the predicated theoretical performance could not be developed in practice with a durable engine.

9.9 Recommendations

It is recommended that the development of the Multi-Jet engine be energetically continued with the design and development of a full scale single row engine concurrently with tests on combustion tubes and rotary valves in the recently designed precision test assembly.

| PREPARED BY | AEROPHYSICS DEVELOPMENT CORPORATION | REPORT NO. 2000-1-R1 |
|---|---|---|
| CHECKED BY | PACIFIC PALISADES, CALIFORNIA | DATE Jan 24 1953 |

## BIBLIOGRAPHY

Reference

1. Schweitzer, P. H.; Van Overbecke, C. W.; Mason, L.; The Kadenacy Effect, page 241, Engineering, Sept. 28, 1945.

2. Emmons, H. W.; Gas Dynamic Tables for Air. Dover Publications (1949), page 31

3. Handbook of Supersonic Aerodynamics, Bureau of Ordnance Publication, Noword Report 1488, Volumes 1 and 2; Superintendent of Documents, U. S. Government Printing Office (1950).

4. Courant, R.; Friedricks, K. D. Supersonic Flow and Shock Waves: First Edition. Interscience Publishers, Inc., New York (1948). pp. 149 and 186.

5. Keenan, J. H., Kaye J.; Thermodynamic Properties of Air, J. Wiley and Sons, New York. (1949).

6. Hottel, H. C.; Williams, G. C.; Sotterfield, C. N.; Thermo dynamic Charts for Combustion Processes; Volumes I and II. J. Wiley and Sons, Inc., New York (1949).

7. Guderley, F.; Nonstationary Gas Flow in Thin Pipes of Variable Cross-section National Advisory Committee of Aeronautics, Technical Memorandum, TM 1196.

8. Sauer, R.; Charakteristikenverfahren für die Eiendimensionale Instationäire Gasstroming, Ingenieur-Archiv, Vol. XIII,(1942).

9. Schultz-Grünow, F.; Nichstationaire Eindimensionale Gasbeweging; Forschung auf dem Gebiet des Ingenieurwesens, Bd. 13, (1942).

10. Hicks, Henry H., Jr.; Weir, Alexander, Jr.; High Mass Flow Ceramic Ram Jet Burner. Aeronautical Research Center, Engineering Research Institute, University of Michigan Report No. UMM-73, Dec. 1950.

11. Howland, A. H.; Simmonds, W. A. A Mechanism of Intense Gaseous Combustion. The Gas Research Board, Beckenham, Kent, England. Publication GRB-49 (1951)

12. Yasecko, J. S. Jet Propelled Rotor for Helicopters. Proceedings of the Fifth Annual Forum, May 12, 13, 1949. American Helicopter Society, Inc., New York.

13. Benson, Igor B. Testing the G. E. 3R-1 Ramjet for Helicopters Proceedings of the Sixth Annual Forum, American Helicopter Society, Inc., New York.

Reference

14. Eckert, E. R. G. Introduction to the Transfer of Heat and Mass. First Edition. McGraw-Hill Book Co., Inc., New York, 1950, p. 113.

15. Keyes, F. G. "A Summary of Viscosity and Heat Conduction Data for He, A, $H_2$, $O_2$, $N_2$, CO, $CO_2$, $H_2O$, and Air." "Measurements of the Heat Conductivity of Nitrogen-Carbon Dioxide Mixtures." Trans. ASME, July, 1951, Vol. 73 No. 5, p. 589-605.

16. Sturn, R. G. A Study of the Collapsing Pressure of Thin-Walled Cylinders, University of Illinois Bulletin, Vol. 39, No. 12, Nov. 11, 1941.

17. Batdorf, S. B. A Simplified Method of Elastic Stability Analysis for Thin Cylindrical Shells, National Advisory Committee for Aeronautics Report No. 874, 1947.

18. American Electro Metals Corporation Summary Report, Cemented Borides, American Electro Metals Corp., Yonkers, New York, Feb. 1, 1949 - Dec. 1, 1950 (Restricted)

19. Haynes Stellite Div., Union Carbide and Carbon Corp., New York, Metamic, Metal Ceramics, F-7480, P-26461.

20. Malmstrom, C.; Keen, R.; Green, L., Jr. Some Mechanical Properties of Graphite at Elevated Temperatures, Jour. of Applied Physics, Vol. 22, No. 5, May, 1951, pp. 593-600.

21. Green, L., Jr. The Behavior of Graphite Under Alternating Stress, ASME Paper No. 51, APM-3, Feb. 6, 1951.

22. Norton Company Technical Bulletin, Norton Fused Stabilized Zirconia, Norton Co., Worcester, Massachusetts.

23. Carborundum Co., Refractories Division, Niagara Falls, N. Y., Carbofrax.

24. Cheng, C. M. Resistance to Thermal Shock, Jour. of the American Rocket Society, Vol. 21, No. 6, Nov. 1951, pp. 147 - 153.

25. Timoshenko, S. & Goodier, J. N. Theory of Elasticity, McGraw-Hill Book Company, Inc., Second Edition, 1951, pp. 412, 415.

26. Jakob, Max Heat Transfer, Vol. I, John Wiley & Sons, Inc., New York, 1950. pp. 285, 288.

Reference

27. Scadron, Marvin D.; Warshwsky, Isidor; Experimental Determination of Time Constants and Nusselt Numbers for Bare-wire Thermocouples in High-Velocity Air Streams and Analytic Approximation of Conduction and Radiation Errors. NACA TN 2599 January 1952.

28. Proceedings of the Royal Society Vol. 209, No. 1097, Oct. 23, 1951.

29. Becker, R. Impact Waves and Detonation NACA TM 505 and 506.

30. Lewis, B., Von Elbe, G. Combustion, Flames and Explosions of Gases Academic Press, Inc., New York (1951).

31. Jost, W. Explosions und Verbrennungs - vorgange in Gasen; Edwards Brothers, Inc., Ann Arbor, Michigan.

32. Payman, W.; Shepherd, W. C. F.; Proceedings of the Royal Society (London) A158, P. 348. (1937)

33. Payman, W.; Proceedings of the Royal Society (London) A120, P. 90 (1928).

34. Damkoehler, G.; Edse, R. Detonation Properties of Fuel-Air Mixtures for Use in Reaction Propulsion. AAF - TS - 978.

35. Berets, D. J.; Greene, E. F.; Kistiakousky, G. P.; American Chemical Society 72, p. 1086 (1950).

36. Shepherd, W. C. F.; Ignition by Impulsive Pressures, Third Symposium on Combustion and Flame and Explosion Phenomena, p. 301 The Williams and Wilkins Company, Baltimore (1949)

37. Zeldovich, Y. B.; Theory of Combustion and Detonation of Gases Technical Report No. F - TS - 1226 - 1A (GDAMA 9-T-4S) May 1949.

| PREPARED BY | AEROPHYSICS DEVELOPMENT CORPORATION | REPORT NO 2000-1-R1 |
|---|---|---|
| CHECKED BY | PACIFIC PALISADES, CALIFORNIA | DATE Jan 24 1953 |

## APPENDIX I

## IDEAL CYCLE PERFORMANCE OF A SINGLE TUBE

This Appendix describes in detail the columns of Tables 1, 2, 3, and 4.

### 1.1 Table 1

Column 1 gives the maximum cycle pressure $\frac{P_3}{P_o}$. For each of the chosen maximum cycle pressures in column 1, the variation of the flow parameters as the pressure drops from $P_3$ to $P_o$ are tabulated.

Column 2, the ratio of the ambient static pressure to the instantaneous pressure in the tube, is chosen arbitrarily. When the exit flow is subsonic $P_o/p = P_n/P$. Column 3 gives the variation of pressure in the tube as the tube discharges. Column 4 gives the time (in the dimensionless form) required for the pressure to drop by the value given in column 3. This is plotted in Figure 4 and is given by equations 13, 14, and 15, and is the ordinate of the curves of Figures 5, 6, 7, and 8. Column 5 gives the instantaneous dimensionless weight flow plotted against $P/P_3$ and is obtained from equation 17 and plotted on Figure 6. Column 6 gives the instantaneous value of the discharge velocity as the pressure drops from $P_3$ to $P_o$, and is obtained from equation (18), and plotted on Figure 7. Column 7 gives the instantaneous values of thrust as the pressure drops from $P_3$ to $P_o$ and is obtained from equation 20 and plotted on Figure 8. Column 8 gives the area under the thrust curves of Figure 8 for each value of $P_3/P_o$. It is given analytically by equation 21 and is plotted on Figure 9.

### 1.2 Table 2

Column 1, the maximum cycle pressure ratio, and column 2, the duct Mach number, are arbitrarily chosen. The choice of $M_1$ (Col. 2) determines the value of $T_2/T_o$ (column 3) and $P_2/P_o$ (column 4). These are obtained from equations 5 and 4 respectively. From columns 4 and 1 we obtain column 5 and $P_3/P_2 = T_3/T_2$ (constant volume combustion). Column 6 is obtained from columns 3 and 5. Column 7, the impulse of the incoming air is calculated by means of equation 23. Column 8 is obtained from Figure 9 and column 9 is the net impulse and is plotted on Figure 10.

### 1.3 Table 3

This table lists the important performance characteristics for a single tube engine operating under an ideal cycle. The arbitrary parameters were $M_1$ (column 1) and $T_3/T_2$ (column 4). Columns

2 to 7 are obtained from Table 2. Column 8 can be obtained from Figure 10. Column 9 is the fuel-air ratio and is obtained from Figure 11. Column 10 lists the specific fuel consumption and is obtained from equation 24. The total duration of a cycle is given in column 11 and is obtained from equations 25, 26, 27, and 28. The average thrust per square foot of combustion chamber area is given in column 12 and is obtained from equation 29. Column 13 gives the weight of air per cycle per cubic foot for combustion tube volume and it is calculated from equation 31. Column 14 gives the air specific impulse, obtained from equation 30.

1.4 Table 4

Table 4 lists for each duct Mach number the maximum allowable value of $\tau_r$ in order for the shock wave to form within 12 inches of the exhaust valve.

| PREPARED BY | AEROPHYSICS DEVELOPMENT CORPORATION | REPORT NO 2000-1-R1 |
|---|---|---|
| CHECKED BY | PACIFIC PALISADES, CALIFORNIA | DATE Jan 24 1953 |

## APPENDIX II

## ACTUAL CYCLE PERFORMANCE OF A SINGLE TUBE

The arbitrary parameters are $M_o$, $M_1$, L, and $T_3$ and are given in columns 1, 2, 3, and 4 of Table 5. The values of the columns 5, 6, 7, 9, 11, 12, 13, 14, and 15 are obtained as described for the ideal case. Columns 8, 10, and 23 give the flow conditions at the outlet end of the tube. These are obtained from equation 62 or Figure 36. Column 25 gives the average density and is computed from equation 72.

The duration of the discharge phase $\tau_E$ is tabulated in column 16 and given by Figure 4 and equation 28. The duration of the pulse compression phase $\tau_c$ (column 17) is given by equation 77 or Figure 41. The duration of the scavenging phase $\tau_s$ (column 18) is given by equation 76 or Figure 41. Column 29 gives the mean effective velocity and is given by equation 69 or Figure 40. Column 22 gives the correction factor for the actual density of the air in the tube and is computed from equation 75. Column 30 gives the air specific impulse which is calculated from equation 71. The thrust per square foot of combustion area (column 31) is computed from columns 30 and 28 and the area of the tube. The fuel-air ratio of column 32 is taken from Figure 42. The specific fuel consumption of column 33 is given by equation (79). Equation 80 gives the thrust coefficient of column 34 and equation 81 gives the characteristic mass flow of column 35. The last two parameters are based on combustion tube area only.

| PREPARED BY | AEROPHYSICS DEVELOPMENT CORPORATION | REPORT NO 2000-1-R1 |
|---|---|---|
| CHECKED BY | PACIFIC PALISADES, CALIFORNIA | DATE Jan 24 1953 |

## APPENDIX III

## PERFORMANCE COMPUTATIONS FOR THE SUPERSONIC ENGINE

The computations of Tables 6 and 7 give the performance calculations for a 36" diameter Multi-Jet operating under an actual cycle. Most of the headings are self-explained. Table 6 gives the supersonic performance computations while Table 7 gives the subsonic performance computations. The numerical subscripts refer to the flow conditions during the different phases of the cycle. Referring to Figure 13, the subscript "o" refers to the ambient conditions of the flow; "1" refers to the flow conditions of the duct flow during scavenging; "2" refers to the flow conditions after the passage of the shock wave; "3" refers to the conditions in the closed combustion chamber after burning is completed and just before discharge. The double primed symbol is used to denote the flow conditions of the inlet phase after the flow has arrived at the rear of the tube and has been influenced by the frictional forces in the duct. It will be noted that $M_1 = 0.6$ for all cases and the tube diverges at a small angle in order to keep $M_1$ = constant throughout the length. Column 18 gives the average density of the fuel-air mixture in the tube. Column 19 gives the ideal total weight of air trapped in the tube. The weight of air per cycle must still be reduced by a correction factor that is determined from the opening and closing times of the valves. The total pressure obtained in the tube must be reduced by this correction factor. Tables 6 and 7 are similar up to column 19. In Table 6 (for the supersonic case) column 20 gives the expansion ratio of the high pressure gasses during the discharge phase for the supersonic flight velocities M 1.00. The impulse during the discharge phase for the various expansion ratios of Column 20 for a given total pressure ratio $P_3 + P_3'' / 2P_o$ is plotted in Figure 88. These curves are obtained from Figures 5 and 8. The given flight Mach number determines the final pressure during discharge and is given by

$$\frac{P_1 + P_1''}{2(2.17)}$$

for the supersonic Mach numbers. Then in Figure 5, $P'/P_3$ would correspond to column 20. From Figure 8 for a given maximum cycle pressure and the value of column 20, the value

$$\frac{\tau_E A_N a_3}{V}$$

is obtained. For the given pressure ratio $\frac{P_3}{P_o} = \frac{P_3 + P_3''}{P_o}$ on Figure 8 the value of

$$\frac{\tau_E A_N a_3}{V}$$

found on Figure 5, is used to find the cut-off point on the thrust

FIGURE 88

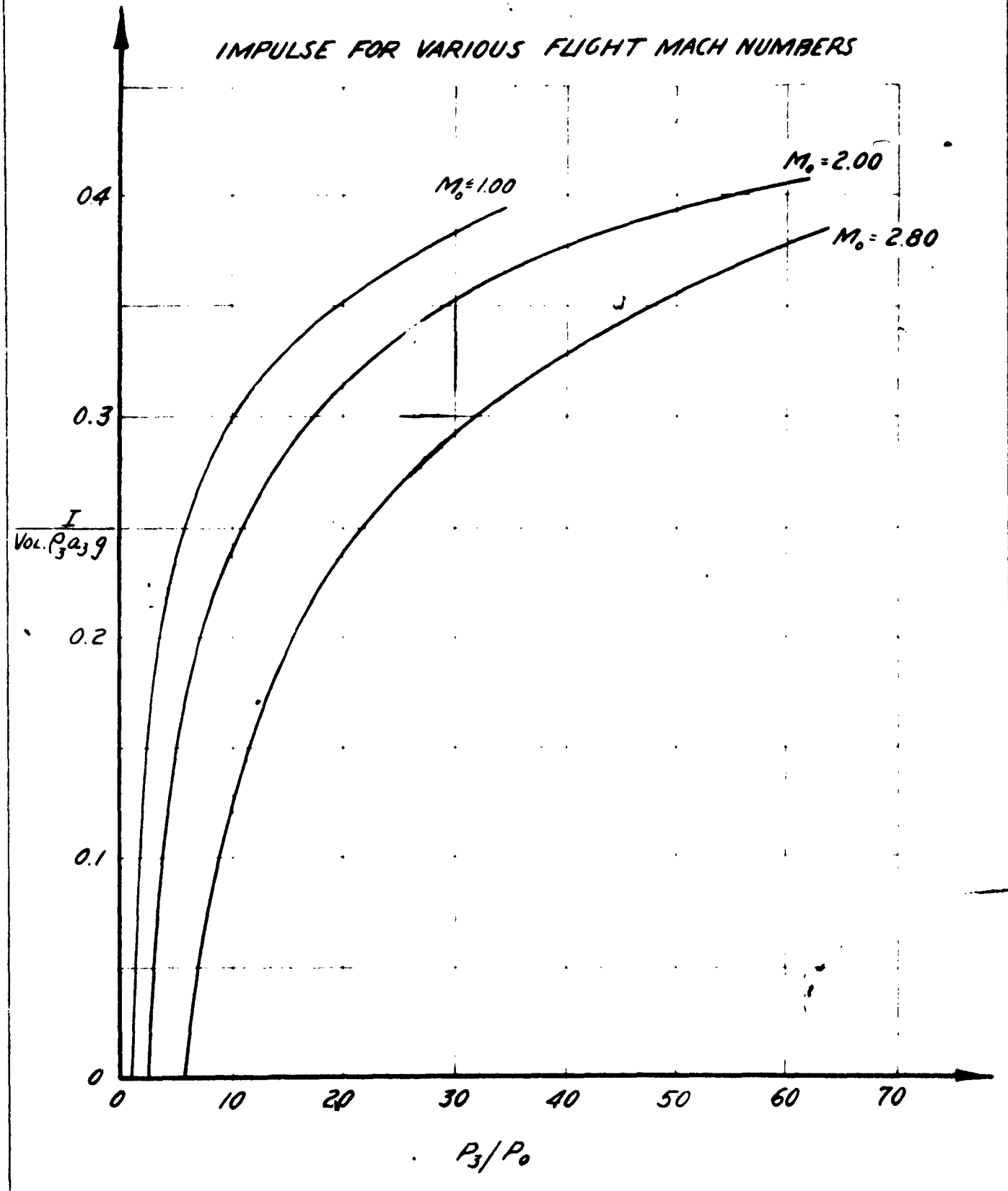
IMPULSE FOR VARIOUS FLIGHT MACH NUMBERS
$M_o = 1.00$
$M_o = 2.00$
$M_o = 2.80$
$\frac{I}{Vol. P_3 a_3 g}$
0.4
0.3
0.2
0.1
0
0
10
20
30
40
50
60
70
$P_3/P_o$

curve. The area is found under the thrust curve between the limits

$$0 \quad \text{to} \quad \frac{\tau_E A_N a_3}{V}$$

(given by Figure 5) and plotted on Figure 88 for the given value of $M_0$. In this way the curves for $M_0 = 2.80$, 2.00, and 1.00 were obtained for Figure 88. From Figure 88 column 21 of Table 6 is obtained. By integration of the curve of Figure 6 from $\tau = 0$ to $\tau = \tau_{DISCH}$ (i.e. the value of $\tau$ found from Figure 5 (using $P'/P_3$ = column 20) gives the percentage of air discharged during the thrust phase (while the pressure dropped from $P_3$ to

$$\frac{P_1 + P_1''}{(P_3 + P_3'')2.17}$$

This can be seen from the following equation where $w_a$ is the weight flow in lbs/sec.

$$\int \frac{w_a}{a_3 \rho_3 g A_N} d\frac{\tau_E A_N a_3}{V} = \int \frac{w_a \, d\tau_E}{g \rho_3 V}$$

where $\int w_a \, d\tau_E$ is the weight of air discharged and $(g \rho_3 V)$ is the total weight of air contained in the tube before discharge. Column 23 gives the percentage of air discharged while 24 gives the weight of the remaining air. Since the gases are expanded isentropically in the tube during the discharge phase, the total temperature at the end of discharge is given in column 26. From the value of the total temperature in the tube the velocity of sound at a nozzle, (discharging at sonic velocity) can be found. This is the velocity of the remainder of the burnt gases during scavenging and is given by column 27. The value of $\tau_s$ for column 28 is obtained from Figures 60 and 63. The impulse of the scavenged gases as they are discharged is given in two parts. The gases first issue at a low nozzle pressure = $\frac{P_1 + P_1''}{2.(2.17)}$

After the pressure effects from the front valve reach the exhaust, the gases issue at a higher pressure = $P_1 + P_1''/2$ . Approximately one-fourth of the remainder of the gases leaves at the low pressure, the other three-fourths leaves at the higher pressure. It was assumed that the nozzle velocity remained the same during the whole scavenging period. Actually the pressure and temperature effects of the opening action of the inlet valve would increase the exit velocity from that given by column 27. This is neglected. Columns 29 and 30 give the two pressures. The impulse of these gases is then computed in columns 31, 32, and 33 which when added give the impulse during scavenging (column 34). The impulse of the intake air is given by column 35. The net impulse is given by column 36. The total duration of the cycles are obtained from Figures 60 and 63.

The losses due to the slow opening and closing actions of the valves are discussed in Subsection 5.4.3. These considerations explain columns 38 to 46 and 49 and 50.

The specific fuel consumption was computed by means of Figure 128. The difference between constant volume burning and constant pressure burning can be seen by comparing Figures 128 and 129. For the same fuel ratios, there is a smaller temperature rise for the constant pressure curves than there is for the constant volume curves. Both of these curves were computed from the data given in the tables and charts in References 5 and 6. The effect of dissociation at the higher temperatures is considered in these curves.

Table 7 gives the computations for the subsonic flight velocities. Since columns 1 to 19 are similar to those of Table 6 they are not described again.

Column 20 gives the expansion ratio during the discharge phase. Column 21 gives the impulse which is found from the curve of Figure 9. For the subsonic flight Mach numbers, the pressure in the tube is allowed to drop to $P_{ot}$ (where $P_o$ defines $P_{ot}$) since the variation of $P_{ot}$ for $0 \leq M_o \leq 0.75$. causes a very small variation in the impulse ($< 3\%$), differences in the impulse curve for the subsonic flight velocities were neglected. The curve of Figure 9 was sufficiently accurate for this purpose. Columns 23, 24, and 25 of Table 7 are similar to columns 23, 24 and 25 of Table 6. The exit nozzle pressure during scavenging was assumed to be equal to the velocity of the inlet fuel-air mixture (i.e. $M_1$ $A_1$). The impulse of the scavenged cases are therefore, given in column 26. The rest of the columns are similar to those of Table 6.

Columns 51 to 57 of Table 6 and Columns 43 to 49 of Table 7 give the drag and thrust coefficients of a typical supersonic missile with a wing area of 425 square feet, powered by 4 of the 36" diameter engines. The thrust and drag coefficients are referred to the wing area and the drag coefficients are obtained from Figure 75.

AERODYNAMIC DEVELOPMENT CORPORATION
P O BOX 657 PACIFIC PALISADES CALIFORNIA

2000-1-R1

DATE Jan 24 1953

FIGURE 128

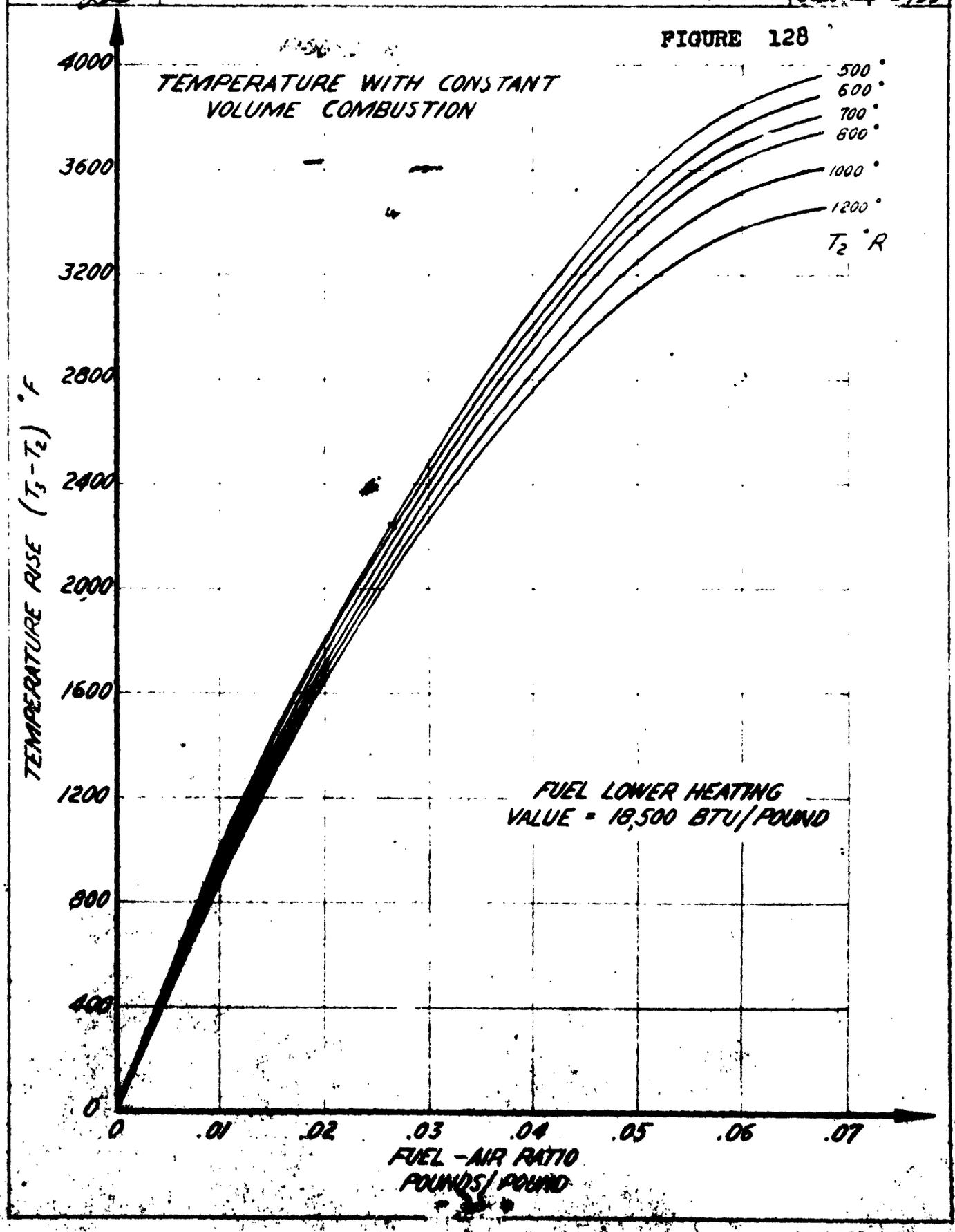

| PREPARED BY | AEROPHYSICS DEVELOPMENT CORPORATION | REPORT NO 2000-1-R1 |
|---|---|---|
| CHECKED BY | PACIFIC PALISADES, CALIFORNIA | DATE Jan 24 1953 |

FIGURE 129

TEMPERATURE RISE WITH CONSTANT PRESSURE COMBUSTION

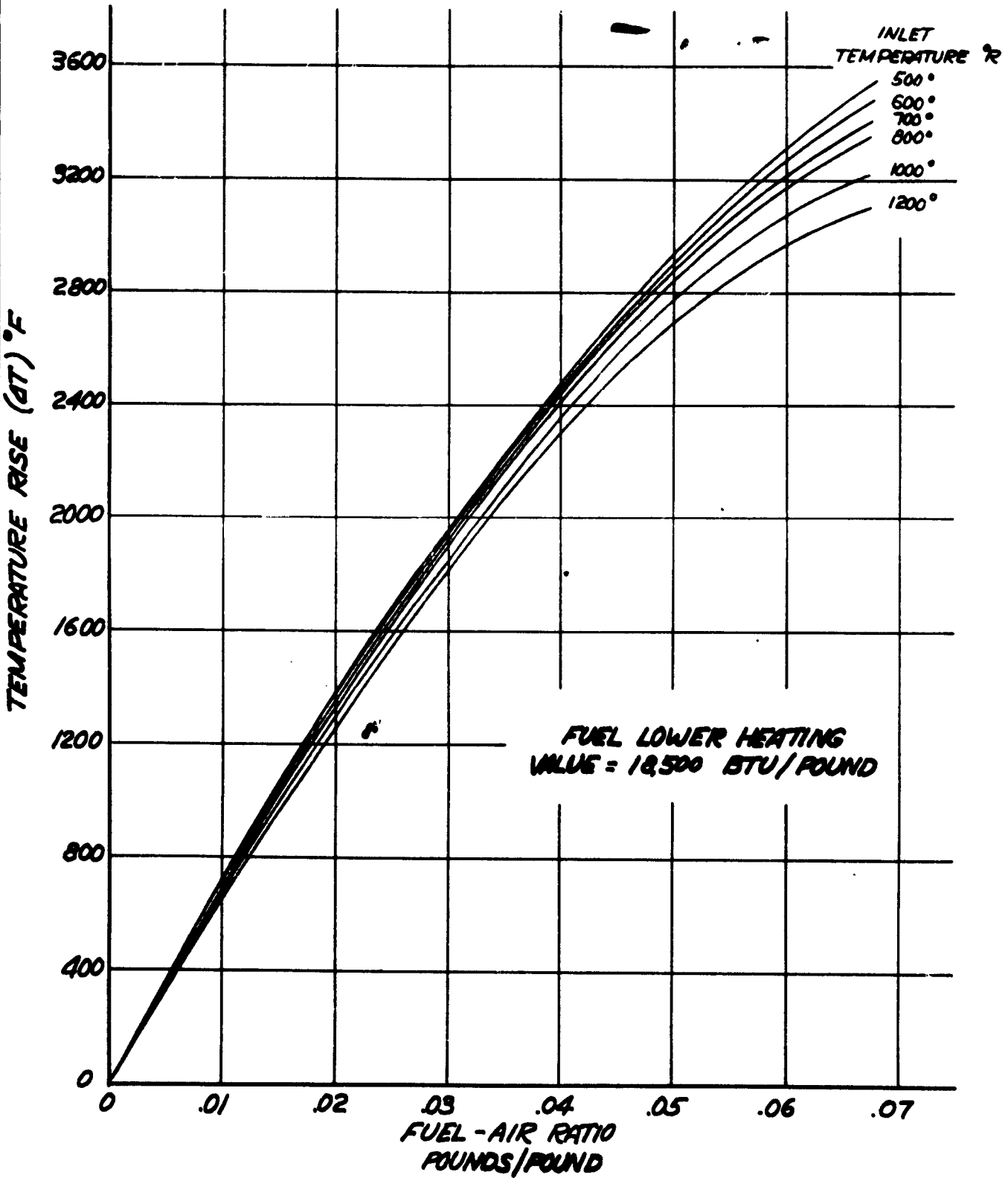

| PREPARED BY | AEROPHYSICS DEVELOPMENT CORPORATION | REPORT NO 2000-1-R1 |
|---|---|---|
| CHECKED BY | PACIFIC PALISADES, CALIFORNIA | DATE 24 Jan 1953 |

## APPENDIX IV

## COMPUTATION FOR THE IDEAL CYCLE

The columns of Table 8 give the performance computations for an 8½" diameter Multi-Jet operating under an ideal cycle. Most of the headings of the columns are obvious. The numerical subscripts refer to the flow conditions during the different phases of the cycle. Referring to the Table 8 and Figure 13, the subscript "o" refers to the ambient conditions of the flow; "1" refers to the flow conditions of the incoming fuel-air mixture during scav - enging; "2" refers to the flow conditions after the passage of the shock wave; "3" refers to the conditions in the closed combustion chamber after burning is completed and just before discharge. It will be noted that $M_1 = 0.6$ for all values of $M_o$. Column 14 gives the total weight of air trapped in the chamber during each cycle. Column 15 gives the expansion ratio of the high pressure gases during the discharge phase. Column 12 gives the total pressure ratio of the hot high pressure gases. From Figure 5, the curve for the total pressure ratio $P_3/O_o$ is picked out and the point on this curve is marked where $P_{ot}/P_3^o = P/P_3$. For this point the value of

$$\frac{\tau_E A_N a_3}{Vol}$$

is tabulated in column 16. In columns 16 and 17, $L$ is the length of the tubes. ( = 0.50 feet.)

The values of column 18 are obtained from Figure 9 and, column 19 gives the values of the impulse $I_v$. Integration of the curve of Figure 6 between the limits for $\tau a_3/L$ from 0 to the value of $\tau_E a_3/L$ given in column 16, gives the percentage of air discharged while the pressure dropped from $P_3$ to $P_{ot}$. This can be seen from the following equation where $w$ is the weight flow in lbs/sec.

$$\int \frac{w}{a_3 \rho_3 g} d\frac{\tau_E a_3}{Vol} = \int \frac{w\, d\tau_E}{g \rho_3 Vol}$$

where $\int w\, d\tau_E$ is the weight of air discharged and $g\rho_3$ Vol. is the total weight of air contained in the tube before discharge. Column 22 therefore gives the weight of air remaining after discharge and this air is discharged during scavenging at a velocity = $V_1$. The Impulse $I_3$ is given in column 23 and added to $I_v$ to give the gross impulse. The impulse due to the inlet flow, given in column 24, is subtracted to give the net impulse in column 25.

| PREPARED BY | AEROPHYSICS DEVELOPMENT CORPORATION | REPORT NO 2000-1-R1 |
|---|---|---|
| CHECKED BY | PACIFIC PALISADES, CALIFORNIA | DATE 24 Jan 1953 |

The time required for scavenging is given in column 26 and is found from the following relation:

$$\tau_s = \frac{L}{M_1 a_1}$$

The time required for pulse compression is given in column 27 and is found from the following relation:

$$\tau_c = \frac{L}{M_w a_1}$$

where $M_w$ is given by equation 3.

The time required for burning was assumed to be 0.0015 secs.

The value of the fuel-air ratio is obtained from Figure 129.

# APPENDIX V

## COMPUTATIONS FOR AN ACTUAL CYCLE

The columns of Table 9 give the performance computations for an 8¼" diameter Multi-Jet operating under an actual predicted cycle. The numerical subscripts are similar to those in Table 8 and refer to the conditions at the entrance of the tube. The double primed symbol is used to denote the conditions of the flow after it has arrived at the rear of the tube and has been influenced by the frictional forces in the duct. The columns of Table 9 up to column 24 are similar to those of Table 8. In order to find $P_1''$, $P_2''$, $P_3''$ and the loss in pressure in a duct of given $L/D$ with flow Mach number $M_1 = 0.6$ is found from Figure 36.

The description given in Appendix IV for the columns 1 to 25 apply to Table 9 also. The value of $\tau_{TOT}$ in column 26 is obtained from Figures 89 and 90 as are the values of $\tau_v$ and $\tau_o$ in columns 27 and 28. The reduction or correction factors are given in columns 31, 32, 33, and 34. Column 31 gives the losses due to the leakage through the valves. Column 32 gives the reduction of mass due to the slow opening and closing actions of the valves. The loss in mass flow due to leakage was computed to be 8.4% (see Sub-Section 6.2.4). The actual performance values are then computed and tabulated in columns 35, 36, 39, 40, 41, 42 and 43.

| PREPARED BY | AEROPHYSICS DEVELOPMENT CORPORATION | REPORT NO 2000-1-A1 |
|---|---|---|
| CHECKED BY | PACIFIC PALISADES, CALIFORNIA | DATE Jan 24 1953 |

## APPENDIX VI

## HELICOPTER MULTI-JET FUEL SYSTEM

Figure 130 gives the flow diagrams presently devised for the fuel system and its control. The fuel is regeneratively heated by the engine exhaust to allow a substantial amount of the fuel to be flash vaporized upon injection in the air flowing through the engine. The flash vaporization should allow more efficient use of the fuel in the motor.

The fuel control system is based on the pressure generated by the fuel at the engine location due to centrifugal action by the well-known formula

$$P = \frac{\rho v^2}{g}$$

$P$ = pressure

$\rho$ = fluid density

$v$ = engine velocity at rotor tip

Consequently, the rotor blade rpm which is proportional to $v$ may be held constant by allowing more or less fuel flow which accelerates or decelerates the rotor so as to hold the pressure, P, constant. The valve A accomplishes this control. The rotary valve in each engine must also be controlled at a constant rpm. This will be accomplished having on the rotary valve shaft a small fuel pump whose output pressure is proportional to the rotary valve rpm (within the required accuracy). This output pressure is applied on one side of a piston, while on the other side of the piston the inlet pressure and spring is applied. This will position a valve which allows more or less fuel to bypass the positive displacement drive (form similar to hydraulic motor) thus regulating the rotary valve rpm.

Examination of the formula for the pressure developed by centrifugal action shows that the pressure is proportional to the fuel density. Consequently, a temperature control heat exchanger is required on the inlet fuel line - the fuel to the motor being preheated to a constant temperature of 120° F ± 5° F.

Starting of the engines is presently considered to be accomplished as follows: A line from a pressurized gas container will drive the rotary valve independently of the fuel motor by means of a small gas turbine at a rate higher than in steady state operation. Rotation of the valves will induce a small air flow through the engine. The ejector action of the air from the gas turbine will also induce an air flow through the engine. A small fuel flow also results by the

| | | |
|---|---|---|
| | AERODYNAMICS DEVELOPMENT CORPORATION | 2000-1-R1 |
| 283 | P.O. BOX 657 FAIRFIELD, CALIFORNIA | Jan 24 1953 |

FIGURE 130

## HELICOPTER MULTI-JET FUEL SYSTEM

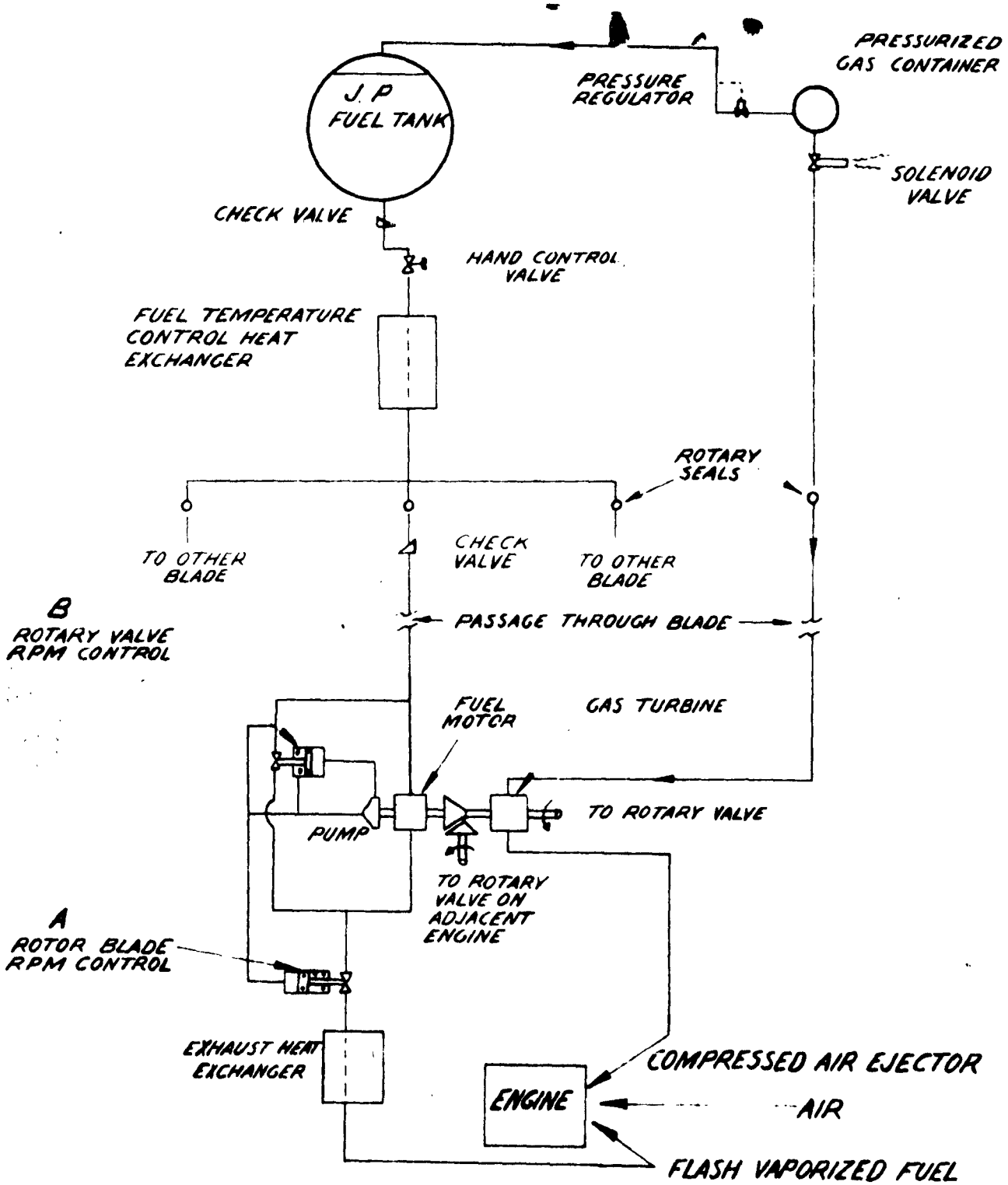

fuel motor acting as a pump and this fuel is injected at the front of the engine. Ignition is obtained in this region by means of spark plugs. The fuel-air mixtures burning partially expand through the engine developing a small amount of thrust while heating the combustion tubes. When the combustion tubes are sufficiently heated to cause auto ignition of the incoming fuel-air mixture, thrust will increase rapidly allowing the blades to rotate. As the rotational speed increases, the fuel pressure increases and the rotary valve may then be driven by the fuel motor instead of the compressed gas turbines. This "bootstrap" arrangement is believed to be a practical way of starting the engines but, of course, must be experimentally demonstrated.

External heated air supplies could, of course, be used for preheating the combustion tubes, but such an arrangement involves rather bulky and heavy equipment which may not be easily available at various places the helicopter may desire to land.

The amount of power available from the fuel during cruise operation (rotor tip speed - 600 ft/sec) is considerable. With a radius of the rotor tip equal to 20.5 feet, the developed pressure is 3500 psia and if a pressure drop of 3000 psia is taken through the fuel motor, then 0.705 horsepower is available for turning the rotary valves (100% efficiency). Hydraulic motor efficiencies may be 60% so that about 0.42 horsepower is available. Calculation of the required rotary valve horsepower is, however, only a small fraction of one horsepower (see section 2) so that under normal cruise conditions most of the fuel will bypass the fuel motor.

Of interest in the starting sequence is the power requirement to accelerate the blades to full speed. Assuming 150 pounds per blade uniformly distributed along the blade as a first approximation, a moment of inertia of 650 slug $ft^2$ is obtained which for a 41 foot diameter blade gives the required torque to accelerate as follows:

$$T = \frac{19050}{t} \text{ ft pounds}$$

T = torque

t = time (seconds)

The required thrust of each engine is

$$F = \frac{19050}{t \cdot r} = \frac{929}{t} \text{ pounds}$$

Or if $t$ = 30 seconds

F = 31 pounds or a total of 93 pounds from three engines

| PREPARED BY | AEROPHYSICS DEVELOPMENT CORPORATION | REPORT NO 2000-1-11 |
|---|---|---|
| CHECKED BY | PACIFIC PALISADES, CALIFORNIA | DATE Jan 24 1953 |

The total static thrust expected under normal operating conditions from three engines (one in each of three blades) is 270 pounds. Consequently, an ample safety factor should exist in accelerating the blades to normal rpm.

Pg 229
MISSING

Disregard
Last Page

Pg 228

MISSING

# TABLE 1

| 1 | 2 | 3 | 4 | 5 | 6 | 7 | 8 |
|---|---|---|---|---|---|---|---|
| $P_3/P_0$ | $P_0/P'$ | $P'/P_3$ | $\tau_E' \frac{A_N a}{Vol.}$ | $\frac{Mr}{\rho_3 a_3 A_N g}$ | $V_N/a_3$ | $\frac{F}{a_3^2 \rho_3 A_N g}$ | $I/a_3 \rho_3 Vol.$ |
| 1.82 | 0.548 | 1.000 | 0 | 0.586 | 0.937 | 0.0170 | 0.0066 |
| | 0.600 | 0.915 | 0.119 | 0.537 | 0.860 | 0.0144 | |
| | 0.700 | 0.785 | 0.336 | 0.446 | 0.714 | 0.0099 | |
| | 0.800 | 0.687 | 0.539 | 0.350 | 0.539 | 0.00586 | |
| | 0.900 | 0.610 | 0.768 | 0.239 | 0.381 | 0.00282 | |
| | 1.000 | 0.549 | 1.239 | 0 | 0 | 0 | |
| 3.00 | 0.333 | 1.000 | 0 | 0.586 | 0.937 | 0.0222 | 0.0128 |
| | 0.548 | 0.608 | 0.682 | 0.358 | 0.890 | 0.0103 | |
| | 0.600 | 0.555 | 0.812 | 0.345 | 0.816 | 0.00874 | |
| | 0.700 | 0.476 | 1.041 | 0.286 | 0.680 | 0.00603 | |
| | 0.800 | 0.417 | 1.258 | 0.225 | 0.536 | 0.00375 | |
| | 0.900 | 0.371 | 1.492 | 0.153 | 0.364 | 0.00173 | |
| | 1.000 | 0.333 | 1.998 | 0 | 0 | 0 | |
| 5.00 | 0.200 | 1.000 | 0 | 0.586 | 0.937 | 0.0254 | 0.0209 |
| | 0.333 | 0.600 | 0.682 | 0.358 | 0.890 | 0.0131 | |
| | 0.548 | 0.365 | 1.423 | 0.227 | 0.836 | 0.00590 | |
| | 0.600 | 0.333 | 1.562 | 0.220 | 0.765 | 0.00521 | |
| | 0.700 | 0.286 | 1.797 | 0.183 | 0.633 | 0.00358 | |
| | 0.800 | 0.250 | 2.031 | 0.143 | 0.496 | 0.00219 | |
| | 0.900 | 0.222 | 2.275 | 0.097 | 0.335 | 0.00100 | |
| | 1.000 | 0.200 | 2.835 | 0 | 0 | 0 | |
| 10.00 | 0.100 | 1.000 | 0 | 0.586 | 0.937 | 0.0278 | 0.0301 |
| | 0.200 | 0.500 | 0.682 | 0.358 | 0.890 | 0.0126 | |
| | 0.333 | 0.300 | 1.423 | 0.227 | 0.836 | 0.00635 | |
| | 0.548 | 0.183 | 2.500 | 0.1223 | 0.776 | 0.00294 | |
| | 0.600 | 0.167 | 2.636 | 0.1188 | 0.712 | 0.00262 | |
| | 0.700 | 0.143 | 2.904 | 0.0981 | 0.584 | 0.00178 | |
| | 0.800 | 0.125 | 3.156 | 0.0767 | 0.460 | 0.00110 | |
| | 0.900 | 0.111 | 3.421 | 0.0525 | 0.314 | 0.00051 | |
| | 1.000 | 0.100 | 3.958 | 0 | 0 | 0 | |
| 15.00 | 0.067 | 1.000 | 0 | 0.586 | 0.937 | 0.0287 | 0.0336 |
| | 0.100 | 0.670 | 0.682 | 0.358 | 0.890 | 0.0183 | |
| | 0.200 | 0.335 | 1.423 | 0.227 | 0.836 | 0.00912 | |
| | 0.333 | 0.202 | 2.50 | 0.122 | 0.776 | 0.00375 | |
| | 0.548 | 0.122 | 3.17 | 0.0850 | 0.741 | 0.00196 | |
| | 0.600 | 0.111 | 3.33 | 0.0821 | 0.684 | 0.00174 | |
| | 0.700 | 0.0952 | 3.60 | 0.0687 | 0.569 | 0.00121 | |
| | 0.800 | 0.0832 | 3.86 | 0.0537 | 0.444 | 0.00074 | |
| | 0.900 | 0.0741 | 4.15 | 0.0362 | 0.296 | 0.00033 | |
| | 1.000 | 0.0667 | 4.69 | 0 | 0 | 0 | |

TABLE I (CONT'D)

| 1 | 2 | 3 | 4 | 5 | 6 | 7 | 8 |
|---|---|---|---|---|---|---|---|
| $R_g/P_o$ | $R_g/P'$ | $P'/R_g$ | $\tau = \frac{A_N a_g}{Vol.}$ | $\frac{w}{R_g a_g A_{Ng}}$ | $V_N/a_g$ | $\frac{F}{a_g^2 R_g A_{Ng}}$ | $I/a_g R_g Vol$ |
| 20.00 | 0.050 | 1.000 | .0 | 0.586 | 0.937 | 0.02910 | 0.0355 |
| | 0.067 | 0.747 | 0.68 | 0.358 | 0.890 | 0.02100 | |
| | 0.100 | 0.500 | 1.42 | 0.227 | 0.836 | 0.01385 | |
| | 0.200 | 0.250 | 2.50 | 0.122 | 0.776 | 0.00625 | |
| | 0.333 | 0.150 | 3.17 | 0.0850 | 0.741 | 0.00315 | |
| | 0.548 | 0.0913 | 3.66 | 0.0661 | 0.725 | 0.00149 | |
| | 0.600 | 0.0833 | 3.81 | 0.0637 | 0.660 | 0.00131 | |
| | 0.700 | 0.0715 | 4.10 | 0.0527 | 0.547 | 0.00089 | |
| | 0.800 | 0.0625 | 4.36 | 0.0416 | 0.427 | 0.00055 | |
| | 0.900 | 0.0556 | 4.66 | 0.0283 | 0.284 | 0.00025 | |
| | 1.000 | 0.0500 | 5.29 | 0 | 0 | 0 | |
| 25.00 | 0.040 | 1.000 | 0 | 0.586 | 0.937 | 0.0293 | 0.0369 |
| | 0.050 | 0.800 | 0.68 | 0.358 | 0.890 | 0.0161 | |
| | 0.067 | 0.597 | 1.42 | 0.227 | 0.836 | 0.00728 | |
| | 0.100 | 0.400 | 2.50 | 0.122 | 0.776 | 0.00440 | |
| | 0.200 | 0.200 | 3.17 | 0.0850 | 0.741 | 0.00260 | |
| | 0.333 | 0.120 | 3.66 | 0.0661 | 0.725 | 0.00175 | |
| | 0.548 | 0.0730 | 4.06 | 0.0542 | 0.703 | 0.00117 | |
| | 0.600 | 0.0667 | 4.20 | 0.0524 | 0.639 | 0.00104 | |
| | 0.700 | 0.0572 | 4.52 | 0.0426 | 0.534 | 0.00071 | |
| | 0.800 | 0.0500 | 4.79 | 0.0340 | 0.415 | 0.00044 | |
| | 0.900 | 0.0444 | 5.09 | 0.0233 | 0.280 | 0.00020 | |
| | 1.000 | 0.0400 | 5.72 | 0 | 0 | 0 | |

# TABLE 2
## IDEAL NET IMPULSE

| 1 | 2 | 3 | 4 | 5 | 6 | 7 | 8 | 9 |
|---|---|---|---|---|---|---|---|---|
| $P_3/P_0$ | $M_1$ | $T_2/T_0$ | $P_2/P_0$ | $P_3/P_2 = T_3/T_2$ | $T_3/T_0$ | $\frac{I_D}{a_0 \rho_0 \text{ Vol}}$ | $\frac{I_{GROSS}}{a_0 \rho_0 \text{ Vol}}$ | $\frac{I_{NET}}{a_0 \rho_0 \text{ Vol}}$ |
| 1.32 | 0.20 | 1.080 | 1.316 | 1.38 | 1.49 | 0.00757 | 0.00936 | 0.00229 |
| | 0.40 | 1.173 | 1.710 | 1.07 | 1.258 | 0.0181 | 0.0114 | - - |
| | 0.60 | 1.27 | 2.19 | - - | - - | 0.0322 | 0.0117 | - - |
| | 0.80 | 1.38 | 2.78 | - - | - - | 0.0500 | 0.0127 | - - |
| 3.00 | 0.20 | 1.080 | 1.316 | 2.273 | 2.46 | 0.00757 | 0.0244 | 0.0169 |
| | 0.40 | 1.173 | 1.710 | 1.754 | 2.06 | 0.0181 | 0.0267 | 0.0086 |
| | 0.60 | 1.27 | 2.19 | 1.369 | 1.733 | 0.0322 | 0.0291 | - - |
| | 0.80 | 1.38 | 2.78 | 1.182 | 1.63 | 0.0500 | 0.0328 | - - |
| 5.00 | 0.20 | 1.080 | 1.316 | 3.795 | 4.10 | 0.00757 | 0.0520 | 0.0444 |
| | 0.40 | 1.173 | 1.710 | 2.925 | 3.44 | 0.0181 | 0.0569 | 0.0388 |
| | 0.60 | 1.27 | 2.19 | 2.280 | 2.895 | 0.0322 | 0.0619 | 0.0297 |
| | 0.80 | 1.38 | 2.78 | 1.805 | 2.49 | 0.0500 | 0.0670 | 0.0170 |
| 10.00 | 0.20 | 1.080 | 1.316 | 7.595 | 8.20 | 0.00757 | 0.1054 | 0.0978 |
| | 0.40 | 1.173 | 1.710 | 5.850 | 6.87 | 0.0181 | 0.1151 | 0.0970 |
| | 0.60 | 1.27 | 2.19 | 4.563 | 5.79 | 0.0322 | 0.1254 | 0.0932 |
| | 0.80 | 1.38 | 2.78 | 3.618 | 4.99 | 0.0500 | 0.1351 | 0.0856 |

PREPARED BY

CHECKED BY

AEROPHYSICS DEVELOPMENT CORPORATION
PACIFIC PALISADES, CALIFORNIA

REPORT NO 2000-1-R1

DATE Jan 24, 1953

SECURITY INFORMATION
RESTRICTED

# TABLE 2 (CONT'D)

| 1 | 2 | 3 | 4 | 5 | 6 | 7 | 8 | 9 |
|---|---|---|---|---|---|---|---|---|
| $P_3/P_0$ | $M_1$ | $T_2/T_0$ | $P_2/P_0$ | $P_3/P_2 = T_3/T_2$ | $T_3/T_0$ | $\frac{I_D}{a_0 g P_0 Vol}$ | $\frac{I_{GROSS}}{a_0 g P_0 Vol}$ | $\frac{I_{NET}}{a_0 g P_0 Vol}$ |
| 15.00 | 0.20 | 1.080 | 1.316 | 11.39 | 12.30 | 0.00757 | 0.1437 | 0.1361 |
| | 0.40 | 1.173 | 1.710 | 8.775 | 10.30 | 0.0131 | 0.1574 | 0.1393 |
| | 0.60 | 1.27 | 2.19 | 6.345 | 8.09 | 0.0322 | 0.1711 | 0.1389 |
| | 0.80 | 1.38 | 2.78 | 5.425 | 7.43 | 0.0500 | 0.1853 | 0.1352 |
| 20.00 | 0.20 | 1.080 | 1.316 | 15.19 | 16.40 | 0.00757 | 0.1751 | 0.1681 |
| | 0.40 | 1.173 | 1.710 | 11.70 | 13.73 | 0.0131 | 0.1921 | 0.1740 |
| | 0.60 | 1.27 | 2.19 | 9.13 | 11.60 | 0.0322 | 0.2095 | 0.1773 |
| | 0.80 | 1.38 | 2.78 | 7.33 | 9.98 | 0.0500 | 0.2263 | 0.1762 |
| 25.00 | 0.20 | 1.080 | 1.316 | 18.9[illegible] | 20.50 | 0.00757 | 0.204 | 0.1964 |
| | 0.40 | 1.173 | 1.710 | 14.6[illegible] | 17.20 | 0.0131 | 0.223 | 0.2049 |
| | 0.60 | 1.27 | 2.19 | 11.41 | 14.50 | 0.0322 | 0.243 | 0.2107 |
| | 0.80 | 1.38 | 2.78 | 9.[illegible]5 | 12.49 | 0.0500 | 0.263 | 0.2127 |

# TABLE 3

| 1 | 3 | 4 | 2 | 5 | 6 | 7 | 8 | 9 | 10 | 11 | 12 | 13 | 14 |
|---|---|---|---|---|---|---|---|---|---|---|---|---|---|
| $M$ | $T/T_o$ | $T$ °R | $\frac{T}{T}$ | $T/T_o$ | $P/P_o$ | $P/P_o$ | $I/W_a a_o$ | $W_f/W_a$ | $f/\sqrt{\theta}$ | $\tau/L$ | $\frac{F_o}{A_N \delta}$ | $W_A/V_{ac.}$ lbs./cycle | $S_t/\sqrt{\theta}$ |
| 0.20 | 1.080 | 560.3 | 2 | 2.16 | 1.316 | 2.63 | 0.00944 | 0.00600 | 2.088 | 0.00764 | 129 | 0.0932 | 10.4 |
| | | | 3 | 3.24 | | 3.95 | 0.0250 | 0.0125 | 1.637 | | 352 | | 27.8 |
| | | | 4 | 4.32 | | 5.26 | 0.0390 | 0.0196 | 1.596 | | 531 | | 44.1 |
| | | | 6 | 6.48 | | 7.90 | 0.0636 | 0.0348 | 1.752 | | 866 | | 71.4 |
| | | | 8 | 8.64 | | 10.52 | 0.0836 | 0.0537 | 2.057 | | 1138 | | 93.9 |
| | | | 10 | 10.80 | | 13.16 | 0.1009 | 0.0884 | 2.818 | | 1370 | | 113.0 |
| 0.40 | 1.173 | 608.5 | 2 | 2.35 | 1.710 | 3.42 | 0.0103 | 0.00661 | 2.042 | 0.00545 | 235 | 0.1116 | 11.6 |
| | | | 3 | 3.52 | | 5.13 | 0.0277 | 0.0138 | 1.590 | | 632 | | 31.2 |
| | | | 4 | 4.70 | | 6.84 | 0.0435 | 0.0216 | 1.587 | | 984 | | 49.0 |
| | | | 6 | 7.05 | | 10.26 | 0.0682 | 0.0384 | 1.810 | | 1550 | | 76.3 |
| | | | 8 | 9.40 | | 13.68 | 0.0880 | 0.0627 | 2.279 | | 2010 | | 98.9 |
| 0.60 | 1.27 | 659.0 | 2 | 2.54 | 2.193 | 4.38 | 0.0113 | 0.00726 | 2.010 | 0.00477 | 350 | 0.1322 | 12.99 |
| | | | 3 | 3.81 | | 6.58 | 0.0295 | 0.0152 | 1.605 | | 912 | | 34.1 |
| | | | 4 | 5.08 | | 8.77 | 0.0463 | 0.0238 | 1.652 | | 1431 | | 51.8 |
| | | | 6 | 7.62 | | 13.16 | 0.0715 | 0.0422 | 1.895 | | 2210 | | 80.1 |
| | | | 8 | 10.16 | | 17.53 | 0.0915 | 0.0742 | 2.610 | | 2830 | | 102.2 |
| 0.80 | 1.38 | 716.0 | 2 | 2.76 | 2.778 | 5.55 | 0.0127 | 0.00803 | 2.040 | 0.00446 | 488 | 0.1540 | 14.1 |
| | | | 3 | 4.14 | | 8.33 | 0.0315 | 0.0169 | 1.678 | | 1212 | | 36.2 |
| | | | 4 | 5.52 | | 11.10 | 0.0484 | 0.0264 | 1.760 | | 1862 | | 53.8 |
| | | | 6 | 8.27 | | 16.66 | 0.0740 | 0.0475 | 2.069 | | 2850 | | 82.6 |
| | | | 8 | 11.05 | | 22.2 | 0.0954 | — | — | | 3680 | | 106.8 |

| | | |
|---|---|---|
| | AEROPHYSICS DEVELOPMENT CORPORATION | 2000-1-71 |
| | PACIFIC PALISADES, CALIFORNIA | DATE Jan 4, 1953 |

# TABLE 4

## MAXIMUM CLOSING TIME FOR THE EXHAUST VALVE

| $M_1$ | $\tau_v$ |
|---|---|
| 0.2 | 0.00026 |
| 0.4 | 0.00066 |
| 0.6 | 0.00145 |
| 0.8 | 0.00572 |

PREPARED BY

CHECKED BY

**AEROPHYSICS DEVELOPMENT CORPORATION**
**PACIFIC PALISADES, CALIFORNIA**

REPORT NO 2000-1-R1

DATE JAN 24 1953

ACTUAL PERFORMANCE OF A SINGLE TUBE ENGINE — TABLE 5

| COLUMN | 1 | 2 | 3 | 4 | 5 | 6 | 7 | 8 |
|---|---|---|---|---|---|---|---|---|
| FUNCTION | $M_0$ | $M_d = M_1$ | L. | $T_3$ °R | $P_{0c}/P_0$ | $P_{2c}/P_0$ | $P_1/P_0$ | $P_1''/P_0$ FOR D= ½ |
| | 0.25 | 0.40 | 3 | 1960 | 1.045 | 1.030 | .924 | 0.918 |
| | | | 3 | 2960 | | | | 0.918 |
| | | | 10 | 1960 | | | | 0.913 |
| | | | 10 | 2960 | | | | 0.913 |
| | | | 20 | 1960 | | | | 0.904 |
| | | | 20 | 2960 | | | | 0.904 |
| | | | 30 | 1960 | | | | 0.867 |
| | | | 30 | 2960 | | | | 0.867 |
| | | 0.60 | 3 | 1960 | | | .806 | 0.794 |
| | | | 3 | 2960 | | | | 0.794 |
| | | | 10 | 1960 | | | | 0.766 |
| | | | 10 | 2960 | | | | 0.766 |
| | | | 20 | 1960 | | | | 0.732 |
| | | | 20 | 2960 | | | | 0.732 |
| | | | 30 | 1960 | | | | 0.701 |
| | | | 30 | 2960 | | | | 0.701 |
| | 0.50 | 0.40 | 3 | 1960 | 1.186 | 1.171 | 1.050 | 1.043 |
| | | | 3 | 2960 | | | | 1.043 |
| | | | 10 | 1960 | | | | 1.038 |
| | | | 10 | 2960 | | | | 1.038 |
| | | | 20 | 1960 | | | | 1.027 |
| | | | 20 | 2960 | | | | 1.027 |
| | | | 30 | 1960 | | | | .985 |
| | | | 30 | 2960 | | | | .985 |
| | | 0.60 | 3 | 1960 | | | 0.919 | .905 |
| | | | 3 | 2960 | | | | .905 |
| | | | 10 | 1960 | | | | .874 |
| | | | 10 | 2960 | | | | .874 |
| | | | 20 | 1960 | | | | .835 |
| | | | 20 | 2960 | | | | .835 |
| | | | 30 | 1960 | | | | .798 |
| | | | 30 | 2960 | | | | .798 |
| | 0.75 | 0.40 | 3 | 1960 | 1.45 | 1.435 | 1.285 | 1.277 |
| | | | 3 | 2960 | | | | 1.277 |
| | | | 10 | 1960 | | | | 1.27 |
| | | | 10 | 2960 | | | | 1.27 |
| | | | 20 | 1960 | | | | 1.257 |
| | | | 20 | 2960 | | | | 1.257 |
| | | | 30 | 1960 | | | | 1.205 |
| | | | 30 | 2960 | | | | 1.205 |
| | | 0.60 | 3 | 1960 | | | 1.125 | 1.109 |
| | | | 3 | 2960 | | | | 1.109 |
| | | | 10 | 1960 | | | | 1.07 |
| | | | 10 | 2960 | | | | 1.07 |
| | | | 20 | 1960 | | | | 1.022 |
| | | | 20 | 2960 | | | | 1.022 |
| | | | 30 | 1960 | | | | 0.977 |
| | | | 30 | 2960 | | | | 0.977 |

AEROPHYSICS DEVELOPMENT CORPORATION
PACIFIC PALISADES, CALIFORNIA

2000-1-R1
Jan 2, 1953

TABLE 5 (CONT'D)

| 9 | 10 | 11 | 12 | 13 | 14 | 15 | 16 | 17 |
|---|---|---|---|---|---|---|---|---|
| $P_E/P_0$ | $\frac{P''}{P_0}$ FOR $\delta=\frac{1}{2}$ | $T_L$ °R | $T_1$ °R | $T_2$ °R | $T_3/T_2$ | $P_3/P_0$ | $\tau_{E/L}$ SECS/FT | $\frac{\tau_C}{L}$ SECS/FT |
| 1.[illegible] | 1.57 | [illegible] | 510 | [illegible] | 3.28 | 5.18 | .00266 | .00104 |
| | 1.57 | | | | 4.95 | 7.82 | .00265 | |
| | 1.56 | | | | 3.28 | 5.18 | .00265 | |
| | 1.[illegible] | | | | 4.95 | 7.82 | .00265 | |
| | 1.543 | | | | 3.28 | 5.18 | .00260 | |
| | 1.540 | | | | 4.95 | 7.82 | .00262 | |
| | 1.[illegible] | | | | 3.28 | 5.18 | .00255 | |
| | 1.[illegible] | | | | 4.95 | 7.82 | .00269 | |
| 1.790 | 1.74 | | 491 | 624 | 3.14 | 5.32 | .00275 | .00112 |
| | 1.74 | | | | 4.75 | 8.50 | .00272 | |
| | 1.[illegible] | | | | 3.14 | 5.32 | .00270 | |
| | 1.[illegible] | | | | 4.75 | 8.50 | .00269 | |
| | 1.[illegible] | | | | 3.14 | 5.32 | .00260 | |
| | 1.[illegible] | | | | 4.75 | 8.50 | .00262 | |
| | 1.[illegible] | | | | 3.14 | 5.32 | .00251 | |
| | 1.[illegible] | | | | 4.75 | 8.50 | .00256 | |
| 1.7[illegible] | 1.7[illegible] | [illegible] | [illegible] | [illegible] | 3.165 | 5.38 | .00[illegible] | .00102 |
| | 1.7[illegible] | | | | 4.78 | 8.53 | .00276 | |
| | 1.7[illegible] | | | | 3.165 | 5.38 | .00277 | |
| | 1.7[illegible] | | | | 4.78 | 8.53 | .00275 | |
| | 1.7[illegible] | | | | 3.165 | 5.38 | .00261 | |
| | 1.7[illegible] | | | | 4.78 | 8.53 | .00[illegible] | |
| | 1.[illegible] | | | | 3.165 | 5.38 | .00277 | |
| | 1.[illegible] | | | | 4.78 | 8.53 | .00278 | |
| .801 | 1.[illegible] | | [illegible] | 647 | 3.03 | 5.09 | .00289 | .00111 |
| | 1.[illegible] | | | | 4.57 | 9.20 | .00284 | |
| | 1.815 | | | | 3.03 | 5.09 | .00283 | |
| | 1.815 | | | | 4.57 | 9.20 | .00280 | |
| | 1.825 | | | | 3.03 | 5.09 | .00263 | |
| | 1.825 | | | | 4.57 | 9.20 | .00266 | |
| | 1.748 | | | | 3.03 | 5.09 | .00270 | |
| | 1.742 | | | | 4.57 | 9.20 | .00260 | |
| 2.20 | 2.18 | 577 | 553 | 650 | 2.99 | 6.58 | .00300 | .00099 |
| | 2.18 | | | | 4.52 | 9.94 | .00295 | |
| | 2.17 | | | | 2.99 | 6.58 | .00298 | |
| | 2.17 | | | | 4.52 | 9.94 | .00294 | |
| | 2.150 | | | | 2.99 | 6.58 | .00295 | |
| | 2.150 | | | | 4.52 | 9.94 | .00289 | |
| | 2.01 | | | | 2.99 | 6.58 | .00292 | |
| | 2.00 | | | | 4.52 | 9.94 | .00283 | |
| 2.40 | 2.[illegible] | | 588 | 685 | 2.37 | 7.06 | .00310 | .00107 |
| | 2.[illegible] | | | | 4.33 | 10.70 | .00304 | |
| | 2.34 | | | | 2.37 | 7.06 | .00305 | |
| | 2.34 | | | | 4.33 | 10.70 | .00300 | |
| | 2.337 | | | | 2.37 | 7.06 | .00298 | |
| | 2.337 | | | | 4.33 | 10.70 | .00294 | |
| | 2.14 | | | | 2.37 | 7.06 | .00291 | |
| | 2.14 | | | | 4.33 | 10.70 | .00287 | |

| PREPARED BY | AEROPHYSICS DEVELOPMENT CORPORATION | REPORT NO 2000-1-R1 |
|---|---|---|
| CHECKED BY | PACIFIC PALISADES, CALIFORNIA | DATE Jan 24 1953 |

# TABLE 5 (CONT'D)

| 18 | 19 | 20 | 21 | 22 |
|---|---|---|---|---|
| $\tau_3$ SECS / FT | $\tau_2$ SECS / FT | $\tau_{TOT}$ SECS / FT | $\tau_{TOT}$ SECS | CORRECTION FACTOR |
| .00226 | .00380 | .00976 | .0293 | .951 |
| | .00380 | .00975 | .0292 | .951 |
| | .00100 | .00695 | .0695 | .984 |
| | .00100 | .00695 | .0695 | .984 |
| | .00050 | .00640 | .1280 | .992 |
| | .00050 | .00642 | .1284 | .992 |
| | .00033 | .00618 | .185 | .995 |
| | .00033 | .00622 | .187 | .995 |
| .00153 | .00380 | | .0273 | .817 |
| | .00380 | .00917 | .0275 | .817 |
| | .00100 | .00635 | .0635 | .945 |
| | .00100 | .00634 | .0634 | .945 |
| | .00050 | .00575 | .1150 | .9726 |
| | .00050 | .00577 | .1154 | .9726 |
| | .00033 | .00549 | .164 | .9817 |
| | .00033 | .00554 | .166 | .9817 |
| .00222 | .00380 | .00982 | .02941 | .946 |
| | .00380 | .00980 | .0294 | .946 |
| | .00100 | .00701 | .0701 | .9837 |
| | .00100 | .00699 | .0699 | .9837 |
| | .00050 | .00635 | .1302 | .9919 |
| | .00050 | .00637 | .1286 | .9919 |
| | .00033 | .00634 | .190 | .9946 |
| | .00033 | .00635 | .190 | .9946 |
| .00151 | .00380 | .00931 | .0279 | .816 |
| | .00380 | .00926 | .0278 | .816 |
| | .00100 | .00645 | .0645 | .9445 |
| | .00100 | .00642 | .0642 | .9445 |
| | .00050 | .00575 | .1156 | .9734 |
| | .00050 | .00578 | .1162 | .9734 |
| | .00033 | .00565 | .169 | .9816 |
| | .00033 | .00555 | .166 | .9816 |
| .00216 | .00380 | .00995 | .0298 | .944 |
| | .00380 | .00990 | .0297 | .944 |
| | .00100 | .00713 | .0713 | .9833 |
| | .00100 | .00709 | .0709 | .9833 |
| | .00050 | .00660 | .1320 | .9916 |
| | .00050 | .00654 | .1308 | .9916 |
| | .00033 | .00640 | .192 | .9944 |
| | .00033 | | .196 | .9944 |
| .00146 | .00380 | .00943 | .0283 | .839 |
| | .00380 | .00937 | .0281 | .839 |
| | .00100 | .00558 | .0658 | .9535 |
| | .00100 | .00653 | .0653 | .9535 |
| | .00050 | .00601 | .1202 | .9759 |
| | .00050 | .00597 | .1194 | .9759 |
| | .00033 | .00577 | .173 | .9839 |
| | .00033 | .00573 | .172 | .9839 |

| PREPARED BY: | AEROPHYSICS DEVELOPMENT CORPORATION | REPORT NO 2000-1-A1 |
|---|---|---|
| CHECKED BY | PACIFIC PALISADES, CALIFORNIA | DATE Jan 24, 1953 |

TABLE 5 (CONT'D FOR DIAM OF TUBE = 1 FT.)

| 1 | 2 | 3 | 4 | 23 | 24 | 25 | 26 | 27 |
|---|---|---|---|---|---|---|---|---|
| $M_o$ | $M_d = M_1$ | L | $T_3$ °R | $P_3''/P_o$ | $P_{3AVG}$ | $\delta P_{AVG}$ | VOL | $W_a$ CYCLE |
| 0.25 | 0.40 | 3 | 1960 | 5.143 | 5.162 | .1044 | 2.363 | .2468 |
| | | 3 | 2960 | 7.76 | 7.790 | .1044 | 2.363 | .2468 |
| | | 10 | 1960 | 5.07 | 5.125 | .1036 | 7.94 | .823 |
| | | 10 | 2960 | 7.65 | 7.735 | .1036 | 7.94 | .823 |
| | | 20 | 1960 | 4.96 | 5.07 | .1025 | 16.06 | 1.645 |
| | | 20 | 2960 | 7.48 | 7.65 | .1025 | 16.06 | 1.645 |
| | | 30 | 1960 | 4.855 | 5.018 | .1015 | 24.36 | 2.470 |
| | | 30 | 2960 | 7.327 | 7.574 | .1015 | 24.36 | 2.470 |
| | 0.50 | 3 | 1960 | 5.535 | 5.578 | .1128 | 2.374 | .2682 |
| | | 3 | 2960 | 8.38 | 8.44 | .1128 | 2.374 | .2682 |
| | | 10 | 1960 | 5.350 | 5.485 | .1109 | 8.05 | .893 |
| | | 10 | 2960 | 8.095 | 8.298 | .1109 | 8.05 | .893 |
| | | 20 | 1960 | 5.103 | 5.362 | .1084 | 16.50 | 1.789 |
| | | 20 | 2960 | 7.72 | 8.11 | .1084 | 16.50 | 1.789 |
| | | 30 | 1960 | 4.86 | 5.24 | .1059 | 25.37 | 2.690 |
| | | 30 | 2960 | 7.345 | 7.923 | .1059 | 25.37 | 2.690 |
| 0.50 | 0.40 | 3 | 1960 | 5.64 | 5.66 | .1144 | 2.363 | .2708 |
| | | 3 | 2960 | 8.52 | 8.55 | .1144 | 2.363 | .2708 |
| | | 10 | 1960 | 5.55 | 5.615 | .1134 | 7.94 | .9025 |
| | | 10 | 2960 | 8.40 | 8.49 | .1134 | 7.94 | .9025 |
| | | 20 | 1960 | 5.433 | 5.557 | .11225 | 16.06 | 1.805 |
| | | 20 | 2960 | 8.22 | 8.40 | .11225 | 16.06 | 1.805 |
| | | 30 | 1960 | 5.32 | 5.50 | .1111 | 24.36 | 2.708 |
| | | 30 | 2960 | 8.04 | 8.31 | .1111 | 24.36 | 2.708 |
| | 0.60 | 3 | 1960 | 6.00 | 6.045 | .1222 | 2.374 | .2907 |
| | | 3 | 2960 | 9.06 | 9.13 | .1222 | 2.374 | .2907 |
| | | 10 | 1960 | 5.80 | 5.945 | .1201 | 8.05 | .9675 |
| | | 10 | 2960 | 8.76 | 8.98 | .1201 | 8.05 | .9675 |
| | | 20 | 1960 | 5.53 | 5.81 | .1174 | 16.50 | 1.937 |
| | | 20 | 2960 | 8.36 | 8.78 | .1174 | 16.50 | 1.937 |
| | | 30 | 1960 | 5.26 | 5.675 | .1147 | 25.37 | .169 |
| | | 30 | 2960 | 7.95 | 8.575 | .1147 | 25.37 | .169 |
| 0.75 | 0.40 | 3 | 1960 | 6.54 | 6.56 | .1325 | 2.363 | .3137 |
| | | 3 | 2960 | 9.86 | 9.90 | .1325 | 2.363 | .3137 |
| | | 10 | 1960 | 6.44 | 6.51 | .1315 | 7.94 | 1.046 |
| | | 10 | 2960 | 9.72 | 9.83 | .1315 | 7.94 | 1.046 |
| | | 20 | 1960 | 6.30 | 6.44 | .1301 | 16.06 | 2.090 |
| | | 20 | 2960 | 9.507 | 9.724 | .1301 | 16.06 | 2.090 |
| | | 30 | 1960 | 6.17 | 6.375 | .1288 | 24.36 | 3.136 |
| | | 30 | 2960 | 9.31 | 9.625 | .1288 | 24.36 | 3.136 |
| | 0.60 | 3 | 1960 | 6.955 | 7.008 | .1416 | 2.374 | .3372 |
| | | 3 | 2960 | 10.54 | 10.62 | .1416 | 2.374 | .3372 |
| | | 10 | 1960 | 6.725 | 6.893 | .1392 | 8.05 | 1.124 |
| | | 10 | 2960 | 10.19 | 10.445 | .1392 | 8.05 | 1.124 |
| | | 20 | 1960 | 6.41 | 6.735 | .1360 | 16.50 | 2.25 |
| | | 20 | 2960 | 9.72 | 10.21 | .1360 | 16.50 | 2.25 |
| | | 30 | 1960 | 6.10 | 6.580 | .1330 | 25.37 | 3.38 |
| | | 30 | 2960 | 9.25 | 9.975 | .1330 | 25.37 | 3.38 |

| PREPARED BY | AEROPHYSICS DEVELOPMENT CORPORATION | REPORT NO 2000-1-A1 |
|---|---|---|
| CHECKED BY | PACIFIC PALISADES, CALIFORNIA | DATE Jan 24,1953 |

TABLE 5 CONT'D FOR TUBE DIAM D = 1 FT.

| 28 $\frac{w_a}{\delta}$ | 29 $u_e/a_3$ | 30 $\frac{E}{w_a\sqrt{\theta}}$ | 31 $\frac{F}{A_T}$ | 32 $w_2/w_a$ | 33 $f/\sqrt{\theta}$ | 34 $C_T$ | 35 $\chi$ |
|---|---|---|---|---|---|---|---|
| 8.42 | .702 | 36.52 | 372.2 | .0140 | 1.461 | 4.02 | 9.83 |
| 8.455 | .888 | 61.6 | 629. | .0288 | 1.681 | 6.795 | 9.84 |
| 11.85 | .695 | 36.07 | 555. | | 1.480 | 5.78 | 14.31 |
| 11.85 | .883 | 61.2 | 907.5 | | 1.693 | 9.81 | 14.30 |
| 12.86 | .683 | 35.28 | 572.5 | | 1.514 | 6.135 | 15.64 |
| 12.86 | .875 | 60.6 | 983. | | 1.709 | 10.62 | 15.64 |
| 13.35 | .672 | 34.60 | 584.5 | | 1.543 | 6.315 | 16.25 |
| 13.20 | .866 | 59.83 | 1000. | | 1.731 | 10.80 | 16.11 |
| 9.82 | .742 | 39.10 | 400. | .0147 | 1.353 | 4.322 | 9.86 |
| 9.76 | .918 | 63.95 | 654.5 | .0286 | 1.610 | 7.07 | 9.87 |
| 14.06 | .723 | 37.88 | 641.5 | | 1.397 | 6.93 | 16.30 |
| 14.08 | .906 | 63.0 | 1067. | | 1.634 | 11.53 | 16.32 |
| 15.58 | .698 | 36.28 | 699.5 | | 1.459 | 7.56 | 18.56 |
| 15.50 | .887 | 61.4 | 1178. | | 1.675 | 12.73 | 18.50 |
| 16.38 | .673 | 34.62 | 710. | | 1.528 | 7.67 | 19.75 |
| 16.19 | .867 | 59.87 | 1213. | | 1.719 | 13.10 | 19.53 |
| 9.21 | .750 | 30.92 | 343. | .0148 | 1.725 | .926 | 9.58 |
| 9.21 | .925 | 55.8 | 618.5 | .0287 | 1.650 | 1.670 | 9.58 |
| 12.88 | .742 | 30.40 | 490.2 | | 1.755 | 1.324 | 13.92 |
| 12.91 | .919 | 55.3 | 894. | | 1.865 | 2.413 | 13.96 |
| 13.875 | .730 | 29.65 | 519. | | 1.799 | 1.401 | 15.10 |
| 14.04 | .911 | 54.7 | 969. | | 1.887 | 2.616 | 15.30 |
| 14.25 | .720 | 29.02 | 524. | | 1.857 | 1.414 | 15.50 |
| 14.25 | .903 | 54.05 | 974.5 | | 1.909 | 2.630 | 15.56 |
| 10.42 | .779 | 32.82 | 355.3 | .0146 | 1.602 | .959 | 9.35 |
| 10.45 | .946 | 57.45 | 623.5 | .0284 | 1.778 | 1.683 | 9.38 |
| 15.00 | .763 | 31.8 | 578.5 | | 1.654 | 1.562 | 15.72 |
| 15.08 | .934 | 56.55 | 1034. | | 1.805 | 2.790 | 15.79 |
| 16.75 | .740 | 30.30 | 629.5 | | 1.735 | 1.700 | 17.93 |
| 16.67 | .918 | 55.3 | 1142. | | 1.347 | 3.082 | 17.74 |
| 17.23 | .713 | 28.58 | 615. | | 1.840 | 1.660 | 18.58 |
| 17.54 | .899 | 53.75 | 1177. | | 1.900 | 3.177 | 17.90 |
| 10.53 | .817 | 26.61 | 336.1 | .0144 | 1.946 | .404 | .17 |
| 10.57 | .973 | 51.0 | 646. | .0283 | 1.997 | .776 | 9.20 |
| 14.68 | .811 | 26.23 | 482. | | 1.975 | .899 | 13.34 |
| 14.76 | .969 | 50.7 | 936.5 | | 2.008 | 1.125 | 13.41 |
| 15.85 | .802 | 25.61 | 512.5 | | 2.022 | .8155 | 14.51 |
| 15.99 | .962 | 50.2 | 1013. | | 2.028 | 1.216 | 14.63 |
| 16.32 | .792 | 24.98 | 516. | | 2.074 | .620 | 14.98 |
| 15.99 | .956 | 49.7 | 1005.5 | | 2.049 | 1.208 | 14.69 |
| 11.91 | .844 | 28.35 | 361. | .0140 | 1.776 | .4337 | 9.24 |
| 12.00 | .994 | 52.7 | 675. | .0278 | 1.997 | .8105 | 9.30 |
| 17.09 | .830 | 27.46 | 569.5 | | 1.834 | .684 | 15.05 |
| 17.21 | .983 | 51.8 | 1083. | | 1.930 | 1.300 | 15.19 |
| 18.70 | .809 | 26.10 | 606.5 | | 1.930 | .7285 | 16.87 |
| 18.83 | .969 | 50.67 | 1187. | | 1.974 | 1.425 | 17.00 |
| 19.50 | .787 | 24.70 | 604. | | 2.039 | .7255 | 17.75 |
| 19.62 | .953 | 49.47 | 1217. | | 2.021 | 1.461 | 17.85 |

| PREPARED BY | AEROPHYSICS DEVELOPMENT CORPORATION | REPORT NO 2000-1-K1 |
|---|---|---|
| CHECKED BY | PACIFIC PALISADES, CALIFORNIA | DATE Jan 24, 1953 |

TABLE 5 CONT'D FOR TUBE DIAM D = ½ FT

| 1 | 2 | 3 | 4 | 23 | 24 | 25 | 26 | 27 |
|---|---|---|---|---|---|---|---|---|
| $M_0$ | $M_4 = M_1$ | L | $T_3 \cdot R$ | $B''/P_0$ | $P_{3\,AVG}$ | $\gamma P_{AVG}$ | VOL | $W_a$ CYCLE |
| 0.25 | 0.40 | 3 | 1960 | 5.107 | 5.144 | 0.1038 | .5925 | .0615 |
| | | 3 | 2960 | 7.718 | 7.769 | 0.1038 | .5925 | .0615 |
| | | 10 | 1960 | 4.955 | 5.068 | 0.1028 | 2.005 | .2060 |
| | | 10 | 2960 | 7.482 | 7.651 | 0.1028 | 2.005 | .2060 |
| | | 20 | 1960 | 4.753 | 4.9[illegible]7 | 0.1006 | 4.10 | .4125 |
| | | 20 | 2960 | 7.180 | 7.50 | 0.1006 | 4.10 | .4125 |
| | | 30 | 1960 | 4.562 | 4.871 | 0.0983 | 6.28 | .6175 |
| | | 30 | 2960 | 6.890 | 7.355 | 0.0983 | 6.28 | .6175 |
| | 0.60 | 3 | 1960 | 5.455 | 5.538 | 0.1122 | .597 | .0670 |
| | | 3 | 2960 | 8.25 | 8.375 | 0.1122 | .597 | .0670 |
| | | 10 | 1960 | 5.100 | 5.36 | 0.1087 | 2.061 | .2238 |
| | | 10 | 2960 | 7.720 | 8.11 | 0.1087 | 2.061 | .2238 |
| | | 20 | 1960 | 4.680 | 4.650 | 0.1042 | 4.318 | .450 |
| | | 20 | 2960 | 7.083 | 7.792 | 0.1042 | 4.318 | .450 |
| | | 30 | 1960 | 4.313 | 4.967 | 0.1005 | 6.78 | .6815 |
| | | 30 | 2960 | 6.525 | 7.513 | 0.1005 | 6.78 | .6815 |
| 0.50 | 0.40 | 3 | 1960 | 5.605 | 5.643 | 0.1141 | .5925 | .0676 |
| | | 3 | 2960 | 8.467 | 8.524 | 0.1141 | .5925 | .0676 |
| | | 10 | 1960 | 5.440 | 5.560 | 0.1125 | 2.005 | .2255 |
| | | 10 | 2960 | 8.210 | 8.395 | 0.1125 | 2.005 | .2255 |
| | | 20 | 1960 | 5.215 | 5.448 | 0.1101 | 4.10 | .4515 |
| | | 20 | 2960 | 7.875 | 8.228 | 0.1101 | 4.10 | .4515 |
| | | 30 | 1960 | 5.003 | 5.342 | 0.1080 | 6.28 | .6785 |
| | | 30 | 2960 | 7.560 | 8.070 | 0.1080 | 6.28 | .6785 |
| | 0.60 | 3 | 1960 | 5.90 | 5.995 | 0.1210 | .597 | .0722 |
| | | 3 | 2960 | 8.92 | 9.060 | 0.1210 | .597 | .0722 |
| | | 10 | 1960 | 5.53 | 5.37 | 0.1175 | 2.061 | .2420 |
| | | 10 | 2960 | 8.36 | 8.780 | 0.1175 | 2.061 | .2420 |
| | | 20 | 1960 | 5.07 | 5.59 | 0.1126 | 4.318 | .4863 |
| | | 20 | 2960 | 7.66 | 8.43 | 0.1126 | 4.318 | .4863 |
| | | 30 | 1960 | 4.67 | 5.38 | 0.1087 | 6.78 | .737 |
| | | 30 | 2960 | 7.06 | 8.13 | 0.1087 | 6.78 | .737 |
| 0.75 | 0.40 | 3 | 1960 | 6.49 | 6.535 | 0.1320 | .5925 | .07825 |
| | | 3 | 2960 | 9.80 | 9.87 | 0.1320 | .5925 | .07825 |
| | | 10 | 1960 | 6.30 | 6.44 | 0.1300 | 2.005 | .2605 |
| | | 10 | 2960 | 9.50 | 9.72 | 0.1300 | 2.005 | .2605 |
| | | 20 | 1960 | 6.05 | 6.315 | 0.1276 | 4.10 | .523 |
| | | 20 | 2960 | 9.13 | 9.535 | 0.1276 | 4.10 | .523 |
| | | 30 | 1960 | 5.79 | 6.185 | 0.1249 | 6.28 | .784 |
| | | 30 | 2960 | 8.755 | 9.348 | 0.1249 | 6.28 | .784 |
| | 0.60 | 3 | 1960 | 6.86 | 6.96 | 0.1409 | .597 | .0841 |
| | | 3 | 2960 | 10.39 | 10.545 | 0.1409 | .597 | .0841 |
| | | 10 | 1960 | 6.415 | 6.7375 | 0.1365 | 2.061 | .2812 |
| | | 10 | 2960 | 9.72 | 10.21 | 0.1365 | 2.061 | .2812 |
| | | 20 | 1960 | 5.88 | 6.47 | 0.1311 | 4.318 | .566 |
| | | 20 | 2960 | 8.92 | 9.81 | 0.1311 | 4.318 | .566 |
| | | 30 | 1960 | 5.42 | 6.24 | 0.1264 | 6.78 | .856 |
| | | 30 | 2960 | 8.21 | 9.455 | 0.1264 | 6.78 | .856 |

| PREPARED BY | AEROPHYSICS DEVELOPMENT CORPORATION | REPORT NO 2000-1-R1 |
|---|---|---|
| CHECKED BY | PACIFIC PALISADES, CALIFORNIA | DATE: Jan 24, 1953 |

TABLE 5 CONT'D FOR TUBE DIAM D = ½ FT

| 28 | 29 | 30 | 31 | 32 | 33 | 34 | 35 |
|---|---|---|---|---|---|---|---|
| $\mu_2/\mu_1$ | $u_e/a_s$ | $\frac{F}{w_2 V_1}$ | $\frac{F}{A P}$ | $\frac{w_e}{w_2}$ | $\frac{F}{V_1}$ | $C_T$ | $X$ |
| 2.098 | .705 | 36.8 | 374.2 | .0148 | 1.45 | 4.045 | 9.80 |
| 2.104 | .901 | 62.8 | 640. | .0288 | 1.65 | 6.915 | 9.82 |
| 2.963 | .686 | 35.6 | 530. | .0148 | 1.495 | 5.73 | 14.36 |
| 2.963 | .8905 | 61.9 | 921. | .0288 | 1.68 | 9.95 | 14.36 |
| 3.22 | .659 | 33.9 | 552. | .0148 | 1.57 | 5.963 | 15.67 |
| 3.21 | .875 | 60.7 | 986. | .0288 | 1.71 | 10.65 | 15.67 |
| 3.332 | .622 | 31.5 | 532. | .0148 | 1.693 | 5.75 | 16.26 |
| 3.30 | .856 | 59.3 | 989. | .0288 | 1.75 | 10.69 | 16.07 |
| 2.45 | .747 | 39.6 | 406. | .0147 | 1.34 | 4.388 | 9.885 |
| 2.435 | .923 | 64.5 | 654. | .0286 | 1.60 | 7.065 | 9.78 |
| 3.525 | .704 | 36.8 | 627. | .0147 | 1.44 | 6.775 | 16.41 |
| 3.532 | .901 | 62.8 | 1070. | .0285 | 1.64 | 11.56 | 16.41 |
| 3.91 | .650 | 33.4 | 649. | .0147 | 1.585 | 7.01 | 18.70 |
| 3.895 | .8695 | 60.2 | 1164. | .0286 | 1.71 | 12.58 | 18.63 |
| 4.158 | .599 | 30.0 | 615. | .0147 | 1.774 | 6.647 | 19.76 |
| 4.105 | .835 | 57.6 | 1170. | .0286 | 1.79 | 12.64 | 19.58 |
| 2.298 | .761 | 31.8 | 354. | .0148 | 1.675 | .957 | 9.625 |
| 2.298 | .9315 | 56.4 | 627. | .0287 | 1.83 | 1.694 | 9.61 |
| 3.217 | .7445 | 30.6 | 497. | .0148 | 1.74 | 1.343 | 14.03 |
| 3.227 | .921 | 55.7 | 906. | .0287 | 1.86 | 2.441 | 14.05 |
| 3.465 | .718 | 29.03 | 509. | .0148 | 1.836 | 1.375 | 15.14 |
| 3.510 | .908 | 54.6 | 973. | .0287 | 1.89 | 2.629 | 15.40 |
| 3.57 | .691 | 27.3 | 494. | .0148 | 1.95 | 1.335 | 15.56 |
| 3.57 | .894 | 53.5 | 969. | .0287 | 1.93 | 2.618 | 15.64 |
| 2.588 | .789 | 33.6 | 367. | .0146 | 1.565 | .992 | 9.445 |
| 2.595 | .946 | 57.6 | 624. | .0284 | 1.774 | 1.686 | 9.36 |
| 3.757 | .754 | 31.7 | 564. | .0146 | 1.685 | 1.524 | 15.61 |
| 3.772 | .927 | 56.2 | 1020. | .0284 | 1.82 | 2.757 | 15.67 |
| 4.20 | .701 | 27.9 | 580. | .0146 | 1.885 | 1.566 | 17.96 |
| 4.18 | .898 | 53.8 | 1115. | .0284 | 1.90 | 3.012 | 17.90 |
| 4.36 | .647 | 24.4 | 530. | .0146 | 2.155 | 1.432 | 18.76 |
| 4.44 | .868 | 51.5 | 1140. | .0284 | 1.985 | 3.080 | 19.11 |
| 2.625 | .833 | 27.8 | 350. | .0144 | 1.864 | .4205 | 9.13 |
| 2.634 | .973 | 51.0 | 645. | .0283 | 2.00 | .7747 | 9.18 |
| 3.66 | .820 | 26.9 | 493. | .0144 | 1.93 | .592 | 13.30 |
| 3.68 | .964 | 50.4 | 932. | .0283 | 2.02 | 1.120 | 13.44 |
| 3.96 | .801 | 25.8 | 515. | .0144 | 2.01 | .619 | 14.48 |
| 4.00 | .953 | 49.6 | 1000. | .0283 | 2.05 | 1.201 | 14.65 |
| 4.08 | .779 | 24.3 | 502. | .0144 | 2.135 | .603 | 14.99 |
| 3.996 | .941 | 48.5 | 984. | .0283 | 2.100 | 1.182 | 14.73 |
| 2.97 | .8565 | 29.2 | 372.5 | .0140 | 1.726 | .4475 | 9.27 |
| 2.992 | .9885 | 52.3 | 670. | .0278 | 1.914 | .805 | 9.305 |
| 4.28 | .827 | 27.31 | 569. | .0140 | 1.846 | .6835 | 15.12 |
| 4.31 | .9705 | 50.9 | 1069. | .0278 | 1.968 | 1.284 | 15.24 |
| 4.71 | .787 | 24.75 | 579. | .0140 | 2.038 | .6955 | 16.96 |
| 4.74 | .9465 | 48.93 | 1154. | .0278 | 2.048 | 1.386 | 17.10 |
| 4.948 | .742 | 21.81 | 541. | .0140 | 2.310 | .650 | 17.98 |
| 4.975 | .921 | 46.9 | 1155. | .0278 | 2.135 | 1.387 | 17.86 |

| PREPARED BY | AEROPHYSICS DEVELOPMENT CORPORATION | REPORT NO. 2000-1-R1 |
|---|---|---|
| CHECKED BY | PACIFIC PALISADES, CALIFORNIA | DATE Jan 24, 1953 |

TABLE 5 CONT'D FOR TUBE DIAM $D = \frac{1}{3}$ FT

| 1 | 2 | 3 | 4 | 23 | 24 | 25 | 26 | 27 |
|---|---|---|---|---|---|---|---|---|
| $M_o$ | $M_d - M_1$ | $L$ | $T_3$ °R | $B''/P_o$ | $B_{AVG}$ | $q/P_{AVG}$ | $V_{OL}$ | $W_a$ CYCLE |
| 0.25 | 0.40 | 3 | 1960 | 5.09 | 5.13 | .1038 | .265 | .0275 |
| | | 3 | 2960 | 7.65 | 7.73 | .1038 | .265 | .0275 |
| | | 10 | 1960 | 4.87 | 5.02 | .1015 | .901 | .0915 |
| | | 10 | 2960 | 7.34 | 7.58 | .1015 | .901 | .0915 |
| | | 20 | 1960 | 4.55 | 4.86 | .0982 | 1.87 | .1835 |
| | | 20 | 2960 | 6.85 | 7.33 | .0982 | 1.87 | .1835 |
| | | 30 | 1960 | 4.32 | 4.75 | .0960 | 2.882 | .277 |
| | | 30 | 2960 | 6.50 | 7.16 | .0960 | 2.882 | .277 |
| | 0.60 | 3 | 1960 | 5.37 | 5.50 | .1112 | .268 | .02982 |
| | | 3 | 2960 | 8.12 | 8.31 | .1114 | .268 | .02982 |
| | | 10 | 1960 | 4.858 | 5.24 | .1060 | .940 | .0997 |
| | | 10 | 2960 | 7.345 | 7.9225 | .1062 | .940 | .0997 |
| | | 20 | 1960 | 4.237 | 4.93 | .0997 | 2.01 | .2008 |
| | | 20 | 2960 | 6.41 | 7.46 | .1000 | 2.01 | .2008 |
| | | 30 | 1960 | 3.73 | 4.675 | .0945 | 3.20 | .3025 |
| | | 30 | 2960 | 5.64 | 7.07 | .0947 | 3.20 | .3025 |
| 0.50 | 0.40 | 3 | 1960 | 5.57 | 5.625 | .1138 | .265 | .03016 |
| | | 3 | 2960 | 8.41 | 8.50 | .1139 | .265 | .03016 |
| | | 10 | 1960 | 5.34 | 5.51 | .1114 | .901 | .1003 |
| | | 10 | 2960 | 8.06 | 8.32 | .1115 | .901 | .1003 |
| | | 20 | 1960 | 4.96 | 5.32 | .1076 | 1.87 | .2012 |
| | | 20 | 2960 | 7.49 | 8.035 | .1077 | 1.87 | .2012 |
| | | 30 | 1960 | 4.685 | 5.18 | .1047 | 2.882 | .3020 |
| | | 30 | 2960 | 7.06 | 7.83 | .1060 | 2.882 | .3020 |
| | 0.60 | 3 | 1960 | 5.82 | 5.96 | .1205 | .268 | .0323 |
| | | 3 | 2960 | 8.79 | 9.00 | .1205 | .268 | .0323 |
| | | 10 | 1960 | 5.265 | 5.68 | .1149 | .940 | .1080 |
| | | 10 | 2960 | 7.95 | 8.575 | .1150 | .940 | .1080 |
| | | 20 | 1960 | 4.59 | 5.34 | .1080 | 2.01 | .2172 |
| | | 20 | 2960 | 6.935 | 8.068 | .1081 | 2.01 | .2172 |
| | | 30 | 1960 | 4.04 | 5.065 | .1024 | 3.20 | .3275 |
| | | 30 | 2960 | 6.11 | 7.655 | .1025 | 3.20 | .3275 |
| 0.75 | 0.40 | 3 | 1960 | 6.45 | 6.515 | .1317 | .265 | .03492 |
| | | 3 | 2960 | 9.74 | 9.84 | .1318 | .265 | .03492 |
| | | 10 | 1960 | 6.185 | 6.38 | .1290 | .901 | .1162 |
| | | 10 | 2960 | 9.34 | 9.64 | .1291 | .901 | .1162 |
| | | 20 | 1960 | 5.74 | 6.16 | .1246 | 1.87 | .2332 |
| | | 20 | 2960 | 8.68 | 9.31 | .1247 | 1.87 | .2332 |
| | | 30 | 1960 | 5.427 | 6.004 | .1215 | 2.882 | .350 |
| | | 30 | 2960 | 8.20 | 9.07 | .1215 | 2.882 | .350 |
| | 0.60 | 3 | 1960 | 6.75 | 6.905 | .1395 | .268 | .0375 |
| | | 3 | 2960 | 10.23 | 10.47 | .1402 | .268 | .0375 |
| | | 10 | 1960 | 6.10 | 6.58 | .1330 | .940 | .1253 |
| | | 10 | 2960 | 9.25 | 9.975 | .1337 | .940 | .1253 |
| | | 20 | 1960 | 5.325 | 6.193 | .1251 | 2.01 | .2515 |
| | | 20 | 2960 | 8.065 | 9.383 | .1257 | 2.01 | .2515 |
| | | 30 | 1960 | 4.89 | 5.875 | .1187 | 3.20 | .3808 |
| | | 30 | 2960 | 7.105 | 8.903 | .1193 | 3.20 | .3808 |

| PREPARED BY | AEROPHYSICS DEVELOPMENT CORPORATION | REPORT NO 2000-1-R1 |
|---|---|---|
| CHECKED BY | PACIFIC PALISADES, CALIFORNIA | DATE Jan 24, 1953 |

## TABLE 5 CONT'D FOR TUBE DIAM D = ½ FT

| 28 $w_a/g$ | 29 $a_e/a_3$ | 30 $\frac{F}{w_a T_0}$ | 31 $\frac{F}{A_8}$ | 32 $w_f/w_a$ | 33 $f/T_0$ | 34 $C_T$ | 35 $X$ |
|---|---|---|---|---|---|---|---|
| .938 | .695 | 35.4 | 362. | .0148 | 1.505 | 3.91 | 9.84 |
| .941 | .884 | 61.4 | 630. | .0288 | 1.689 | 6.807 | 9.90 |
| 1.518 | .675 | 35.0 | 520. | | 1.523 | 5.62 | 14.32 |
| 1.318 | .870 | 60.4 | 888. | | 1.716 | 9.59 | 14.42 |
| 1.435 | .637 | 32.4 | 530. | | 1.645 | 5.725 | 15.76 |
| 1.435 | .838 | 57.9 | 946. | | 1.790 | 10.22 | 15.75 |
| 1.50 | .610 | 30.6 | 523. | | 1.741 | 5.65 | 16.46 |
| 1.50 | .815 | 56.0 | 958. | | 1.851 | 10.35 | 16.50 |
| 1.093 | .724 | 38.25 | 391. | .0147 | 1.383 | 4.223 | 9.85 |
| 1.086 | .907 | 63.5 | 644. | .0286 | 1.620 | 6.955 | 9.92 |
| 1.568 | .672 | 34.9 | 593.5 | | 1.515 | 6.41 | 16.38 |
| 1.574 | .867 | 60.4 | 1029. | | 1.704 | 11.10 | 16.41 |
| 1.748 | .600 | 30.2 | 579. | | 1.750 | 6.255 | 18.49 |
| 1.742 | .809 | 55.73 | 1080. | | 1.945 | 11.66 | 18.70 |
| 1.843 | .532 | 25.78 | 512. | | 2.051 | 5.53 | 19.12 |
| 1.821 | .750 | 51.0 | 1046. | | 2.018 | 11.30 | 19.78 |
| 1.025 | .743 | 30.75 | 341.7 | .0148 | 1.730 | .924 | 9.60 |
| 1.025 | .920 | 55.85 | 620. | .0287 | 1.949 | 1.875 | 9.59 |
| 1.430 | .721 | 29.3 | 472.3 | | 1.817 | 1.276 | 13.91 |
| 1.435 | .903 | 54.5 | 880.7 | | 1.895 | 2.380 | 13.96 |
| 1.545 | .678 | 26.54 | 467.0 | | 2.005 | 1.262 | 15.16 |
| 1.577 | .875 | 52.3 | 930. | | 1.975 | 2.510 | 15.37 |
| 1.590 | .651 | 24.80 | 448.5 | | 2.147 | 1.212 | 15.61 |
| 1.590 | .852 | 50.4 | 912. | | 2.010 | 2.462 | 15.64 |
| 1.158 | .765 | 32.2 | 548.2 | .0146 | 1.862 | .941 | 9.84 |
| 1.162 | .936 | 57.1 | 820.0 | .0284 | 1.790 | 1.875 | 9.38 |
| 1.675 | .714 | 28.92 | 523.7 | | 1.817 | 1.415 | 15.62 |
| 1.682 | .898 | 54.05 | 984. | | 1.890 | 2.658 | 15.72 |
| 1.678 | .639 | 24.04 | 504.5 | | 2.136 | 1.363 | 18.10 |
| 1.870 | .843 | 49.7 | 1037. | | 2.056 | 2.800 | 18.00 |
| 1.936 | .572 | 19.69 | 429. | | 2.659 | 1.160 | 18.80 |
| 1.971 | .788 | 45.3 | 1005. | | 2.255 | 2.714 | 19.16 |
| 1.172 | .812 | 26.5 | 335.8 | .0144 | 1.955 | .4035 | 9.20 |
| 1.176 | .970 | 51.15 | 651. | .0283 | 1.990 | .782 | 9.24 |
| 1.630 | .793 | 25.25 | 463.5 | | 2.050 | .3565 | 13.31 |
| 1.638 | .957 | 50.10 | 925. | | 2.053 | 1.111 | 13.41 |
| 1.767 | .758 | 23.02 | 463. | | 2.249 | .556 | 14.58 |
| 1.783 | .931 | 48.00 | 974. | | 2.122 | 1.170 | 14.74 |
| 1.8225 | .730 | 21.22 | 441. | | 2.44 | .530 | 15.07 |
| 1.785 | .911 | 46.4 | 945. | | 2.195 | 1.135 | 14.78 |
| 1.325 | .831 | 27.72 | 352.8 | .0140 | 1.817 | .4238 | 9.24 |
| 1.335 | .985 | 52.3 | 670.5 | .0278 | 1.912 | .805 | 9.31 |
| 1.904 | .787 | 24.91 | 517.5 | | 2.021 | .6215 | 15.07 |
| 1.918 | .953 | 49.75 | 1043. | | 2.010 | 1.253 | 15.21 |
| 2.091 | .721 | 20.62 | 483. | | 2.442 | .580 | 16.98 |
| 2.107 | .904 | 45.8 | 1080. | | 2.185 | 1.397 | 17.11 |
| 2.198 | .651 | 16.10 | 388. | | 2.150 | .4792 | 17.98 |
| 2.212 | .853 | 41.77 | 1042. | | 2.395 | 1.251 | 18.10 |

SUPERSONIC PERFORMANCE OF THE MULTI-JET

TABLE 6

| COLUMN | 1 | 2 | 3 | 4 | 5 | 6 | 7 | 8 | 9 | 10 |
|---|---|---|---|---|---|---|---|---|---|---|
| FUNCTION | $M_o$ | $T_3$ °R | $P_o$ PSF | $P_{ot}$ PSF | $P_{1t}$ PSF | $P_1$ PSF | $P_1'$ PSF | $P_2$ PSF | $P_2'$ PSF | $T_{ot}$ °R |
| OPERATION | | | | | | | ⑥ × 0.97 | ⑥ × 2.17 | ⑧ × 0.97 | |
| | 2.80 | 3960 | 2116 | 57,300 | 37,200 | 28,700 | 27,840 | 62,900 | 61,050 | 1330 |
| | | 2960 | | | | | | | | |
| | | 1960 | | | | | | | | |
| | 2.00 | 3960 | 2116 | 16,540 | 14,900 | 11,500 | 11,150 | 25,700 | 24,400 | 935 |
| | | 2960 | | | | | | | | |
| | | 1960 | | | | | | | | |
| | 1.00 | 3960 | | 4,010 | 4,010 | 3,100 | 3,003 | 6,800 | 6,580 | 623 |
| | | 2960 | | | | | | | | |
| | | 1960 | | | | | | | | |

TABLE 6 (Cont'd)

| 1 | 2 | 11 | 12 | 13 | 14 | 15 | 16 | 17 | 18 | 19 |
|---|---|---|---|---|---|---|---|---|---|---|
| $M_o$ | $T_3$ °R | $T_1$ °R | $T_2$ °R | $T_3/T_2$ | $P_3$ PSf | $P_3'$ PSf | $P_{3\,AVG}$ | $\frac{P_{3\,AVG}}{P_o}$ | $\delta P_{3\,AVG}$ | $W_{(18)\times VOL}$ |
| | | | (11) × 1.27 | | (8) × (13) | (9) × (13) | $\frac{(14)\times(15)}{2}$ | $\frac{(16)}{3}$ | lbs/ft³ | lbs/CYCLE (17) × .E11 |
| 2.80 | 3960 | 1240 | 1575 | 2.51 | 158,000 | 153,300 | 155,500 | 73.8 | .738 | .0896 |
| | 2960 | | | 1.878 | 118,200 | 114,800 | 116,500 | 55.3 | .738 | .0896 |
| | 1960 | | | 1.245 | 78,300 | 76,100 | 77,200 | 36.6 | .738 | .0896 |
| 2.00 | 3960 | 872 | 1108 | 3.68 | 92,700 | 89,800 | 91,250 | 43.2 | .453 | .0525 |
| | 2960 | | | 2.67 | 68,700 | 65,200 | 66,950 | 31.7 | | |
| | 1960 | | | 1.77 | 45,500 | 43,200 | 44,350 | 21.0 | | |
| 1.00 | 3960 | 581 | 738.5 | 5.36 | 36,470 | 35,280 | 35,875 | 17.0 | .1705 | .02065 |
| | 2960 | | | 4.01 | 27,270 | 26,380 | 26,825 | 12.7 | | |
| | 1960 | | | 2.65 | 18,050 | 17,450 | 17,750 | 8.41 | | |

VOL. OF 1 ROW OF TUBES FOR A 34" DIAM ENGINE = 0.1211 cu. ft.

1 ENGINE CONTAINS 32 ROWS OF TUBES

TABLE 6 (Cont'd)

| 1 | 2 | 20 | 21 | 22 | 23 | 24 | 25 | 26 | 27 | 28 |
|---|---|---|---|---|---|---|---|---|---|---|
| $M_o$ | $T_3$ °R | $\frac{P_1+P_1'}{\Sigma P_{3AVG} \times 2.17}$ | $\frac{I_V}{a_3 \rho_3 V_{3L}}$ | $I_V$ lb. SECS | W DISCHARGED | W REMAINING | W DISCHARGED DURING SCAV. | $T_t$ END OF DISCHARGE | VEL. AS EXHAUST FPS | $T_{SCAV}$ |
| | | | | (21)x(18)x$a_3$ | % | % | (24)x(19) lbs | (20)$^{2/7}$ x $T_3$ | 46.95X / 1.875x(26) | |
| 2.80 | 3960 | .084 | .0403 | 10.60 | .8165 | .1835 | .01642 | 1950 | 1930 | .00190 |
| | 2960 | .112 | .0368 | 8.45 | .7848 | .2152 | .0193 | 1580 | 1740 | |
| | 1960 | .169 | .0318 | 5.90 | .718 | .282 | .0252 | 1180 | 1508 | |
| 2.00 | 3960 | .0522 | .0382 | 5.88 | .846 | .154 | .0081 | 1700 | 1850 | .00212 |
| | 2960 | .078 | .03585 | 4.82 | .8264 | .1736 | .00912 | 1430 | 1655 | |
| | 1960 | .118 | .03210 | 3.49 | .776 | .224 | .0118 | 1060 | 1440 | |
| 1.00 | 3960 | .0388 | .0344 | 4.085 | .878 | .122 | .00252 | 1560 | 1730 | .00250 |
| | 2960 | .0524 | .0301 | 1.60 | .846 | .154 | .00318 | 1270 | 1560 | |
| | 1960 | .0792 | .0268 | 1.15 | .826 | .174 | .00360 | 950 | 1340 | |

TABLE 6 (Cont'd)

| 1 | 2 | 29 | 30 | 31 | 32 | 33 | 34 | 35 | 36 | 37 |
|---|---|---|---|---|---|---|---|---|---|---|
| $M_o$ | $T_3$ °R | SCAV. PRESS. 1st 1/4 OF PHASE PSF | SCAV. PRESS LAST 3/4 OF PHASE | PRESS. IMP. 1ST 1/4 OF SCAV. | PRESS. IMP LAST 3/4 OF SCAV. | VEL. IMP. DURING SCAV. | $I_3$ lb SECS | INTAKE IMPULSE | $I_{NET}$ lb SECS | $t_{TOT}$ |
| | | (6)+(7) / 2 X 2.17 | (6)+(7) / 2 PSF | (29)−2.116(0.0958) × $\tau_{SCAV}$ / 4 | (30−2.116)0.0958 × $3\tau_{SCAV}$ / 4 | (25)×(27) / 32.2 | (5)+(32)+(33) | (3)×$M_o$×$a_3$ / 32.2 | (26)+(34)−(35) | SECS |
| 2.80 | 3960 | 13,000 | 28,270 | 0.517 | 3.73 | 0.985 | 5.232 | 8.70 | 7.132 | .00589 |
| | 2960 | | | | | 1.04 | 5.287 | | 5.037 | |
| | 1960 | | | | | 1.18 | 5.427 | | 2.627 | |
| 2.00 | 3960 | 5,210 | 11,325 | 0.164 | 1.48 | 0.458 | 2.102 | 3.64 | 4.549 | .00681 |
| | 2960 | | | | | 0.468 | 2.112 | | 3.092 | |
| | 1960 | | | | | 0.528 | 2.172 | | 2.022 | |
| 1.00 | 3960 | 1,530 | 3,051 | - .0366 | .175 | .135 | .270 | 0.716 | 1.639 | .00806 |
| | 2960 | | | | | .154 | .289 | | 1.17 | |
| | 1960 | | | | | .150 | .285 | | .716 | |

AREA OF 1 ROW OF TUBES OF A 34" DIA. ENGINE = .0958 FT²

TABLE 6 (Cont'd)

| 1 | 2 | 38 | 39 | 40 | 41 | 42 | 43 | 44 | 45 | 46 | 47 |
|---|---|---|---|---|---|---|---|---|---|---|---|
| $M_o$ | $T_3$ °R | $\tau_o$ | $\tau_v$ | $\tau_v/\tau_o$ | K | $1-\frac{\tau_v}{\tau_o}$ | $1-K\frac{\tau_v}{\tau_o}$ | $K\frac{\tau_v}{\tau_o}-\frac{\tau_v}{\tau_o}$ | THRUST | SPECIFIC THRUST | $J_3-J_2$ |
| | | SECS | SECS | | | | | | | | |
| 2.80 | 3960 | .00285 | .00050 | .176 | .015 | .824 | .997 | .822 | 36,650 | 79.5 | 8586 |
| | 2960 | | | | .025 | | .996 | .821 | 25,150 | 56.0 | 1384 |
| | 1960 | | | | .036 | | .994 | .820 | 13,125 | 28.7 | 365 |
| 2.00 | 3960 | .00326 | .00055 | .168 | .031 | .832 | .995 | .829 | 19,800 | 85.5 | 2858 |
| | 2960 | | | | .040 | | .993 | .827 | 13,400 | 57.8 | 1952 |
| | 1960 | | | | .055 | | .991 | .825 | 8,790 | 38.0 | 952 |
| 1.00 | 3960 | .00395 | .000680 | .172 | .065 | .828 | .99 | .82 | 5,980 | 78.5 | 3282 |
| | 2960 | | | | .105 | | .98 | .815 | 4,350 | 55.0 | 2222 |
| | 1960 | | | | .230 | | .96 | .805 | 2,570 | 33.2 | 1382 |

$$\frac{\text{AREA OF 34" DIAM ENGINE}}{\text{AREA OF 36" DIAM ENGINE}} = 0.893$$

TABLE 6 (Cont'd)

| 1 | 2 | 48 | 49 | 50 | 51 | 52 | 53 | 54 | 55 | 56 | 57 |
|---|---|---|---|---|---|---|---|---|---|---|---|
| $M_o$ | $T_3$ °R | FUEL / AIR | SPECIFIC FUEL CONSUMPTION lbs/hr/lb thrust | THRUST / FRONTAL AREA | $C_T$ - 4 ENGINES CLUSTERED ON 425 | $C_D$ SEA LEVEL | $C_D$ 5000' ALT | $C_D$ 15000' ALT | $C_D$ 25000' ALT | $C_D$ 35000' ALT | DRAG SEA LEVEL |
| | | lb / lb | (48) x (49) / (46) | lbs / ft² | (47) / A x 425 | | | | | | lbs. |
| 2.80 | 3960 | .0338 | 1.53 | 5,050 | .0297 | .0230 | .0231 | .0232 | .0235 | .0241 | |
| | 2960 | .0170 | 1.09 | 3,560 | .0204 | | | | | | |
| | 1960 | .0044 | 0.552 | 1,820 | .0107 | | | | | | |
| 2.00 | 3960 | .0440 | 1.84 | 2,790 | .0314 | .0258 | .0259 | .0260 | .0270 | .0290 | |
| | 2960 | .0228 | 1.42 | 1,900 | .0213 | | | | | | |
| | 1960 | .0099 | 0.990 | 1,175 | .0139 | | | | | | |
| 1.00 | 3960 | .0455 | 2.09 | 846 | .0380 | .0302 | .0327 | .0358 | .0435 | .0636 | 19,000 |
| | 2960 | .0276 | 1.80 | 606 | .0276 | | | | | | |
| | 1960 | .0133 | 1.44 | 364 | .0163 | | | | | | |





SECURITY INFORMATION
RESTRICTED

TABLE 6 (CONT'D)

| 1 | 2 | 58 | 59 |
|---|---|---|---|
| $M_o$ | $T_3$ 'R | $C_T$ | $\chi$ |
| | | $\frac{(50)}{g}$ | $\frac{(50)}{(49)} \times \frac{\sqrt{T_{RC}}}{P_{RC}/P_{RS}}$ |
| 2.90 | 3960 | .4347 | [illegible] |
| | 2960 | .3065 | [illegible] |
| | 1960 | .1537 | [illegible] |
| 2.00 | 3960 | .371 | [illegible] |
| | 2960 | .3203 | [illegible] |
| | 1960 | .1782 | [illegible] |
| 1.00 | 3960 | .4715 | [illegible] |
| | 2960 | .419 | [illegible] |
| | 1960 | .2457 | [illegible] |

SUBSONIC PERFORMANCE OF THE MULTI-JET

TABLE 7

| COLUMN | 1 | 2 | 3 | 4 | 5 | 6 | 7 | 8 | 9 | 10 | 11 |
|---|---|---|---|---|---|---|---|---|---|---|---|
| FUNCTION | $M_o$ | $T_3$ °R | $P_s$ psf | $P_{ot}$ psf | $P_{it}$ psf | $P_1$ psf | $P_1'$ psf | $P_2$ psf | $P_2'$ psf | $T_{ot}$ °R | $T_1$ °R |
| OPERATION | | | | | | | ⑥ × 0.97 | ⑥ × 2.17 | ⑧ × 0.97 | | |
| | 0.75 | 3960<br>3960<br>1960 | 2116 | 3070 | 3070 | 2070 | 2300 | 5200 | 5050 | 577 | 539 |
| | 0.50 | 3960<br>3960<br>1960 | | 2510 | 2510 | 1740 | 1880 | 4250 | 4120 | 545 | 509 |
| | 0.25 | 3960<br>3960<br>1960 | | 2210 | 2210 | 1710 | 1660 | 3750 | 3640 | 525 | 490 |
| | 0 | 3960 | | 2116 | 2116 | 1635 | 1587 | 3580 | 3477 | 519 | 484 |





SECURITY INFORMATION
RESTRICTED

TABLE 7 (Cont'd)

| 1 | 2 | 12 | 13 | 14 | 15 | 16 | 17 | 18 | 19 | 20 | 21 |
|---|---|---|---|---|---|---|---|---|---|---|---|
| $M_o$ | $T_3$ °R | $T_2$ °R | $T_3/T_2$ | $P_{3\ PSF}$ | $P_3'$ PSF | $P_{3\ AVG}$ | $\frac{P_{3\ AVG}}{P_o}$ | $\gamma P_{3\ AVG}$ | $W = (18) \times V_{OL}$ | $\frac{P_{3t}}{P_{3\ AVG}}$ | $\frac{I_v}{a_3 \gamma P_3 V_{OL}}$ |
| | | (11) x 1.27 | | (8) x (13) | (9) x (13) | (14) + (15) | (16)/(3) | lbs/ft³ | lbs/cycle (12) x 0.1611 | | |
| 0.75 | 3960 | 684 | 5.79 | 30,100 | 29,200 | 29,650 | 14.05 | .149 | .01709 | .1035 | .0330 |
| | 2960 | | 4.33 | 22,480 | 21,820 | 22,150 | 10.5 | | | .139 | .0300 |
| | 1960 | | 2.87 | 14,910 | 14,470 | 14,690 | 6.95 | | | .209 | .0258 |
| 0.50 | 3960 | 646 | 6.03 | 25,600 | 24,800 | 25,200 | 11.9 | .120 | .01453 | .100 | .0317 |
| | 2960 | | 4.58 | 19,440 | 18,840 | 19,140 | 9.05 | | | .131 | .0291 |
| | 1960 | | 3.04 | 12,910 | 12,510 | 12,710 | 6.03 | | | .1975 | .0236 |
| 0.25 | 3960 | 622 | 6.36 | 23,900 | 23,200 | 23,550 | 11.13 | .1119 | .01357 | .094 | .0310 |
| | 2960 | | 4.76 | 17,850 | 17,320 | 17,585 | 8.32 | | | .126 | .0281 |
| | 1960 | | 3.16 | 11,830 | 11,490 | 11,660 | 5.53 | | | .190 | .0224 |
| 0 | 3960 | 615 | 6.44 | 23,060 | 22,390 | 22,725 | 10.78 | .1078 | .01305 | .093 | .0308 |
| | 2960 | | 4.81 | 17,250 | 16,750 | 17,000 | 8.05 | | | .124 | .0278 |
| | 1960 | | 3.19 | 11,430 | 11,090 | 11,260 | 5.33 | | | .188 | .0217 |

VOL OF 1 ROW OF TUBES FOR 34" DIAM. ENGINE = 0.1211 ft³

1 ENGINE CONTAINS 1 ROW OF TUBES





SECURITY INFORMATION RESTRICTED

TABLE 7 (Cont'd)

| 1 | 2 | 22 | 23 | 24 | 25 | 26 | 27 | 28 | 29 | 30 | 31 |
|---|---|---|---|---|---|---|---|---|---|---|---|
| $M_o$ | $T_3$ °R | $I_{v}$ lb sec | W DISCHARGED | W REMAINING | W DISCHARGED OVER NO DAV | $I_s$ | INTAKE IMPULSE lb SECS | $I_{NET}$ lb SECS | $\tau_{TOT}$ | $\tau_o$ | $\tau_v$ |
| | | (21)x(19)x$a_3$ | % | % | (24)x(19) lbs | (23)x$M_1$x$a_1$ / 32.2 | (13)x$M_o$x$a_o$ / 32.2 | (22)+(26) -(27) | SECS | SECS | SECS |
| 0.75 | 3960 | 1.65 | .798 | .202 | .00345 | .0733 | 0.440 | 1.285 | .00835 | .00405 | .000710 |
| | 2960 | 1.31 | .750 | .25 | .00427 | .0905 | | .96 | | | |
| | 1960 | 0.915 | .68 | .32 | .00547 | .116 | | .591 | | | |
| 0.50 | 3960 | 1.35 | .799 | .201 | .00292 | .060 | 0.252 | 1.158 | .00880 | .00415 | .000750 |
| | 2960 | 1.08 | .758 | .242 | .00352 | .0722 | | .900 | | | |
| | 1960 | 0.71 | .689 | .311 | .00452 | .0927 | | .551 | | | |
| 0.25 | 3960 | 1.23 | .806 | .194 | .00262 | .0553 | 0.105 | 1.178 | .00890 | .00425 | .000760 |
| | 2960 | 0.976 | .78 | .22 | .00298 | .0606 | | .931 | | | |
| | 1960 | 0.629 | .733 | .267 | .00362 | .0756 | | .597 | | | |
| 0 | 3960 | 1.18 | .83 | .17 | .00282 | .0442 | 0 | 1.224 | .00900 | .00435 | .000765 |
| | 2960 | 0.929 | .799 | .201 | .00262 | .0521 | | .981 | | | |
| | 1960 | 0.586 | .750 | .25 | .00326 | .0650 | | .651 | | | |





SECURITY INFORMATION RESTRICTED

TABLE 7 (Cont'd)

| 1 | 2 | 32 | 33 | 34 | 35 | 36 | 37 | 38 | 39 | 40 | 41 |
|---|---|---|---|---|---|---|---|---|---|---|---|
| $M_o$ | $T_3$ °R | $\tau_v/\tau_c$ | K | $1-\frac{\tau_v}{\tau_c}$ | $1-K\frac{\tau_v}{\tau_c}$ | $(1-\frac{\tau_v}{\tau_c})(1-K\frac{\tau_v}{\tau_c})$ | THRUST OF 36" D. ENGINE | SPECIFIC THRUST lb./lb. AIR/SEC | $T_3 - T_2$ | $\frac{FUEL}{AIR}$ | SPECIFIC FUEL CONSUMPTION lb./hr./lb. THRUST |
| | | | | | | | (28)×(26)×32 / (3)×0.893 | (28)/(13) × (35) | °F | $\frac{LB.}{LB}$ | 3600 × (42) / (39) |
| 0.75 | 3960 | .175 | .090 | .825 | .984 | .821 | 4550 | 74.0 | 3276 | .0462 | 2.14 |
| | 2960 | | .160 | | .977 | .815 | 3360 | 54.8 | 2276 | .0279 | 1.83 |
| | 1960 | | .370 | | .935 | .781 | 1990 | 32.4 | 1276 | .0138 | 1.53 |
| 0.50 | 3960 | .183 | .115 | .813 | .979 | .80 | 3770 | 77.9 | 3314 | .0468 | 2.16 |
| | 2960 | | .16 | | .964 | .789 | 2900 | 59.7 | 2314 | .0283 | 1.71 |
| | 1960 | | .53 | | .90 | .735 | 1650 | 34.2 | 1314 | .0143 | 1.50 |
| 0.25 | 3960 | .179 | .13 | .821 | .977 | .801 | 3820 | 84.7 | 3338 | .0470 | 2.00 |
| | 2960 | | .24 | | .957 | .785 | 2950 | 65.7 | 2338 | .0285 | 1.56 |
| | 1960 | | .675 | | .88 | .723 | 1760 | 38.8 | 1338 | .0144 | 1.34 |
| 0 | 3960 | .176 | .14 | .824 | .975 | .803 | 3930 | 91.5 | 3345 | .0470 | 1.85 |
| | 2960 | | .26 | | .954 | .785 | 3070 | 71.6 | 3345 | .0785 | 1.43 |
| | 1960 | | .73 | | .87 | .716 | 1850 | 43.5 | 1345 | .0144 | 1.19 |

# TABLE 7 (CONT'D)

| 1 | 2 | 42 | 43 | 44 | 45 | 46 | 47 | 48 | 49 |
|---|---|---|---|---|---|---|---|---|---|
| $M_o$ | $T_3$ °R | THRUST / FRONTAL AREA | $C_T$ - 4 ENGINES BASED ON 425[2] | $C_D$ SEA LEVEL | $C_D$ 5000' ALT | $C_D$ 15000' ALT | $C_D$ 25000' ALT | $C_D$ 35000' ALT | DRAG SEA LEVEL |
| | | $\frac{lbs}{ft^2}$ | $\frac{4 \times 37}{4 \times 425}$ | | | | | | lbs |
| 0.75 | 3960 | 642 | .0515 | .0156 | .0242 | .0351 | .0615 | .131 | 5,530 |
| | 2960 | 476 | .0380 | | | | | | |
| | 1960 | 281 | .0225 | | | | | | |
| 0.50 | 3960 | 534 | .0960 | .0500 | .0651 | .1226 | .2646 | .2646 | 7,850 |
| | 2960 | 410 | .0738 | | | | | | |
| | 1960 | 234 | .0420 | | | | | | |
| 0.25 | 3960 | 540 | .388 | .582 | .825 | 1.7556 | 4.05 | 10.12 | 22,900 |
| | 2960 | 417 | .300 | | | | | | |
| | 1960 | 249 | .179 | | | | | | |
| 0 | 3960 | 555 | | | | | | | |
| | 2960 | 435 | | | | | | | |
| | 1960 | 262 | | | | | | | |





SECURITY INFORMATION
RESTRICTED

TABLE 7 (CONT'D)

| 1 | 2 | 50 | 51 | |
|---|---|---|---|---|
| | | $C_T$ (42) $C_{l_\beta}/\beta$ | $K$ (42) $C_{n_\beta}$ (38) Rolling | |
| 0.75 | 3960 | .771 | 1.50 | |
| | 2960 | .572 | 1.305 | |
| | 1960 | .3575 | 1.30 | |
| 0.50 | 3960 | 1.445 | 5.12 | |
| | 2960 | 1.110 | 5.13 | |
| | 1960 | .6045 | 5.11 | |
| 0.25 | 3960 | 5.84 | 6.15 | |
| | 2960 | 4.505 | 6.12 | |
| | 1960 | 2.69 | 6.135 | |
| 0 | 3960 | | 6.09 | |
| | 2960 | | 6.07 | |
| | 1960 | | 6.04 | |

IDEAL PERFORMANCE OF THE MULTI-JET  TABLE 8

| COLUMN NO. | 1 | 2 | 3 | 4 | 5 | 6 | 7 | 8 | 9 |
|---|---|---|---|---|---|---|---|---|---|
| FUNCTION | $M_0$ | $T_3$ °R | $P_0$ PSF | $P_{0t}$ PSF | $P_1$ PSF | $P_2$ PSF | $T_{0t}$ °R | $T_1$ °R | $T_2$ °R |
| OPERATION | | | | | | | | | ⑧ x 1.27 |
| | 0.75 | 2960 | 2116 | 3070 | 2407 | 5225 | 577 | 539 | 684.5 |
| | | 2460 | | | | | | | |
| | | 1960 | | | | | | | |
| | 0.50 | 2960 | | 2510 | 1968 | 4270 | 545 | 509 | 646.5 |
| | | 2460 | | | | | | | |
| | | 1960 | | | | | | | |
| | 0.25 | 2960 | | 2210 | 1732 | 3760 | 525 | 490 | 622.5 |
| | | 2460 | | | | | | | |
| | | 1960 | | | | | | | |
| | 0 | 2960 | | 2116 | 1658 | 3597 | 519 | 484 | 615 |
| | | 2460 | | | | | | | |
| | | 1960 | | | | | | | |

IDEAL PERFORMANCE OF THE MULTI-JET TABLE 8 Cont'd

| 1 | 2 | 10 | 11 | 12 | 13 | 14 | 15 | 16 | 17 |
|---|---|---|---|---|---|---|---|---|---|
| $M_o$ | $T_3$ °R | $T_3/T_2$ | $P_{3_{PSF}}$ | $P_3/P_o$ | $\rho_{3\,AVG}$ | W | $P_{oc}/P_3$ | $\tau_E a_3/L$ | $\tau_E$ SECS |
| | | | ⑥ x ⑩ | ⑪/⑬ | $\frac{32.2 \times P_3}{1716 \times T_3}$ | lbs/CYCLE | | | ⑯ x 0.50 / $a_3$ |
| 0.75 | 2960 | 5.493 | 22600 | 10.675 | .1435 | .01245 | .1359 | 3.00 | .0005955 |
| | 2460 | 4.567 | 18780 | 8.875 | | | .1635 | 2.68 | .000575 |
| | 1960 | 3.638 | 14960 | 7.07 | | | .2050 | 2.33 | .000560 |
| 0.50 | 2960 | 5.815 | 19540 | 9.23 | .1241 | .01077 | .1287 | 3.13 | .0006213 |
| | 2460 | 4.835 | 16240 | 7.675 | | | .1545 | 2.83 | .0006073 |
| | 1960 | 3.852 | 12950 | 6.113 | | | .1939 | 2.48 | .000596 |
| 0.25 | 2960 | 6.043 | 17880 | 8.45 | .1134 | .00986 | .1237 | 3.40 | .000675 |
| | 2460 | 5.020 | 14860 | 7.02 | | | .1488 | 3.10 | .0006653 |
| | 1960 | 4.002 | 11850 | 5.60 | | | .1864 | 2.74 | .000658 |
| 0 | 2960 | 6.117 | 17330 | 8.185 | .1100 | .00955 | .1221 | 3.58 | .000711 |
| | 2460 | 5.085 | 14410 | 6.807 | | | .14675 | 3.28 | .000704 |
| | 1960 | 4.050 | 11475 | 5.425 | | | .1842 | 2.95 | .000709 |

IDEAL PERFORMANCE OF MULTI-JET

TABLE 8 Cont'd

| 1 | 2 | 18 | 19 | 20 | 21 | 22 | 23 | 24 | 25 | 26 |
|---|---|---|---|---|---|---|---|---|---|---|
| $M_o$ | $T_3$ °R | $\frac{I_v}{a_3 \& \beta_{VOL}}$ | $I_v$ lb. SECS | W DISCHARGED | W REMAINING | W DISCHARG. DURING SCAVENGING | $I_s$ lb SECS | $I_D$ lb SECS | $I_{NET}$ lb SECS | $\tau_s$ |
| | | | (18)×(14)×$a_3$ | % | % | (21)×(14) lbs | $\frac{(22)\times M_1 \times a_1}{32.2}$ | $\frac{(14)\times M_o \times a_o}{32.2}$ | (19)+(23)−(24) | SECS |
| 0.75 | 2960 | .0307 | .962 | .758 | .242 | .003013 | .0640 | .3233 | .7027 | .00073 |
| | 2460 | .0289 | .838 | .8006 | .2094 | .002607 | .0554 | | .570 | |
| | 1960 | .0261 | .675 | .8336 | .1664 | .002071 | .04395 | | .3963 | |
| 0.50 | 2960 | .02925 | .794 | .7462 | .2538 | .002736 | .0565 | .1867 | .6633 | .000752 |
| | 2460 | .02715 | .6807 | .7747 | .2253 | .002429 | .0501 | | .5445 | |
| | 1960 | .0240 | .5375 | .8142 | .1858 | .002005 | .0414 | | .3925 | |
| 0.25 | 2960 | .0283 | .703 | .7244 | .2756 | .002713 | .05505 | .0854 | .673 | .000766 |
| | 2460 | .0259 | .5945 | .7488 | .2512 | .002475 | .0501 | | .5595 | |
| | 1960 | .0226 | .463 | .784 | .2160 | .002130 | .0431 | | .421 | |
| 0 | 2960 | .02795 | .6725 | .7116 | .2884 | .002750 | .0554 | 0 | .728 | .00077 |
| | 2460 | .02555 | .5685 | .7336 | .2664 | .002541 | .05117 | | .620 | |
| | 1960 | .0221 | .439 | .7628 | .2372 | .002264 | .04555 | | .4845 | |

IDEAL PERFORMANCE OF THE MULTI-JET

TABLE 8 Cont'd

| 1 | 2 | 27 | 28 | 29 | 30 | 31 | 32 | 33 | 34 | 35 |
|---|---|---|---|---|---|---|---|---|---|---|
| $M_o$ | $T_3$ °R | $\tau_c$ | $\tau_{TOT}$ SECS | THRUST LBS | SPECIFIC THRUST LBS/LB/SEC | $T_3 - T_2$ | FUEL / AIR | SPECIFIC FUEL CONSUMPTION LBS/HR/LB F | THRUST / FRONTAL AREA | WEIGHT / THRUST |
| | | SECS | (17)+(26)+(27) +0.0015 | (25)/(28) | (29)/(19) | °F | lb/lb | 3600 x (32)/(30) | LBS/IN² | LB/LB |
| 0.75 | 2960 | .000536 | .003362 | 20910 | 56.45 | 2276 | .0279 | 1.780 | 4.18 | .1675 |
| | 2460 | | .003342 | 170.5 | 45.80 | 1776 | .0205 | 1.61 | 3.410 | .205 |
| | 1960 | | .003327 | 119.3 | 31.84 | 1276 | .0137 | 1.549 | 2.386 | .294 |
| 0.50 | 2960 | .000552 | .003426 | 193.6 | 61.65 | 2314 | .02825 | 1.650 | 3.872 | .181 |
| | 2460 | | .003412 | 159.5 | 50.60 | 1814 | .0209 | 1.486 | 3.190 | .2195 |
| | 1960 | | .003401 | 115.3 | 36.45 | 1314 | .0141 | 1.394 | 2.306 | .304 |
| 0.25 | 2960 | .000563 | .003505 | 191.8 | 68.27 | 2338 | .0285 | 1.504 | 3.836 | .1825 |
| | 2460 | | .003495 | 160.0 | 56.75 | 1838 | .0212 | 1.346 | 3.200 | .219 |
| | 1960 | | .003488 | 120.7 | 42.72 | 1338 | .0145 | 1.221 | 2.414 | .291 |
| 0 | 2960 | .000566 | .003548 | 205.1 | 76.2 | 2345 | .0285 | 1.347 | 4.102 | .170 |
| | 2460 | | .003541 | 174.9 | 64.9 | 1845 | .0212 | 1.177 | 3.498 | .200 |
| | 1960 | | .003546 | 136.6 | 50.7 | 1345 | .0145 | 1.030 | 2.732 | .258 |

TABLE 8 (CONT'D)

| 1 | 2 | 36 | 37 |
|---|---|---|---|
| $M_0$ | $T_3$ °R | $C_T$ | $\chi$ |
| | | (34)/8 | (34) Ft²/Sec²<br>(30) Ft²/Sec²/°R |
| .75 | 2450 | .722 | 1.75 |
| | 2450 | .593 | 1.80 |
| | 1950 | .413 | 1.73 |
| 0.50 | 2450 | 1.078 | 1.71 |
| | 2450 | 1.24 | 1.85 |
| | 1950 | .977 | 1.84 |
| .25 | 2450 | .995 | 1.80 |
| | 2450 | 1.16 | 1.82 |
| | 1950 | 1.26 | 1.85 |
| 0 | 2450 | | 1.75 |
| | 2450 | | 1.75 |
| | 1950 | | 1.75 |

ACTUAL PERFORMANCE OF THE MULTI-JET

TABLE 9

| Column | 1 | 2 | 3 | 4 | 5 | 5(a) | 6 | 6(a) | 7 |
|---|---|---|---|---|---|---|---|---|---|
| Function | $M_o$ | $T_3$ °R | $P_o$ psf | $P_{ot}$ psf | $P_1$ psf | $P_1'$ psf | $P_2$ psf | $P_2'$ psf | $T_{ot}$ °R |
| Operation | | | | | | ⑤ x 0.97 | ⑤ x 2.17 | ② x 0.97 | |
| | 0.75 | 2960 | 2116 | 3070 | 2407 | 2336 | 5225 | 5067 | 577 |
| | | 2460 | | | | | | | |
| | | 1960 | | | | | | | |
| | 0.50 | 2960 | | 2510 | 1968 | 1910 | 4270 | 4145 | 545 |
| | | 2460 | | | | | | | |
| | | 1960 | | | | | | | |
| | 0.25 | 2960 | | 2210 | 1732 | 1680 | 3758 | 3646 | 525 |
| | | 2460 | | | | | | | |
| | | 1960 | | | | | | | |
| | 0 | 2960 | | 2116 | 1658 | 1609 | 3600 | 3490 | 519 |
| | | 2460 | | | | | | | |
| | | 1960 | | | | | | | |

ACTUAL PERFORMANCE OF THE MULTI-JET

# TABLE 9

| 1 | 2 | 8 | 9 | 10 | 11(a) | 11(b) | 11 | 12 | 13 |
|---|---|---|---|---|---|---|---|---|---|
| $M_o$ | $T_3$ °R | $T_1$ °R | $T_2$ °R | $T_3/T_2$ | $P_3$ psf | $P_3'$ psf | $P_{3\,AVG}$ psf | $\frac{P_{3\,AVG}}{P_o}$ | $qP_{3\,AVG}$ lbs/ft² |
| | | | (8)×1.27 | | (6)×(10) | (6a)×(10) | $\frac{(11a)+(11b)}{2}$ | | |
| 0.75 | 3460 | 539 | 684.5 | 5.06 | 26,450 | 25,600 | 26,025 | 12.30 | .1411 |
| | 2960 | | | 4.33 | 22,600 | 21,920 | 22,260 | 10.69 | |
| | 2460 | | | 3.66 | 19,780 | 18,200 | 18,490 | 8.74 | |
| | 1960 | | | 2.86 | 14,960 | 14,510 | 14,735 | 6.96 | |
| 0.50 | 3460 | 509 | 646.5 | 5.35 | 22,950 | 22,190 | 22,520 | 10.63 | .1222 |
| | 2960 | | | 4.68 | 19,540 | 18,960 | 19,250 | 9.10 | |
| | 2460 | | | 3.98 | 16,240 | 15,760 | 16,000 | 7.56 | |
| | 1960 | | | 3.04 | 12,950 | 12,560 | 12,755 | 6.027 | |
| 0.25 | 3460 | 490 | 622.5 | 5.56 | 20,850 | 20,300 | 20,575 | 9.70 | .1113 |
| | 2960 | | | 4.75 | 17,800 | 17,350 | 17,615 | 8.327 | |
| | 2460 | | | 3.95 | 14,860 | 14,410 | 14,635 | 6.915 | |
| | 1960 | | | 3.15 | 11,850 | 11,490 | 11,670 | 5.515 | |
| 0 | 3460 | 484 | 615 | 5.53 | 20,300 | 19,650 | 19,975 | 9.44 | .1082 |
| | 2960 | | | 4.81 | 17,330 | 16,820 | 17,075 | 8.07 | |
| | 2460 | | | 4.00 | 14,410 | 13,980 | 14,195 | 6.71 | |
| | 1960 | | | 3.185 | 11,475 | 11,130 | 11,255 | 5.32 | |

AERODYNAMICS DEVELOPMENT CORPORATION
PACIFIC PALISADES, CALIFORNIA

REPORT NO. 2000-1-R1
DATE Jan 24 1953

| PREPARED BY | AEROPHYSICS DEVELOPMENT CORPORATION | REPORT NO 2000-1-R1 |
|---|---|---|
| CHECKED BY | PACIFIC PALISADES, CALIFORNIA | DATE Jan 21 1953 |

ACTUAL PERFORMANCE OF THE MULTI-JET

TABLE 9 (CONT'D)

| 1 | 2 | 14 | 15 | 16 | 17 | 18 | 19 | 20 | 21 |
|---|---|---|---|---|---|---|---|---|---|
| $M_o$ | $T_3$ °R | W lbs/cycle | $\beta_{AVG}/P_{OR}$ | $\frac{\tau_E \alpha_3}{L}$ | $\tau_E$ SECS ⑯ x 0.50 / $q_i$ | $\frac{I'}{\alpha_3 \beta_3 V_{OL}}$ | $I_r$ lb. SECS ⑱x⑲x$\alpha_3$ | W DISCHARGED % | W REMAINING % |
| 0.75 | 3460 | .01227 | 8.49 | 3.25 | .000564 | .0320 | 1.130 | .779 | .221 |
| | 2960 | | 7.26 | 2.94 | .000584 | .0307 | .950 | .7638 | .2362 |
| | 2460 | | 6.025 | 2.66 | .000571 | .02865 | .819 | .7928 | .2072 |
| | 1960 | | 4.805 | 2.28 | .000548 | .0258 | .558 | .8400 | .1600 |
| 0.50 | 3460 | .010625 | 6.96 | 3.45 | .000583 | .0307 | .941 | .7895 | .2105 |
| | 2960 | | 7.57 | 3.12 | .000620 | .0291 | .779 | .7470 | .2530 |
| | 2460 | | 6.37 | 2.82 | .000605 | .0269 | .6655 | .7758 | .2242 |
| | 1960 | | 5.08 | 2.45 | .000589 | .0237 | .524 | .8174 | .1826 |
| 0.25 | 3460 | .00970 | 9.30 | 3.65 | .000666 | .0281 | .687 | .7283 | .2717 |
| | 2960 | | 7.77 | 3.35 | .000634 | .0297 | .630 | .7938 | .2062 |
| | 2460 | | 6.62 | 3.06 | .000656 | .02575 | .582 | .7524 | .2476 |
| | 1960 | | 5.28 | 2.71 | .000652 | .0223 | .4495 | .7873 | .2127 |
| 0 | 3460 | .009405 | 9.35 | 3.75 | .000650 | .0295 | .800 | .7955 | .2045 |
| | 2960 | | 7.97 | 3.54 | .000704 | .0278 | .659 | .7148 | .2852 |
| | 2460 | | 6.705 | 3.25 | .000697 | .0253 | .554 | .7360 | .2640 |
| | 1960 | | 5.32 | 2.84 | .000683 | .02175 | .4252 | .7737 | .2263 |

ACTUAL PERFORMANCE OF THE MULTI-JET

TABLE 9

| 1 | 2 | 22 | 23 | 24 | 25 | 26 | 27 | 28 | 29 |
|---|---|---|---|---|---|---|---|---|---|
| $M_o$ | $T_3$ °R | $W_{DISCH}$ DURING SCAVENGING | $I_s$ lb SECS | $I_D$ lb SECS | $I_{NET}$ lb SECS | $\tau_{TOT}$ | $\tau_o$ | $\tau_v$ | $\tau_v/\tau_o$ |
| | | (21)×(14) lbs | $\frac{(22)\times M_o \times a_o}{32.2}$ | $\frac{(14)\times M_o \times a_o}{32.2}$ | (19)+(23)-(24) | SECS | SECS | SECS | |
| 0.75 | 3460 | .00271 | .0575 | .3188 | .8687 | | | | |
| | 2960 | .00290 | .0615 | | .6927 | | | | |
| | 2460 | .00254 | .0540 | | .5542 | .00340 | .001510 | .0004 | .265 |
| | 1960 | .00196 | .0416 | | .3808 | | | | |
| 0.50 | 3460 | .00224 | .0462 | .1839 | .8033 | | | | |
| | 2960 | .00269 | .0555 | | .6506 | | | | |
| | 2460 | .00238 | .0491 | | .5307 | .00350 | .001518 | | .2635 |
| | 1960 | .00194 | .04000 | | .3800 | | | | |
| 0.25 | 3460 | .00201 | .0407 | .0840 | .7903 | | | | |
| | 2960 | .00264 | .0533 | | .6563 | | | | |
| | 2460 | .00239 | .0485 | | .5465 | .00360 | .001525 | | .2622 |
| | 1960 | .00206 | .0417 | | .4072 | | | | |
| 0 | 3460 | .00192 | .0386 | | .8386 | | | | |
| | 2960 | .00268 | .0540 | | .7130 | | | | |
| | 2460 | .00248 | .0500 | | .6040 | .00360 | .001525 | | .2622 |
| | 1960 | .00213 | .0428 | | .4680 | | | | |

ACTUAL PERFORMANCE OF THE MULTI-JET

TABLE 9

| 1 | 2 | 30 | 31 | 32 | 33 | 34 | 35 | 36 | 37 |
|---|---|---|---|---|---|---|---|---|---|
| $M_o$ | $T_3$ °R | K | $\eta_c$ −0.08 | $(\frac{P_x}{P_o})(\eta_c - 0.08)$ | $\frac{(1-K\frac{P_x}{P_o})}{(1-0.08K)}$ | $(\frac{P_x}{P_o})(1-K\frac{P_x}{P_o})$ / $(\eta_c-0.08)(1-0.08K)$ | THRUST lbs | AIR SPECIFIC IMPULSE lbs/lb/sec | $T_3 - T_e$ |
| | | | | | | (32) × (33) | (25)/(26) × (34) | (25)/(14) × (33) | °F |
| 0.75 | 3460 | .110 | .992 | .676 | .934 | .652 | 166.5 | 68.2 | 2775 |
| | 2960 | .142 | .9908 | | .925 | .645 | 131.2 | 53.9 | 2275 |
| | 2460 | .214 | .9829 | | .926 | .627 | 102.3 | 41.9 | 1775 |
| | 1960 | .370 | .966 | | .872 | .590 | 66.0 | 27.1 | 1275 |
| 0.50 | 3460 | .145 | .9881 | .677 | .950 | .643 | 149.0 | 71.3 | 2013 |
| | 2960 | .197 | .9842 | | .934 | .633 | 117.5 | 57.1 | 2313 |
| | 2460 | .307 | .9754 | | .897 | .608 | 92.1 | 44.8 | 1813 |
| | 1960 | .528 | .9577 | | .825 | .560 | 64.9 | 29.5 | 1313 |
| 0.25 | 3460 | .170 | .9864 | .678 | .943 | .640 | 141.0 | 76.8 | 2337 |
| | 2960 | .240 | .9808 | | .920 | .625 | 113.4 | 62.3 | 2337 |
| | 2460 | .382 | .9694 | | .872 | .592 | 90.0 | 49.2 | 1837 |
| | 1960 | .690 | .9448 | | .775 | .525 | 59.5 | 32.5 | 1337 |
| 0 | 3460 | .180 | .9854 | .678 | .939 | .636 | 148.0 | 83.5 | 2845 |
| | 2960 | .260 | .9792 | | .912 | .619 | 122.5 | 69.1 | 2345 |
| | 2460 | .412 | .967 | | .872 | .592 | 99.5 | 56.0 | 1845 |
| | 1960 | .770 | .9503 | | .820 | .564 | 66.2 | 37.3 | 1345 |

AEROPHYSICS DEVELOPMENT CORPORATION
PACIFIC PALISADES CALIFORNIA

REPORT NO 2000-1-R1
DATE Jan 24 19

SECURITY INFORMATION
RESTRICTED

ACTUAL PERFORMANCE OF THE "ULTI-JET TABLE 9

| 1 | 2 | 38 | 39 | 40 | 41 | 42 | 43 |
|---|---|---|---|---|---|---|---|
| $M_o$ | $T_3$ °R | FUEL / AIR | SPECIFIC FUEL CONSUMPTION lbs/hr/lb | THRUST / FRONTAL AREA | WEIGHT / THRUST | CT | X |
| | | $\frac{lb}{lb}$ | $\frac{3600 \times (38)}{(36)}$ | $\frac{lb_3}{in^2}$ | $\frac{lb}{lb}$ | $(40)/q$ | $\frac{(40)\ \text{Thrust}}{(38)\ \text{Fuel/Eng}}$ |
| 0.75 | 3460 | .0363 | 1.92 | 3.330 | .258 | .579 | 5.11 |
| | 2960 | .0279 | 1.865 | 2.624 | .333 | .454 | 5.09 |
| | 2460 | .0205 | 1.765 | 2.040 | .428 | .354 | 5.10 |
| | 1960 | .0137 | 1.820 | 1.320 | .665 | .228 | 5.09 |
| 0.50 | 3460 | .0368 | 1.86 | 2.960 | .290 | 1.190 | 5.17 |
| | 2960 | .0238 | 1.700 | 2.350 | .376 | 0.915 | 5.12 |
| | 2460 | .0209 | 1.675 | 1.842 | .475 | 0.716 | 5.13 |
| | 1960 | .0141 | 1.720 | 1.218 | .720 | 0.473 | 5.13 |
| 0.25 | 3460 | .0370 | 1.735 | 2.920 | .305 | 4.38 | 5.11 |
| | 2960 | .0285 | 1.645 | 2.260 | .386 | 3.52 | 5.05 |
| | 2460 | .0212 | 1.550 | 1.800 | .487 | 2.90 | 5.08 |
| | 1960 | .0145 | 1.605 | 1.190 | .736 | 1.85 | 5.08 |
| 0 | 3460 | .0372 | 1.605 | 2.960 | .290 | | 5.10 |
| | 2960 | .0285 | 1.490 | 2.450 | .358 | | 5.10 |
| | 2460 | .0212 | 1.365 | 1.990 | .440 | | 5.10 |
| | 1960 | .0145 | 1.400 | 1.324 | .561 | | 5.10 |

PREPARED BY

CHECKED BY

AEROPHYSICS DEVELOPMENT CORPORATION

PACIFIC PALISADES, CALIFORNIA

REPORT NO. 2000-1-11

DATE Jan 24 1953

SECURITY INFORMATION RESTRICTED



SECURITY INFORMATION RESTRICTED

TORQUE ON VALVE BLADES DUE TO AERODYNAMIC DRAG

TABLE 10

| 1 | 2 | 3 | 4 | 5 | 6 | 7 | 8 | 9 | 10 | |
|---|---|---|---|---|---|---|---|---|---|---|
| SECTION | RADIAL ARM | VELOCITY | REYNOLDS $N_o$ | THICKNESS / CHORD | $C_D$ | AREA | $q$ | DRAG | TORQUE PER BLADE | TOTAL TORQUE FOR 5 BLADES |
| | INCHES | F P S | | | | D ft | PS F | LBS | IN. LBS | IN LBS. |
| 1 | 3.6" | 130 | $2.5 \times 10^5$ | 0.045 | .0103 | 2.00 | 20.0 | .00286 | .0103 | .0825 |
| 2 | 2.7" | 85 | $1.22 \times 10^5$ | 0.086 | .0128 | 2.37 | 8.56 | .00180 | .00485 | .0388 |
| 3 | 1.9" | 60 | $0.61 \times 10^5$ | 0.206 | .115 | 1.01 | 4.27 | .00344 | .00654 | .0522 |
| | | | | | | | | | | .1735 |

# TABLE II

## TOTAL PRESSURE DURING DISCHARGE

| INDEX POINT | $\mu$ | $P_t/P_T$ |
|---|---|---|
| 0, 0 | 0 | 1.000 |
| 1, 1 | -.175 | .796 |
| 2, 2 | -.350 | .631 |
| 3, 3 | -.525 | .496 |
| 4, 4 | -.700 | .388 |
| 5, 5 | -.875 | .301 |
| 6, 6 | -1.050 | .232 |
| 7, 7 | -1.225 | .177 |
| 8, 8 | -1.400 | .135 |
| 9, 9 | -1.575 | .101 |
| 10, 10 | -1.750 | .0755 |
| 11, 11 | -1.925 | .0555 |
| 12, 12 | -2.100 | .0406 |
| 13, 13 | -2.275 | .0293 |
| 14, 14 | -2.450 | .0207 |
| 15, 15 | -2.625 | .0148 |
| 16, 16 | -2.800 | .0102 |
| 17, 17 | -2.975 | .0068 |

# TABLE 12

## HIGH TEMPERATURE COMBUSTION TUBE MATERIAL COMPARISON

PREPARED BY

CHECKED BY

AEROPHYSICS DEVELOPMENT CORPORATION
P O BOX 657, PACIFIC PALISADES, CALIFORNIA

REPORT NO: 2000-1-R1

DATE: JAN 24 1953

| MATERIAL AND SOURCE | COEFFICIENT OF THERMAL EXPANSION $\epsilon$ = in. in./°F | THERMAL CONDUCTIVITY Btu/hr/ft²/°F/in | MODULUS OF ELASTICITY E = psi | DENSITY $\rho$ = lbs/cu.in. | POISSON'S RATIO $\frac{1}{\sigma}$ | SPECIFIC HEAT $C_p$ = Btu/lb/°F | TENSILE STRENGTH $\sigma$ = psi | THERMAL DIFFUSIVITY $\alpha$ = ft²/hr. | REMARKS |
|---|---|---|---|---|---|---|---|---|---|
| Borolite Zirconium Boride ($ZrB_2$) 5% Nickel American Electro Metal Corp. | 5.5 x 10⁻⁶ at T 1840° F for $ZrB_2$ only | 160 @ 60°F | | .101 | | | Short time Rupture strength is 12,000 psi at 2,000 | | Small samples have been heated to 4710° F and plunged into water without cracking. Very oxidation resistant |
| Graphite (EBP) National Carbon Company | 1.2 x 10⁻⁶ over wide range of temperature | 1200 @ 60°F 87 @ 1000°F estimated at 40 @ 3000°F | .12 x 10⁷ @ 3000°F | .061 | @ 60°F | .165 Mean from 70°F to 1000°F .2 Mean from 1000°F to 3000°F | 2000 @ 2000°F 3000 @ 3000°F 4000 @ 4000°F 6700 @ 6000°F 0 @ 6300°F Short time tests | .5 x 10⁻² @ 3000°F estimated | Oxidizes above 700°F Extremely thermal shock resistant but must be coated to resist oxidation. |
| Stabilized Zirconium Oxide (Dense) (Norton Co.) | 3 x 10⁻⁶ from 60°F to 3000°F | 5.5 @ 60°F 6.2 @ 2000°F 7.5 @ 3000°F | 2.5 x 10⁷ @ 1800° F | .152 | | .17 Mean from 70°F to 2000°F | 6700 @ 1800° F | 1.3 x 10⁻² @ 3000°F estimated | Very low thermal conductivity at high temperatures. Somewhat sensitive to thermal shock. |
| Carbofrax (>85% SiC) The Carborundum Co. | 2.6 x 10⁻⁶ from 60°F to 2500°F | 105 @ 1200°F 109 @ 2200°F 112 @ 2800°F | | .098 | | .2 | Rupture strength is 2000-3120 @ 2400°F | | Oxidation resistant. Good thermal shock resistance. Low tensile strength at 3000° F. |
| Metamic LT-1 70% Cr 30% $Al_2O_3$ Haynes Stellite Div. Union Carbide & Carbon Corp. | 4.7 x 10⁻⁶ Mean from 32°F to 1832°F Estimated at 7.10⁻⁶ @ 2400°F | 83 Mean from 60°F to 1000°F Estimated at 50 @ 2400°F | Estimated 10⁷ @ 2400°F | .22 | Estimated .2 | Estimated .25 | 17500 @ 1800°F 12000 @ 2000°F 7000 @ 2200°F 3200 @ 2400°F Short time | 4.4 x 10⁻² @ 2400°F estimated | M.P. = 3362° F, so strength @ 3000° F is probably low. |
| Kentanium K151A 80% TiC 20% Ni Kennametal, Inc. | 4.5 x 10⁻⁶ up to 1200°F | 240 @ 60°F | 5.67 x 10⁷ | .21 | varies little from .25 for most materials | $C_p$ varies little from .3 for most materials | 40000 @ 2000° F Short time test 10500 @ 1800° F for stress rupture at 10 hours | | Good material at 2000° F, but probably has little strength at 3000° F. |

PREPARED BY:
CHECKED BY:
AEROPHYSICS DEVELOPMENT CORPORATION
P O BOX 657, PACIFIC PALISADES, CALIFORNIA
REPORT NO: 2000-1-R1
DATE: JAN 24 1958

# TABLE 12 (CONT'D)

| MATERIAL AND SOURCE | COEFFICIENT OF THERMAL EXPANSION $\epsilon$ = in./in./°F | THERMAL CONDUCTIVITY $k$ BTU/hr/ft²/°F/in | MODULUS OF ELASTICITY E = psi | DENSITY $\rho$ = lbs/cu.in. | POISSON'S RATIO $\nu$ | SPECIFIC HEAT $C_p$ = BTU/lb/°F | TENSILE STRENGTH $\sigma$ = psi | THERMAL DIFFUSIVITY $\alpha$ = ft²/hr. | REMARKS |
|---|---|---|---|---|---|---|---|---|---|
| Stupalith Lithium Alumina Silicate - Stupakoff Ceramic & Mfg. Co. | $.035 \times 10^{-6}$ (A-2417) $.47 \times 10^{-6}$ (A-2209) | | | .058 .085 | | | 3000 @ 60°F 5000 @ 60°F | | Material melts at 2450°F or under. Dimensions of cast pieces can be held accurately. Excellent thermal shock properties. |
| Alumina 96% $Al_2O_3$ Al-200 (low porosity) Coors Porcelain Co. | | 28 @ 60°F | $55 \times 10^6$ | .145 | | | | | Very high melting point. Poor thermal shock properties. |
| Kentanium K151-A Kennametal, Inc. | $5.10^{-6}$ | 160 @ 60°F | $56.7 \times 10^6$ @ 60° | .209 | | | Short time tests 80000 @ 60°F 55000 @ 1500° F 30000 @ 2000° F 12500 @ 2200° F 3000 @ 2400° F | | Stress - Rupture Times Curves indicate no appreciable strength is retained for 100 hours at 2100° F. Material has excellent thermal shock properties, but is rather costly. |
| Molybdenum coated with Molybdenum Disilicide - Fansteel Metallurgical Corporation | $3.10^{-6}$ | 240 @ 60°F | $42.10^6$ | .368 | | .065 | 150000 @ 60° F 100000 @ 1600° F 30000 @ 2000° F 3000 @ 3000°F | | Stress - Rupture Time Curve not known, but the coated material appears to be quite satisfactory, though heavy and rather costly for high temperature service |
| Quartz Translucent General Electric Company | $.55.10^{-6}$ | 9.5 @ 60°F | 7100 | .075 | .14 | .18 | 26 @ 60° F | | Tensile strength is poor but otherwise material has excellent properties up to 3000°F. |
| Adamant Fire Brick Cement-Rotfield Refractories Company | | Low | | .05 | | | 800 @ 60°F 1270 @ 2000° F | | Tensile strength is good for cement material. |
| Fiberfrax 50% $Al_2O_3$ 50% $SiO_2$ -The Carborundum Co. | | .25 @ 60°F 1.00 @ 1000°F 2.00 @ 1700°F 4.00 @ 2500°F | | .007 .0035 | | | | | Excellent insulation material for temperatures to 2500°F |

TABLE 13

HIGH TEMPERATURE COMBUSTION TUBE MATERIAL COMPARISON

| MATERIAL | DESIGN TENSILE STRENGTH ASSUMED AT 3000° F psi | AT 400 psi PRESSURE WALL THICKNESS OF 275" I.D. TUBE (S) | ESTIMATED FOURIER NUMBER FOR t = .01 hrs. | ESTIMATED THERMAL RESISTANCE NUMBER R = 1/bs | CALCULATED MAXIMUM STRESS UPON COOLING FROM 3000° F (STEADY FLOW) psi |
|---|---|---|---|---|---|
| Zirconium Boride ($ZrB_2$) 5% Nickel | 15000 | .0367" | 45.6 | 5.74 | 19000 |
| Graphite (EBP) | 3000 | .1833" | 1.9 | 1.09 | 1100 |
| Stabilized Zirconium Oxide (Dense) Norton | 5000 | .110" | 1.6 | .359 | 78000 |
| Metamic LT-1 | Design Tensile Strength Assumed at 2500°F psi 725 | At 180 psi pressure wall thickness of 1.00" I.D. Tube .125" | | Estimated Thermal Resistance Number 14.1 | Calculated maximum stress upon cooling from 2500°F (Pulsating flo 3270 psi |